MASSACHUSETTS INSTITUTE OF TECHNOLOGY

Ocean Engineering

Cambridge, Massachusetts 02139

MASSACHUSETTS INSTITUTE OF TECHNOLOGY
DEPARTMENT OF OCEAN ENGINEERING
CAMBRIDGE, MASS. 02139

Phase Report
Under Contract No. NAS8-24365
M.I.T. DSR 71648

Analysis of Thermal Stresses and Metal Movement During Welding

by

T. Muraki
and
K. Masubuchi

to

George C. Marshall Space Flight Center
National Aeronautics and Space Administration

June 21, 1973

Report No. 73-16

1.0 INTRODUCTION

The original research contract on "Analysis of Thermal Stresses and Metal Movement during Welding" was initiated on May 15, 1969 with a appropriation of $35,390. The study was completed on October 14, 1970, and the final report of the study was published on December 15, 1970, as the NASA Contractor Report CR-61351.

The extension of the contract became effective on October 14, 1970 with an appropriation of $19,735. In June 1972, the contract was further extended with an additional appropriation of $10,000. In June 1973, the contract was again extended until June 30, 1974 with no additional funding. This report covers the work from October 14, 1970 to date.

2.0 SCOPE OF THE EXTENDED RESEARCH CONTRACT

The scope of the extended research contract is described in Modification No. 3 of Contract No. NAS8-24055, issued in November 1970. The revised contract covered the following phases and tasks:

Phase B, Task 4. To develop a system of mathematical solutions and computer programs for one (1) dimensional analysis and for two (2) dimensional analysis.

Phase D. Adapt Phase B system of mathematical solution of temperature change, stress and strain to refractory metal alloys Cb752 and Ta222 as have been developed for aluminum. The emphasis of analyses should be made for GTWA process, 20-60 inches per minute, 0.10-0.020 inches thick and heat input widely ranging about 200,000 joules/inch/inch. Necessary metal movement and stress measurements or materials will be furnished by the government as determined by MSFC.

As decided in Modification No. 7, issued in June 1972, the scope of research was expanded to cover the following phases:

Phase E. Perform a mathematical study of bending stresses and distortion of 2219-T87 in the thickness direction-aluminum only.

Phase F. Perform a mathematical study of thermal

stresses and metal movement in joining thin cylindrical shells-theoretical portion only.

In June 1973, the program has been further expanded to include:

Phase G. Perform experiments on thermal stresses and metal movement in joining thin cylindrical shells.

3.0 PROGRESS OF RESEARCH

Phase B, Task 4 and Phase D

Appendix A of this report, which is the thesis entitled "Investigation of Thermal Stress and Buckling During Welding of Tantalum and Columbium Sheet" prepared by Mrs. K. Anne S. Hirsch describes the work on Phase B, Task 4, and Phase D.

Chapter II of the thesis describes mathematical analyses on thermal stresses.

Chapters III and IV describe experimental procedures and results. Experimental results were compared with analytical predictions. Important results obtained are as follows:

(1) Temperature changes during welding of tantalum and columbium sheets were comparable to those predicted by the mathematical analysis.

(2) The one-dimensional program was found to be very accurate in predicting thermal strains parallel to the weld. Experimental results and theoretical results were in excellent agreement.

(3) Since the one-dimensional program was capable of analyzing only one strain (or stress) component, a study was made to develop a two-dimensional program capable of analyzing all the three

components under the plane-stress condition. To overcome mathematical difficulties involved in the two-dimensional analysis, the finite-element analysis was used. The problem, however, is a compromise between the accuracy of calculation and computation cost. The accuracy of calculation can be improved by using a finer grid system, but as the number of elements increases, computation cost increases tremendously. The two-dimensional program as developed by January, 1972, was not able to provide results with satisfactory accuracy.

Phase E

Appendix B of this report, which is the thesis entitled "Analysis of Two-Dimensional Thermal Strains and Metal Movement During Welding" prepared by LCDR Jon J. Bryan, USN, describes the work on Phase E.

Chapter II of the thesis describes mathematical formulations of the two-dimensional finite-element analysis of thermal stresses during welding. The significant contribution that LCDR Bryan has made is to develop a mathematical system for expressing temperature dependencies of various material properties, including yield stress, coefficient of linear thermal expansion, thermal conductivity, etc.

Chapters III, IV, and V describe experimental procedures, data reproduction, and results, respectively. Experiments were conducted on butt welds and bead-on-plate welds in aluminum. Measurements were made of temperature changes, thermal strains and relative movements between both sides of the weld line. Computer programs were developed to process a large number of data generated. An important scope of the study by LCDR Bryan was to generate reliable experimental data. Important results obtained are as follows:

(1) Butt vs. Bead-on-plate Characteristics. Figures 41 through 44 of Bryan's thesis provide temperature distribution data for the tests with strain gages installed and Figures 45 through 51 provide data on transverse and longitudinal strain distribution resulting from these tests. Ideally, a butt weld becomes more and more like a bead-on-plate weld for multipass situations. One would hope for a two-dimensional model which could cover both cases. However, Figures 43 and 44 show a different initial temperature distribution for bead-on-plate and butt welds. This implies that for the plate thickness utilized in this study, which was 1/4 inch, the two types of weld will behave somewhat differently in the way of thermally-

induced strains, moments, and distortions. The bead-on-plate weld is not a two-dimensional situation, but the butt weld clearly is. This is because the arc force penetrates into the joint gap and the plate edges in the joint are evenly heated in the thickness direction. Figures 45, 46, 48, and 49 seem to agree with this observation for strains, since bead-on-plate values do not match the top ones.

(2) Use of Strain Invariant. When one deals with transient thermal stresses during welding plates, he faces a difficult task of analyzing three stress components, σ_x, σ_y and τ_{xy}, which change with time. During the experiments at M.I.T., difficulties were experienced in analyzing data and obtaining some trends.

In order to simplify the analysis, an attempt was made to utilize strain invariant, I, as follows (see Equation (64) in page 81):

$$I = (\sigma_x^2 - \sigma_x\sigma_y + \sigma_y^2 + 3\tau_{xy}^2)^{1/2}$$

On the basis of the theory of plasticity, the material is in the plastic condition when I is larger than the value of yield stress.

Figures 56, 57, and 58 show changes of I/σ_{ys}

during welding. Values of I/σ_{ys} give rather consistent, explainable results compared to other values such as σ_x σ_y, and the direction of pron-cipal stress (ϕ_x), shown in Figures 45 through 55. Figures 56, 57, and 58 also show some regions near the weld undergo plastic deformation when the temperatures reach their maximum values.

The study by LCDR Bryan provided useful experimental data. However, he did not have enough time to compare experimental data with analytical predictions. This effort is being carried out by Dr. T. Muraki.

Phase F.

Efforts have been made by Dr. T. Muraki to develop mathematical analysis of thermal stresses and metal move-ment in joining thin cylindrical shells. Basic equations have been developed and numerical computations are being made.

4.0 PLAN FOR THE FUTURE STUDY

A plan for the future study from July 1, 1973 through June 30, 1974 is as follows:

(1) Phase G experiment

(2) Complete description of theoretical studies

4.1 Phase G

Although basic equations have been developed to analyze thermal stresses and metal movement in joining thin cylindrical shells, it is important to compare analytical solutions with experimental results. Efforts will be made to generate experimental data on cylindrical shells. The extent of the efforts, however, depends upon the availability of naval officer students.

4.2 Complete Description of Theoretical Studies

As described earlier in this report, a major problem in the theoretical study is how to develop a computer program with satisfactory accuracy and reasonable cost. During the entire course of this research, persistent efforts have been made to achieve that goal and computer progrmas have been modified for many times.

At the end of the current research program, a complete description will be given of most progressed computer programs.

APPENDIX A

Thesis by Mrs. K. A. S. Hirsch

INVESTIGATION OF THERMAL STRESS AND BUCKLING DURING WELDING OF TANTALUM AND COLUMBIUM SHEET

BY

KATHRYN ANNE STREET HIRSCH

B.S., MATALLURGY AND MATERIAL SCIENCE

MASSACHUSETTS INSTITUTE OF TECHNOLOGY

(1969)

SUBMITTED IN PARTIAL FULFILLMENT

OF THE REQUIREMENTS FOR

THE DEGREE OF

MASTER OF SCIENCE

AT THE

MASSACHUSETTS INSTITUTE OF TECHNOLOGY

JANUARY, 1972

SIGNATURE OF AUTHOR: Kathryn Anne Street Hirsch

Department of Ocean Engineering
January, 1972

CERTIFIED BY: Kenji Masubuchi

Thesis Supervisor

ACCEPTED BY: _____

Chairman, Departmental Committee on Graduate Students

INVESTIGATION OF THERMAL STRESS AND BUCKLING DURING WELDING OF TANTALUM AND COLUMBIUM SHEET

BY

KATHRYN ANNE STREET HIRSCH

Submitted to the Department of Ocean Engineering on January 21, 1972, in partial fulfillment of the requirements for the degree of Master of Science.

ABSTRACT

The heat flow and stress-strain analyses of bead-on-plate welds is discussed and current efforts to apply the theory are outlined. Temperature and strain data from welding experiments on tantalum and columbium (niobium) sheet are presented.

The experimental data are compared to analytical predictions obtained from both one- and two-dimensional computer programs developed for the National Aeronautics and Space Administration. Results indicate that the one-dimensional program can be used to predict and analyze bead-on-plate weldments. The two-dimensional program, however, needs more programmer work in order to become a viable tool. Analytical and experimental evidence indicate that tantalum and columbium may be welded in thin sheet form but with a measure of local thermal buckling.

ACKNOWLEDGEMENT

I wish to thank Professor Koichi Masubuchi of M.I.T. for his invaluable technical assistance over a period of several years now and his guidance in the direction and magnitude of my work. I also wish to thank Mr. Anthony Zona of the Materials Joining Laboratory and Mr. Fred Merlis of the Aerolastics Laboratory for their assistance in running the welding experiments. I am truly indebted to Miss Diane Wyszomirski for her efficient typing of this thesis.

Finally, I thank my husband, Jack, who put up with more than his share of leftover casseroles and wifely bad moods during the completion of this paper.

TABLE OF CONTENTS

LIST OF FIGURES

I INTRODUCTION

A. Background

Welding is one of the most widely used methods for the fabrication of complex structures, because welding offers various advantages over other fabrication processes such as riveting and casting. There are, however, several undesired effects inherent in this process. Among these are residual stresses, distortion, and buckling. The primary cause of these phenomena is the presence of thermally induced plastic strain brought about during the welding process. It is the object of this thesis to study the effects of elevated temperature on the amount of residual stress, distortion and buckling in the material.

Residual stresses in a material may lead to low stress brittle fracture. Below a certain transition temperature, normally ductile materials may fracture catastrophically in brittle mode in the presence of high tensile stresses and notch defects. Such defects are common in welding and are present as cracks or lack-of-fusion spots. Since residual stresses in the heat affected zone may be at or near the yield strength of the material, very little applied stress may be necessary to cause fracture.

Distortion and buckling reduce joint strength by causing mismatching. They may also impart initial deflection in structural members which can result in premature yielding.

Work has already been done at M.I.T. developing one-and two-dimensional computer analyses of strains induced by non-uniform heating. These programs have been compared with experimental data obtained from aluminum and steel sheet. This thesis was undertaken with the thought in mind of broadening the previous scope by considering new materials and adding a buckling analysis to the wealth of strain information already obtained.

Tantalum and columbium exhibit excellent high temperature properties. Figure 1 compares the yield strength versus temperature curves of tantalum and columbium to those several of other structural materials. This is particularly important for aerospace applications where reentry temperatures range from 2000° to 4000° F depending on the trajectory. The melting point of tantalum is 5425° F--well within the safe range. It exhibits a low ductile-to-brittle transition temperature and excellent fabricability for a refractory metal. Columbium (also called niobium) melts at 4474° F and is currently being used in several experimental high-temperature structural alloys. In comparison to the previously studied alloys of aluminum and steel, these should give investigators an idea of the promise of refractory metals as structural materials.

As represented in Figure 1, the ultrahigh strength steel has an excellent yield stress capability but only over a limited temperature range. Heat treated aluminum and low carbon steel retain their respective strengths only as far along the temperature scale as does high strength steel. For

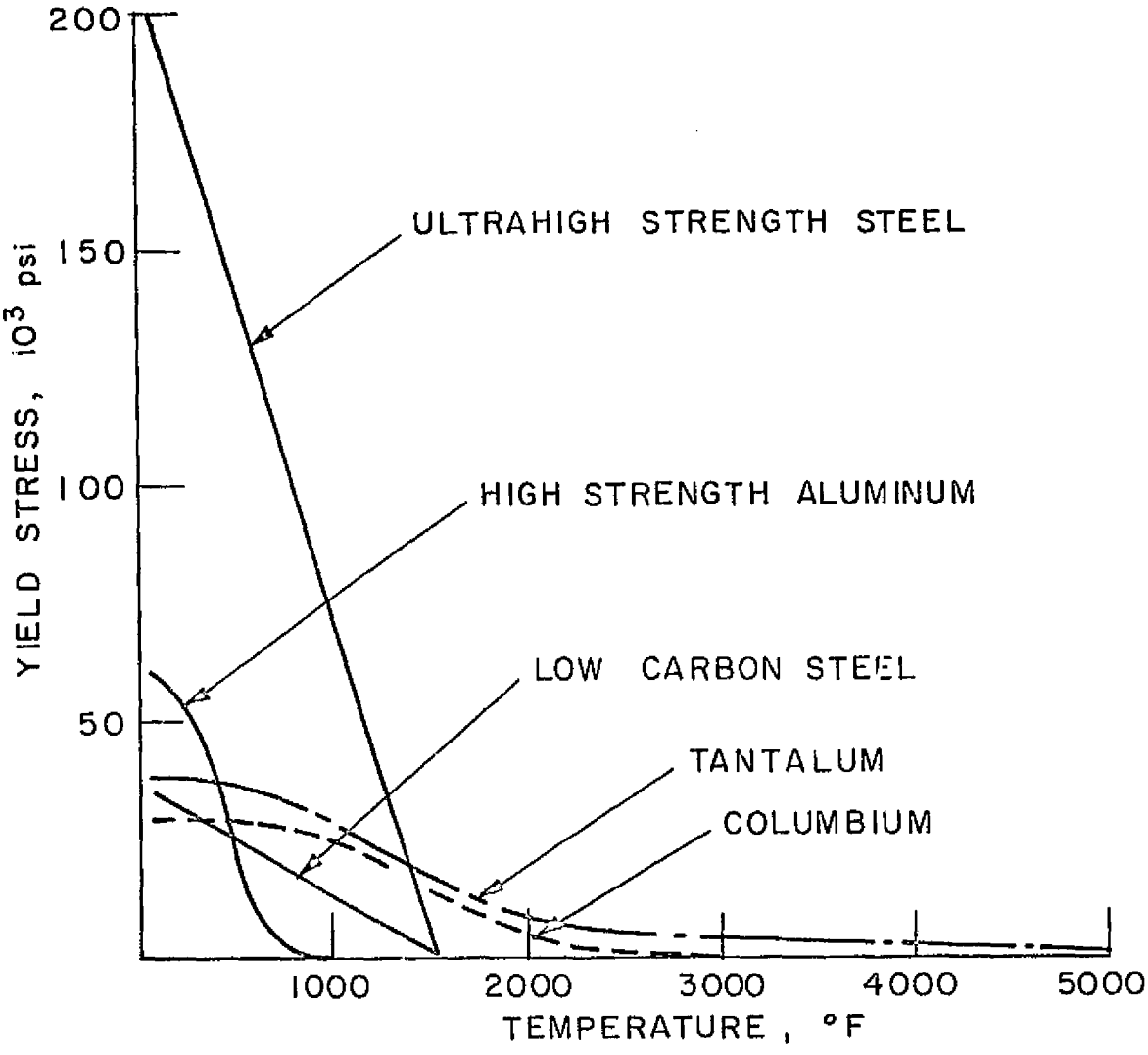

Figure 1 Yield Stress vs. Temperature of Several Structural Materials

any application over 1500° F these materials will suffer severe decreases in desirable material properties. Columbium and, more specifically, tantalum fall into a different category of materials. They demonstrate a reduction in strength at approximately 1500° F, however, they retain at least a moderate yield stress beyond this point. This indicates that these two materials show promise for use in applications which call for service in a wide range of temperature, while retaining structural stability. Thus, application to the NASA space shuttle program seems most appropriate.

B. Welding Stress-Strain Development

Because a weldment is locally heated by the welding arc, the temperature distribution in the weldment is not uniform and changes as welding progresses. This nonuniform temperature distribution causes thermal stresses in the weldment which also change during the process.

Figure 2 shows schematically how welding thermal stresses are formed. Figure 2a indicates a bead-on-plate weld in which a weld bead is being deposited at a speed, v. O-xy is the coordinate system; the origin, O, is on the surface underneath the welding arc, and the x-direction lies in the direction of arc travel.

Figure 2b shows the temperature distribution along several cross sections. Along Section A-A, which is ahead of the arc, the temperature change due to welding, ΔT, is almost

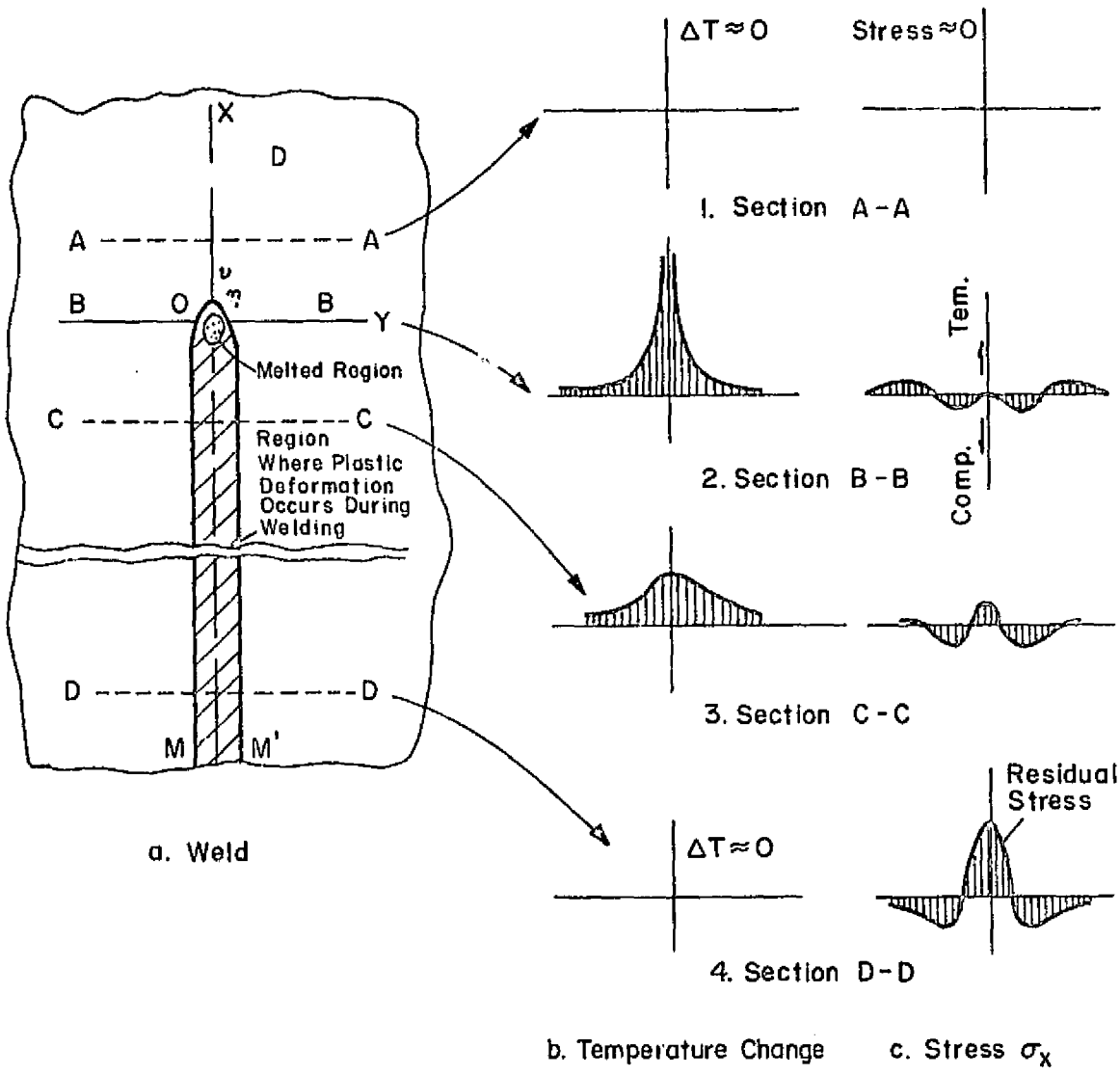

Figure 2 Schematic Representation of Changes of Temperature and Stresses during Welding

zero (Figure 2b-1). Along Section B-B, which crosses the welding arc, the temperature distribution is very steep (Figure 2b-2). Along Section C-C, some distance behind the arc, the distribution of temperature is as indicated in Figure 2b-3. Far behind the arc (Section D-D), the temperature change due to welding again diminishes (Figure 2b-4).

Figure 2c shows the distribution along these sections of the x-direction stress, σ_x. Stress in the y-direction, σ_y, and shear stress, τ_{xy}, also exist in a two-dimensional stress field but are secondary and are neglected in this discussion. Along Section A-A, thermal stresses due to welding are essentially zero (Figure 2c-1). The stress distribution along Section B-B is shown in Figure 2c-2. In the area beneath the welding arc stresses are near zero because molten metal cannot support loads. Immediately outside the weld puddle, stresses are compressive because thermal expansion of these areas is restrained by surrounding areas that are heated to lower temperatures. Since the temperatures of the areas immediately adjacent to the puddle are quite high and the strength of the material is correspondingly low, stresses in these areas are as high as the yield strength and plastic straining occurs. Stresses in areas away from the weld are tensile and balance with the compressive stresses near the weld. In other words, $\int \sigma_x \cdot dy = 0$, across Section B-B.

The distribution along Section C-C is shown in Figure 2c-3. Here the weld metal and base metal regions near the weld are

cooling and tend to shrink. This causes tensile stresses in these regions near the weld and compressive stresses in areas further away.

Figure 2c-4 shows the stress distribution along Section D-D. Continued cooling and shrinkage has left very high tensile stresses in and near the weld, and offsetting compressive stresses across the rest of the section. This is the residual stress distribution after complete cool-down.

Note that the cross-hatched area, MM', in Figure 2a indicates the region where plastic deformation occurs during the welding thermal cycle. The region outside MM' remains elastic during the entire cycle.

C. Previous Investigations

Under the sponsorship of NASA an ongoing series of projects on welding parameters has been undertaken. These projects comprise the first concise look at welding technology in this country as seen by the engineer rather than the welder.

The first project in the series consisted of an improvement of earlier attempts by Battelle Memorial Institute, Columbus Laboratories to develop a computer program for calculating longitudinal stresses during bead-on-plate welds. The results of the Battelle study are covered in a report (RSIC-820) published by the Redstone Scientific Information Center, U. S. Army Missile Command.[1] The M.I.T. work added to the scope of the previous program by considering, in

addition, an investigation of the temperature changes caused by the welding arc, including an analysis of temperature distribution due to the heat generated by the welding arc. A system of mathematical statements was developed describing the phenomenon of thermal stresses and plastic strains during welding. Computer programs for a one-dimensional analysis of the problem and subsequently a finite element two-dimensional analysis were written.[2]

The next phase of the program was to compare the analytic results with experimental data. Bead-on-plate welds were made on 2219 aluminum alloy plate, 1/4-inch thick. Various welding conditions were used during the experiments. The correlation of data proved the computer program to be an accurate and highly useful tool for predicting the magnitudes and directions of residual stresses.[3] In general, longitudinal strains (along the axis of the weld) were predominant. Transverse and shear strains were of smaller magnitude, except in the immediate area of the welding arc. For this reason, the one-dimensional computer predictions were essentially verified. Heat input significantly affected the extent of the tensile residual stress zone. High compressive stresses occurred in areas ahead of the moving arc. Figure 3 is a schematic of the development of the current welding analysis.

The next step in the development of a suitable weld analysis technique was to experiment on different materials under different conditions. Transient strain and temperature data were obtained from welding experiments on low-carbon and high-strength steels with different strength levels (up to

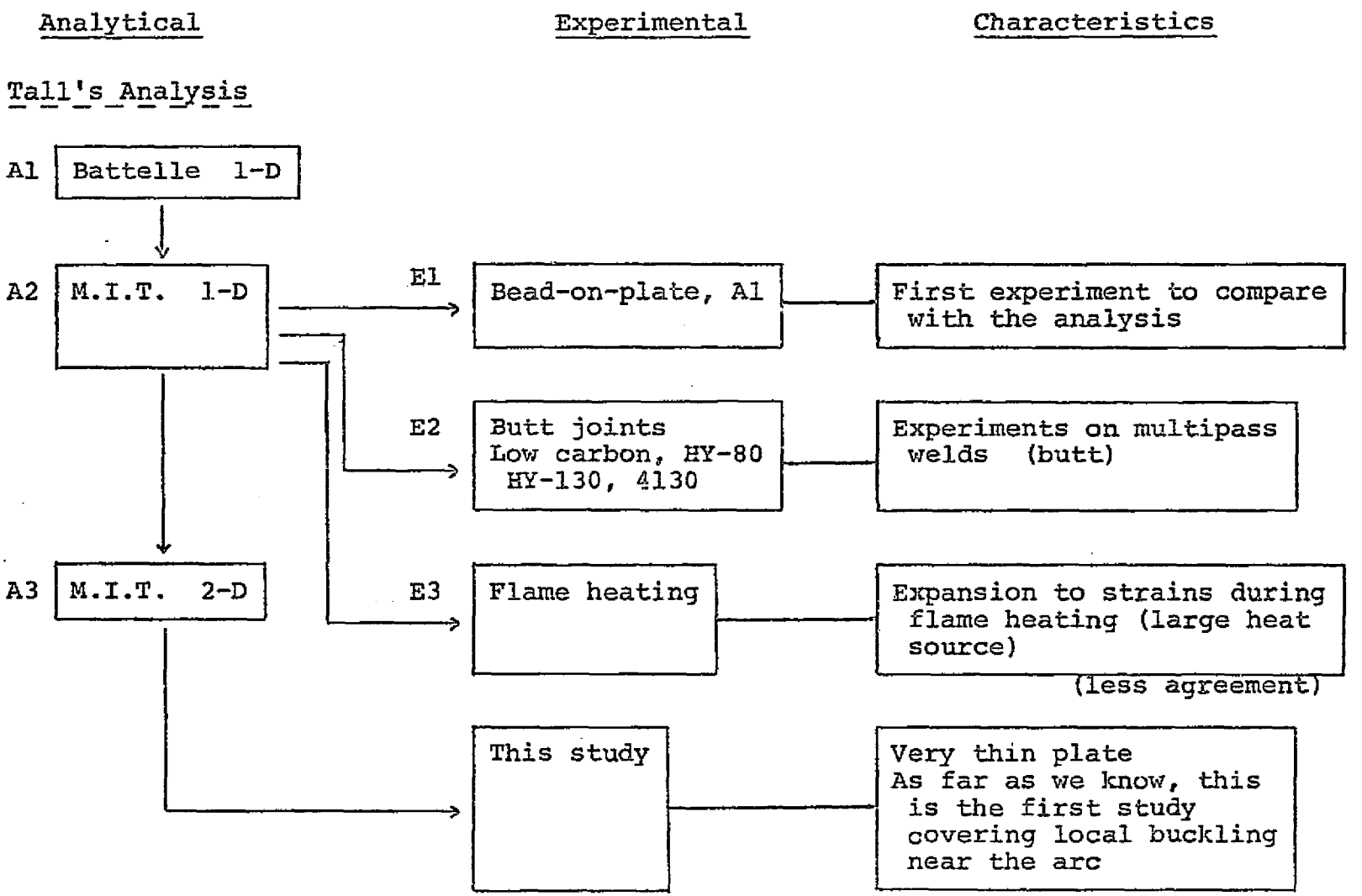

Figure 3 Development of the Current Welding Analysis

180,000 psi yield strength). These experiments were designed to approximate ship structural weldments including thick-section, multi-pass butt welds. The experimental data were compared to the computer programs and results indicated that the programs could be used to analyze complex structural weldments applicable to ship and submarine fabrication.

It was now apparent that the programs had merit for weld analysis, therefore, another attempt at fundamental application of the computer was proposed. Johnson[5] performed experiments on flame heating to remove the residual stresses induced by weldments in steel. He again used thick plate sections. The program was not as successful as previously, due to the large area of the flame heat source.

D. Objective of This Study

This particular investigation is an attempt to broaden the scope of previous investigations even further. Two new materials are being used--namely, tantalum and columbium. These refractory metals have previously defied all attempts at welding due to the ease at which they oxidixe in the presence of elevated temperatures. Thin sheets are being used on the order of .012 to .015 inches thick instead of the 1/4-inch plate sections used in the past. This means that the necessity has arisen for which we must take heat loss by convection from the sheet surface into consideration. All equations and the subsequent computer program must be modified to include these convection terms.

This investigation is of particular interest to NASA because they are considering manufacturing the space shuttle from tantalum or columbium. In sponsoring the contract, they requested the experimental welds be made using a gas tungsten arc apparatus in order that this report might simulate welds which could be made on a production-line basis.

As a follow up to previous studies using the NASA computer program, this investigation will use the one- and two-dimensional weld analyses.

Some study of buckling of sheet after welding has already been done[1] but little progress was made. This paper devotes a section to an attempt to develop an extremely simplified buckling analysis applicable to welded structures.

As far as we know, this is the first study ever published covering transient local buckling near the arc. Studies on transient thermal strains near the arc exist as do works on buckling of the entire plate after welding,[6] however, none has been published on local buckling which moves with the arc. This is a significant problem in the fabrication of structures using thin sheet. Without the use of a computer, such a study is virtually impossible.

II THEORY

A. Heat Flow Analysis

Derivations of the heat flow equations have been set forth by several authors. Chief among these are Myers, et al[7] who give a derivation and a number of solutions which are applicable to various welding processes. Unfortunately, it is not yet possible to calculate with satisfactory accuracy, the thermal cycles in the vicinity of the weld made under given welding conditions.

Figure 4 shows schematically the temperature distribution in a plate on whose surface a weld bead is being laid at a speed, v. Curves 1 to 6 represent isothermal curves on the surface, while the dotted curves represent isothermal curves on the transverse section, ABCD. O-xy is the coordinate axis; the origin, O, is on the surface underneath the welding arc, the x-axis lies in the direction of welding, and the z-axis is placed in the thickness of the plate, downward.

The fundamental expression for heat conduction is given by the Fourier heat flow equation, as follows:

$$\frac{\partial \theta}{\partial t} = \kappa \left(\frac{\partial^2 \theta}{\partial x^2} + \frac{\partial^2 \theta}{\partial y^2} + \frac{\partial^2 \theta}{\partial z^2} \right)$$

The mathematical analysis of heat flow in a weldment is essentially a solution of this equation for a given initial condition (initial temperature distribution) and a boundary condition (shape and intensity of the heat source, geometry of the weldment, etc.).

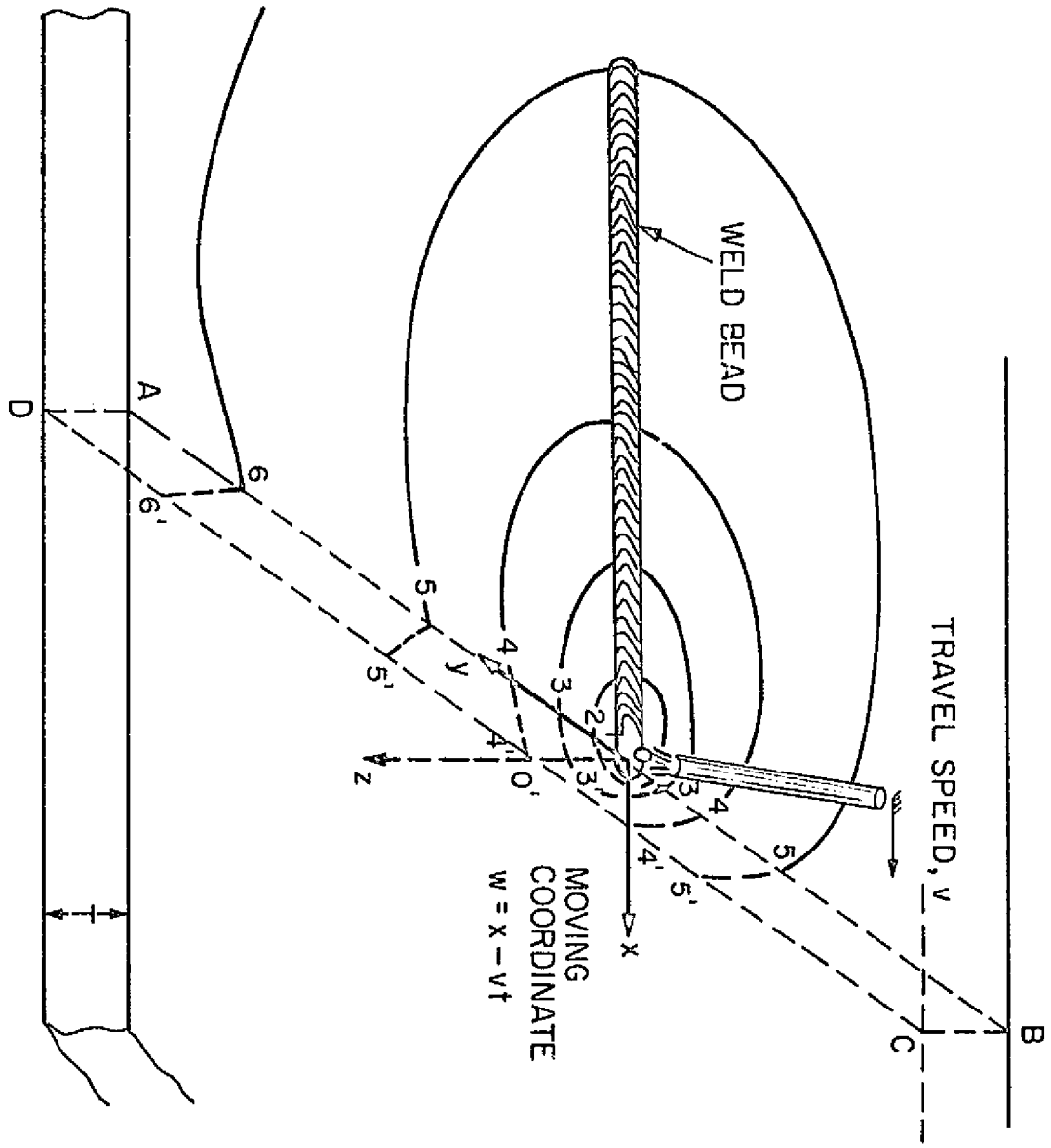

Figure 4 Temperature Distribution in a Plate When a Weld Bead is Laid on the Surface

Two features of heat flow during metal-arc welding are:

1) The heat source moves, usually at a constant speed, on or near the surface of the workpiece.
2) The size of the heat source (welding arc) is small compared to the size of the workpiece.

Consider the case of a solid through which heat is flowing but in which no heat is generated. The temperature θ at the point $P(x,y,z)$ will be a continuous function of x, y, z and t, and the first differential coefficients of θ will also be continuous. If we define $\dot{Q} = dQ/dt$ to be the rate of heat transfer across one face of a rectangular parallelepiped, where ρ is the density and c the specific heat of the solid, we have the time rate of change of internal energy per unit volume equal to:

$$\dot{Q}_v = \rho \cdot c \left(\frac{\partial \theta}{\partial t}\right) \tag{1}$$

If we expand this expression:

$$\rho \cdot c \left(\frac{\partial \theta}{\partial t}\right) = \frac{\partial}{\partial x}\left(\lambda \frac{\partial \theta}{\partial x}\right) + \frac{\partial}{\partial y}\left(\lambda \frac{\partial \theta}{\partial y}\right) + \frac{\partial}{\partial z}\left(\lambda \frac{\partial \theta}{\partial z}\right) \tag{2}$$

This then becomes

$$\rho \cdot c \left(\frac{\partial \theta}{t}\right) = \lambda\left(\frac{\partial^2 \theta}{\partial x^2} + \frac{\partial^2 \theta}{\partial y^2} + \frac{\partial^2 \theta}{\partial z^2}\right) + \frac{\partial \lambda}{\partial \theta}\left[\left(\frac{\partial \theta}{\partial x}\right)^2 + \left(\frac{\partial \theta}{\partial y}\right)^2 + \left(\frac{\partial \theta}{\partial z}\right)^2\right] \tag{3}$$

We assume that $\partial\lambda/\partial\theta = 0$, thus removing the last terms of the equation.

Such a condition is realized in many cases of practical importance.

The temperature distribution for welding is calculated from the analytic solution of the linearized heat flow equation

for a moving line source. This equation is linear because the material properties have been assumed to be constant with temperature. The linear heat flow equation for a flat plate is:

$$\frac{\partial \theta}{\partial t} = \kappa \left(\frac{\partial^2 \theta}{\partial x^2} + \frac{\partial^2 \theta}{\partial y^2} + \frac{\partial^2 \theta}{\partial z^2} \right) \tag{4}$$

where

θ = temperature change

$\kappa = \lambda / c_\rho$, thermal diffusivity

c = specific heat

ρ = density

λ = thermal conductivity

Quasi-stationary. In the case of a moving heat source, it is convenient to express this equation in a coordinate system moving with the heat source. The equation then becomes:

$$\frac{\partial^2 \theta}{\partial w^2} + \frac{\partial^2 \theta}{\partial y^2} + \frac{\partial^2 \theta}{\partial z^2} = - \frac{v}{\kappa} \frac{\partial \theta}{\partial w} \tag{5}$$

where

$w = x - vt$

v = speed of moving source

If this equation is solved for a moving line source of intensity, q, where

$q = Q/h$

H = plate thickness

Q = net heat input

The following solution is obtained

$$\theta - \theta_o = \frac{q}{2\pi\lambda} e^{-\frac{v}{2\kappa} w} K_o\left(\frac{v}{2\kappa} r\right) \qquad (6)$$

in which

$$v = \sqrt{w^2 + y^2}$$

$K_o(z)$ is the modified Bessel function of the second kind and zero order.

Nonstationary. For two-dimensional nonstationary heat flow, consider an instantaneous line source, q; cal/cm occurring at P'(x',y') in an infinite plate at a time, t', and then extinguishing the equation for temperature change at P(x,y) and at time, T, then becomes:

$$\theta - \theta_o = \frac{e^{-\frac{(x-x')^2 + (y-y')^2}{4\kappa(t-t')}}}{4\pi\kappa(t-t')} \frac{q_i}{c\rho} \qquad (7)$$

Temperature change due to a moving point source can now be obtained using equation (7) in the integrated form:

$$\theta - \theta_o = \int_0^{t_o} \frac{e^{-\frac{(x - vt)^2 + y^2}{4\kappa(t_o + t_1 - t)}}}{4\kappa\pi(t_o + t_1 - t)} \frac{q}{c\rho} dt \qquad (8)$$

Equation (8) can also be expressed as follows:

$$\theta - \theta_o = \frac{q}{4\pi\lambda} e^{-\frac{v}{2\kappa} w} \int_{\frac{v^2}{4\kappa} t_1}^{\frac{v^2}{4\kappa}(t_0+t_1)} \frac{e^{-\zeta - \frac{\gamma^2}{\zeta}}}{\zeta} d\zeta \qquad (9)$$

where $w = x - v(t_o + t_1)$

$\gamma^2 = (v/4\kappa)^2(w^2 + y^2)$

Equation (9) represents a general solution for two-dimensional heat flow when laying a straight weld bead. By assuming that welding continued from $t_o = 0$ to $t_o = +\infty$, the temperature in the nonstationary state is obtained as follows:

$$\theta - \theta_o - \frac{q}{4\pi\lambda} e^{-\frac{v}{2\kappa}w} \int_0^{\infty} \frac{e^{-\zeta - \frac{\gamma^2}{\zeta}}}{\zeta} d\zeta = \frac{q}{2\pi\lambda} e^{-\frac{v}{2\kappa}w} K_o\left(\frac{v}{2\kappa} r\right) \tag{10}$$

Consider a plate lying in the xy-plane and its thickness, b in the direction of z to be so small that the temperature may be taken to be constant over it. This is a plausible assumption using the generalized plane problem:

$$\frac{1}{b} \int_{-b/2}^{b/2} \theta(x,y,z)dz = \bar{\theta}(x,y) \tag{11}$$

Let E be the outer conductivity of the material, λ its thermal conductivity, ρ its density, and c its specific heat, then the differential equation satisfied by the temperature in the plate is found to be:

$$\frac{\partial^2\bar{\theta}}{\partial x^2} + \frac{\partial^2\bar{\theta}}{\partial y^2} - \frac{\rho c}{\lambda} \frac{\partial\bar{\theta}}{\partial t} - \frac{2E}{\lambda} (\bar{\theta} - \bar{\theta}_o) = 0 \tag{12}$$

where $\bar{\theta}_o$ is the temperature of the surrounding medium. Defining a^2, the radiation constant, as:[8]

$$a^2 = \frac{2E}{\rho cb} \tag{13}$$

The equation becomes:

$$\frac{\partial^2\bar{\theta}}{\partial x^2} + \frac{\partial^2\bar{\theta}}{\partial y^2} - a^2\bar{\theta} = 0 \qquad (14)$$

For the sake of simplicity, we will use θ instead of $\bar{\theta}$ in the rest of this thesis.

If we solve this new radiation equation using the modified Bessel function as we did before, the new solution becomes:

$$\theta - \theta_o = \frac{q}{4\pi\lambda} e^{-\frac{v}{2\kappa}w} K_o(\sqrt{a'^2/\kappa}\, r) \qquad (15)$$

where

$$\gamma^2 = \frac{a'}{4\kappa}(w^\varepsilon + y^2)$$

$$a' = a^2 + \frac{v^2}{4\kappa}$$

a^2 is defined as the radiation constant with units of 1/sec and is obtained from the formula:

$$a^2 = 2E/c\rho b$$

where

E = radiation heat from the unit surface by unit temperature difference per unit time, cal/cm^{2}sec °C

b = thickness of the plate, cm.

E can be determined experimentally from the formula[9]

$$E = \frac{w}{s} \cdot \frac{c}{\theta - \theta_o} \cdot V_c \qquad (16)$$

where

w = weight of specimen, gm

s = surface area, cm^2

θ = temperature of plate

θ_o = room temperature

V_c = cooling rate, °c/sec

By this method we can treat the heat flow in a thin sheet as a two-dimensional heat flow problem with a^2 representing a heat sink. In this case, a^2 is not constant but varies with temperature.

The problem is not purely heat loss due to radiation into the atmosphere, because copper backing plates were used in the experiment. These undoubtedly had an effect on heat dissipation. Since the problem is somewhat complicated for a precise analysis, we simply use a^2 to represent the heat sink.[17]

B. Stress Analysis

The second major aspect of the analysis of welding processes is the calculation of stresses and strains which result from temperature distributions.

Although many problems may involve only elastic effects, considerable work has been done on plastic deformation. In general, metals behave elastically up to some limiting value of stress or equivalently some limiting value of strain. For most, this behavior may be considered to be linear, that is, the stress is proportional to the strain. The constant of proportionality is the Young's modulus of the material. If the material is strained beyond the yield point, the stress increases, but at a lower rate than before. For some materials very little strain occurs, and they may be considered perfectly plastic.

If the stress is then removed, the material behaves elastically and returns to the zero stress level with a finite amount of strain. When the load is again applied, the material behaves elastically up to the maximum previous stress.

When a material has undergone plastic deformation, this deformation remains after the load has been removed. Although the phenomenon is not time dependent, the material does remember its past history. It is possible to obtain different distributions of strain for the same stress distributions if loading histories are different. As a result, stress and strain must be calculated for small increments of loading not merely for the final loading if plastic deformation occurs.

There are several different theories for predicting the yield point of a material which has first undergone plastic deformation in tension and is then loaded in compression or vice versa. They are illustrated in Figure 5. For a purely plastic material, all of these theories are equivalent. The present analysis employs the second theory in which the initial yield points are independent.

A normal stress-strain curve is obtained from a uniaxial tension test. If such tests are run at different temperatures, different curves will result. In general, both the yield strength and Young's modulus will decrease with temperature. In this way a family of curves is obtained which may be pictured as a three-dimensional surface with the third coordinate representing temperature as shown in Figure 6. This surface, however, has been constructed by considering the

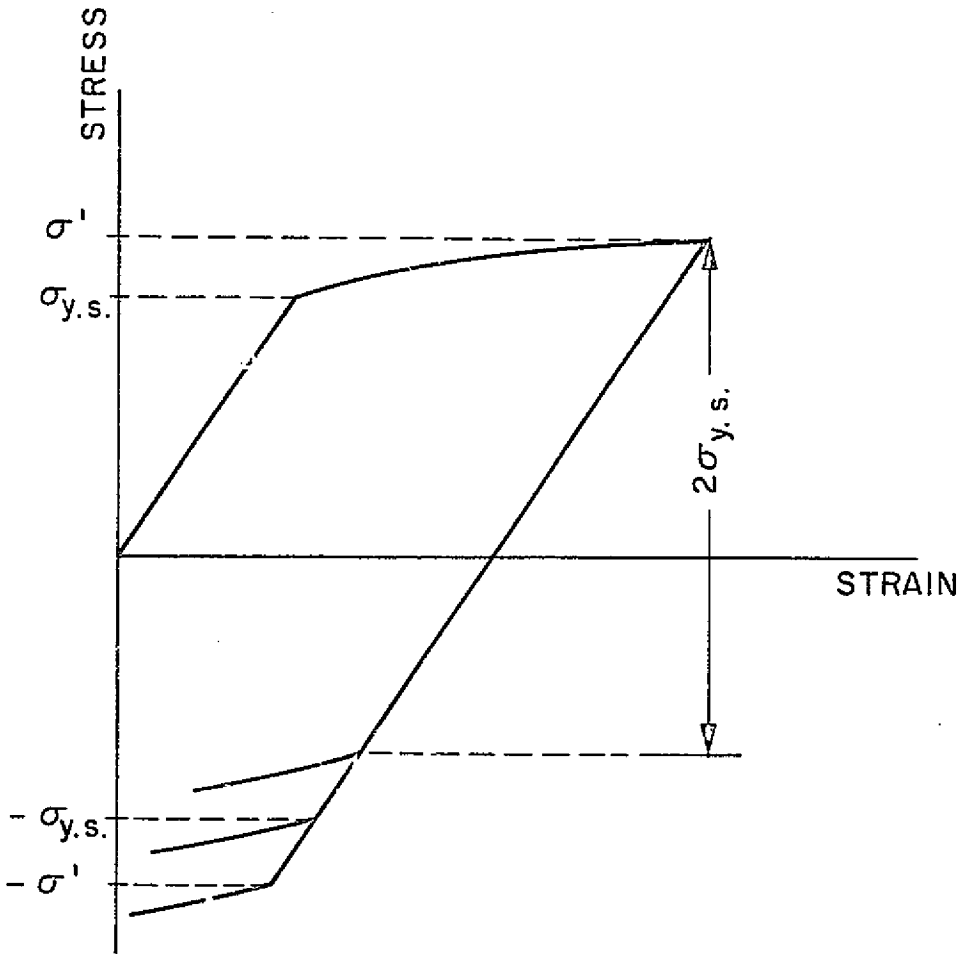

Figure 5 Theories of Reverse Yielding

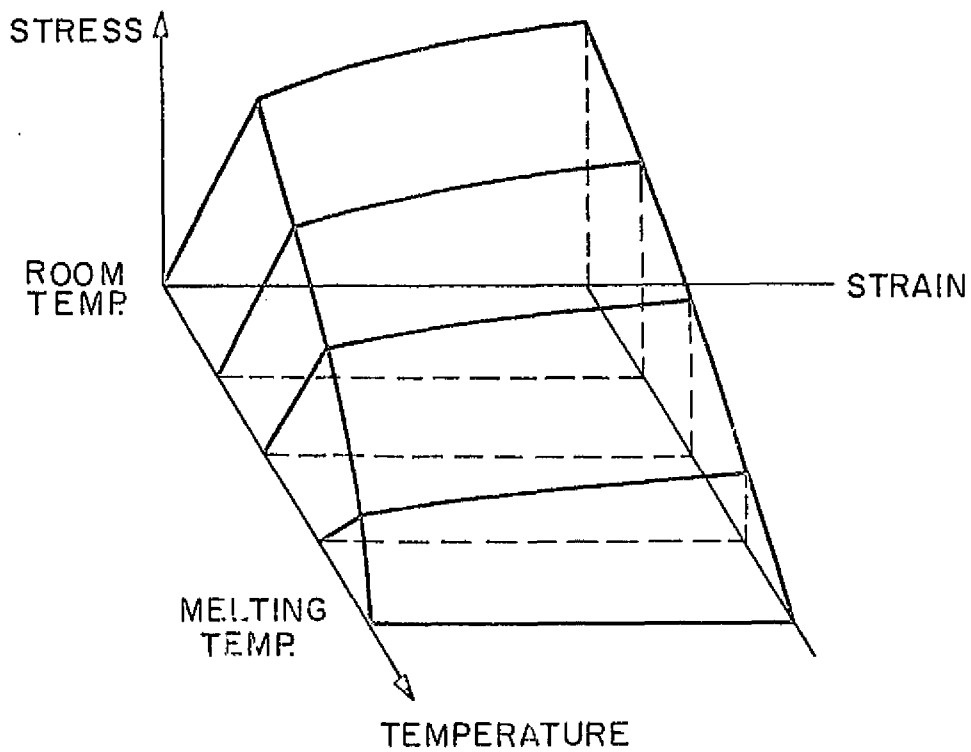

Figure 6 Stress-Strain Relationships at Various Temperatures

material behavior at a fixed temperature only, and does not really indicate how the material behaves under changing temperatures.

As has been mentioned in the section on heat flow, the two-dimensional approximation gives a fairly realistic model of the welding of thin sheet since the temperature does not vary with thickness. In this case the plane stress formulation may be used with stress and strain being considered uniform in the thickness direction, and σ_z, the stress in this direction assumed to be zero.

The equilibrium equations involve the longitudinal and transverse stresses σ_x and σ_y and the shear stress τ_{xy}, these equations are:

$$\frac{\partial \sigma_x}{\partial x} + \frac{\partial \tau_{xy}}{\partial y} = 0 \tag{17}$$

$$\frac{\partial \sigma_y}{\partial y} + \frac{\partial \tau_{xy}}{\partial x} = 0 \tag{18}$$

where there are no body forces acting on the material.

In order for the material to remain continuous, the longitudinal and transverse strains ε_x and ε_y, and the shear strain, ε_{xy}, must satisfy the relation:

$$\frac{\partial^2 \varepsilon_x}{\partial y^2} + \frac{\partial^2 \varepsilon_y}{\partial x^2} - 2 \frac{\partial^2 \varepsilon_{xy}}{\partial x \partial y} = 0 \qquad \text{compatibility equation} \tag{19}$$

The stresses and strains are related by the following:

$$\varepsilon_x = 1/E(\sigma_x - \mu\sigma_y) + \alpha T + \varepsilon_x^p + \Delta\varepsilon_x^p \tag{20}$$

$$\varepsilon_y = 1/E(\sigma_y - \mu\sigma_x) + \alpha T + \varepsilon_y^p + \Delta\varepsilon_y^p \tag{21}$$

$$\varepsilon_{xy} = 1/G \quad \tau_{xy} + \varepsilon_{xy}^p + \Delta\varepsilon_{xy}^p \tag{22}$$

where

E = Young's modulus

μ = Poisson's ratio

G = shear modulus = $E/2(1 + \mu)$

α = coefficient of linear thermal expansion

T = temperature above reference temperature

$\Delta\varepsilon_x^p$, $\Delta\varepsilon_y^p$, $\Delta\varepsilon_{xy}^p$ are the plastic strains due to the last increment of load.

ε_x^p, ε_y^p, ε_{xy}^p are the plastic strains due to previous increments of load.

The incremented plastic strains are found from the stresses using the following relations:

$$\Delta\varepsilon_x^p = \frac{\Delta\varepsilon_p}{2\sigma_e}(2\sigma_x - \sigma_y) \tag{23}$$

$$\Delta\varepsilon_y^p = \frac{\Delta\varepsilon_p}{2\sigma_e}(2\sigma_y - \sigma_x) \tag{24}$$

$$\Delta\varepsilon_{xy}^p = \frac{3}{2} \quad \frac{\Delta\varepsilon_p}{\sigma_e} \quad \tau_{xy} \tag{25}$$

where

$$\sigma_e = (\sigma_x^2 + \sigma_y^2 - \sigma_x\sigma_y + 3\tau_{xy}^2)^{1/2} \tag{26}$$

$$\Delta\varepsilon_p = 2/\sqrt{3}\ [(\Delta\varepsilon_x^p)^2 + (\Delta\varepsilon_y^p)^2 + \Delta\varepsilon_x^p\,\Delta\varepsilon_y^p + (\Delta\varepsilon_{xy}^p)^2]^{1/2} \tag{27}$$

There are several types of strains involved in this discussion. The first type is the total strains, ε_x, ε_y, etc. These strains are related to the actual displacements in the material and are the strains that are actually measured.

The thermal strain, αT, is related to the expansion that would take place if each part of the material were completely free to expand. That is, the surfaces of the material are not restrained, and the temperature distribution is such that the thermal strains satisfy the compatibility equations.

For most temperature distributions, however, the thermal strains alone do not satisfy compatibility, and additional strain is present. This is the mechanical strain or stress-producing strain. This strain has, in general, both an elastic and a plastic component and is related to stress by the stress-strain diagram and the Prandtl-Reuss relation. These stresses must satisfy the equilibrium equations and boundary conditions involving surface forces.

The problem of an infinitely long plate with width, 2c, has been solved in the following manner. Using the stress-strain relation:

$$\varepsilon_x = 1/E\ \sigma_x + \alpha T + \varepsilon_x^p \tag{28}$$

if we introduce the nondimensional quantities:

$$S = \sigma_x/\sigma_o \qquad e = \varepsilon_x/\varepsilon_o \qquad \tau = \alpha T/E_o \qquad e_p = \varepsilon_x^p/\varepsilon_o$$

$$\eta = y/c \qquad H = E/E_o \tag{29}$$

where σ_o is the yield stress at some reference temperature, ε_o, and, E_o is the Young's modulus at that temperature, the

stress-strain relation becomes:

$$e_x = S/H + \tau + e_p \tag{30}$$

The integrals for the net force and the moments become

$$\int_{-1}^{1} S \cdot dy = 0 \tag{31}$$

$$\int_{-1}^{1} S \cdot y \cdot dy = 0 \tag{32}$$

If we consider an infinitely long plate containing a bead-on-plate weld, the magnitude of the stresses are as follows:

$$\frac{\partial \sigma_x}{\partial x} << \frac{\partial \sigma_x}{\partial y} \tag{33}$$

$$\frac{\partial \sigma_y}{\partial x} << \frac{\partial \sigma_y}{\partial y} \tag{34}$$

$$\frac{\partial \tau_{xy}}{\partial x} << \frac{\partial \tau_{xy}}{\partial y} \tag{35}$$

Therefore, we can assume

$$\sigma_x = f(y) \tag{36}$$

and from the equilibrium condition

$$\frac{\partial \sigma_x}{\sigma x} = 0 \qquad \tau_{xy} = \sigma_y = 0 \tag{37}$$

Then

$$\frac{\partial^2 \epsilon_x}{\partial y^2} = 0 \tag{38}$$

This is considered the one-dimensional analysis of welding. The theory is not applicable in the region near the welding

arc, however, it can be used as an approximation for a stress field in which

$$\frac{\partial \sigma_x}{\partial x} << \frac{\partial \sigma_x}{\partial y} \tag{39}$$

This analysis was developed by Tall and was the forerunner of the original research program at Battelle Memorial Institute.[10]

As previously stated, the compatibility equation[3] reduces to

$$\frac{\partial^2 e_x}{\partial y^2} = 0$$

which implies that the strain distribution is linear. That is: $e_x = a + by$ (40)

When the linear form of the strain is substituted into the integral equations using the stress-strain relation, the resulting equations may be solved for the unknown coefficients a and b.

In this way, the final expression for the total strain is obtained as:

$$e_x = (A_1 - A_2\eta)\left[\int_{-1}^{1} H(T + e_p)d\eta\right] - (A_2 - A_3\eta)\left[\int_{-1}^{1} H(T + e_p)\eta d\eta\right] \tag{41}$$

where

$$A_i = \frac{\int_{-1}^{1} H\eta^2 d\eta}{\int_{-1}^{1} Hd\eta \int_{-1}^{1} H\eta^2 d\eta - \left(\int_{-1}^{1} H\eta d\eta\right)^2} \tag{42}$$

$$A_2 = \frac{\int_{-1}^{1} H\eta d\eta}{\int_{-1}^{1} Hd\eta \int_{-1}^{1} H\eta^2 d\eta - \left(\int_{-1}^{1} H\eta d\eta\right)^2} \tag{43}$$

$$A_3 = \frac{\int_{-1}^{1} Hd\eta}{\int_{-1}^{1} Hd\eta \int_{-1}^{1} H\eta^2 d\eta - \left(\int_{-1}^{1} H\eta d\eta\right)^2} \tag{44}$$

The nondimensional thermal strain, τ, and the variation of the nondimensional Young's modulus, H, are calculated from the temperature distribution, T. Since the plastic strain, E_p, is not known, the strain cannot be calculated directly; however, an initial approximation to the total strain can be obtained by assuming that the plastic strain is zero. The mechanical strain is then calculated from the expression

$$e_n = e_x - \tau \tag{45}$$

This mechanical strain may be used to obtain a first approximation to the plastic strain using the stress-strain curve as shown in Figure 7.

C. Stress Calculation

At this point it would perhaps, be helpful to understand exactly how the computer uses the stress-strain calculations to produce results.

The time units and corresponding temperature are inputted into the program and may come from the analytic

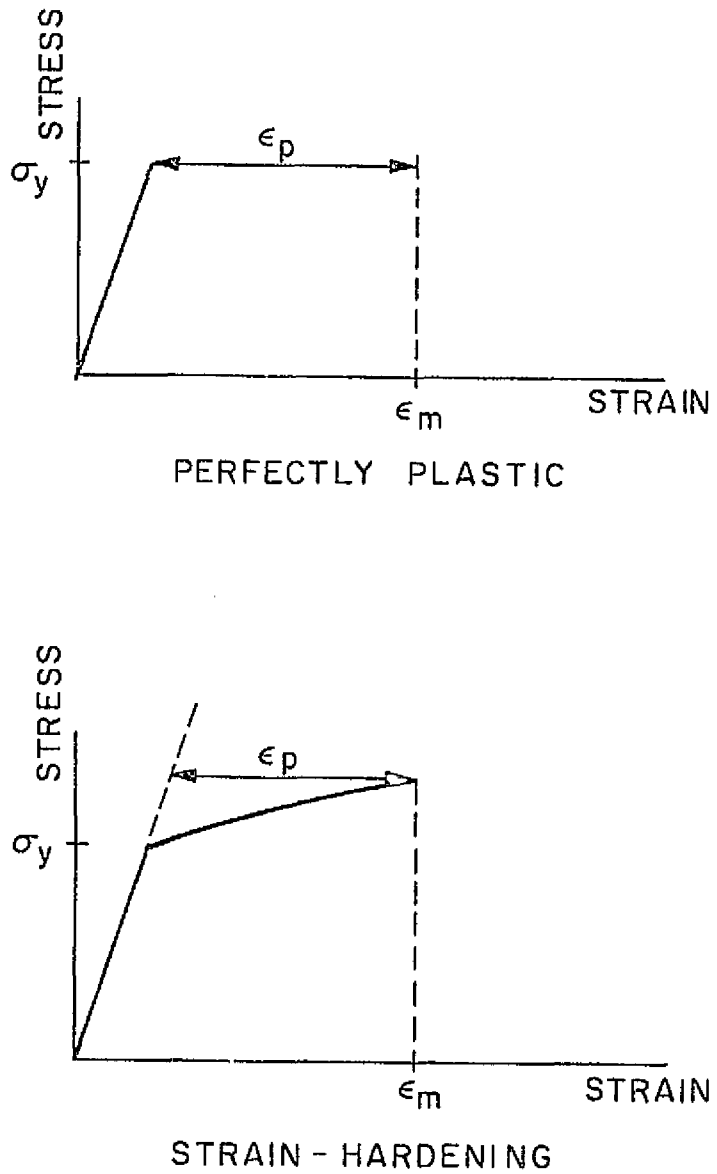

Figure 7 Obtaining Plastic Strain from Stress-Strain Curve

temperature program or experimental data. The time at which the arc reaches the gages is also read in. The material properties used include Young's modulus, E, the initial yield stress, σ_y, the coefficient of linear thermal expansion, α, and a strain-hardening parameter, m.

The program performs calculations at several nondimensional transverse positions. These positions range from the weld center line to the edge of the plate with finer divisions nearer the center line.

In the expression for total strain, ε_x, the integrals are taken across the entire plate, however, the program uses values across only half the plate. The resulting expression for total strain ahead of the weld is given by:

$$\varepsilon_x = (A_1 - A_3\eta) \int_0^1 H(T+\varepsilon_p)d\eta + (A_4\eta - A_2) \int_0^1 H(T+\varepsilon_p)\left(\frac{\eta-1}{2}\right)dy \quad (46)$$

where

$$A_1 = \frac{\int_0^1 H\eta(\eta - t)d\eta}{D} \quad (47)$$

$$A_2 = \frac{\int_0^1 H\eta d\eta}{D} \quad (48)$$

$$A_3 = \frac{\int_0^1 H(\eta - 1/2)d\eta}{D} \quad (49)$$

$$A_4 = \frac{\int_0^1 Hd\eta}{D} \quad (50)$$

where

$$D = \int_0^1 Hd\eta \int_0^1 H\eta(\eta-1/2)d\eta - \int_0^1 H\eta d\eta \int_0^1 H(\eta-1/2)d\eta \quad (51)$$

Behind the weld the total strain is given by the simpler expression:

$$\varepsilon_x = A \int_0^1 H(T + \varepsilon_p)d\eta \tag{52}$$

where

$$A = \frac{1}{\int_0^1 H d\eta} \tag{53}$$

In the program these integrals are evaluated using Simpson's Rule.

At the start of the calculation, the material is assumed to be free of any plastic strain. The plastic strain is accumulated during successive iterations until reverse yielding occurs.

At each time step the plastic strain is calculated using the mechanical strain component only of the total measured amount. Figure 8 illustrates several possible situations of elastic and plastic strains as well as reverse yielding. For clarity the curves are shown as being independent of temperature but the actual calculation takes such changes into account.

Each value of plastic strain calculated is compared with the previous one until either subsequent values agree within one percent or the program has performed twenty iterations and ceases.

If convergence is obtained, the stress for each point is calculated and printed out along with total, mechanical,

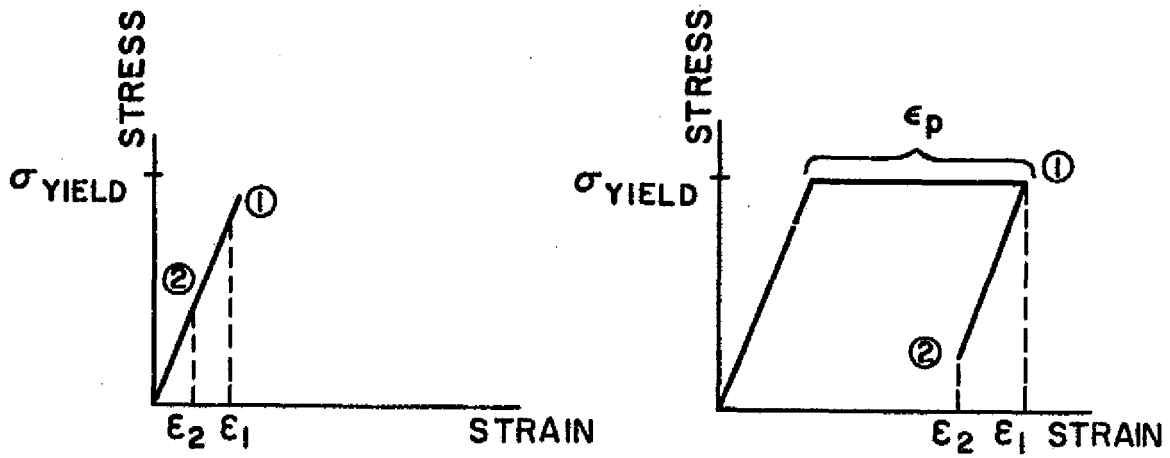

a) Elastic Loading and Unloading

b) Plastic Loading--
Elastic Unloading

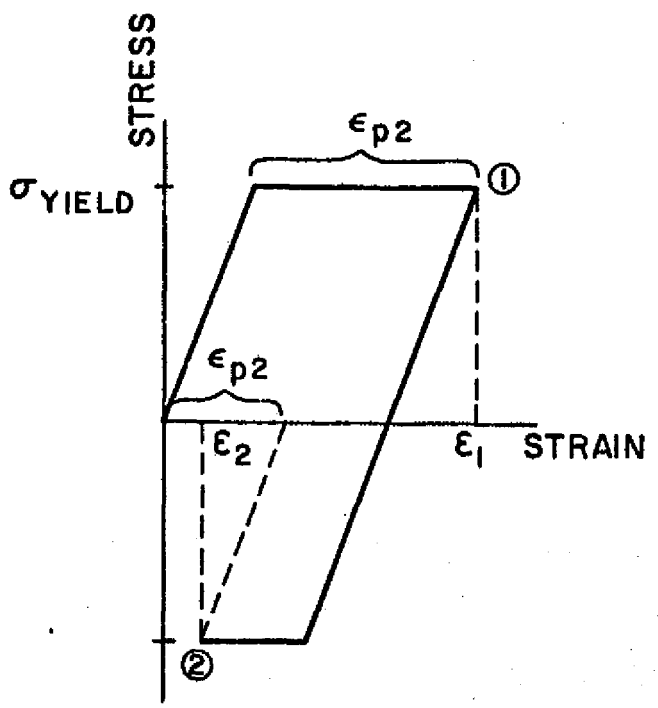

c) Plastic Loading--Reverse Yielding

Figure 8 Loading and Unloading

and plastic strains. When the last time step is completed, the calculation is repeated at all points at the reference temperature (0° F). This gives the residual stress distribution.

Two-dimensional Program. The current two-dimensional program considers the average stress over an entire block in a preset grid. As the arc is moved closer to that particular grid block, the stress is calculated. The grid shape has a finer spacing nearer the weld to give more precise values in the area of greatest interest. One major disadvantage of a finite element program is the cost-effective decision necessary for determining the fineness of the grid. Obviously, for best results the grid should be made as small as possible. This is, unfortunately, not possible where money for running programs is limited; therefore some compromise must be made.

First, the temperature distribution around the moving arc is calculated. Then the stress field is divided into a set of similar blocks of width, h_o, shown in Figure 9. The time intervals represented by the block width must be short enough so that the temperature and thermal stress for each increment may be regarded as being constant. Since the greatest changes in temperature occur near the arc, narrow strips are used in areas near the arc.

The calculation starts on a block some distance ahead of the welding arc where the temperature change is negligible,

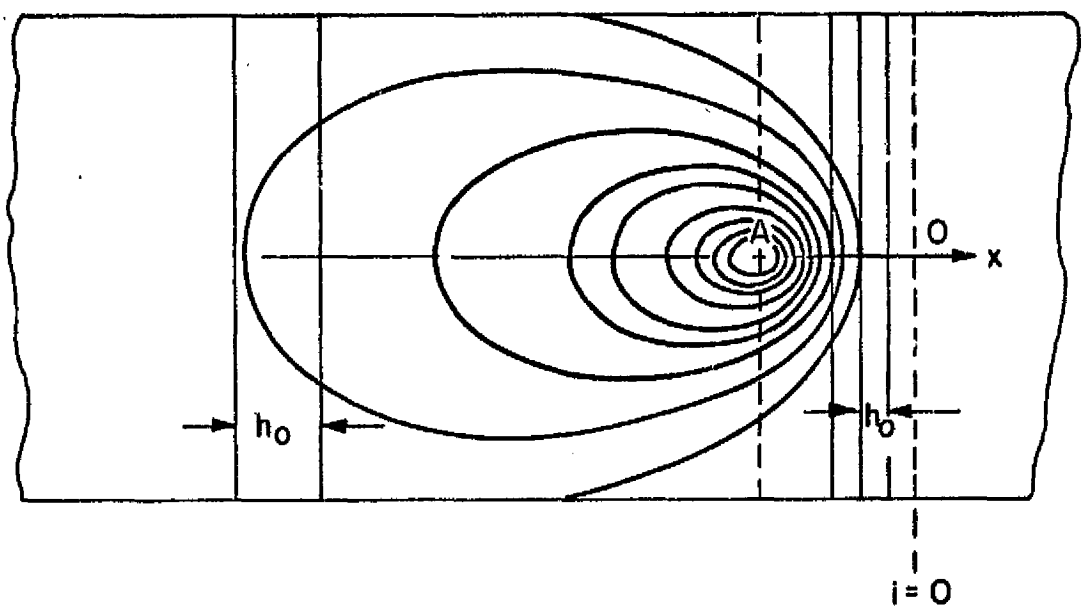

Figure 9 Computer Division of Specimens

and the stresses are purely elastic. Time zero is fixed on the block.

First stresses in the block crossing the origin, O, are calculated based on elasticity theory. Then stresses in the second block are calculated by adding stresses, due to the temperature increment. In this case, analysis is made whether or not any plastic deformation takes place. It is assumed that the amount of stresses at a given point does not exceed the yield stress of the material at the temperature of that point. Similar analyses are conducted step by step on the following blocks. Thus the stress distribution in the entire field is determined.[11]

D. Thermal Buckling

Buckling type distortion of welded plate can be classified into the following two types. First is the buckling of the whole plate after welding has been completed. The second is local buckling near the arc during welding.

In practice we clamp the plate to avoid buckling. Therefore, in most applications the first type is the problem. The plate does not buckle while it is clamped, but when it is released. This phenomenon has been studied by both Masubuchi and Watanabe and Satoh.[16] No work has been done on the second type, because it requires complicated analysis.

In the experiments conducted in this study, buckling of the entire plate was not observed, probably because the small weld produced by the gas tungsten arc process did not produce

enough residual compressive stresses. Local buckling was observed. Figure 10 illustrates its appearance.

The complete analysis of local buckling is very complicated. The ideal solution would be to develop a simple model to determine the critical free distance, that is, the distance between the clamps. Only a simple introduction is developed here.

In welding of a thin plate, buckling may occur due to compressive thermal stresses during cooling. Compressive thermal stress is considered to be caused by inherent shrinkage due to welding. As a result, the critical inherent shrinkage of buckling is obtained by assuming that compressive thermal stress is equivalent to stress in the plate produced by concentrated compressive forces, $P = Eh(\varepsilon_1)$, acting at both ends of the weld line.

Where

E = Young's Modulus

h = plate thickness (cm)

ε_1 = inherent shrinkage (cm)

When the value of P_{cr} (critical) is reached, buckling occurs. Stresses can be obtained using the theory of elasticity. For an aspect ratio (length/width) less than or equal to 2, the equation is given by:

σ_x (at the reference points) =

$$\frac{P}{Eh}\left[1 + 4 \sum_{n=2,4,6}^{\infty} (-1)^{n/2} (n\pi\mu + 1)e^{-n\pi\mu}\right] \qquad (54)$$

where $\mu = L/B$.

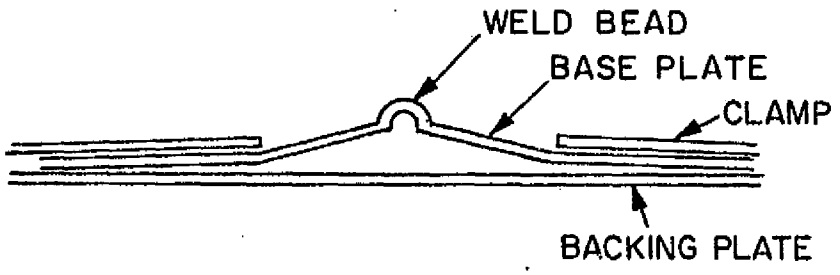

Figure 10 Buckling Appearance after Welding

The formula for inherent shrinkage is:

$$(\varepsilon_1)_{cr} = \frac{P_{cr}}{Eh} \frac{k\pi^2 h^2}{12(1 - \nu^2)B} \tag{55}$$

where

ν = Poisson's ratio

k = numerical factor dependent upon the aspect ratio L/B.

k is approximately represented by:

$$k = 11 + 50(B/L)^2 \tag{56}$$

and is independent of material.

It is considered that a plate will buckle in the longitudinal direction when the magnitude of ε_1 exceeds the critical value determined by the previous equation. Watanabe and Satoh analyzed the relationship between inherent shrinkage and welding conditions in carbon steel. They found the formula to be:

$$(\varepsilon_1) = 0.136 \times 10^{-6}\left(\frac{I}{h\sqrt{v}}\right)^2 \tag{57}$$

where

I = welding current (A)

v = arc travel speed (cm/sec)

Extensive experimental evidence is necessary to determine a similar formula for other materials.

Consider a long strip of width 2a, length, L, and welded along the center line. (see Figure 11) The following assumptions are made regarding residual stress components:

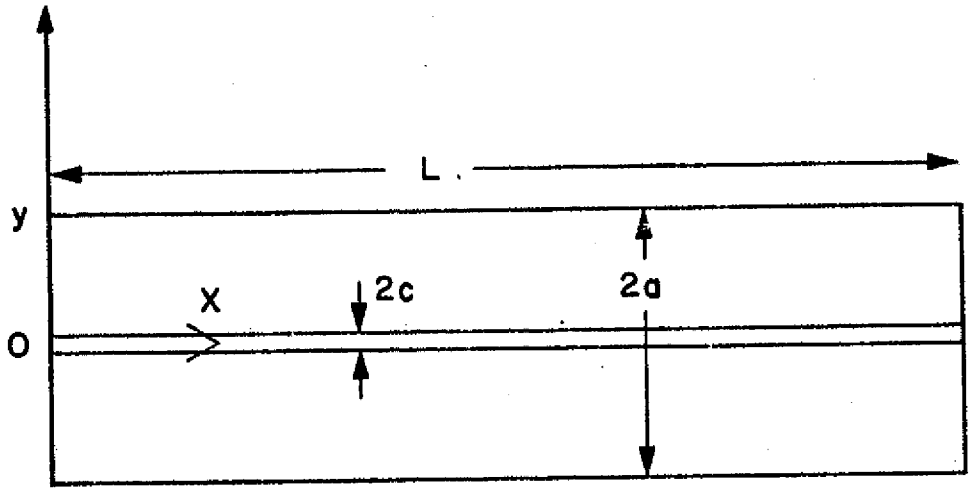

Figure 11 Schematic of Specimen

$$\text{longitudinal stress, } \sigma_x = \begin{cases} -\sigma' & |y| > c \\ \sigma'' & 0 < |y| < c \end{cases} \tag{58}$$

$$\text{transverse, } \sigma_y = 0 \tag{59}$$

$$\text{shear, } \tau_{xy} = 0 \tag{60}$$

Since the residual stress must be symmetric:

$$\int_0^a \sigma_x dy = 0 \tag{61}$$

and

$$\sigma' = \frac{c}{a - c} \sigma'' \tag{62}$$

If we denote the deformation in the z-direction as w, the equation of equilibrium is:

$$D = \left(\frac{\partial^4 w}{\partial x^4} + 2\frac{\partial^4 w}{\partial x^2 \partial y^2} + \frac{\partial^4 w}{\partial y^4}\right) = T_x \frac{\partial^2 w}{\partial x^2} \tag{63}$$

where

$$D = \text{rigidity of the plate} = \frac{Eh^3}{12(1 - \nu^2)} \tag{64}$$

also called bending stiffness.

$$T_x = \sigma_x h$$

For boundary conditions, it was assumed that the plate is simply supported at both ends, $x = 0, L$ and that the plate is free along $y = \pm A$.

If we consider a plate symmetrically heated and supported on rigid edge members, the most important temperature parameters are the average temperature rise of the plate over that of the edge member, and the nonuniformity parameter representing

the difference between the maximum and minimum temperature rise.

A temperature distribution of the form

$$T_{(y)} = T_o - \Delta T\left(\frac{y}{b}\right) \tag{65}$$

is chosen to represent the tent-like distribution obtained in welding.

The boundary conditions for a clamped edge determine both deflection and slope normal to the boundary to be zero:

$$\omega = 0 \qquad \frac{\partial \omega}{\partial n} \equiv \frac{\partial \omega}{\partial x} \cos \alpha + \frac{\partial \omega}{\partial y} \sin \alpha = 0 \tag{66}$$

where α is the angle between the normal, n, and the direction of x. (See Figure 12.)

Thus, the bending moments m_x, and m_y, and the twisting moment m_{xy} are given by:

$$m_x = m_y - (1 + \nu) D \alpha M_\theta \tag{67}$$

$$m_{xy} = 0 \tag{68}$$

where

$$m_\theta = \frac{12}{h^3} \int_{-\frac{h}{2}}^{+\frac{h}{2}} \theta z dz \qquad \text{temperature moment} \tag{69}$$

In most pure buckling problems $m_\theta = 0$. Hence, also

$$\sigma_{xx} = \frac{n_x}{h} + \frac{E\alpha}{1 - \nu} (n_\theta - \theta) \tag{70}$$

$$\sigma_{yy} = \frac{n_y}{h} + \frac{E\alpha}{1 - \nu} (n_\theta - \theta) \tag{71}$$

$$\sigma_{xy} = \frac{n_{xy}}{h} \tag{72}$$

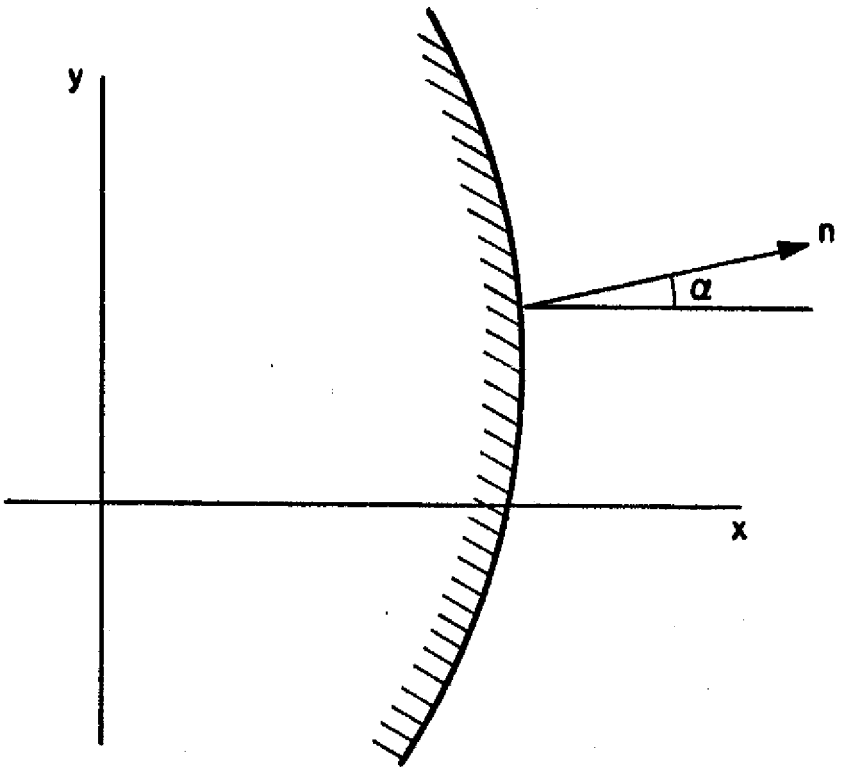

Figure 12 Boundary Conditions for Clamped Edge

where

$$n_\theta = \frac{1}{h}\int_{-h/2}^{+h/2} \theta\,dz \qquad \text{Mean temperature} \tag{73}$$

θ = temperature distribution

ε_{xx}^o, ε_{yy}^o, ε_{xy}^o = strain components in the midplane

$$n_x = D[\varepsilon_{xx}^o + \nu\varepsilon_{yy}^o - (1 + \nu)\alpha n_\theta] \tag{74}$$

$$n_y = D[\varepsilon_{yy}^o + \nu\varepsilon_{xx}^o - (1 + \nu)\alpha n_o] \tag{75}$$

$$n_{xy} = n_{yx} = \frac{1 - \nu}{2} D\varepsilon_{xy}^o \tag{76}$$

If the plate is held fixed along its entire edge

$$\varepsilon_{xx}^o = \varepsilon_{yy}^o = \varepsilon_{xy}^o = 0 \tag{77}$$

$$n_x = n_y = -(1 + \nu)\alpha k n_\theta \tag{78}$$

$$n_{xy} = 0 \tag{79}$$

where

$$k = \frac{Eh}{1 - \nu^2} \qquad \text{stretching stiffness} \tag{80}$$

Since in thermal buckling problems in contrast to ordinary buckling problems, the membrane forces n_x, n_y, and n_{xy} are not constants, but functions of x, y--expecially in this case of the tent-like temperature distribution--it is, in general, not possible to find exact solutions. The added burden of the clamped boundary conditions puts this problem well into the realm of a doctorate thesis by itself and,

subsequently will not be attempted here. There is, unfortunately, no reference available today which even attempts to solve this problem. Parts, however, can be found in Parkus, Johns, Timoshenko, Nowacki, Cox.[12,13,14,15,16]

III PROCEDURES

A. Strain Measurement

Thermal strains in welding are measured frequently by the use of electrical resistance strain gages. These operate on the principle that certain conductors exhibit a change in electrical resistance with a change in strain. Gages are mounted on the test specimens and the resistance variation across the gage is measured as welding progresses. In the case of thermal strains in welding, the observed resistance change, ΔR, consists of:

$$\Delta R = \Delta R_1(\varepsilon_e) + \Delta R_2(\varepsilon_p) + \Delta R_3(\alpha T) + \Delta R_4(T)$$

where

$\Delta R_1(\varepsilon_e)$ = the resistance change corresponding to elastic mechanical strain, ε_e.

$\Delta R_2(\varepsilon_p)$ = the resistance change corresponding to plastic mechanical strain, ε_p.

$\Delta R_3(\alpha T)$ = the resistance change corresponding to temperature induced thermal strain, αT.

$\Delta R_4(T)$ = the resistance change caused by thermo-electric effects in the gage itself.

It is not possible to separate strain into its elastic and plastic components, but $\Delta R_3(\alpha T)$ and $\Delta R_4(T)$ can be subtracted by either calculation or experiment. This so-called "apparent strain" may be measured by heating a mounted strain gage in an oven and obtaining a plot of apparent strain versus temperature.

A schematic diagram of the experimental set-up is shown in Figure 13. One strain gage and thermocouple was cut out from each of the original tantalum and niobium sheets to which a weld bead had been applied. The pieces cut out were approximately two inches by three inches in size so that the strain recorded by each of the gages would have a negligible mechanical component. The pieces of tantalum and niobium with their respective gages, along with a third unmounted strain gage and thermocouple were then placed into a furnace. As the temperature in the furnace was raised from room temperature to 1000°F, strain change (resistance change) of each of the electric-resistance strain gages was measured via a wheatstone bridge set up. The induced EMF created by the temperature gradient between the thermocouples in the furnace and a 32° F reference bath was also measured, from which temperature was determined.

The data plotted as temperature versus strain is shown in Figure 14.

B. Apparatus and Procedure

1. Test specimens. Plate dimensions and gage locations are shown in Figure 15. The arrangement of constraining clamps is shown in Figure 16. The room temperature material properties of the test plates are found in Table 1.

2. Strain gages and thermocouples. The gages used in this investigation were type HT-1212-5B, manufactured by BLH Electronics, Waltham, Massachusetts. These are high temperature, free-filament gages which include a thermocouple as an

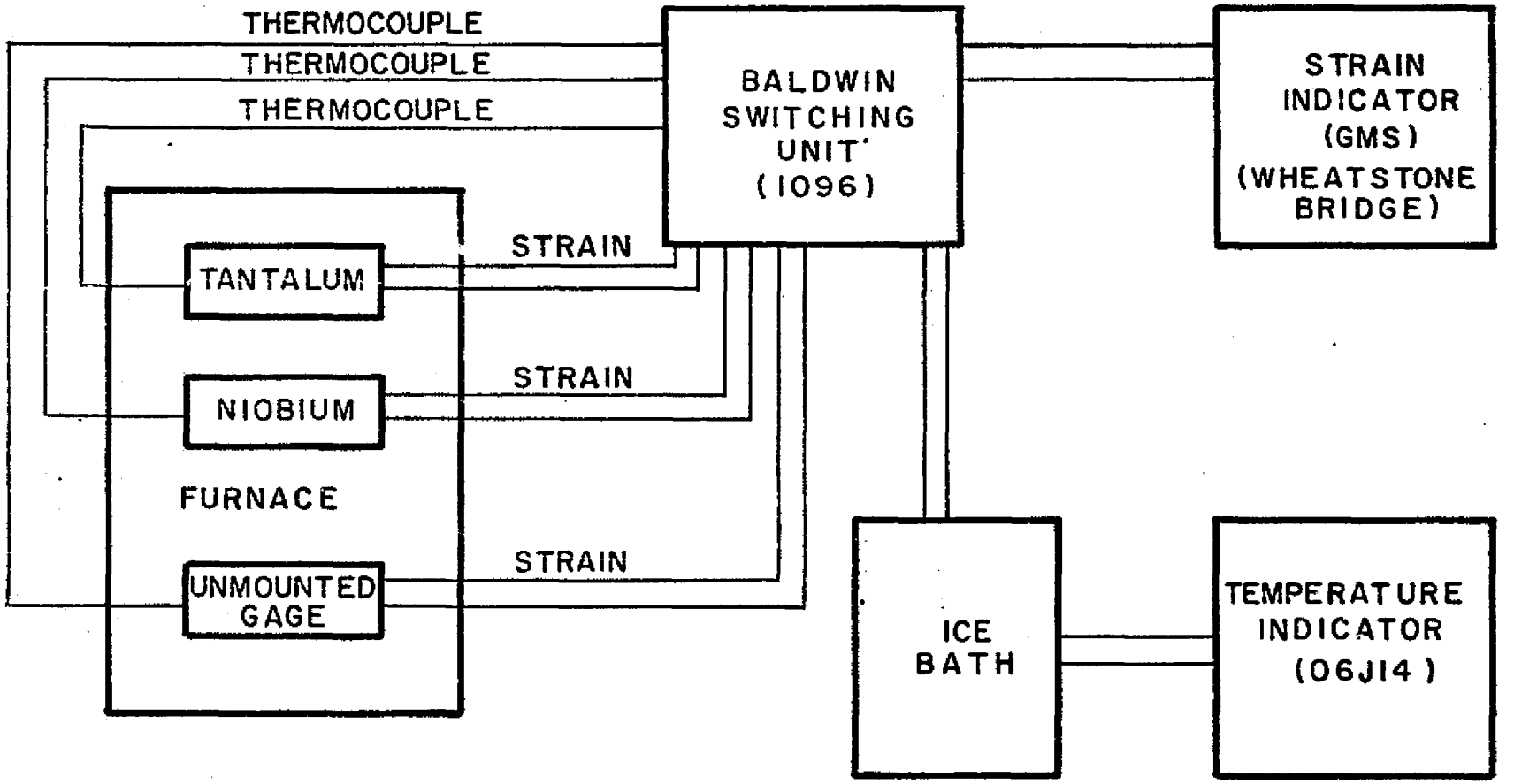

Figure 13 Schematic of Experimental Wheatstone Bridge

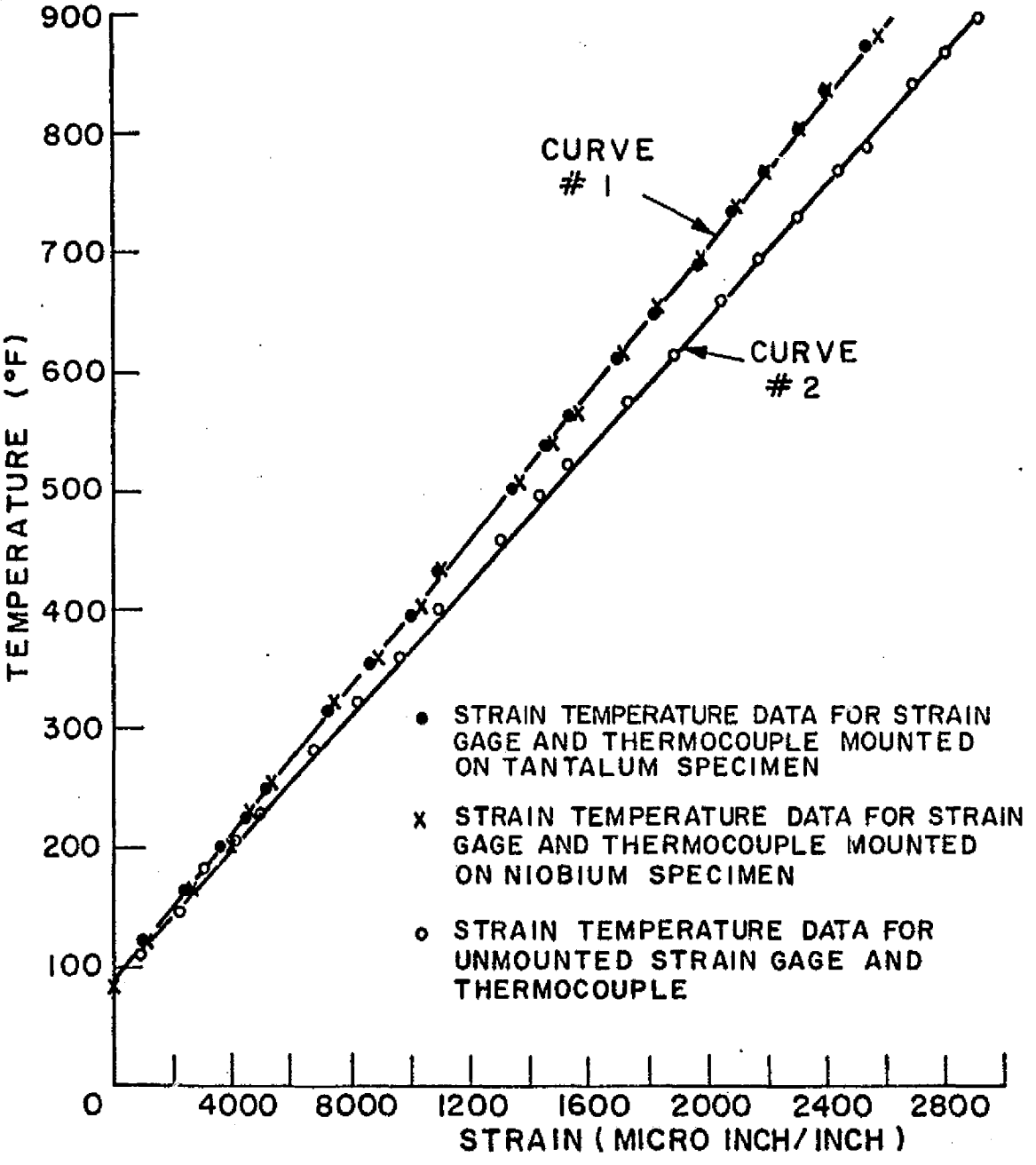

Figure 14 Temperature vs Strain Curve for Thermocouple

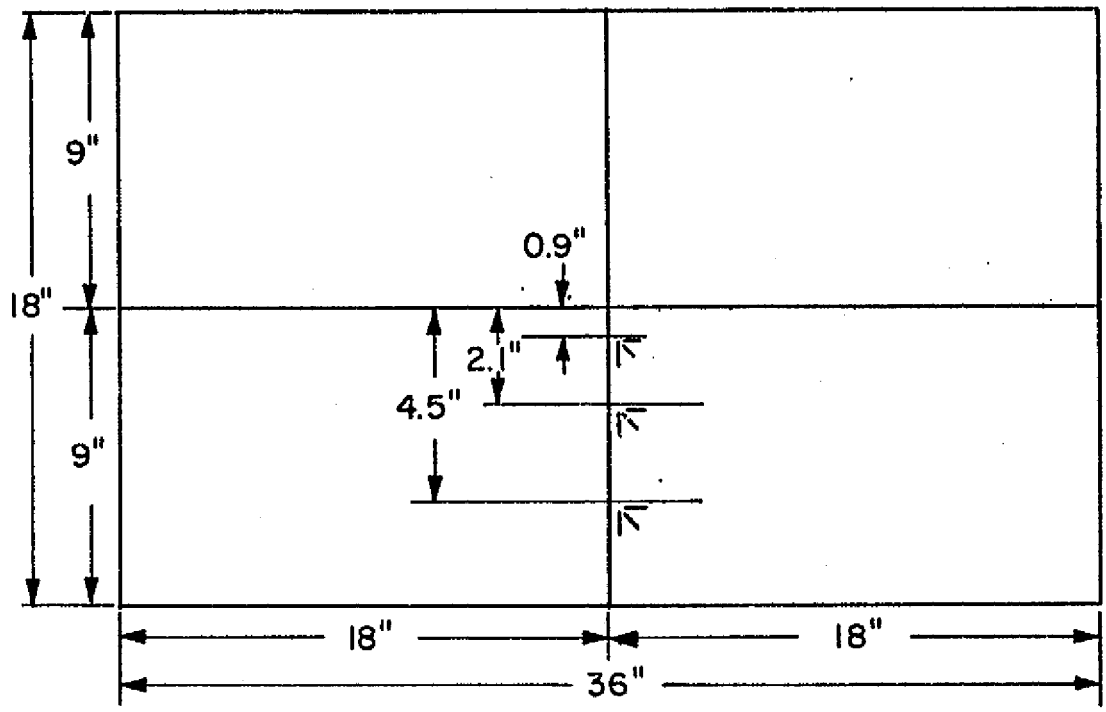

Figure 15 Specimen Dimensions

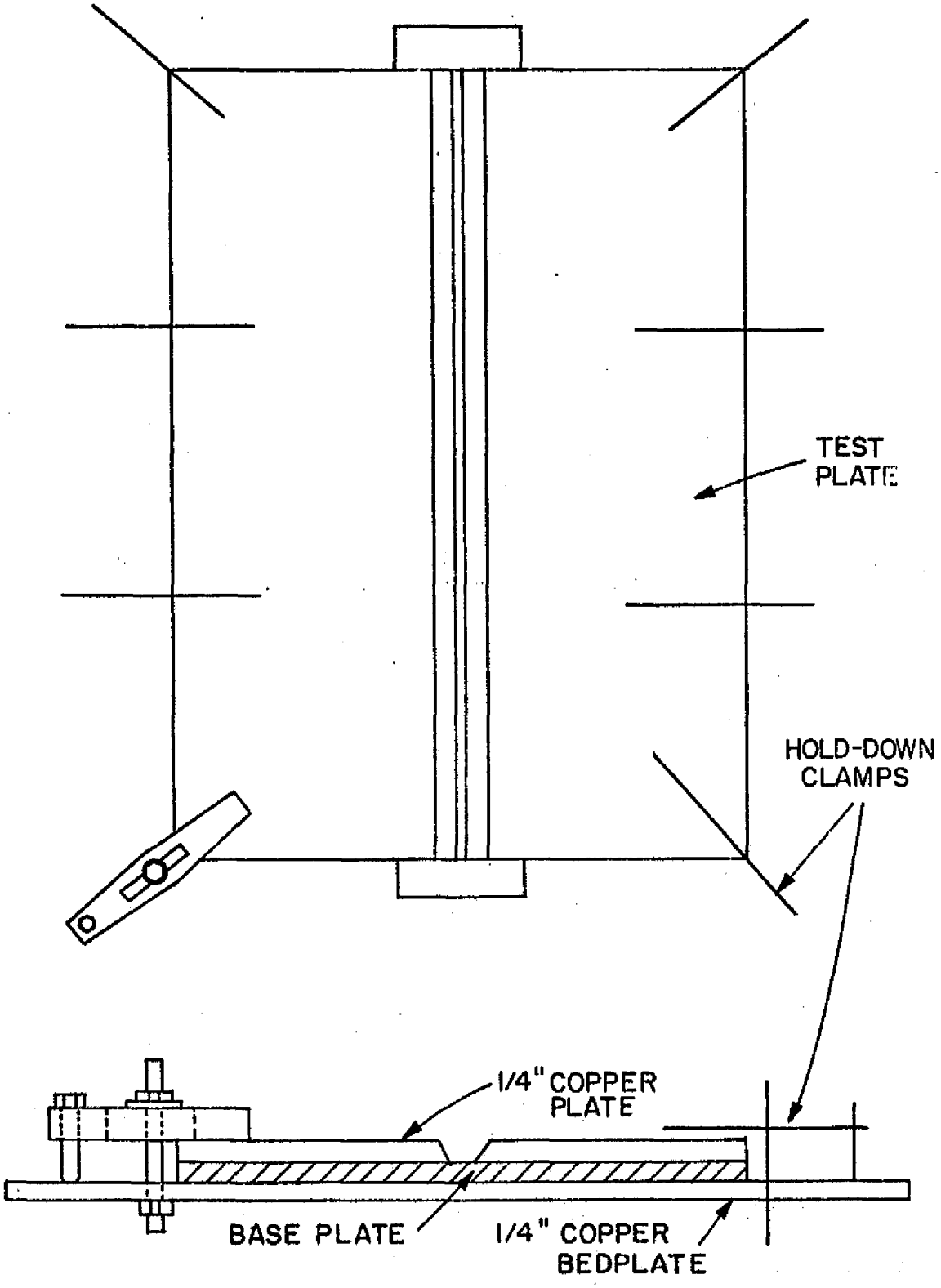

Figure 16 Clamp Arrangement

TABLE 1

Material	Tensile Strength psi	0.2% Yield Strength psi	Young's Modulus psi	Coefficient of Linear Thermal Expansion per °C	Density g/cm^3	Thermal Conductivity $cal/sec/cm^2/oc/cm$	Specific Heat cal/gm °C
Tantalum	55,000	-	27×10^6	6.5×10^{-6}	16.6	0.13	0.034
Columbium	85,000	32,000	22.7×10^6	7.06×10^{-6}	8.57	0.13	0.067

integral part of the mechanism. Gage properties are:

Designation	HT-1212-5B
Gird Length	5/16 inch
Grid Width	3/32 inch
Temperature Range	-320° to +1200° F
Resistance	120 ohms
Gage Factor	4.11 ±1%
Cement	Rokide--BLH

3. Instrumentation. Strain gages were connected into a potentiometric circuit (half-Wheatstone bridge) and calibrated as indicated in Figure 17. Figure 18 shows the calibration circuit of the thermocouples which were referenced to a 32° F ice bath. Both circuits were fed into a Honeywell continuous recording 12-channel Visicorder. Temperature and strain were recorded simultaneously at the gage location. Weld passes were timed by means of an electric stop watch as well as a timer integral to the chart recorder.

C. Welding Equipment and Conditions

The power source used was an ac-dc Heliwelder (manual GTA) manufactured by the Air Reduction Company. The torch from this machine was wired to an automatic beam and carriage electronic governor manufactured by the Linde Division of Union Carbide Corporation. This was done to insure constant travel speed which could not be guaranteed using only the manual apparatus. The travel speed, arc voltage, and amperage

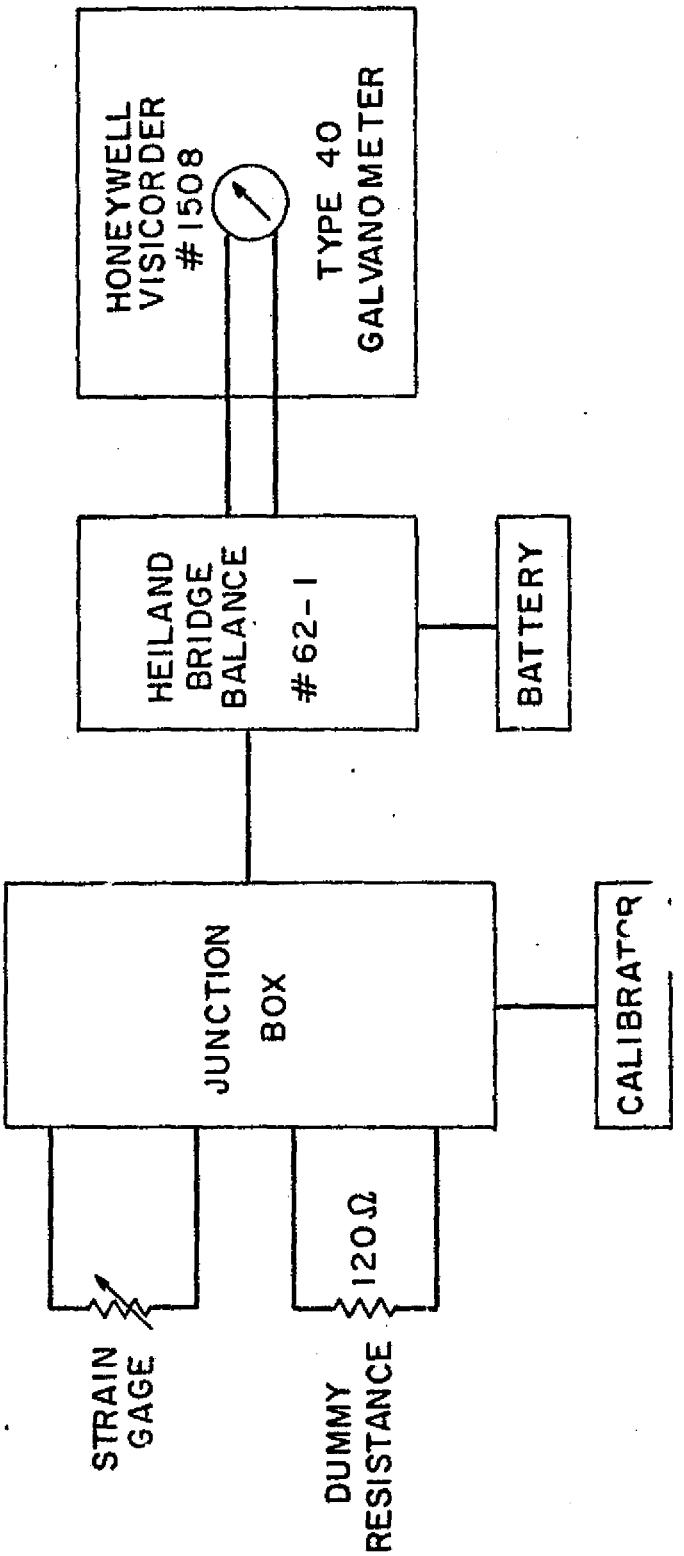

Figure 17 Strain Gage Circuit

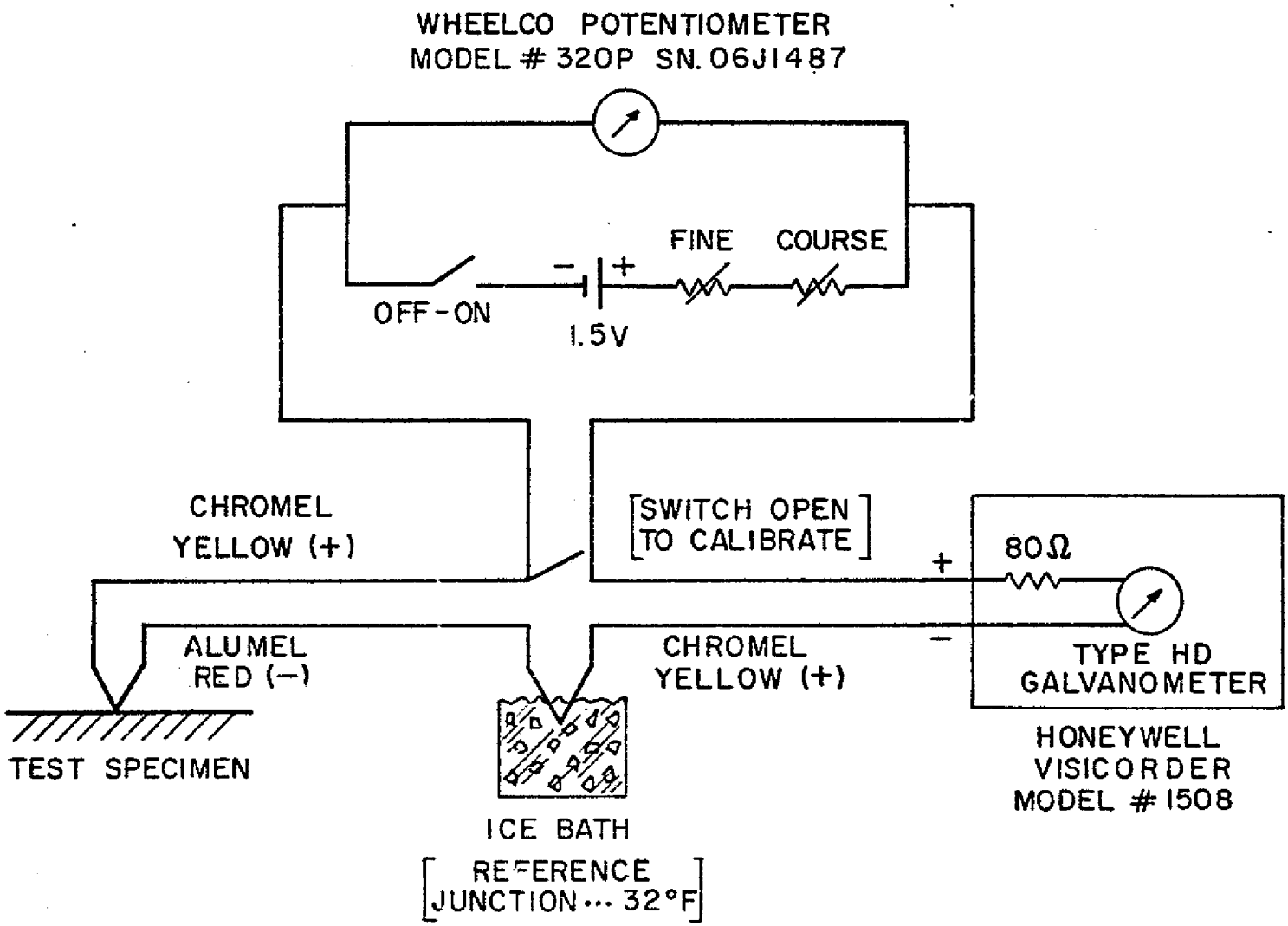

Figure 19 Thermocouple Circuit

were preset before each pass. Arc length was adjustable during the weld.

D. Experimental Procedures

The experimental operation is shown schematically in Figure 19. The test plate, instrumented at BLH, was clamped between copper plates to insure no buckling during the welding process. Welding speed was preset at 8 ipm, arc voltage at 10, and amperage at 40. The visicorder was actuated and the arc was struck. As the welding torch began to move down the plate, the arc length was adjusted and the timer started. The recorder output was marked when the arc passed the strain gage location. When the welding head reached the end of the plate the arc was extinguished and the plate allowed to cool. The recorder continued to monitor the gages for approximately three minutes until conditions appeared stable. Periodical readings were taken until the sheet cooled to room temperature. The clamps were then released while the recorder was still monitoring.

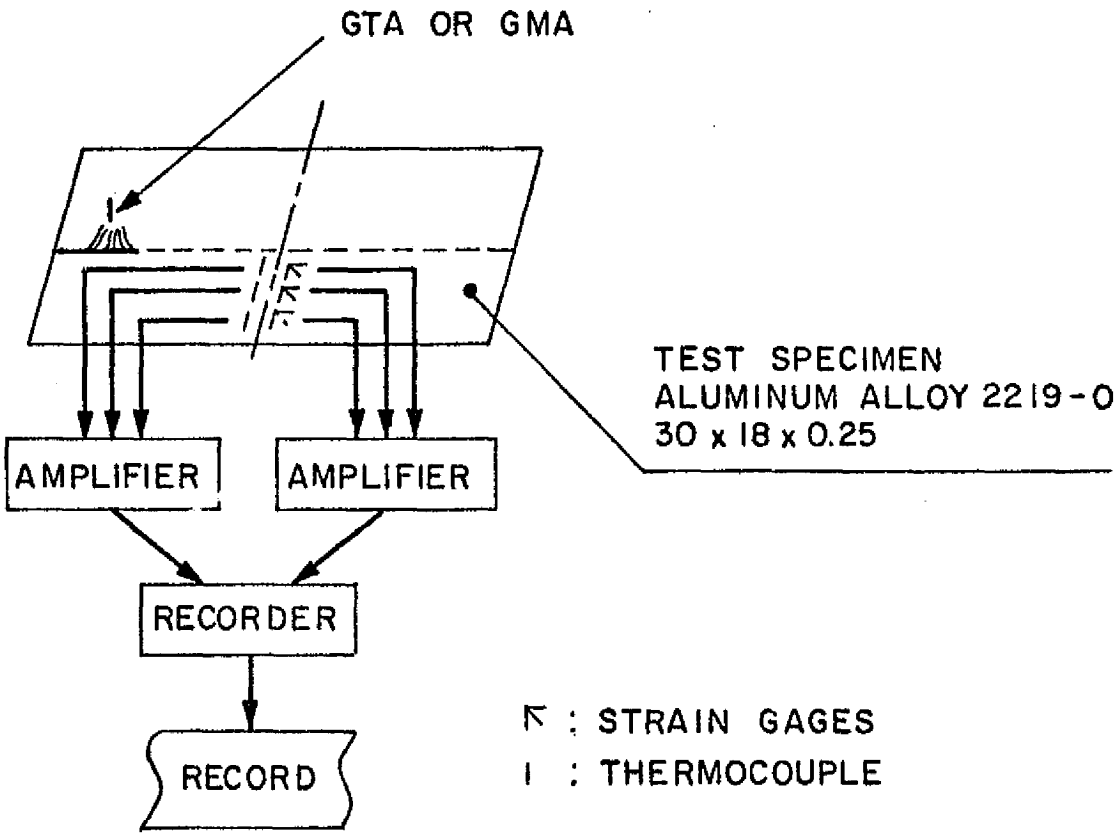

Figure 19 Schematic of Apparatus and Procedure

IV EXPERIMENTAL RESULTS

The results of this investigation consist of mechanical strain data recorded during the welding of test specimens. The data is presented below in the form of plots of mechanical strain versus time and temperature versus time. For comparison purposes, each experimental strain curve is preceded by theoretical strain curves obtained from the NASA one-dimensional and two-dimensional computer programs. Only longitudinal strains are plotted from the two-dimensional program due to the fact that the transverse strains are of a significantly smaller magnitude.

The horizontal axis of all graphs is a scale of time measured in seconds. Zero time is arbitrary, occurring some time after the arc has stabilized and is moving down the plate toward the gage location. The point at which the arc passes this location is indicated on the graph. The limiting time on the scales merely represents a time by which the plates had reached steady conditions.

The vertical scale of the first two graphs is temperature in degrees Fahrenheit measured from the thermocouples on the samples. The subsequent graphs are calibrated in μ in/in strain on the vertical axis. Positive values indicate tensile strain and negative values indicate compressive strain.

A. Discussion and Analysis--General

The weld appearance showed the presence of a white powder which was thought to be an oxide of the base plate.

When the plate was forcibly bowed after the clamps were removed, the weld area demonstrated severe brittleness and cracked in many places. The weld itself was not as continuous as it might have been due to the difficulty in maintaining a constant arc length. Several times during welding the arc extinguished but this is thought to have only minor effect.

Local buckling was observed in the weld region but no attempt was made to measure the amount. This would have been impossible in this experiment due to the presence of longitudinal oxide-induced cracks along the crown of the weld bead which would prevent any precise measurement of deformation.

A major purpose of this thesis was to compare experimental results on thin sheet to the previously tested one-dimensional computer analysis and the new two-dimensional model.

Tantalum strain gage number 3 which was located 4.5 inch from the weld showed a continuous tension response. The program predicted compression. Such disagreement did not occur on the columbium specimen. This can be attributed to the fact that tantalum gage number 3 was not located far enough from the weld to fall into the compression region. (See Figure 2.) The program had been previously used on aluminum and steel and used the same criterion to predict the location of the compressive region in tantalum. This is evidently not a correct assumption due to the unique temperature properties of this material discussed in the previous section.

In both tantalum and columbium gage number 3 was located so far from the weld center line than the copper backing

became a major factor and significantly lower readings were recorded. These should generally be ignored when analyzing the worth of the computer model compared with experimental data.

B. Heat Flow

In order to begin a heat flow calculation, it is necessary to determine a quantity known as arc efficiency, η. This factor is related to heat in the following manner:

$$Q = \eta \cdot v \cdot I$$

where

Q = thermal power of heat source in watts

v = welding speed in in/sec

I = currents in amperes

Figures 20 through 32 show calculated temperature changes during welding. Measured temperature changes are shown in Figures 33 and 34.

In order to determine the correct value for arc efficiency, η, calculations were made with three values of η, 0.2, 0.3, 0.4. Figures 20 through 34 show the calculations for each of these values. For $\eta = 0.4$ the theoretical values were significantly higher than the experimental ones. For $\eta = 0.3$ the values were closer but not quite low enough. The $\eta = 0.2$ value showed closest agreement.

For most GTA welding processes the arc efficiency is 0.2 to 0.5. (See Figure 35.) This discrepancy was due to not including heat loss by radiation in the analysis.

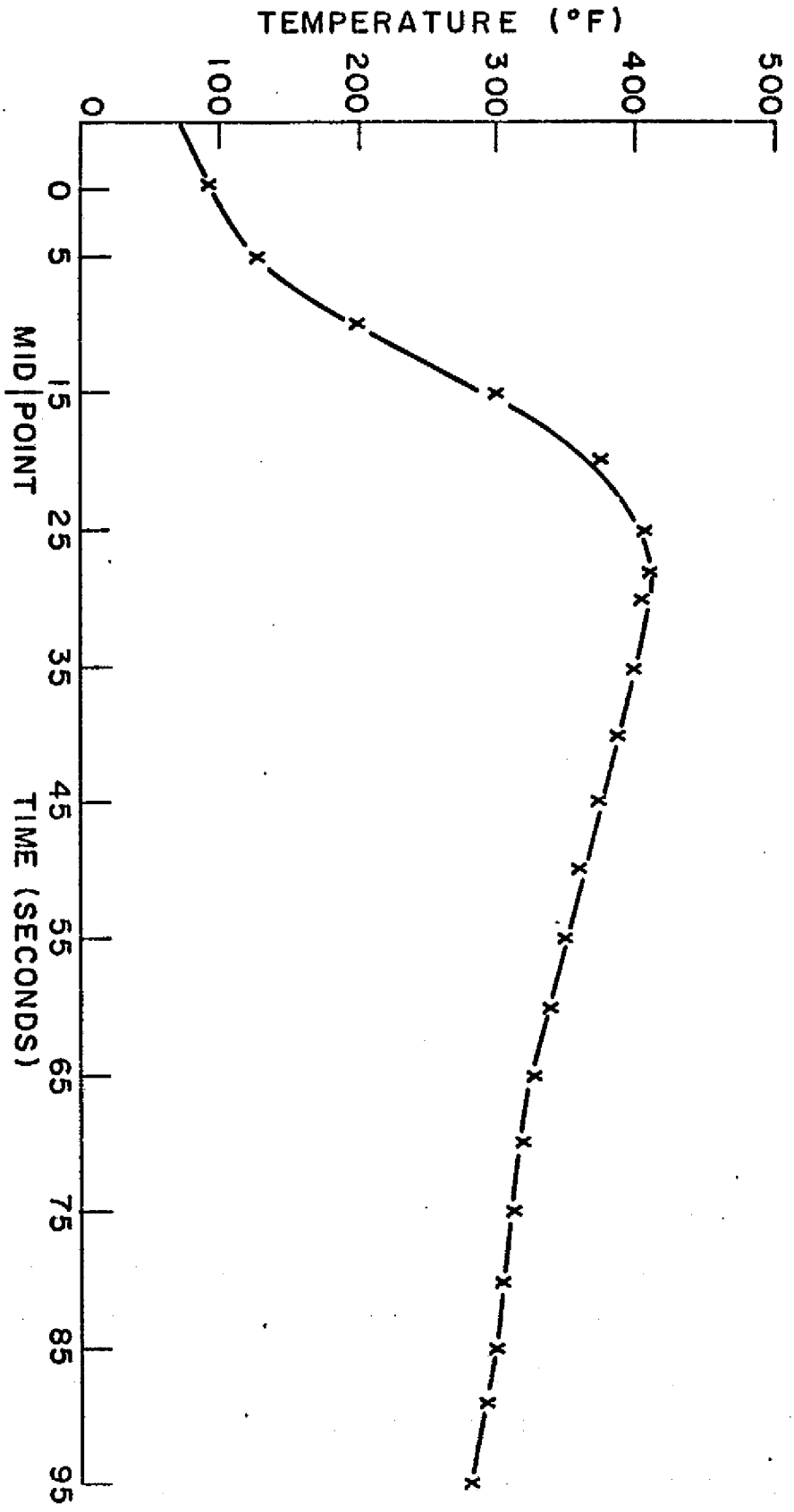

Figure 20 Calculated Temperature Change during Welding of Tantalum (efficiency = 0.1, 0.9 inch from Weld center)

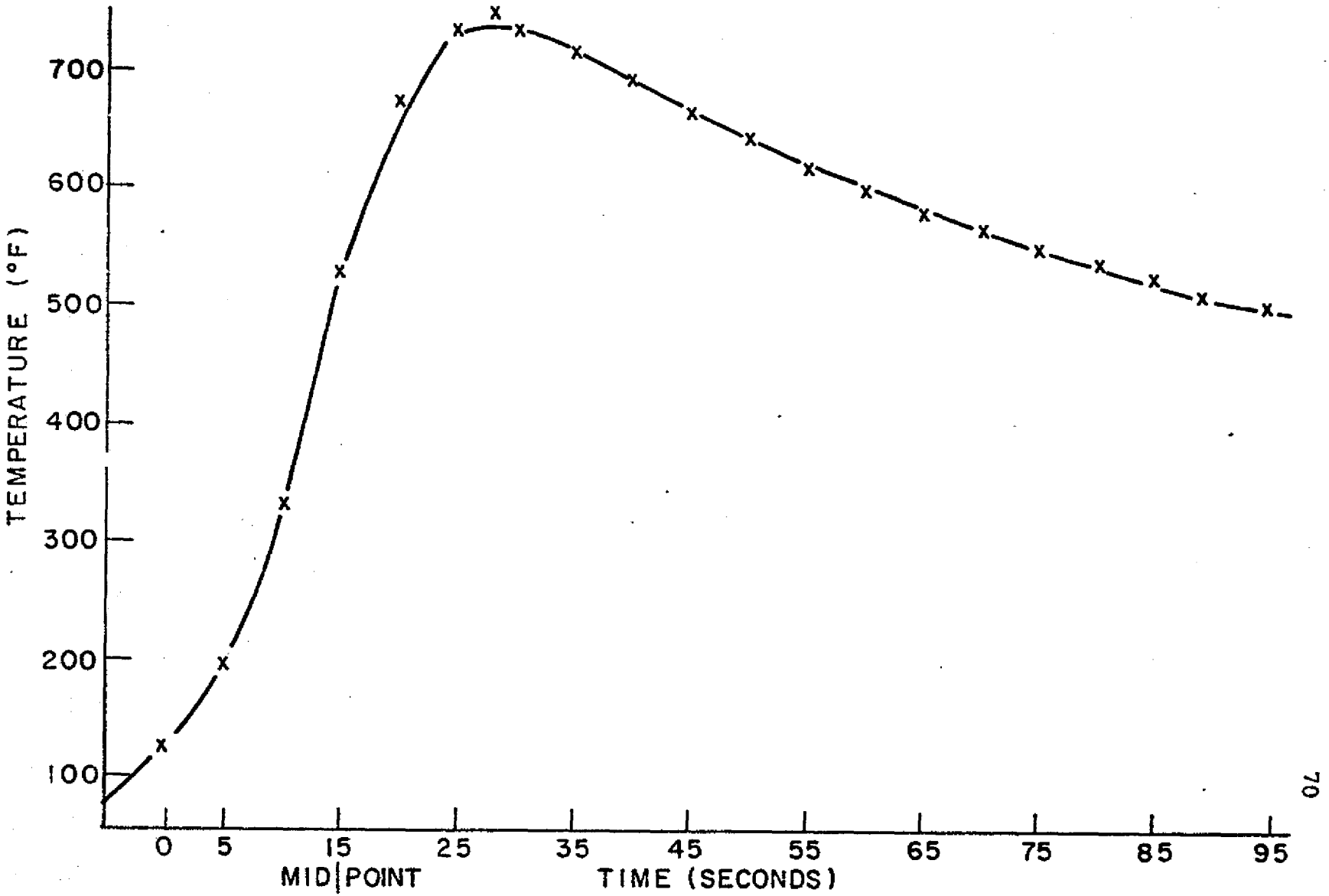

Figure 21 Calculated Temperature Change during Welding of Tantalum (efficiency = 0.2, 0.9 inch from weld center)

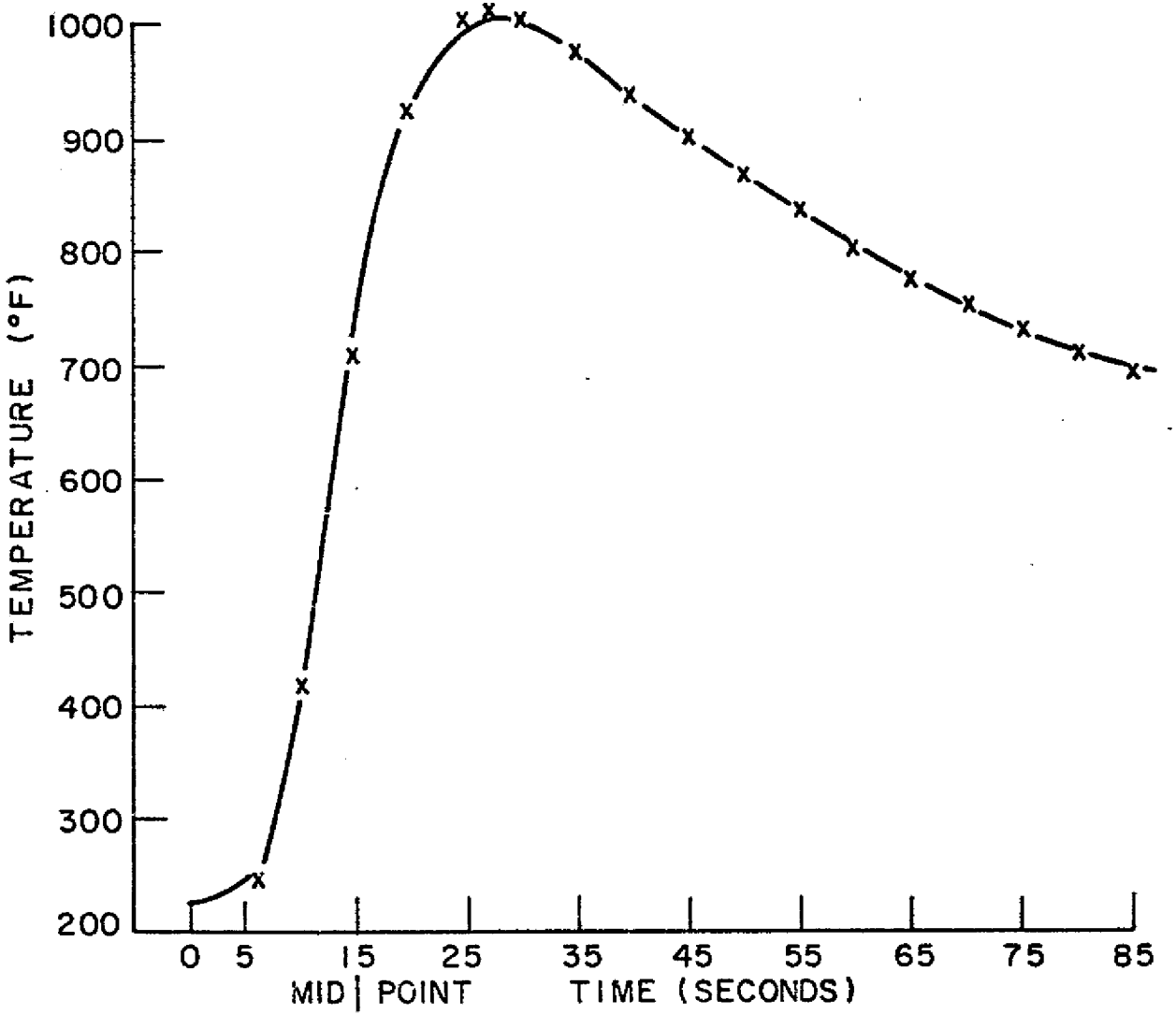

Figure 22 Calculated Temperature Change during Welding of Tantalum (efficiency = 0.3, 0.9 inch from weld center)

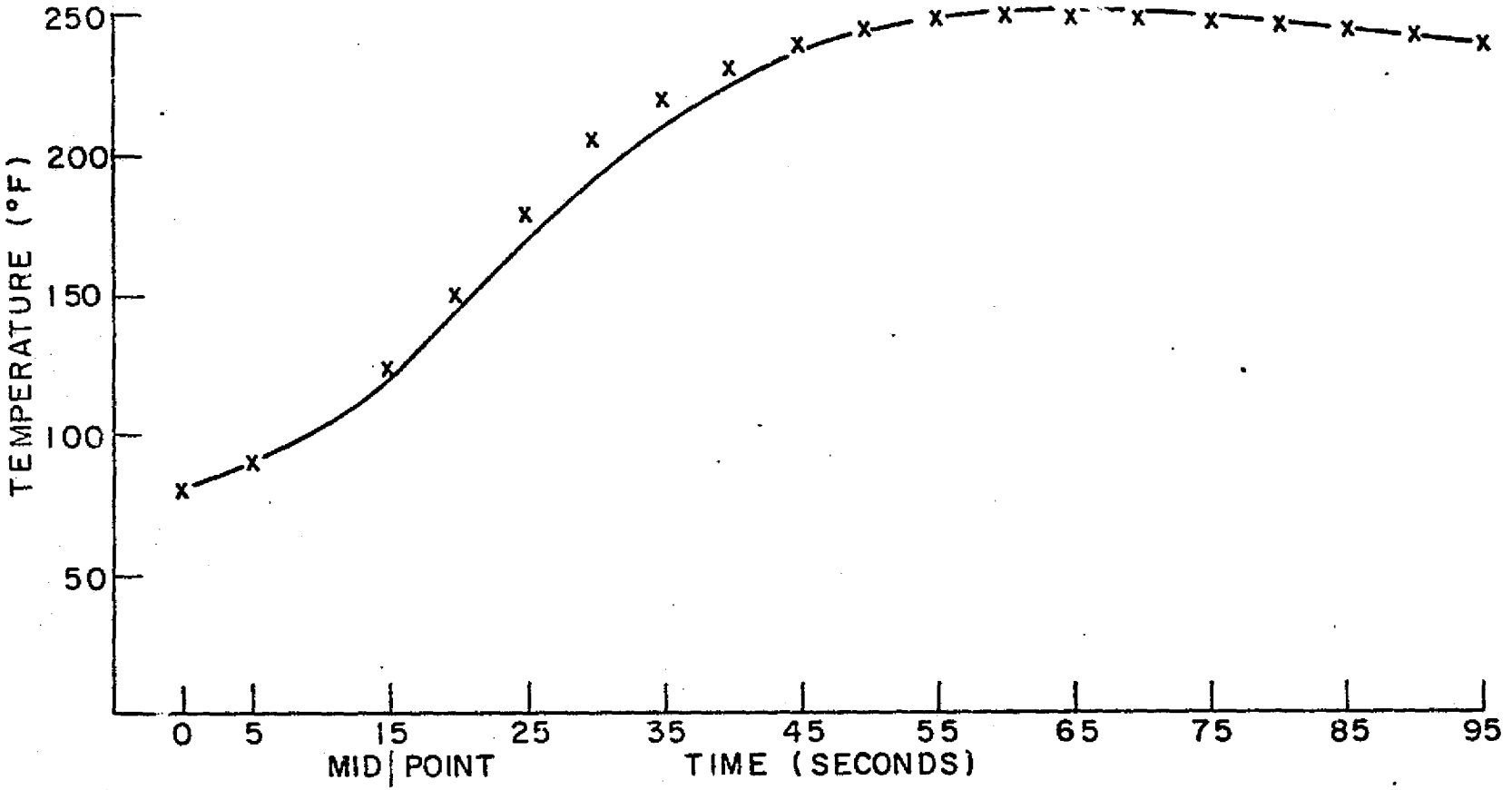

Figure 23 Calculated Temperature Change during Welding of Tantalum (efficiency = 0.1, 2.1 inch from weld center)

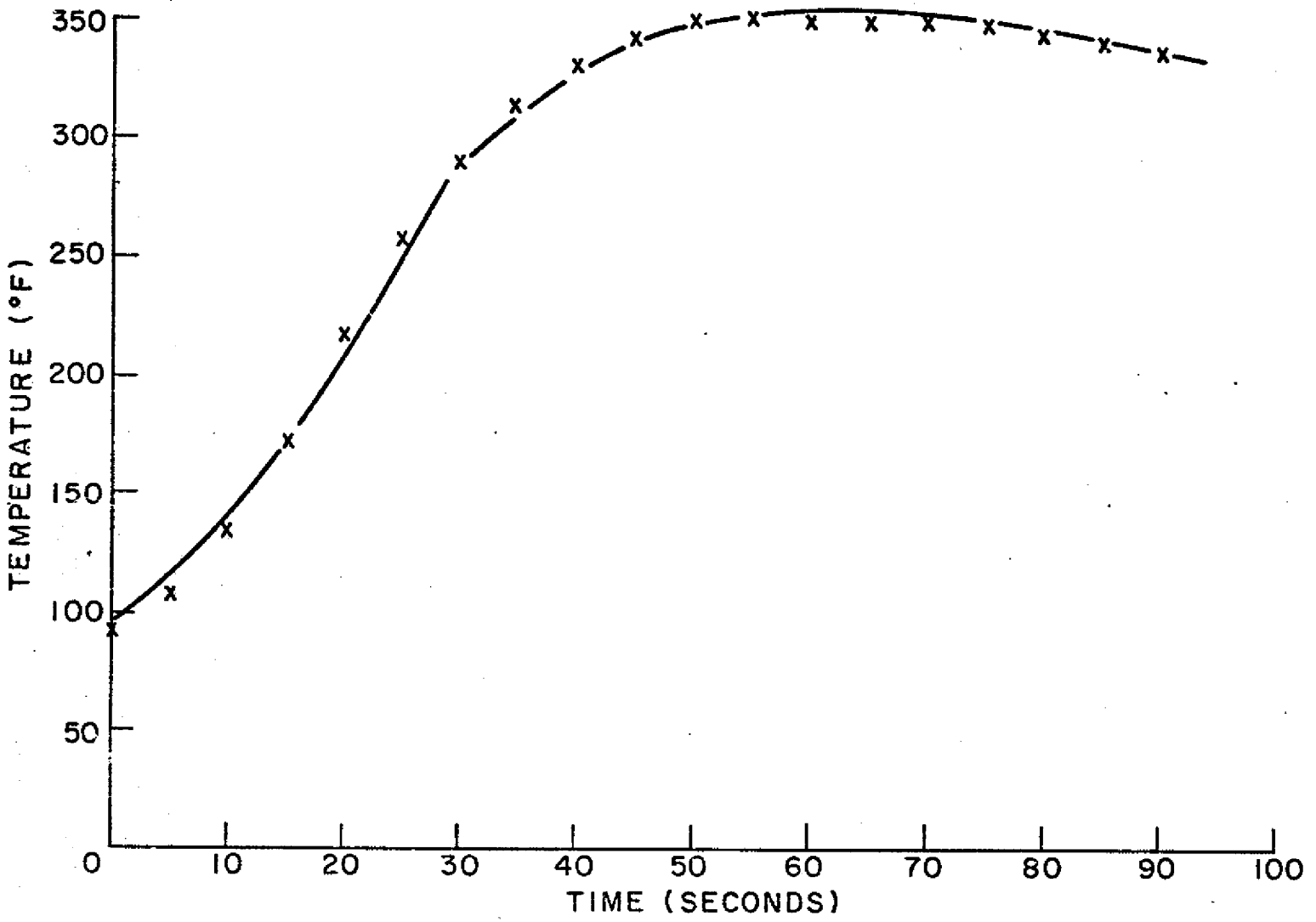

Figure 24 Calculated Temperature Change during Welding of Tantalum (efficiency = 0.2, 2.1 inch from weld center)

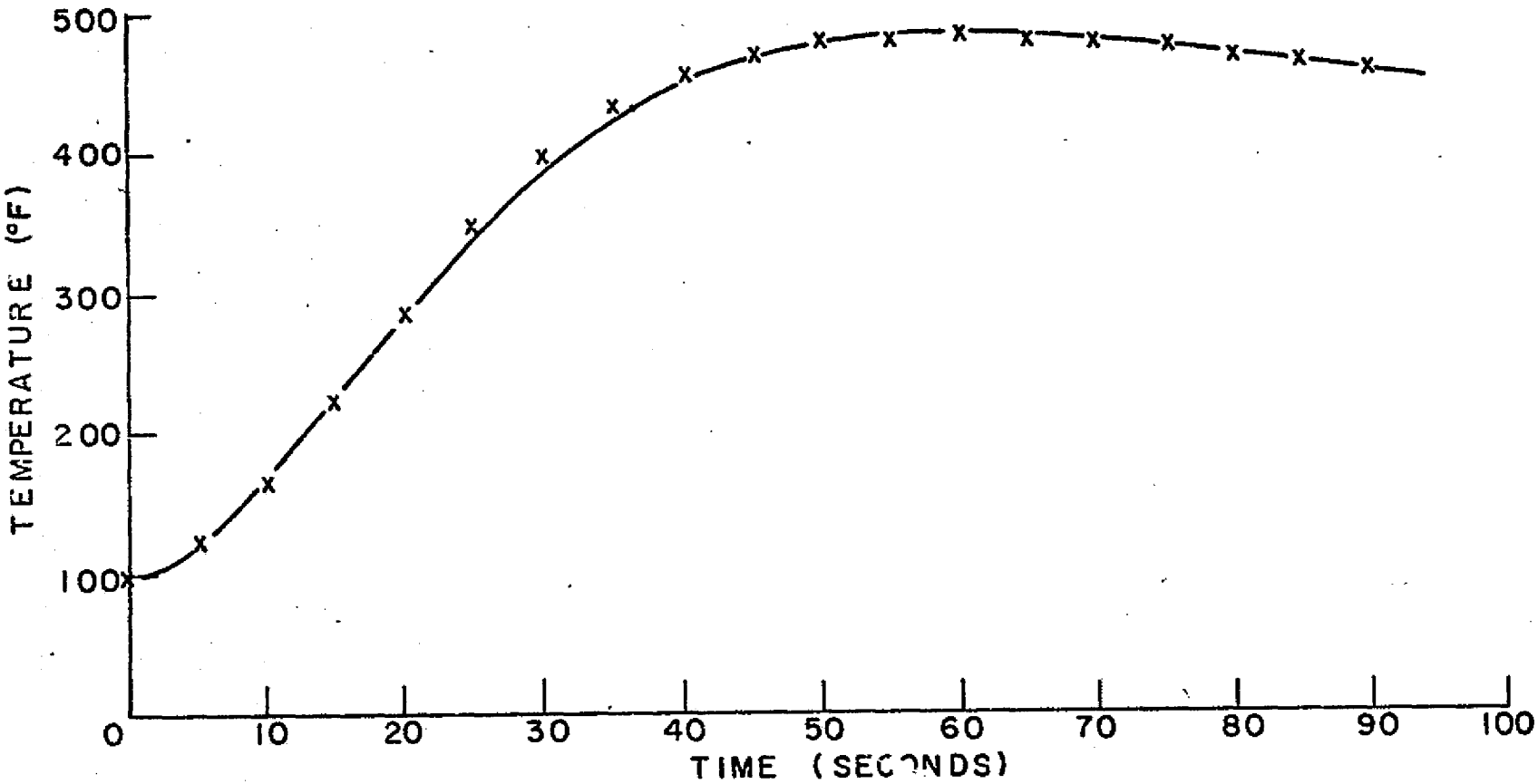

Figure 25 Calculated Temperature Change during Welding of Tantalum (efficiency = 0.3, 2.1 inch from weld center.)

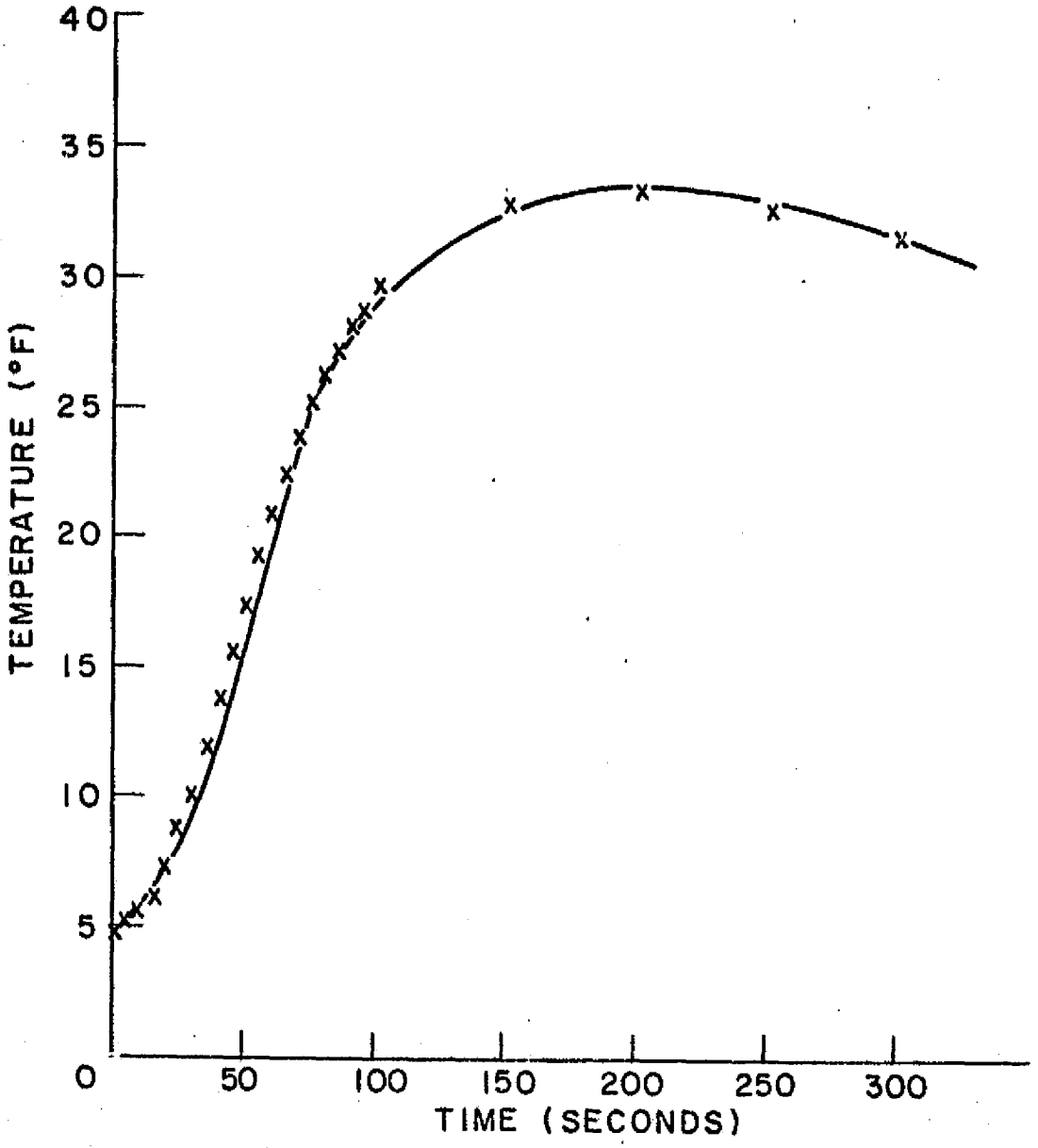

Figure 26 Calculated Temperature Change during Welding of Tantalum (efficiency = 0.1, 4.5 inch from weld center)
Note: Time and Temperature Scales Are Reversed

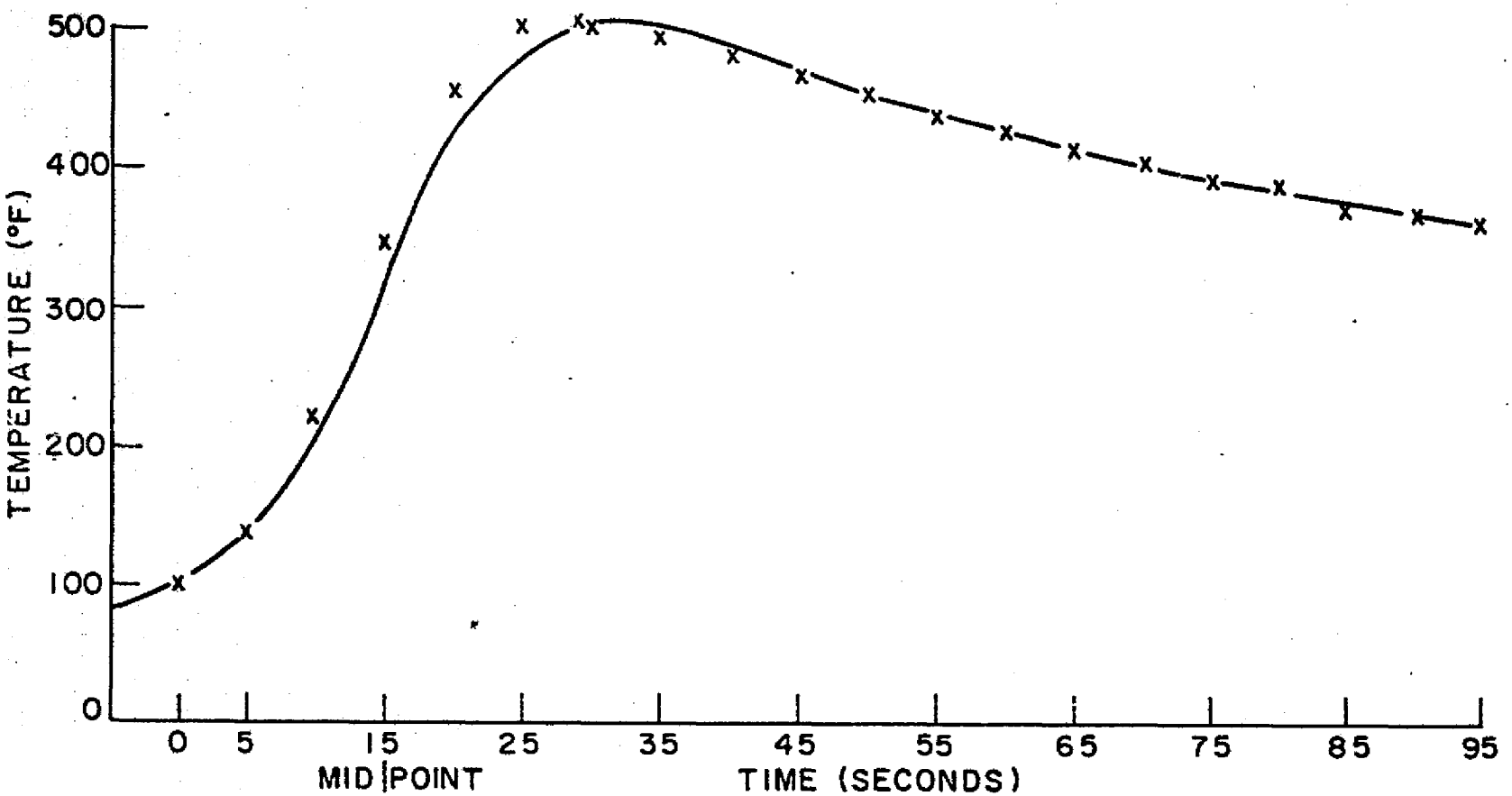

Figure 27 Calculated Temperature Change during Welding of Columbium (efficiency = 0.1, 0.9 inch from weld center)

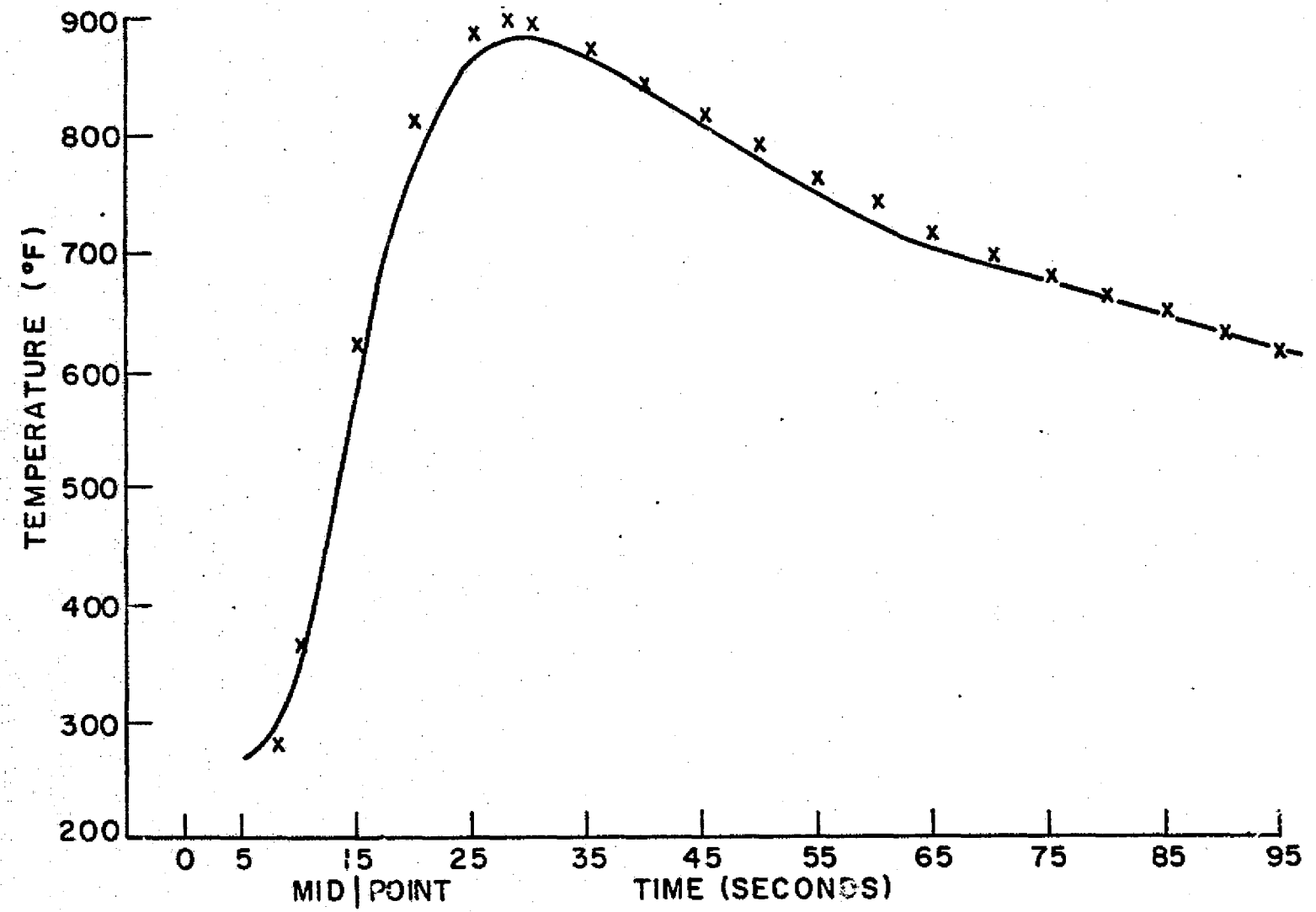

Figure 28 Calculated Temperature Change during Welding of Columbium (efficiency = 0.2, 0.9 inch from weld center)

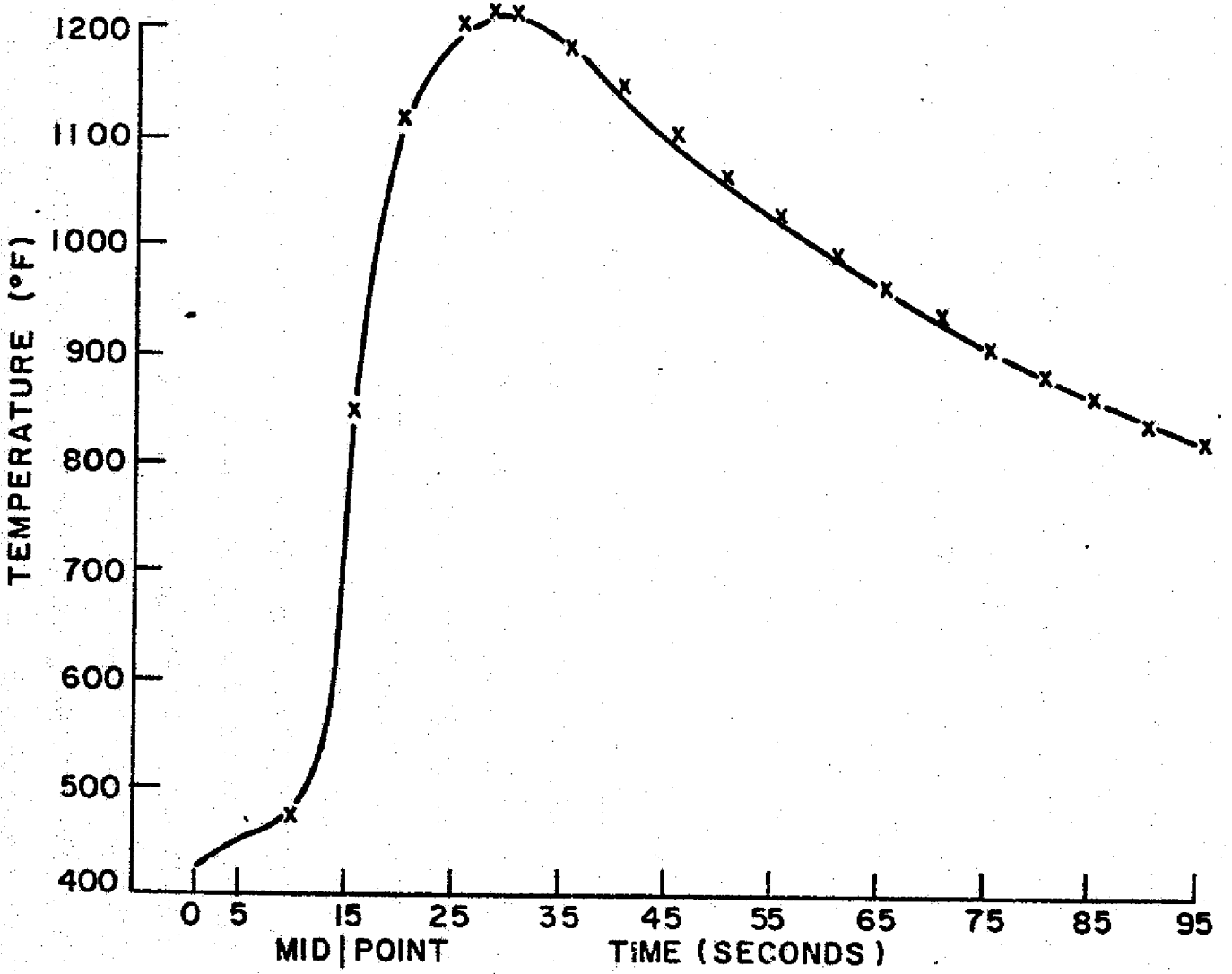

Figure 29 Calculated Temperature Change during Welding of Columbium (efficiency = 0.3, 0.9 inch from weld center)

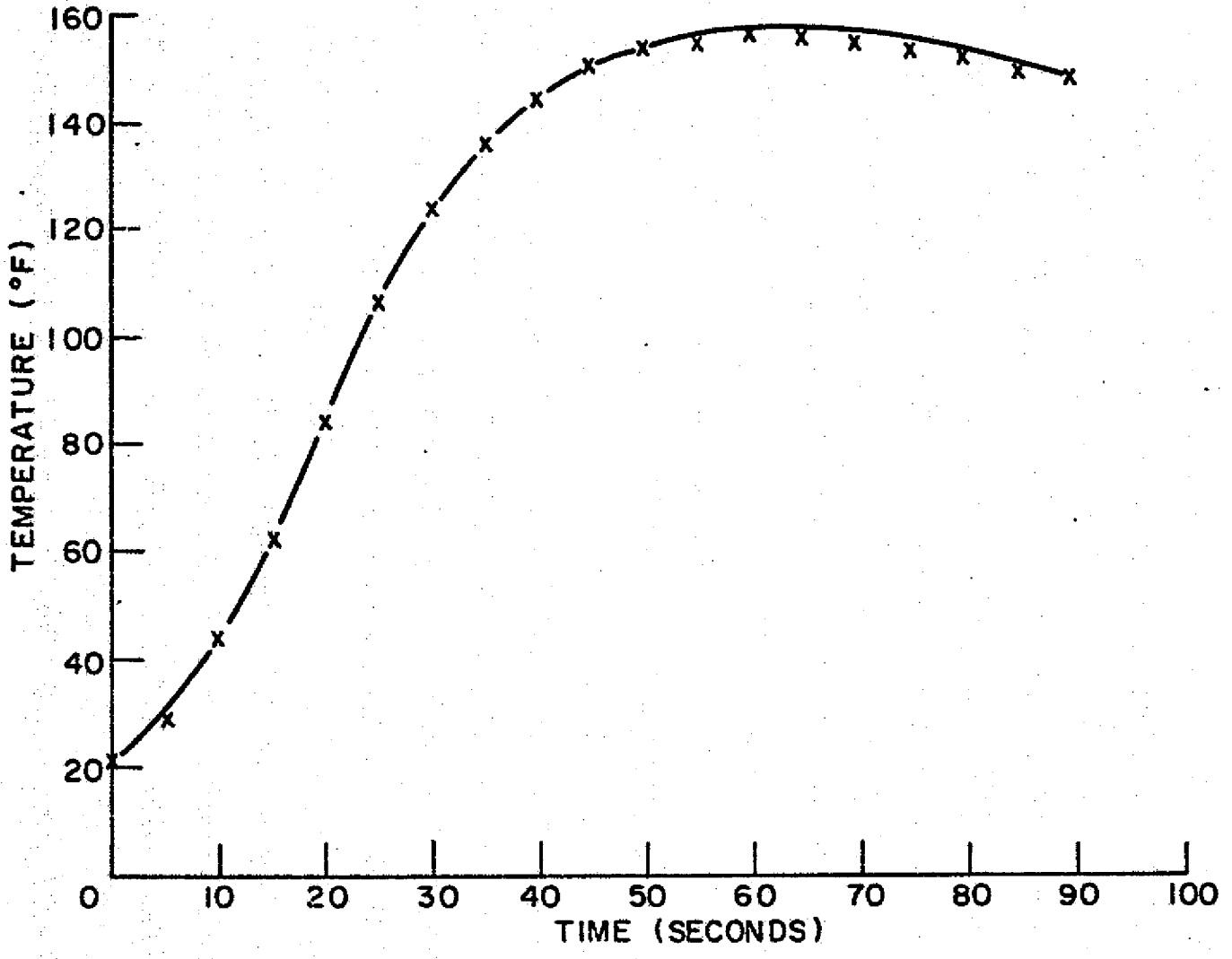

Figure 30 Calculated Temperature Change during Welding of Columbium (efficiency = 0.1. 2.1 inch from weld center)
Note: Add 75° F to all values.

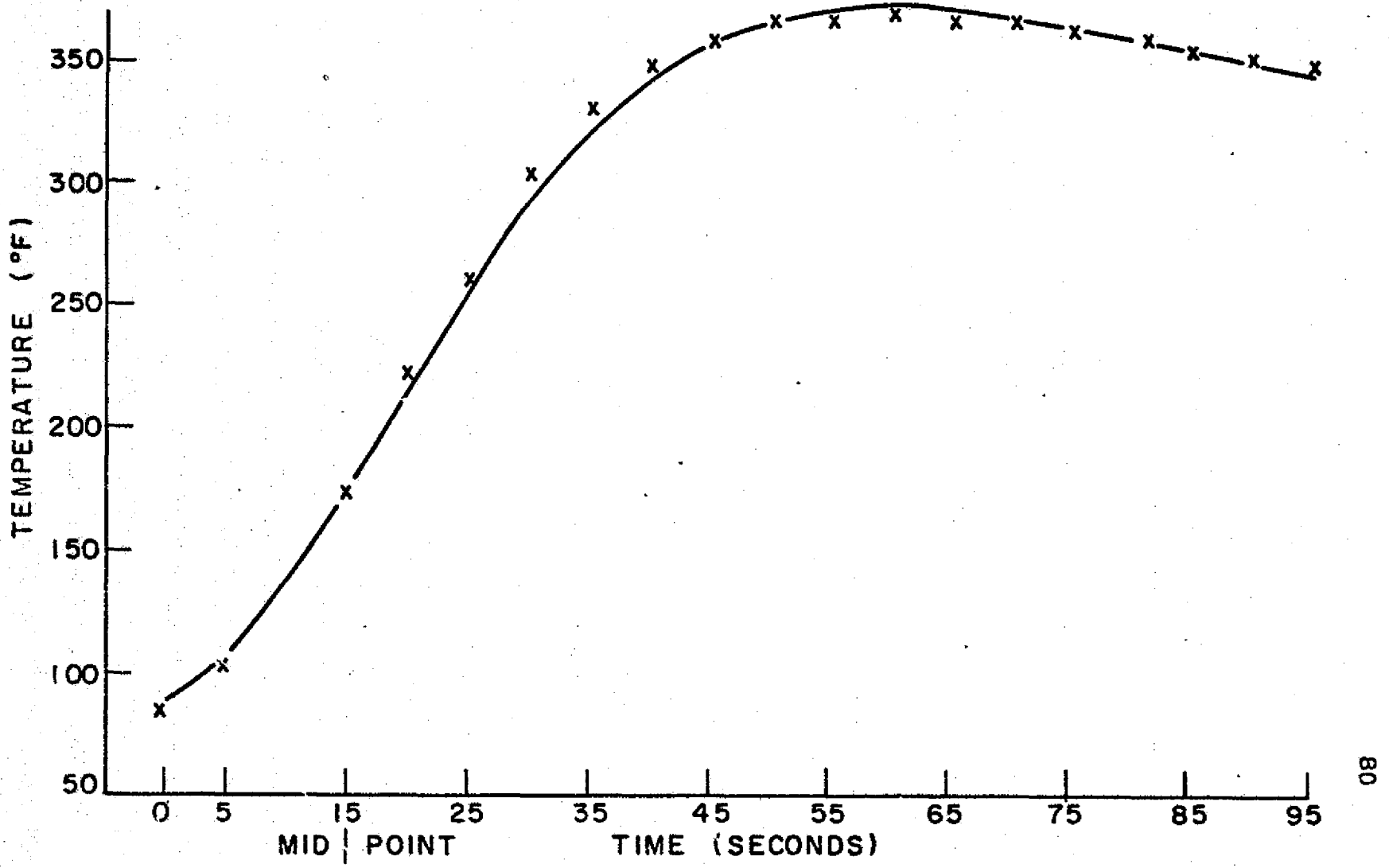

Figure 31 Calculated Temperature change during Welding of Columbium (efficiency = 0.2, 2.1 inch from weld center)

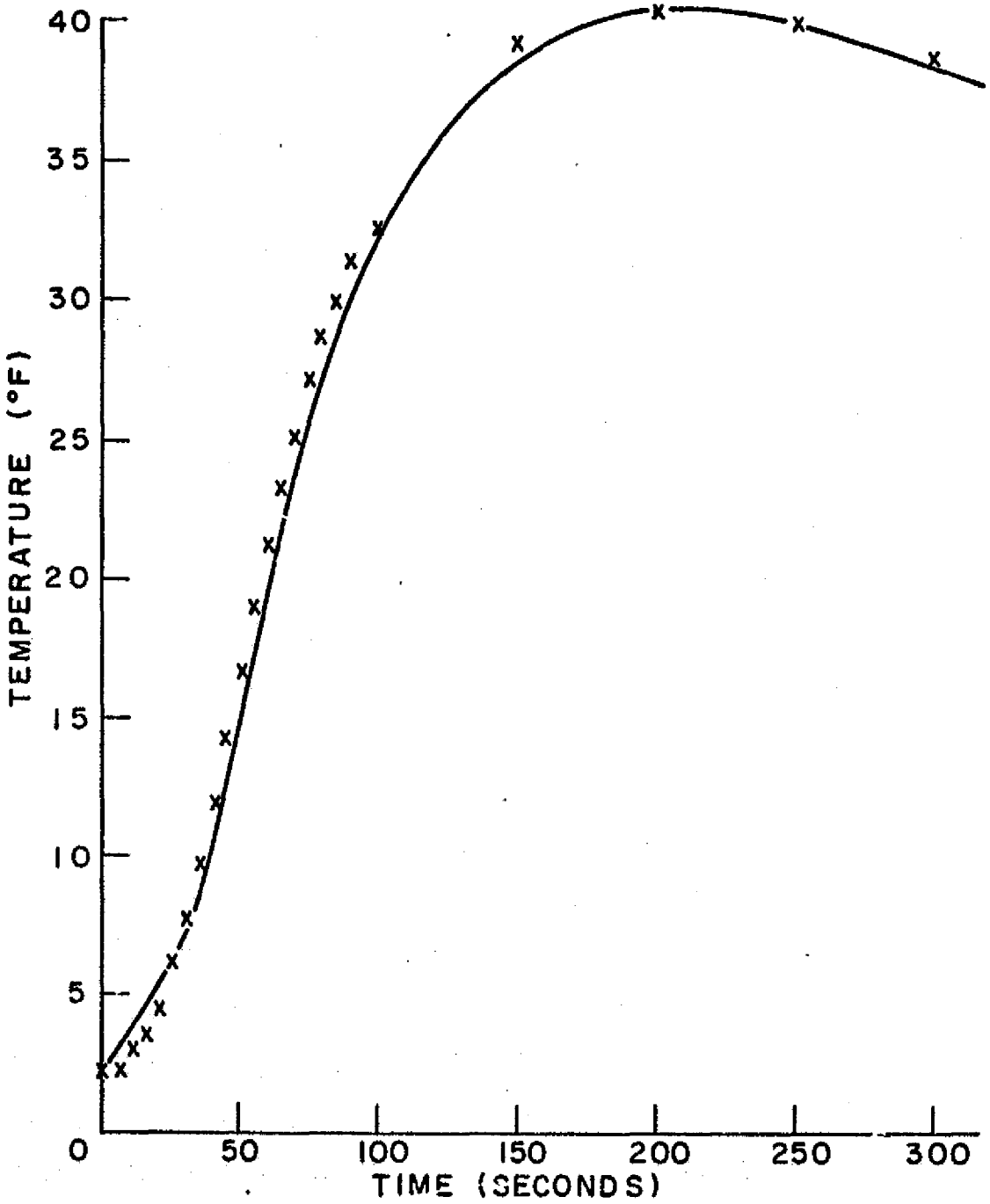

Figure 32 Calculated Temperature Change during Welding of Columbium (efficiency = 0.1, 4.5 inch from weld center)
Note: Time and Temperature Scales are Reversed.

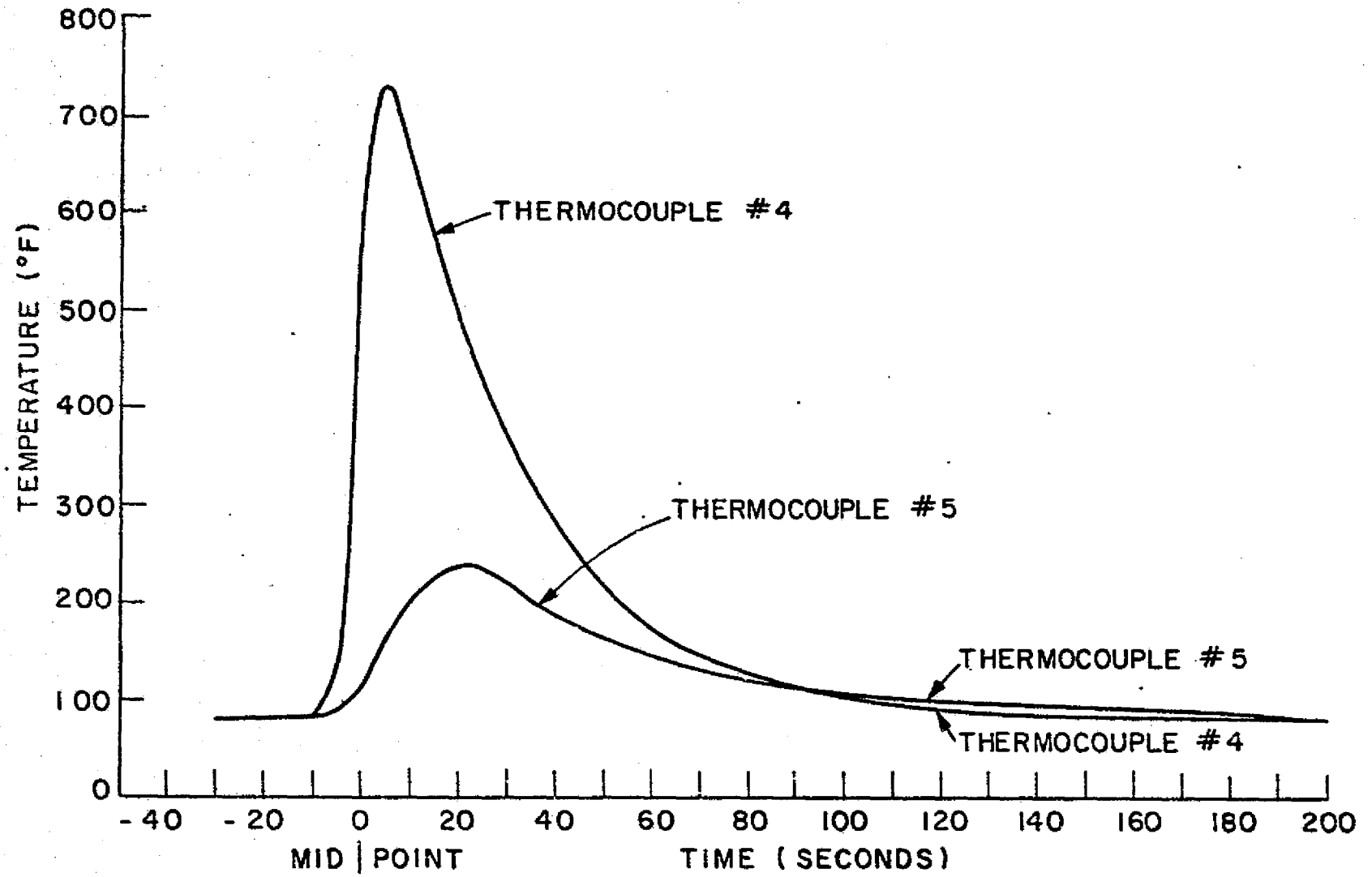

Figure 33 Experimental Temperature Change During Welding of Tantalum

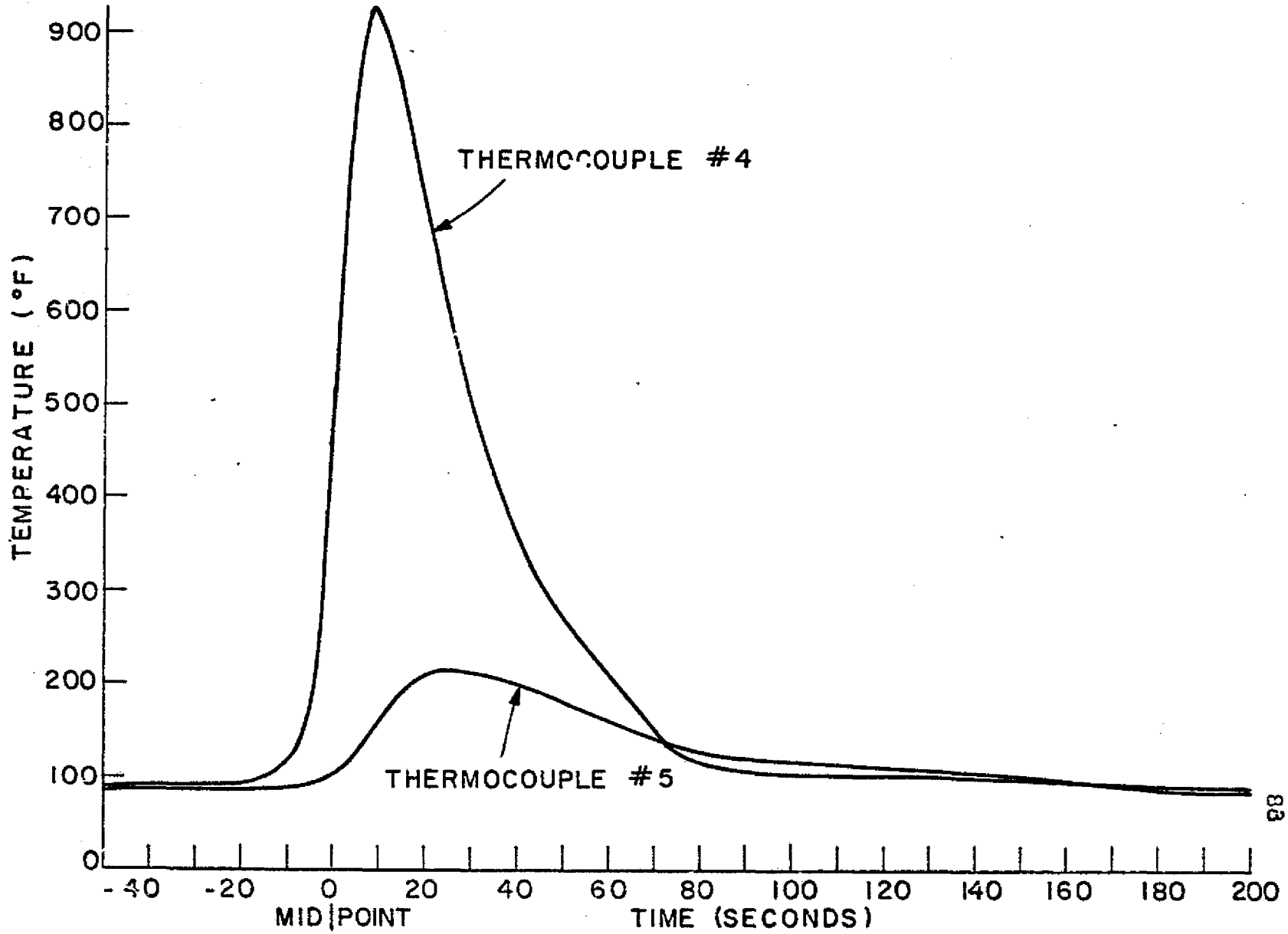

Figure 34 Experimental Temperature Change during Welding of Columbium

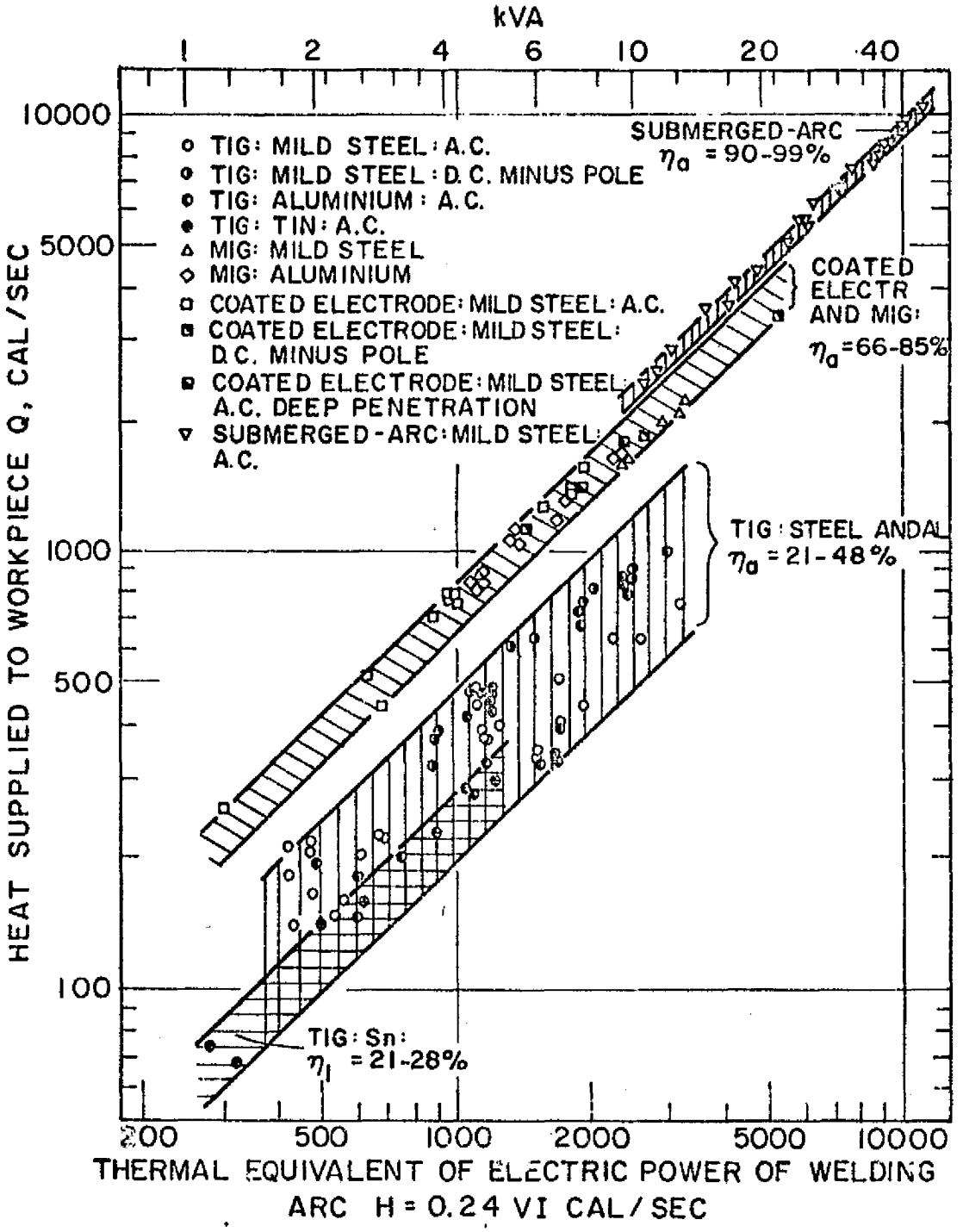

Figure 35 Measured Values of Efficiency for Various Processes and Materials (taken from Ref. 1)

Next, the radiation term, E, was added to the temperature calculation program. The best curve fit obtained by varying E and η is given in Figure 36. This corresponded to an E value of approximately 40 times that obtained by Naka[8] (E = watts/in^2 · °F), and an η of 0.3. This was thought to be the best temperature correlation possible. The figures show that the computed and measured temperature tends to peak slightly earlier than the calculation and decreases more rapidly. This is probably a further effect of heat loss from the surface.

When the arc efficiency calculation was done at a point further away from the weld center line than the original calculation, the efficiency tended to take on a slightly lower value. This was due to the presence of the copper backing plate acting as a heat sink.

C. Strains--Stress Analysis

One-Dimensional

Figures 37 and 38 show that longitudinal strains calculated by the one-dimensional computer program coincide extremely well with measured results (Figures 39 and 40). Peaks occur approximately 5 seconds sooner after the arc passes in the measured graphs than they do in the calculated graphs. Peak heights agree within a maximum of 400 μ in/in for the tantalum specimens and 100 μ in/in for the columbium specimens.

The tantalum strain maximum was of a lower magnitude than the columbium values. This was not the trend predicted

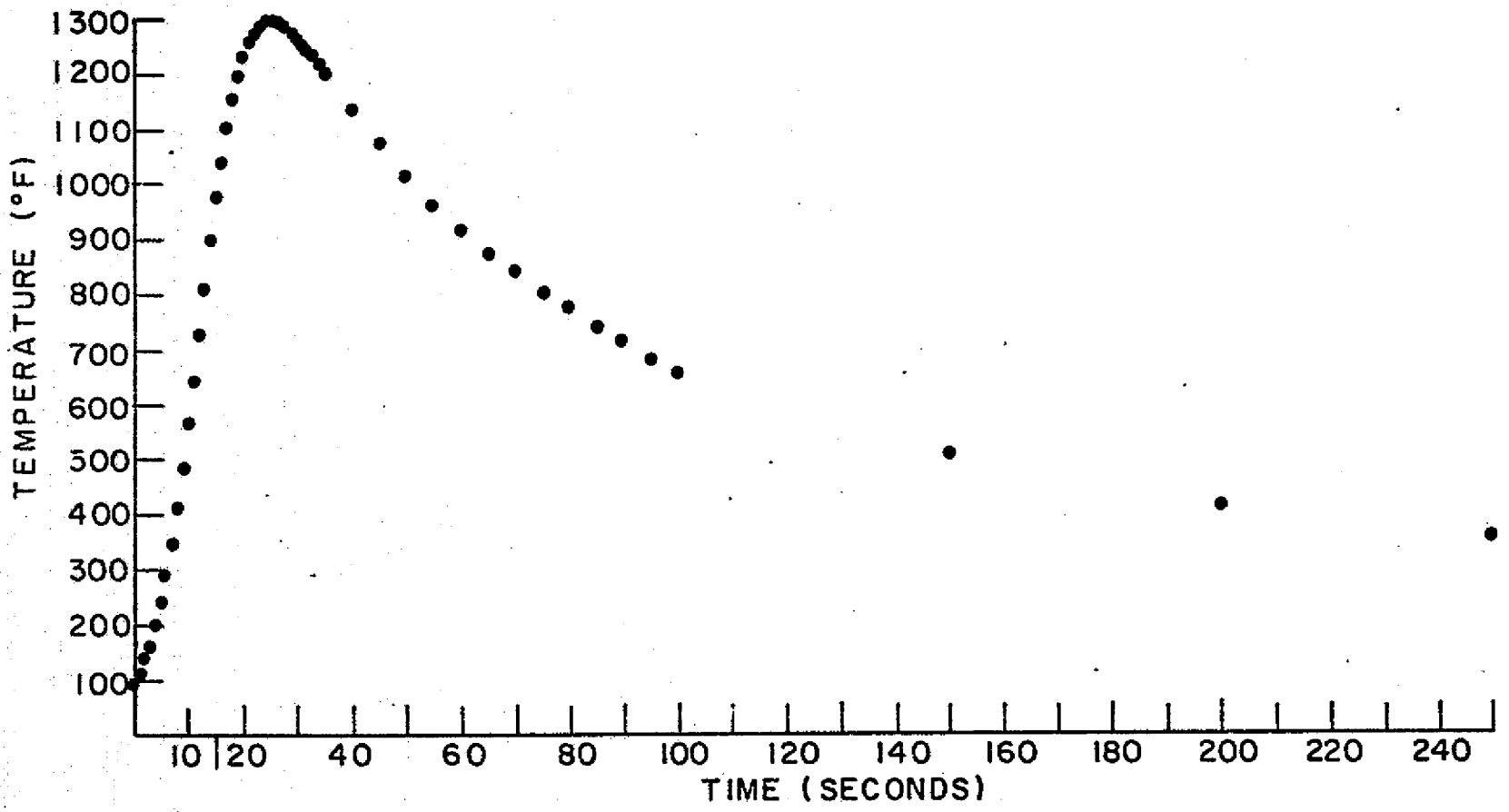

Figure 36 Calculated Temperature Change during Welding for Efficiency = 0.3, E = watts/in^2 x ^{o}F

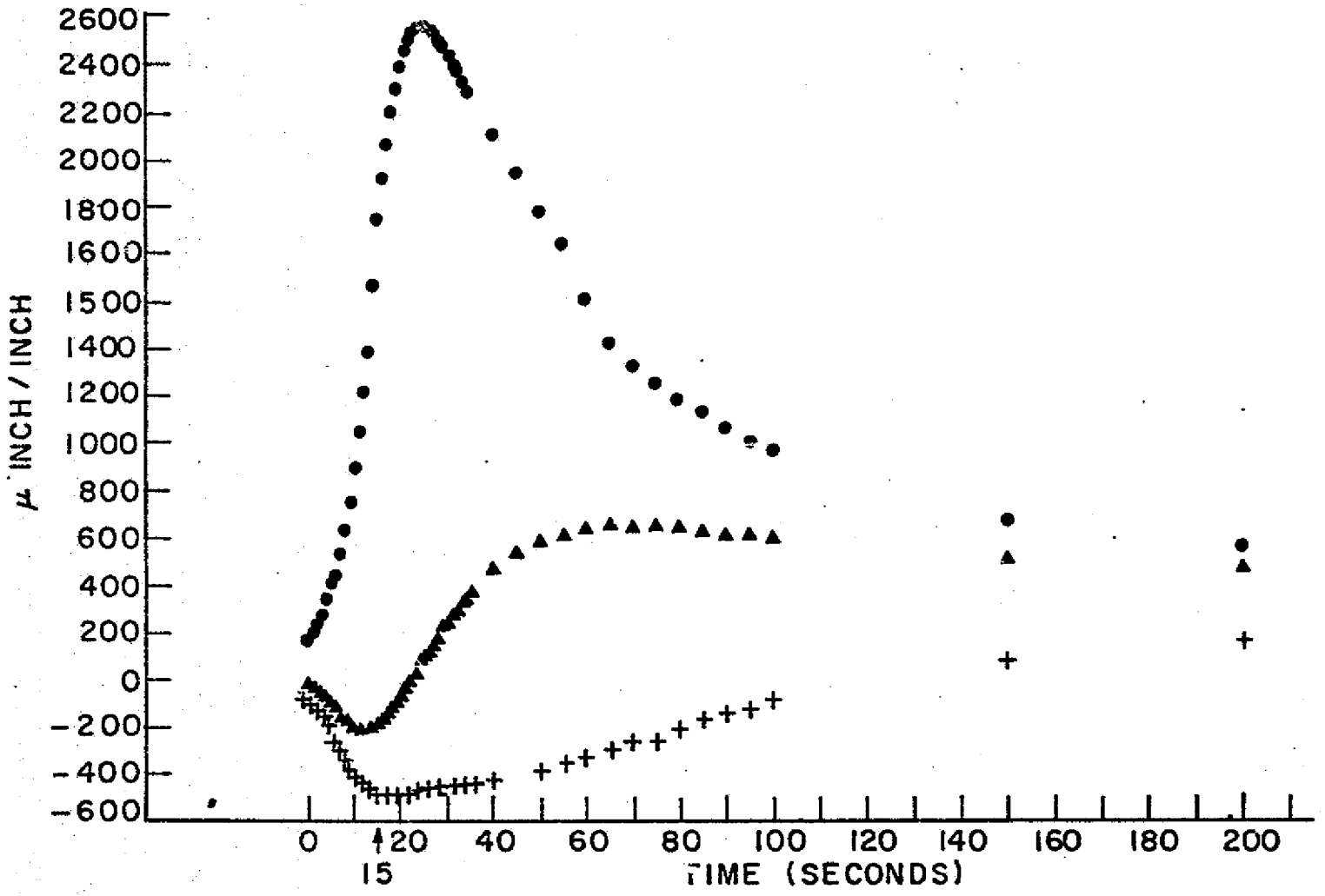

Figure 37 Calculated Strain Change during Welding of Tantalum Using the One-Dimensional Program

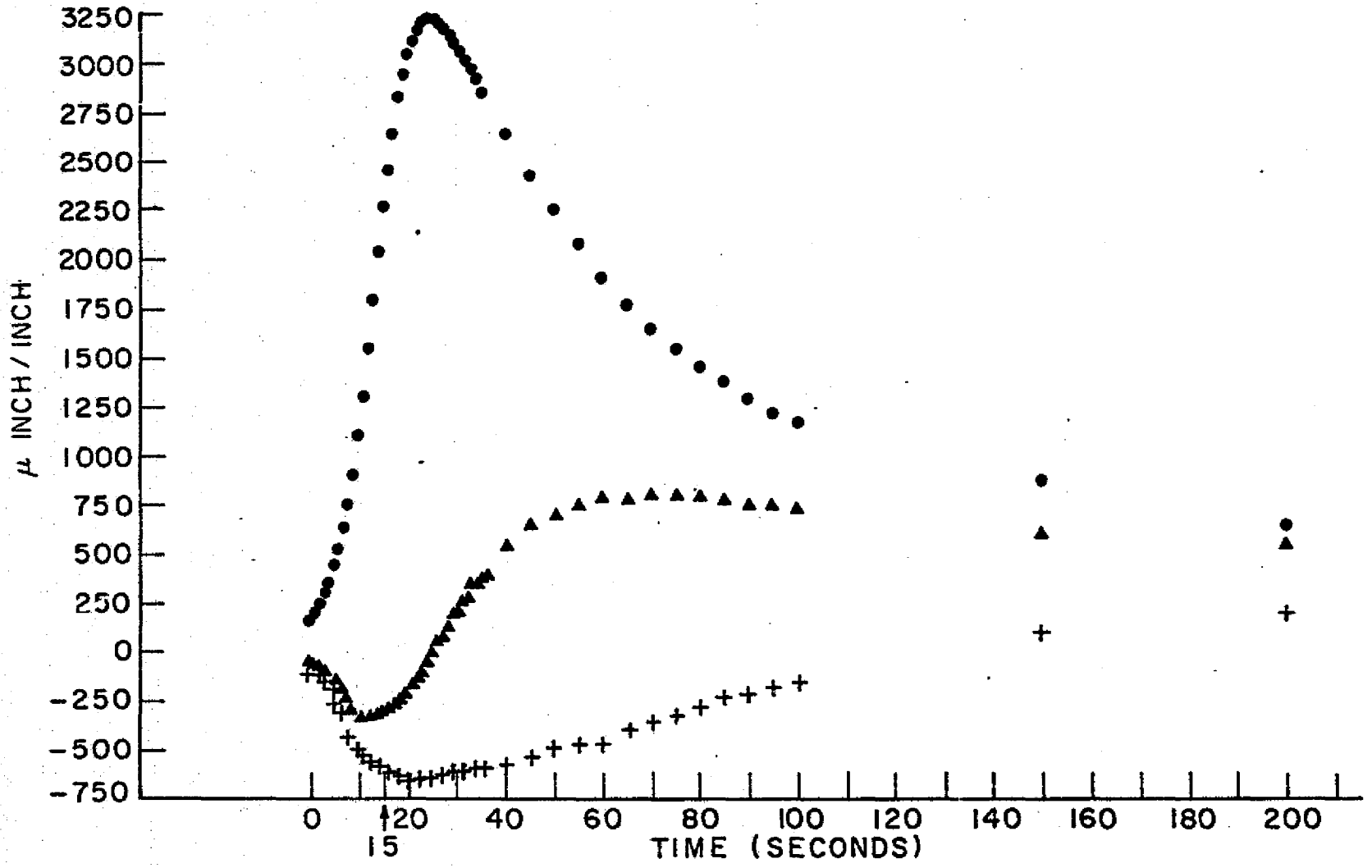

Figure 38 Calculated Strain Change during Welding of Columbium Using the One-dimensional Program

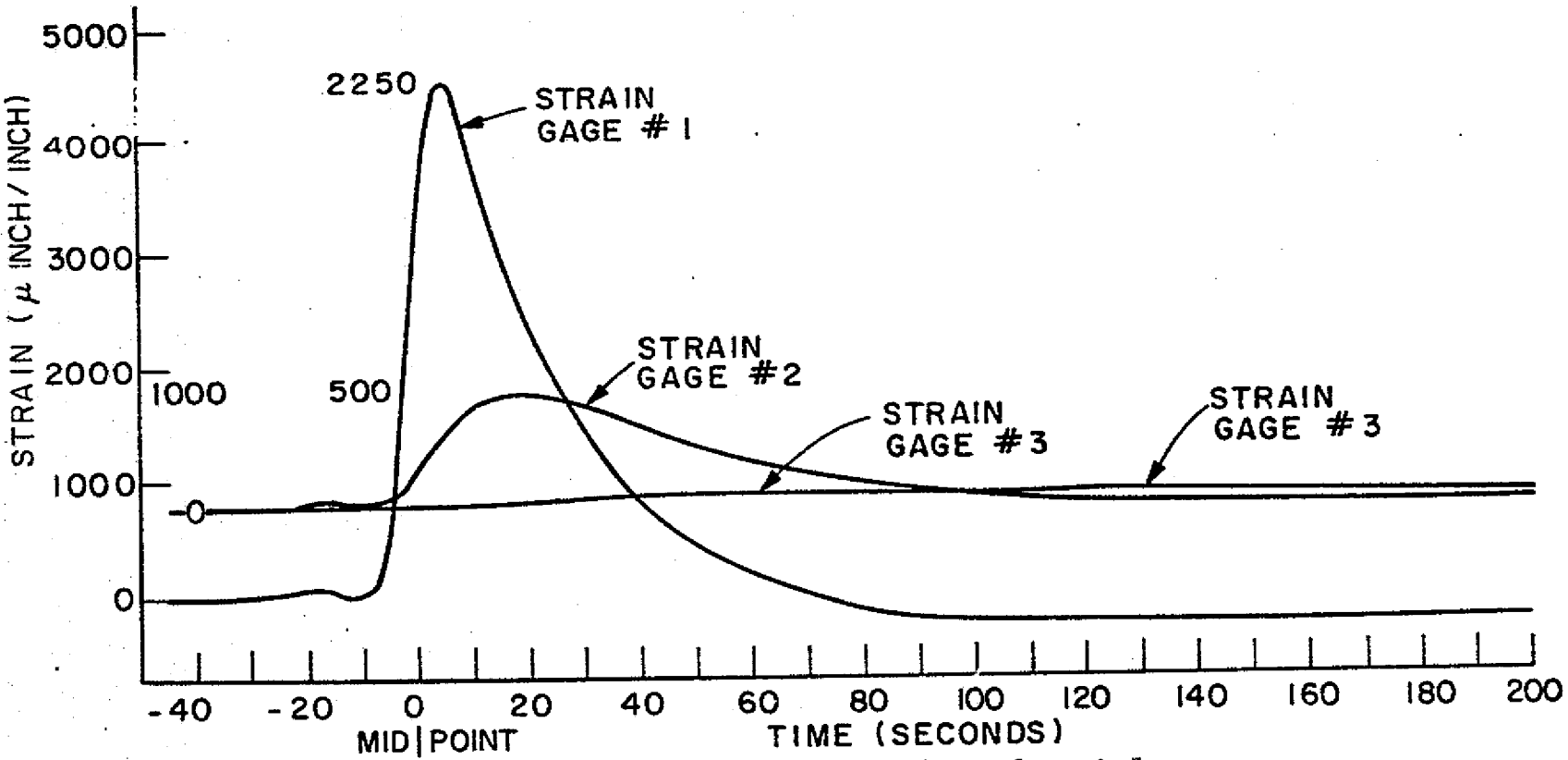

Figure 39 Experimental Cahnge during Welding of Tantalum
Note: Strain Scale incorrect--Read Correct Values from the Numbers Located on the Graph Itself

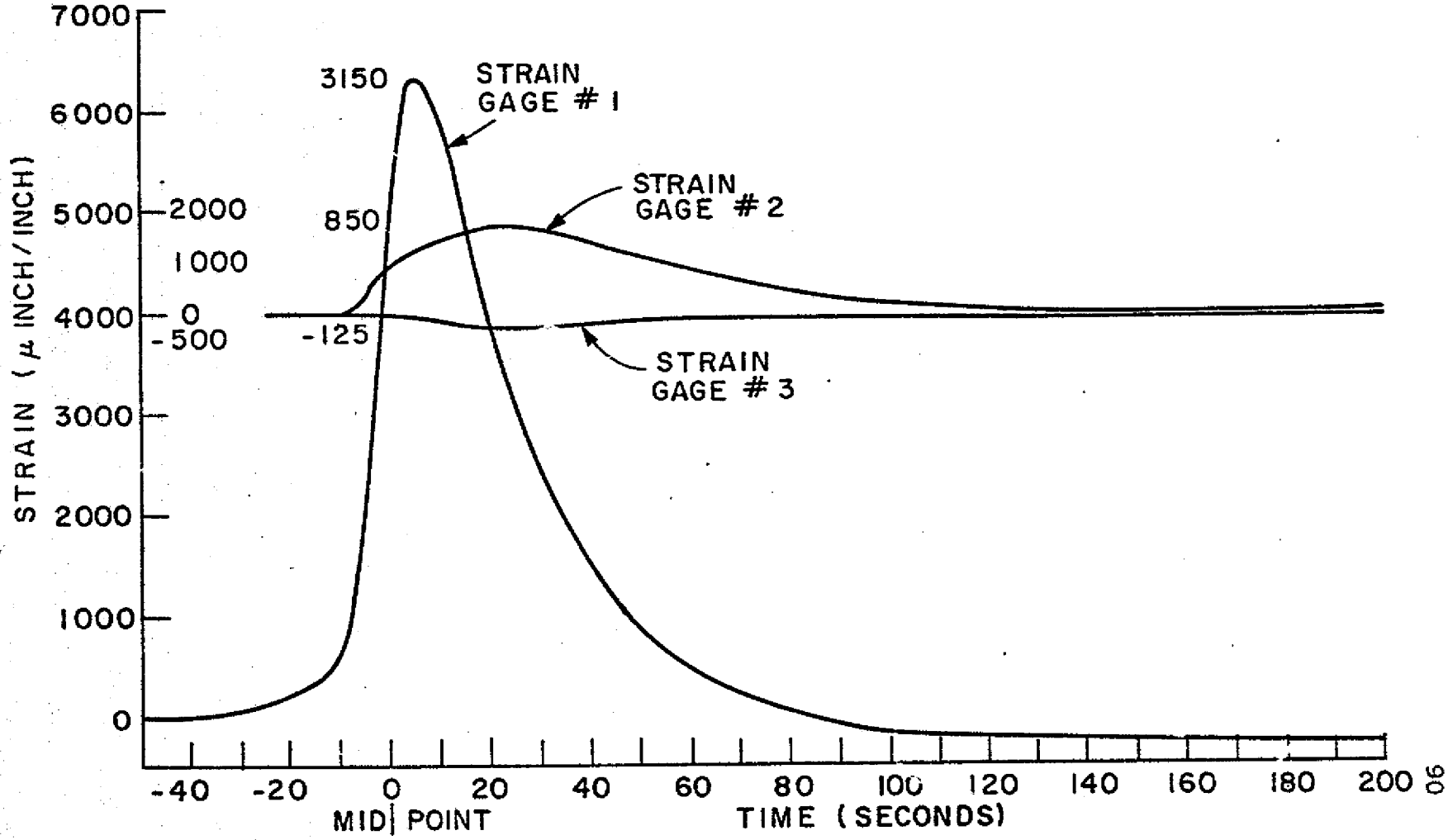

Figure 40 Experimental Strain Change during Welding of Columbium
Note: Strain Scale incorrect--Read correct values from the Numbers Located on the Graph Itself.

in Figure 41. The error occurred due to the uncertain value of yield stress of columbium. For annealed products the value is 45,000 psi but for wrought products a high of 55,000 psi is reached. Figure 41 utilizes the lower value while the program uses the higher one.

The peak values obtained for both specimens of approximately 3,000 μ in/in corresponds to the values achieved for 1/4 inch thick 2219 aluminum alloy by Arita. This demonstrates the conjecture made earlier that columbium and tantalum will be competitive with aluminum for structural purposes.

Two-Dimensional

In the two-dimensional calculation all strains followed the same pattern of peak shape and all showed a similar lag time of 5 seconds behind measured values. The two-dimensional calculation results appear in Figures 42 through 45.

There were two great disparities in the comparison of two-dimensional theoretical and measured results. The first was the actual numerical value the peak obtained. This was significantly (1000 μ in/in compared to 3000 μ in/in) lower than the measured value. Since the one-dimensional values agree with the experimental results, and taking into consideration the fact that the two-dimensional program is still in the developmental stage, these values can be discounted as programmer error. This does not negate the worth of the two-dimensional analysis, however, because the peak shapes and locations were correct.

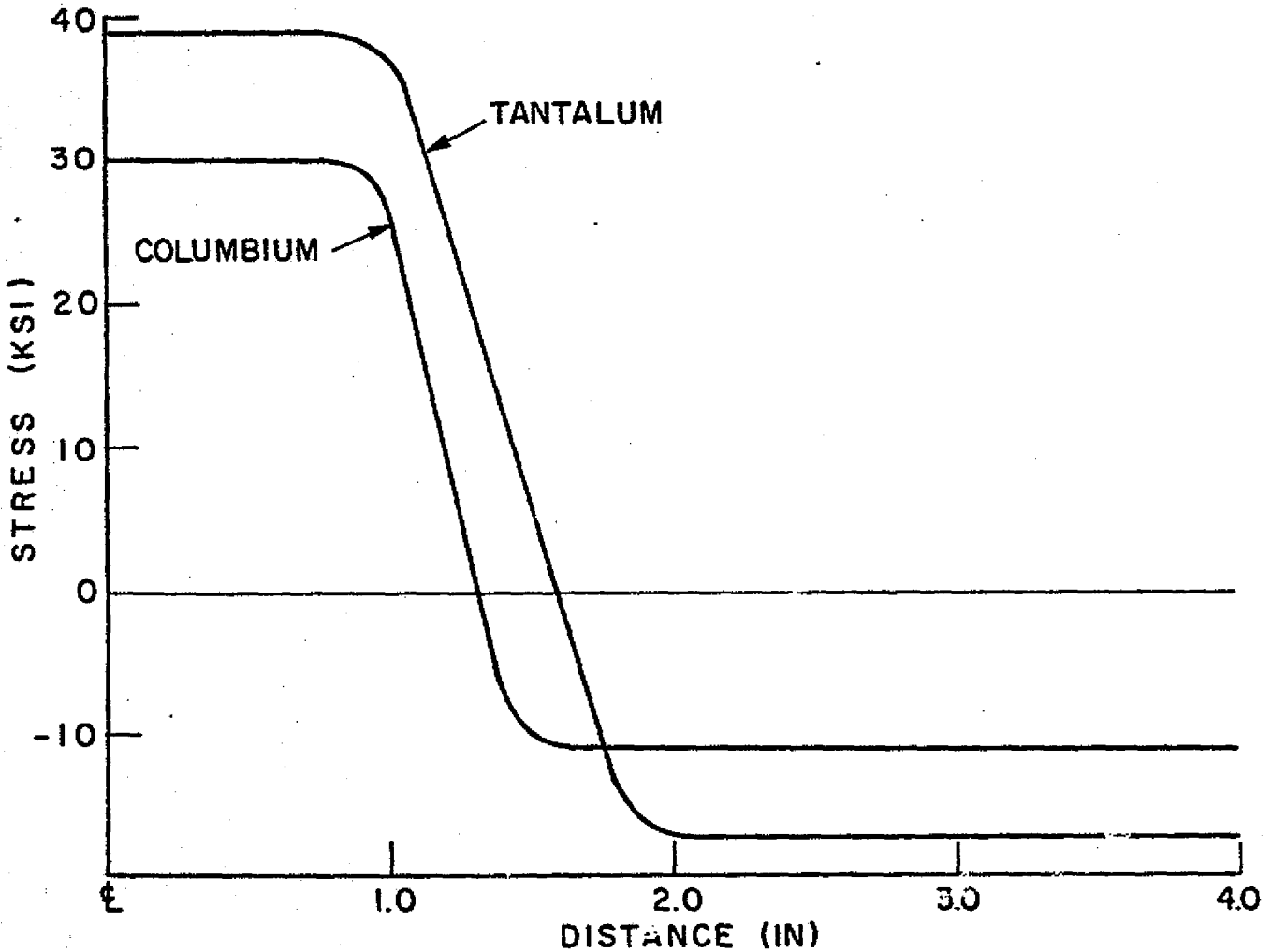

Figure 41 Previous Stress vs Distance from Weld Center Taken from Ref.

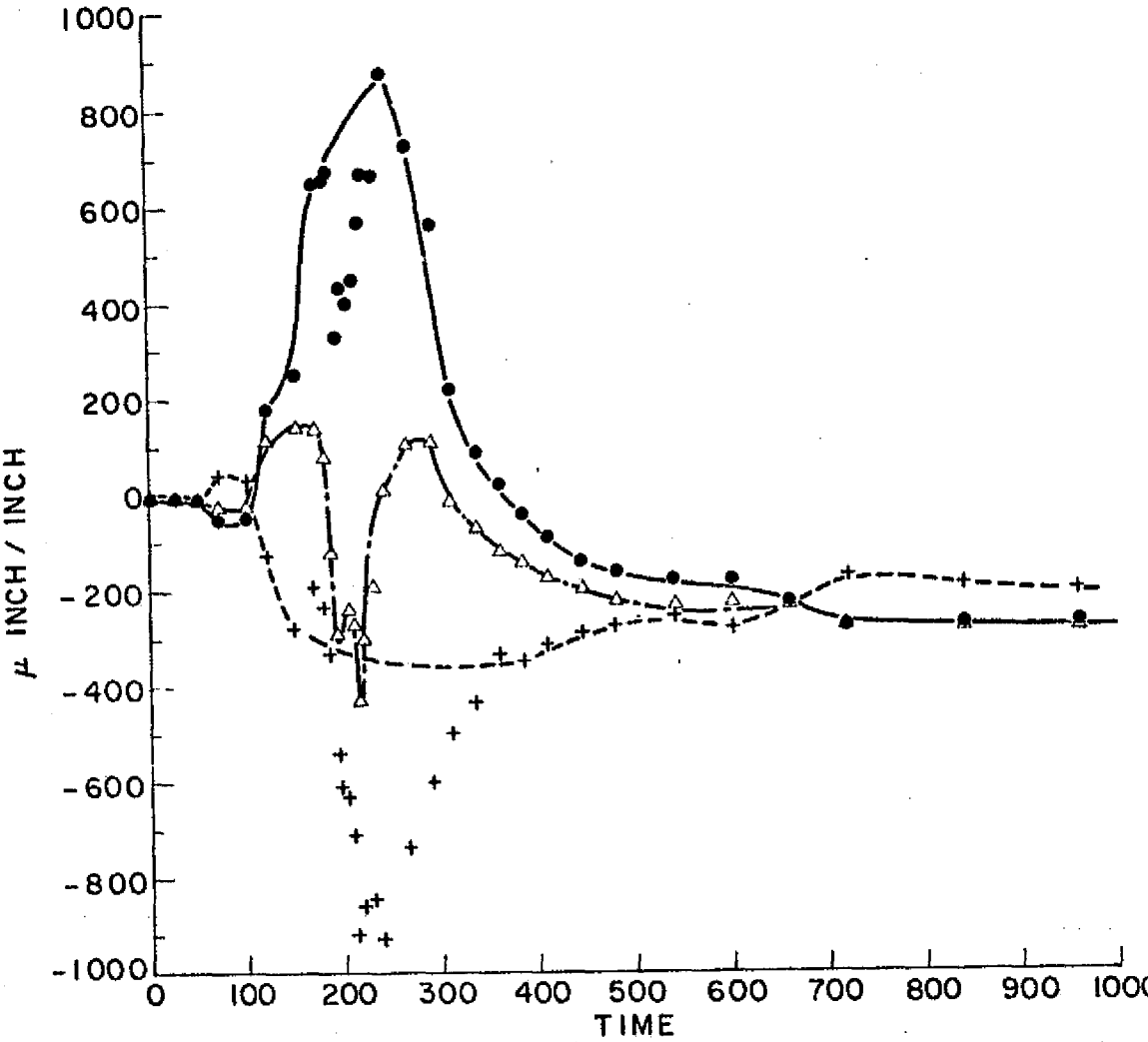

Figure 42 Calculated Strain Change during Welding of Tantalum Using the Two-dimensional Program

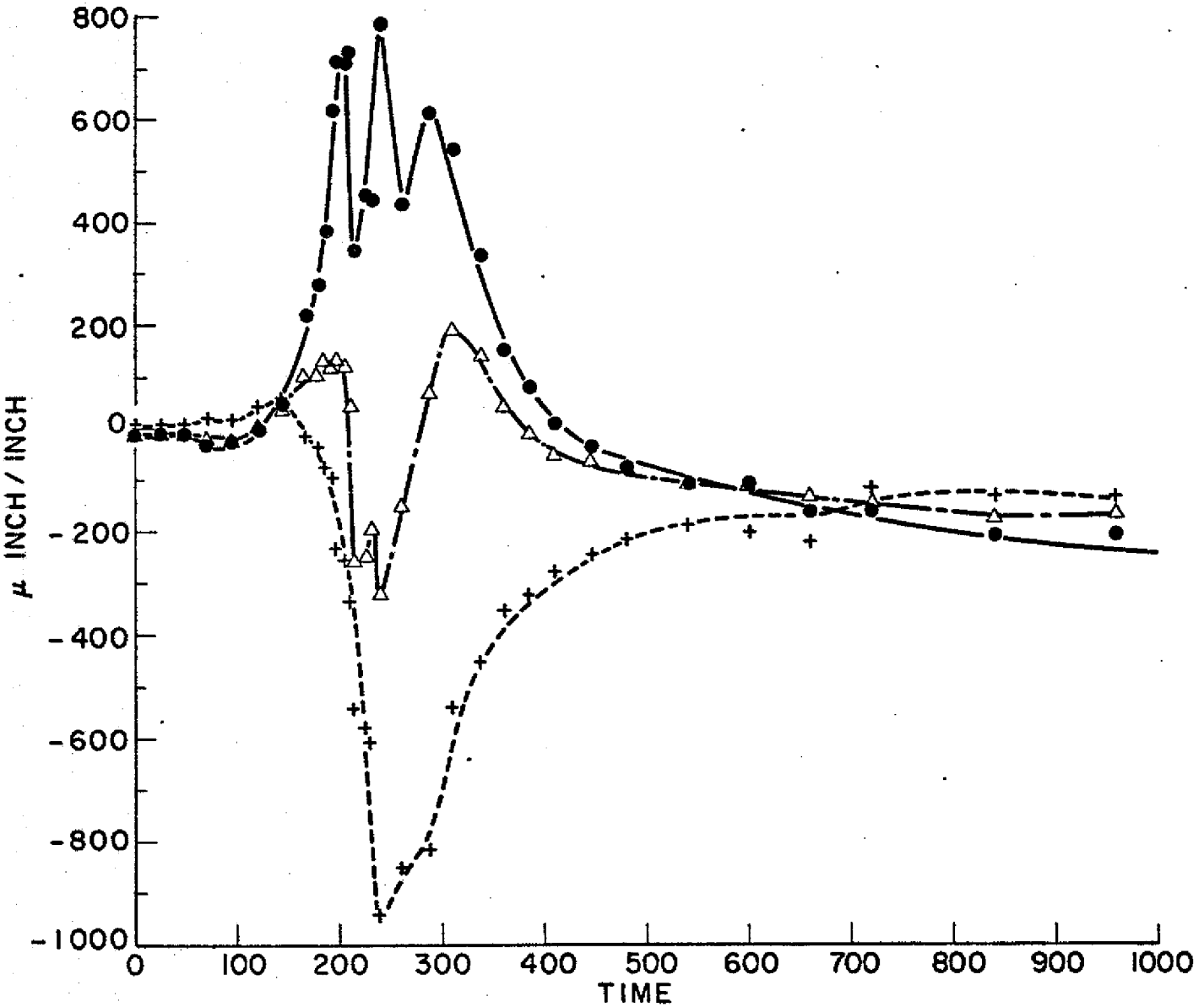

Figure 43 Calculated Strain Change during Welding of Tantalum Using Two-dimensional Program at Time Step after that Used in Figure 42.

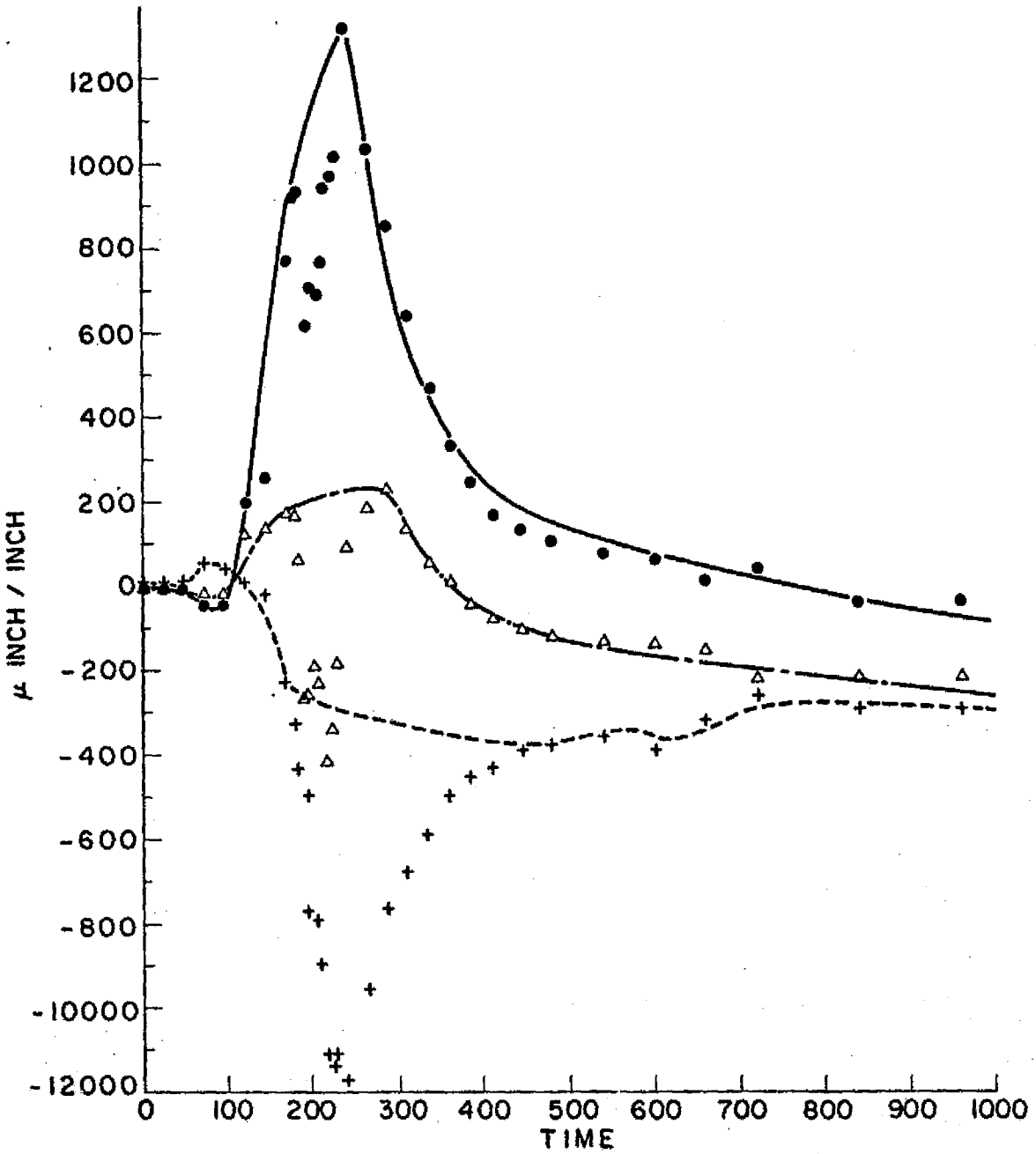

Figure 44 Calculated Strain Change during Welding of Columbium Using Twp-dimensional Program

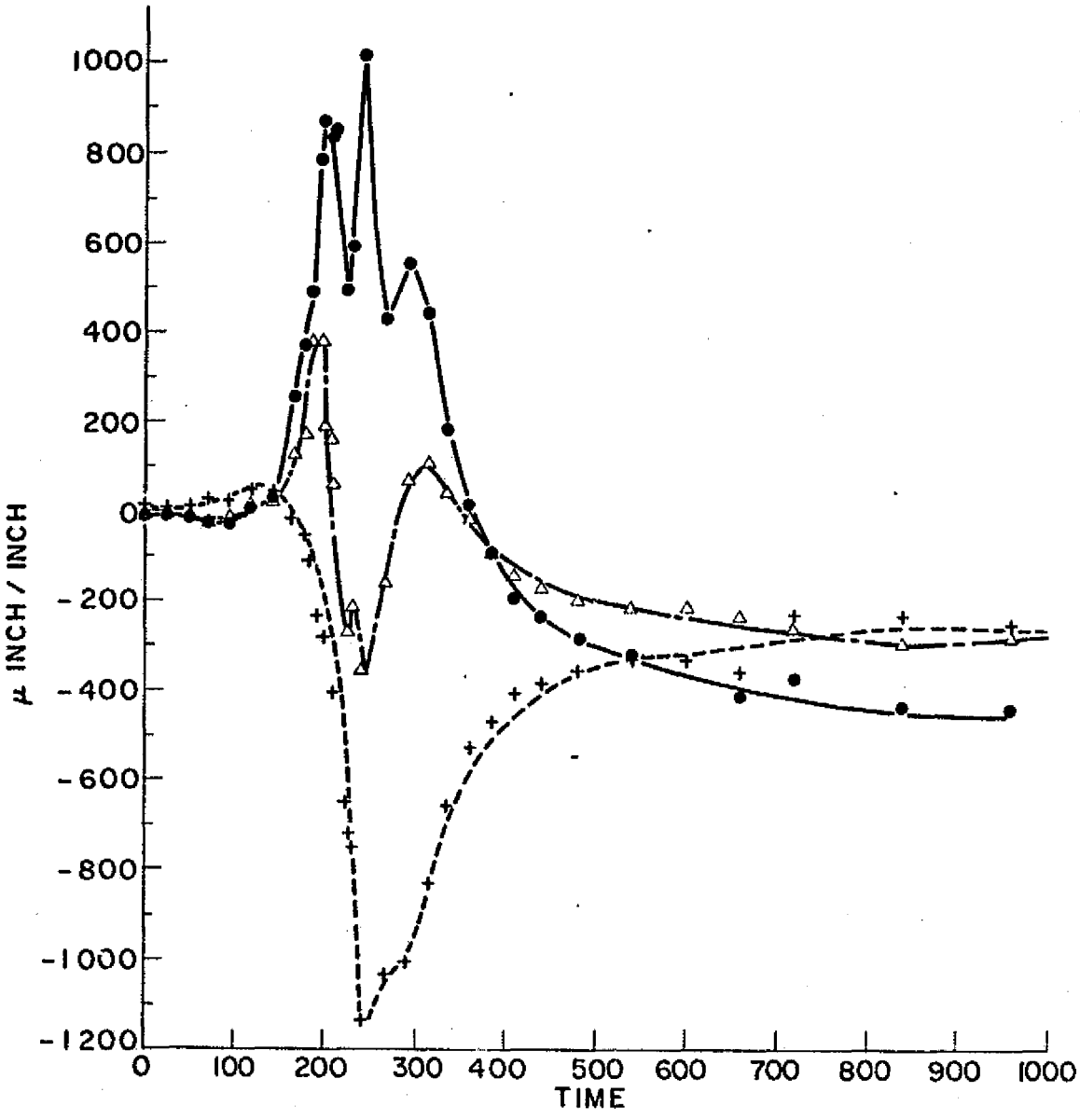

Figure 45 Calculated Strain Change during Welding of Columbium Using the Two-dimensional Program at Time Step after that used in Figure 44.

Also, the ratio of tantalum_{max} to columbium_{max} strain values were computed. Although the numbers did not agree, the peak height ratios fell in the 1.25-1.7 range the same as the one-dimensional and experimental results.

The second discrepancy with experimental results occurred as a dip in the theoretical peak at the point where the arc passed the strain gages. This was due to the nature of the finite element program. The time steps were unfortunately arranged such that the computer passed from one grid block to another just as the torch passed the gages. This is a correctable factor if the size and placement of grid blocks is changed. By ignoring the dip, the correct peak shape is obtained.

D. Residual Stress

Graphs of residual stress versus distance from the weld center line at successive times are shown in Figures 46 through 50. These values were taken from the one-dimensional program. The fact that the area near the weld becomes tensile as time progresses while the area away from the weld is compressive demonstrates the validity of the discussion on residual stress in the introductory section. The narrow width of the tensile zone indicates that there will be little post-weld buckling by the Watanabe-Satoh analysis.[6]

Figure 51 shows how the stress field changes with time at three different distances from the weld. The closest distance of .9 inches shows the greatest variation and

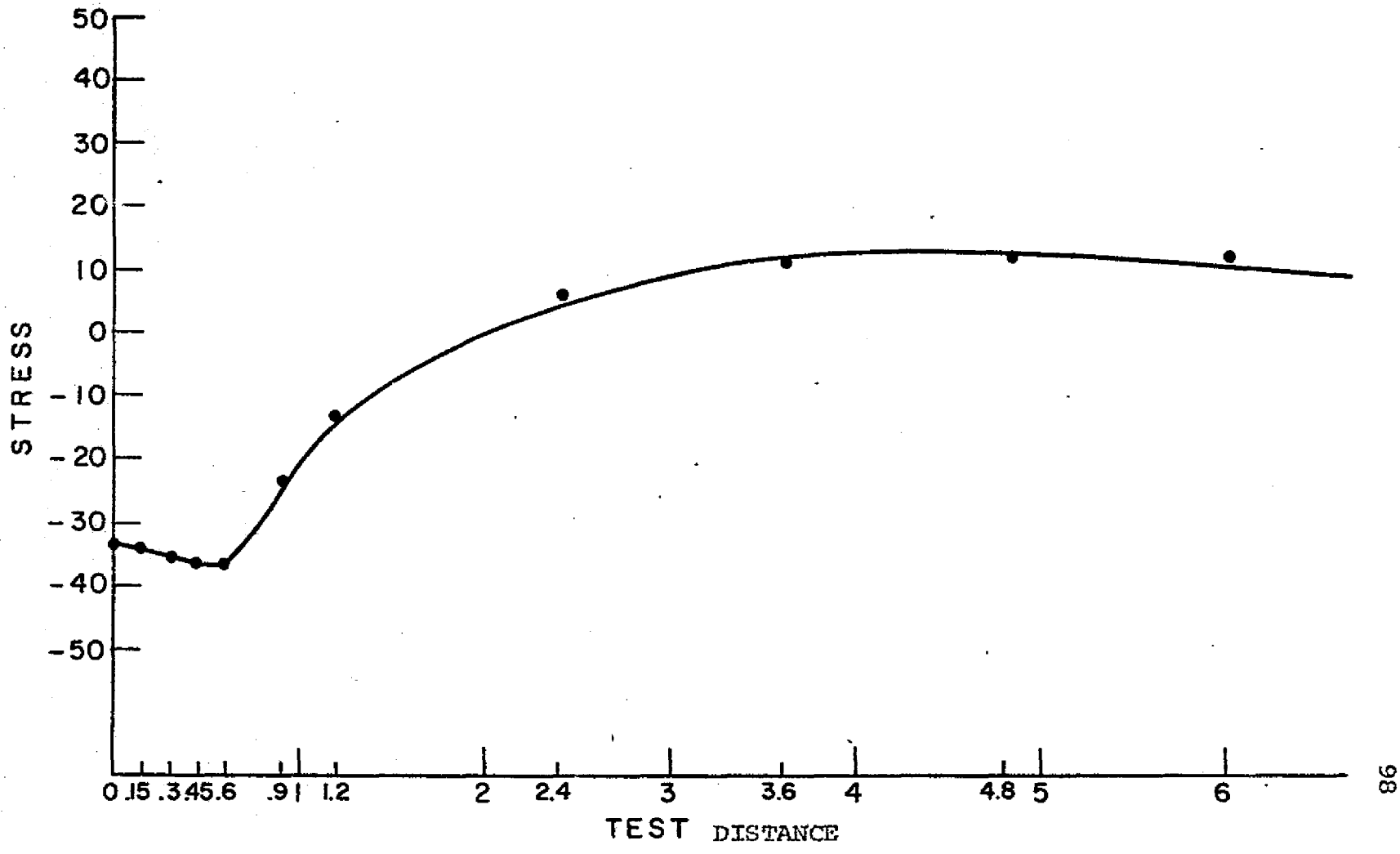

Figure 46 Calculated Change in Residual Stress with Distance from Weld Center during Welding of Tantalum, 5 seconds before arc reaches point of measurement.

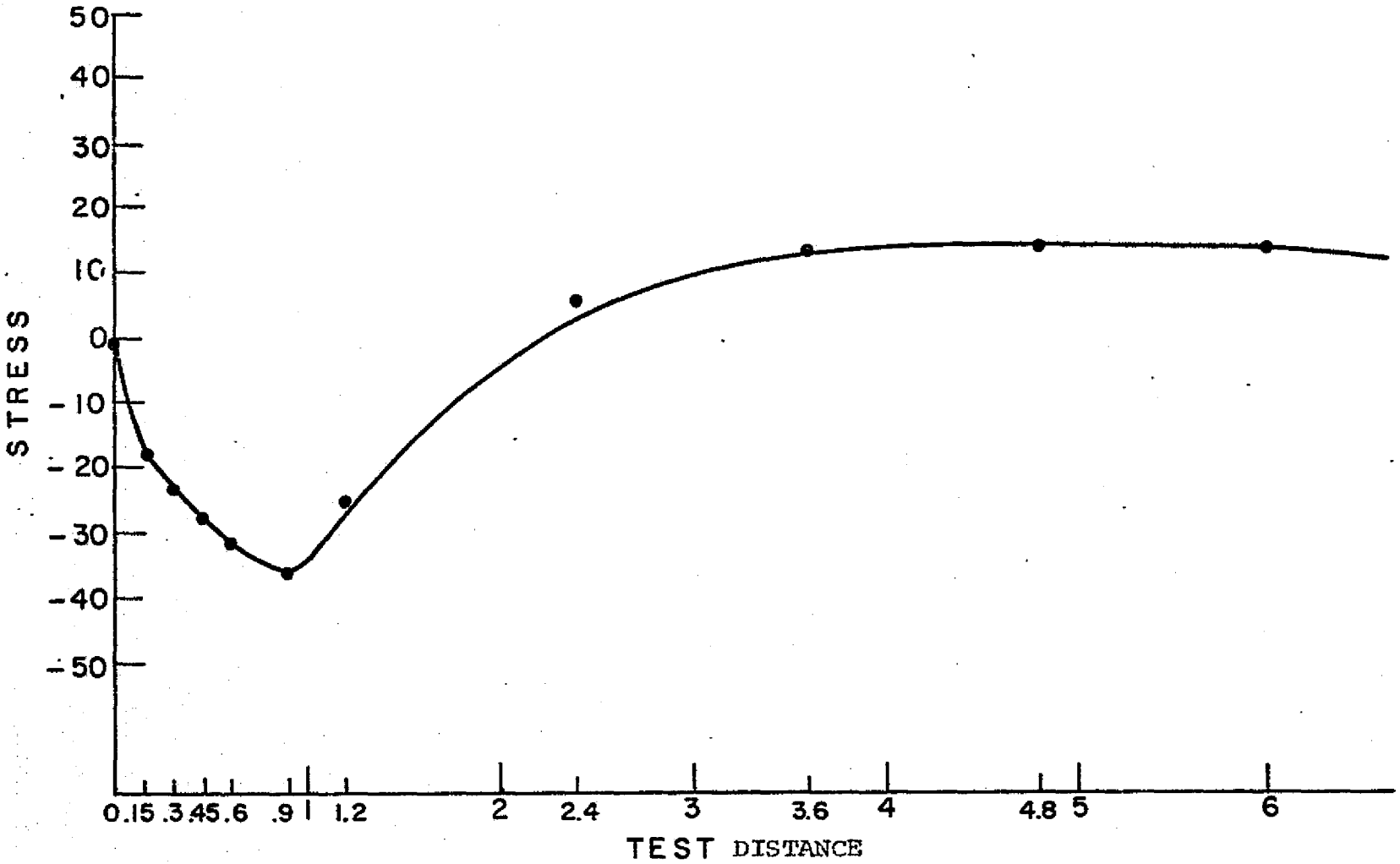

Figure 47 Calculated Change in Residual Stress with Distance from Weld Center during Welding of Tantalum Just as Arc Passes Point of Measurement

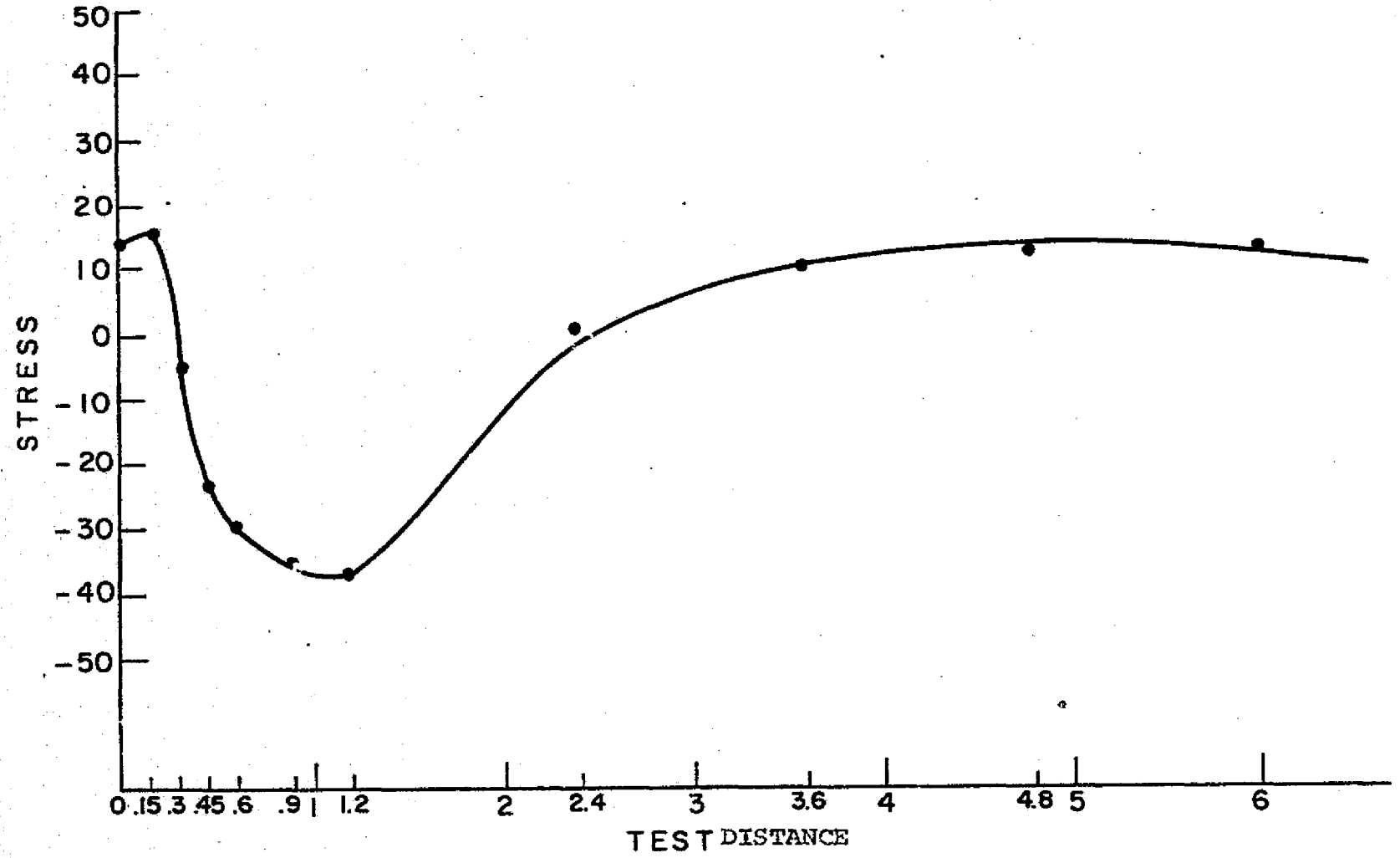

Figure 48 Calculated Change in Residual Stress with Distance from Weld Center during Welding of Tantalum, 5 seconds after Arc Passed Point of Measurement

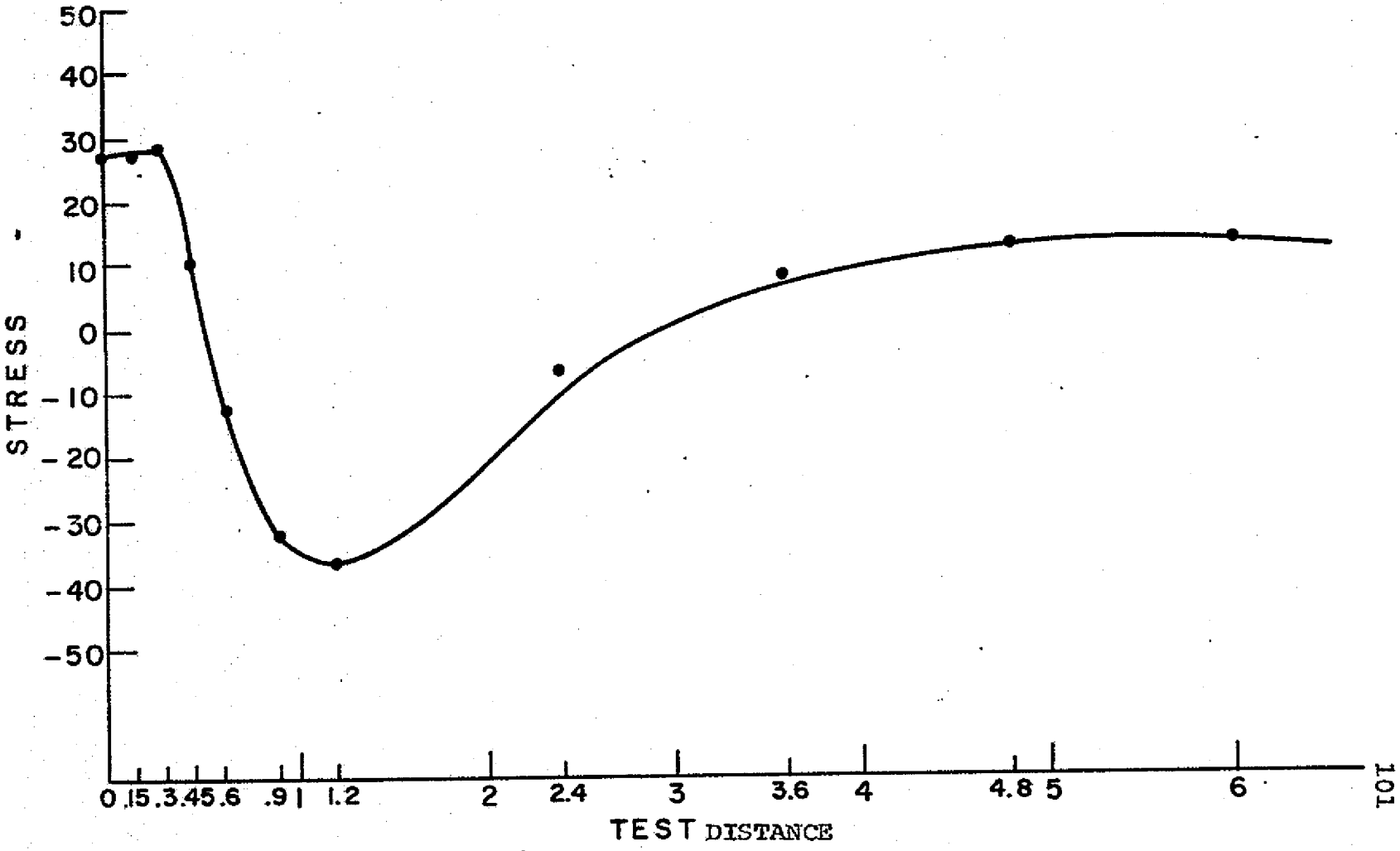

Figure 49 Calculated Change in Residual Stress with Distance from Weld Center during Welding of Tantalum, 15 Seconds after Arc Passed Point of Measurement

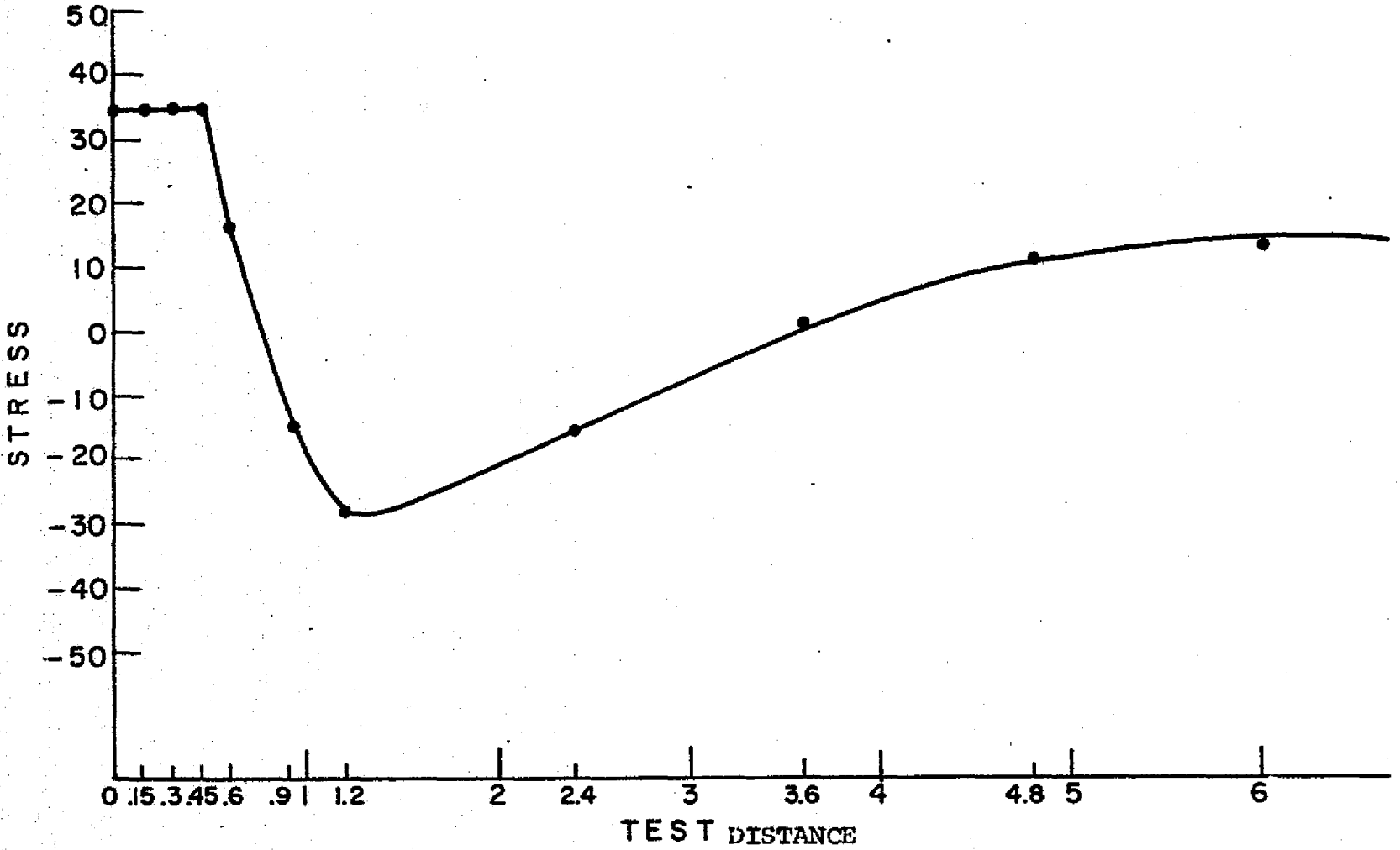

Figure 50 Calculated Change in Residual Stress with Distance from Weld Center during Welding of Tantalum, 35 seconds after Arc Passed Point of Measurement

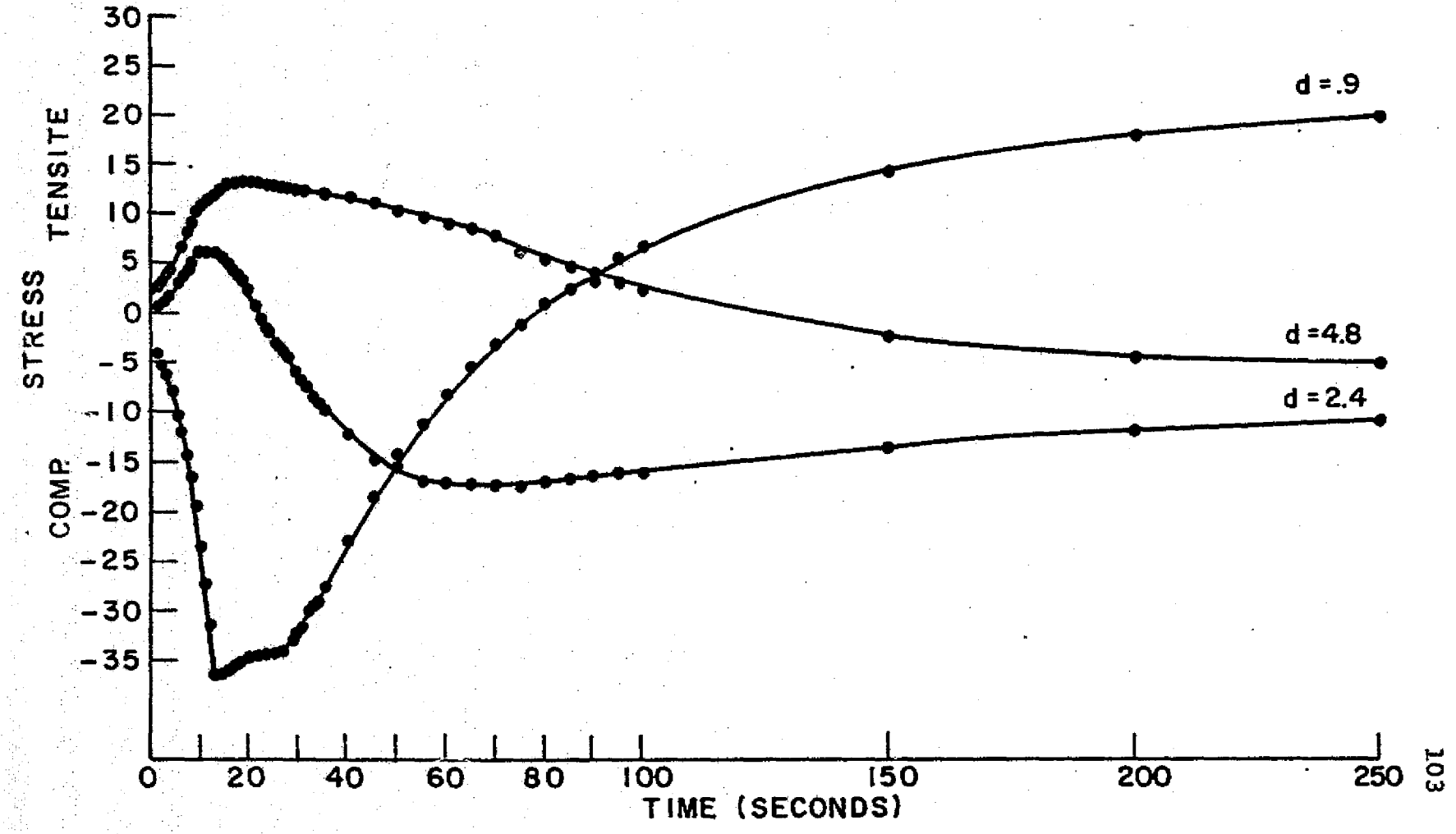

Figure 51 Calculated Change in Residual Stress with Time during Welding of Tantalum

stabilizes in the tensile region. The farthest distance from the weld varies only slightly from tensile to compressive. This is merely another method of demonstrating the same information that appears in Figures 46 through 50.

CONCLUSIONS

The purpose of this investigation was to determine the reactions produced by welding Tantalum and Columbium sheet and compare them with computer predictions.

1. The temperature distribution during welding of Tantalum and Columbium is comparable to that expected in other structural materials of similar thickness. This results in a thermal stress of suitable proportion to allow the use of Tantalum and Columbium as a structural material.

2. The weldability of Tantalum and Columbium was not sufficiently studied to be able to recommend the "best" technique, however, it appears that weldability is possible using present, but carefully controlled, production techniques.

3. Local thermal buckling may well be a major consideration in any attempt at fabrication using large Tantalum or Columbium sheet. Theoretical predictional ability is not currently state-of-the-art.

4. The previously developed one-dimensional computer program is an excellent tool for predicting expected stresses and strains. Experimental results and theoretical results were in complete agreement.

5. The two-dimensional program appears to be able to be developed in the future into a viable prediction tool. Currently the program needs some adjustment to give correct strain magnitudes.

RECOMMENDATIONS

1. Future welding of tantalum and columbium should be done in a more controlled atmosphere to prevent oxide contamination.

2. Asbestos lining should be used from the standpoint of analysis between any necessary backing plates and the base plate to prevent any unnecessary heat flow complications.

3. An extensive theoretical analysis of local buckling should be undertaken in an attempt to supply a viable mathematical model which can then be experimentally tested.

4. Further research should be done on how small the finite element grid size can be made and still remain cost effective.

5. The premise of the two-dimensional program should be changed in that the arc should never have to jump from one block to another, but the block should move along with the arc.

REFERENCES

[1] Masubuchi, K., et al, "Analysis of Thermal Stresses and Metal Movement during Welding," RSIC-820, Redstone Scientific Information Center, 1968

[2] Andrews, J. B., Masubuchi, K., "Analysis of Thermal Stress and Metal Movement during Welding," Report for M.I.T. of the Department of Naval Architecture and Marine Engineering, May, 1970

[3] Masubuchi, K., et al, "Analysis of Thermal Stresses and Metal Movement during Welding," Report to G. C. Marshall Space Flight Center, NASA, Contract No. NAS8-24365, 2 Vol. M.I.T., 1970

[4] Klein, K. M., "Investigation of Welding Thermal Strains in Marine Steels," Thesis for Master of Science degree, M.I.T., 1971

[5] Johnson, E., "Study of Flame Heating of Steel Plate," Thesis for Master of Science degree, M.I.T., 1971

[6] Watanabe, M., Satoh, K., "Welding Mechanics and Its Application," Asakura Publishing Company, Tokyo, 1965 (Japanese)

[7] Myers, et al, "Fundamentals of Heat Flow in Welding," WRC Bulletin 123, Welding Research Council, 1967

[8] Naka, T., Masubuchi, K., "Temperature Distribution during Welding," Parts I and II, Journal of the Japan Welding Society, Vol. 16, No. 7, pp. 281-290, Vol. 16, No. 12, pp. 374-378, 1947 (Japanese)

[9] Naka, T., Shrinkage and Cracking in Weldments, Komine Industrial Publishing Company, Tokyo, 1949 (Japanese)

[10] Tall, L., "Residual Stresses in Welded Plates--A Theoretical Study," The Welding Journal, Vol. 43, No. 1, pp. 10s-23s, 1964

[11] Masubuchi, K., "Control of Distortion and Shrinkage in Welding," WRC Bulletin 149, Welding Research Council, 1970

[12] Nowacki, W., Thermoelasticity, Addison-Wesley, Reading, Massachusetts, 1962

[13] Timoshenko, S., Theory of Plates and Shells, McGraw-Hill, New York, 1959

[14] Johns, D. J., Thermal Stress Analysis, Pergamon, London, 1965

[15] Parkus, H., Thermoelasticity, Blaisdell, Waltham, Massachusetts, 1968

[16] Cox, H. L., The Buckling of Plates and Shells, MacMillan, New York, 1963

[17] Carslow, H. S., Conduction of Heat in Solids, Oxford, 1948

APPENDIX B

Thesis by LCDR Jon J. Bryan

ANALYSIS OF TWO DIMENSIONAL THERMAL STRAINS AND METAL MOVEMENT DURING WELDING

by

LIEUTENANT COMMANDER JON JASPER BRYAN, USN
B.S., Northwestern University
1961

SUBMITTED IN PARTIAL FULFILLMENT
OF THE REQUIREMENTS FOR THE
DEGREE OF OCEAN ENGINEER AND
FOR THE DEGREE OF
MASTER OF SCIENCE IN NAVAL ARCHITECTURE AND
AND MARINE ENGINEERING

at the

MASSACHUSETTS INSTITUTE OF
TECHNOLOGY

May, 1973

Signature of Author.....
Department of Ocean Engineering
May, 1973

Certified by.....
Thesis Supervisor

Accepted by.....
Chairman, Departmental Committee
on Graduate Students

ANALYSIS OF TWO DIMENSIONAL THERMAL STRESSES AND METAL MOVEMENT DURING WELDING

by

Jon Jasper Bryan

Submitted to the Department of Ocean Engineering on May 11, 1973, in partial fulfillment of the requirements for the degrees of Ocean Engineer and Master of Science of Naval Architecture and Marine Engineering.

ABSTRACT

The strain response of metal plates during welding is discussed and current state-of-the-art efforts to analyze the phenomena are reviewed. Mechanical and physical temperature dependent properties; transient strain and temperature distribution data obtained from experiments on 6061 aluminum alloy in the T651 condition; and a data reduction computer program are presented. The experiments were designed to look at the macroscopic effects of welding upon heat treatable age hardened alloys while at the same time approximating ship structural weldments.

The transient strain response was found to be predominantly longitudinal but transverse strains were significant in the region of the welding arc. It was also found that residual strains correlated reasonably between similar experiments with a variation of the second stress deviator tensor invariant J_2 representing the "state of stress" rather than by individual strain components.

Several recommendations are made concerning continued experimental investigation aimed at further development of the National Aeronautics and Space Adminstration programs.

THESIS SUPERVISOR: Koichi Masubuchi

TITLE: Professor of Ocean Engineering & Materials Science

ACKNOWLEDGEMENT

I am grateful to the U.S. Navy for sponsoring my studies at MIT. Several individuals were of particular assistance: Messrs. Fred Merlis and Al Shaw of MIT's Aerolastics Laboratory and Mr. Anthony Zona of the Materials Joining Laboratory for being especially helpful in the preparation and running of my welding experiments; Mr. James Grant of the Application Engineering Division of ALCOA for allowing me to publish the half-hour heating cycle typical tensile stress-strain curves for the material I utilized and from which I based a considerable portion of my mechanical properties data; and, Miss Maureen Gallagher, who was always cheerful in her assistance in obtaining purchase orders for services and materials and in typing my thesis.

To Professor Koichi Masubuchi, who advised and guided me for the past three years as a professor and a friend, I am forever indebted.

Lastly, I acknowledge those all-encompassing laws governing experimental efforts identified with Murphy and wish to add another corollary: "If you don't understand the problem then you in all probability are part of it." My stay at MIT has directed me more towards understanding, but there will always be a part of us in every problem we deal with.

TABLE OF CONTENTS

LIST OF FIGURES

LIST OF TABLES

I: INTRODUCTION

A. Background:

The phenomenon of thermal stresses and strains resulting from welding processes lead to difficulties in the fabrication of structures. Non-uniform temperature distribution leads to residual stresses which in turn provide problems from stress corrosion, buckling, brittle fracture, fatigue strength, and distortion. Depending upon the type of material being welded, any or all of the above problems may be important considerations in the structure's design and its service performance (1). All contribute to the reliability of the basic structure (2, pp. 2). Masubuchi (2 - 5), Klein and Masubuchi (6), and Klein (7) provide interpretive reports which review the particulars of each of the above phenomena for aluminum and steel as well as comprehensive reviews of the literature. Almost all of the previous studies refer to residual stresses and distortion and only recently has much attention been given to the actual thermal stresses during welding. This is due to the complexity of the problem characterized by large temperature changes in small areas near the welding arc with its resulting non-elastic deformation, temperature dependency of the material properties and/or phase transformations, and complex boundary conditions resulting from conditions of geometry and multi-pass welding (3, pp. 2, 3).

P Thermal Stresses During Welding, Residual Stresses and Distortion:

In order to study the effects of residual stresses and distortion performance of welded structures, it is first necessary to understand the relative magnitude and distribution of residual stresses and distortion in weldments. The mechanism by which thermal stresses and strains are developed in welded plates is best described by Masubuchi (8,3, pp. 4-6) and is repeated here:

Figure 1 shows schematically changes of temperature and stresses during welding. A bead-on-plate weld is being made along the x-axis. The welding arc, which is moving at a speed, v, is presently located at the origin, O, as shown in Figure 1a.

Figure 1b shows temperature distribution along several cross section. Along Section A-A, which is ahead of the welding arc, the temperature change due to welding, ΔT, is almost zero. Along Section B-B, which crosses the welding arc, the temperature distribution is very steep. Along Section C-C, which is some distance behind the welding arc, the distribution of temperature change is as shown in Figure 1b-3. Along Section D-D, which is very far from the welding arc, the temperature change due to welding again diminishes.

Figure 1c shows the distribution of stresses along these sections in the x-direction, σ_x. Stress in the

y-direction, σ_y, and shearing stress, τ_{xy}, also exists in a two-dimensional stress field.*

Along Section A-A, thermal stresses due to welding are almost zero. The stress distribution along Section B-B is shown in Figure 1c-2. Stresses in regions underneath the welding arc are close to zero, because molten metal does not support loads. Stresses in regions somewhat away from the arc are compressive, because the expansion of these areas is restrained by surrounding metal that is at lower temperatures. Since the temperatures of these areas are quite high and the yield strength of the material is low, stresses in these areas are as high as the yield strength of material at corresponding temperatures. The magnitude of compressive stress passes through a maximum with increasing distance from the weld or with decreasing temperature. However, stresses in areas away from the weld are tensile and balance with compressive stresses in areas near the weld. In other words,

$$\int \sigma_x \cdot dY = 0 \qquad (1)$$

across Section B-B.** Thus, the stress distribution along

---

* In general three-dimensional stress field, six stress components, σ_x, σ_y, σ_z, τ_{xy}, τ_{zy}, τ_{zx} exist.

** Equation (1) neglects the effect of σ_y and τ_{xy} on the equilibrium condition.

Section B-B is as shown in Figure 1c-2.

Stresses are distributed along Section C-C as shown in Figure 1c-3. Since the weld metal and base metal regions near the weld have cooled, they try to shrink causing tensile stresses in regions close to the weld. As the distance from the weld increases, the stresses first change to compressive and then become tensile.

Figure 1c-4 shows the stress distribution along Section D-D. High tensile stresses are produced in regions near the weld, while compressive stresses are produced in regions away from the weld. The distribution of residual stresses that remain after welding is completed as is shown in the figure.

The cross-hatched area, M-M, in Figure 1a shows the region where plastic deformation occurs during the welding thermal cycle. The ellipse near the origin O indicates the region where the metal is melted. The region outside the cross-hatched area remains elastic during the entire welding thermal cycle.

As shown in Figure 1, thermal stresses during welding are produced by a complex mechanism which involves plastic deformation at a wide range of temperatures from room temperature up to the melting temperature. Because of the difficulty in analyzing plastic deformation, especially at elevated temperatures, mathematical analyses were limited

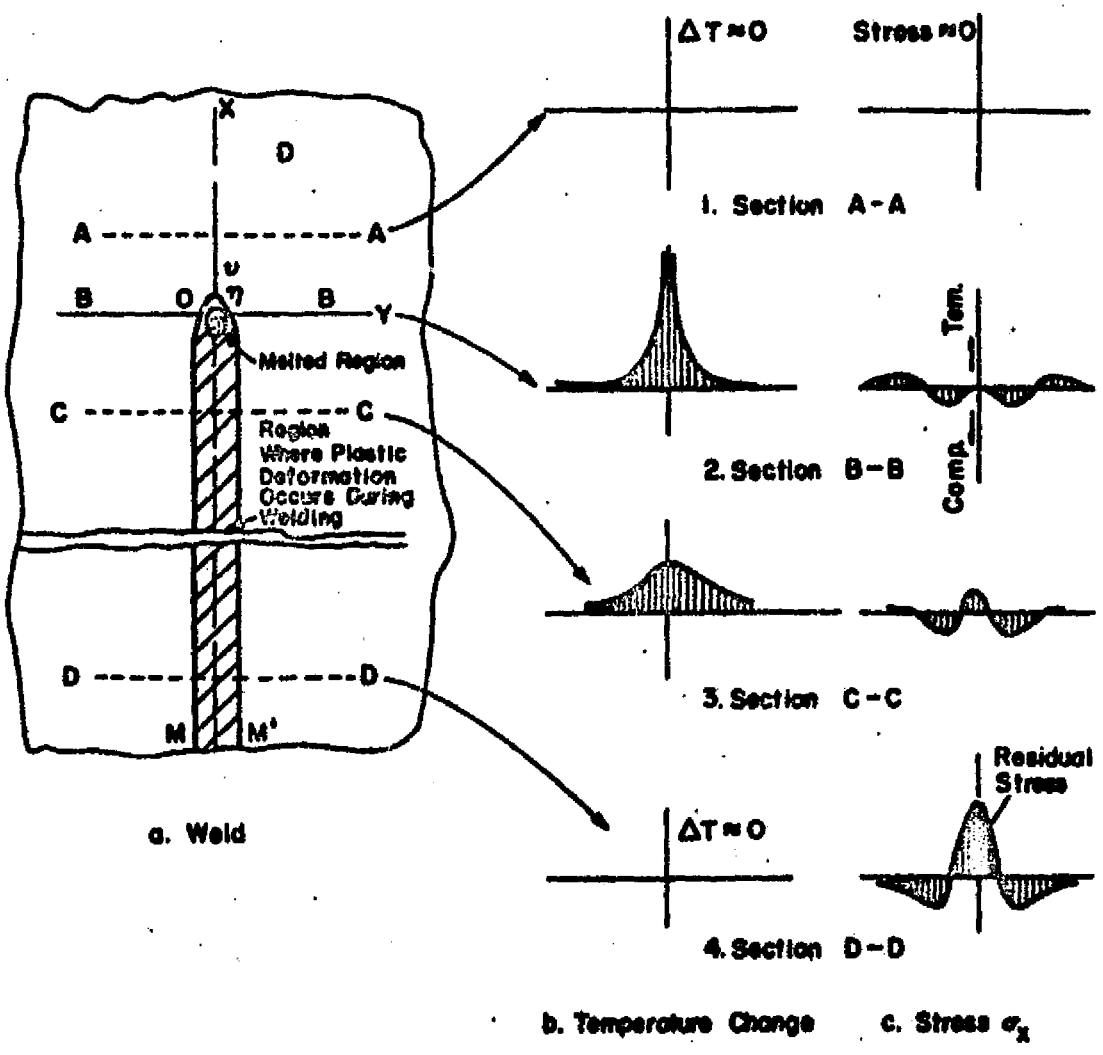

Figure 1 Schematic Representation of Changes of Temperature and Stresses During Welding (3,8).

for very simple cases such as spot welding.

However, on the basis of recent developments in computer technology, it appears that a technological breakthrough as far as the analysis of thermal stresses during welding are concerned is not too far away.

C. Previous Investigations:

The closest approach to a breakthrough to date has been the one-dimensional strip theory approach first presented by Tall (9) and extended by Masubuchi and associates at Battelle Memorial Institute (10) and Massachusetts Institute of Technology (7, 11, 12) under the support of NASA's George C. Marshall Space Flight Center. These studies have been reviewed in detail in references (3- 6) and will not be repeated here.

A great deal of effort in the last several years has been devoted to developing finite element programs which will extend one-dimensional analysis to two and three dimensions (13 - 20). Nearly all hav' met some qualitative success but in general, quantitative results have been lacking. The finite element method utilizes an approximate model to derive a set of equations which is then solved exactly. The flexibility of the finite element method will

allow the extension of the flat plate problem into more complex and real life geometries. It provides a complete strain picture, including longitudinal, transverse, and shear strains. It has the capability to model the restraint conditions in the actual structure and weld. Its greatest drawback is high expense from considerable computer time for large degree of freedom problems and the post analysis of the vast quantities of data the technique generates. Interactive graphics will greatly aid this latter problem in the future.

Masubuchi and Iwaki (13) and Masubuchi and Andrews (14) coupled the elastic-plastic analysis developed by Wang (15) with the thermal loading calculations for moving heat sources previously utilized by the one-dimensional programs. Reference (13) was qualitative and reference (14) provided some quantitative results with course meshes but appeared to have transition element instability when a smaller mesh was utilized. In this situation, an element which reaches yield stress is considered a transition element. However, in the next iteration, the equivalent stress from that element drops below yield and the element becomes elastic again. The whole situation jumps between the two sets of values. In order to overcome this difficulty, a scheme was devised to quarter the time step in which this instability occurred. This worked for a large number of cases

but not all cases. Sometimes increasing the time step also eliminated the instability. Reference (10) may offer a way to correct this problem. Yamada (17) seems to have met with more success dealing with thermal stresses due to rapid heating by controlling the number of elements which yield.

Hibbit and Marcal (18) offer the most analytic of the approaches to date. Their model treats the weld process as a thermo-mechanical problem. A finite element formulation derived from the uncoupled thermal and mechanical energy balances forms the basis of the model. It attempts to deal with material non-linearity due to temperature dependence of thermal properties and in the fusion problem where material phase change is accompanied by a latent heat effect. It includes radiation as a cooldown mechanism and finite strain effects during isothermal loading. However, there was little agreement with experimentally measured residual stresses and they concluded that their finite element model did not include significant material behavior.

Shinn (19) approaches the two-dimensional distortion of a panel structure due to welding with the assumption of elastic deformation during the welding process. Computations were carried out using the one-dimensional experimental values of unconstrained angular changes along the welded edge and its equivalent constrained welding

moment as an input to the computer program. The results were not completely successful because of the elastic assumption and the questionable accuracy of the experimental data input into the program. It is of the opinion of this author that this technique, on the basis of current technology, will provide the most fruitful results in the immediate future in terms of financial and manpower investments. The basic welding problem is highly non-linear and may be too complex to solve in a completely analytical form. A purely empirical approach does not appear very fruitful, either. It is not a simple task to determine thermal stresses in small regions heated to high temperatures. Without proper analysis, it would be difficult to adequately interpret experimental data.

The empirical-analytic technique, however, is only as good as experimental data provided. At present, material and physical properties at the range of temperature from room to melting, even for the most common of structural materials, are sorely lacking in the literature. More effort must be expended in providing this critical information. The approximations utilized in the interim will be the controlling feature of this computational technique.

D. Aim and Purpose of the Present Study:

Muraki and Masubuchi are presently developing a new elasto-plastic finite element computer program at Massachusetts Institute of Technology along the lines described by Yamada (17) with temperature distribution adopted from reference (20). It is the purpose of this report to provide experimental data on a heat treatable tempered aluminum alloy to verify this program. Electric resistance thermocouples, three element strain gage rosetts, single element strain gages, and an extensioneter will be utilized to obtain transient and residual strain and displacement data in the center and near the edge of 30x18 inch panels for an automatic GMA welding process. Experiments will be performed for bead-on-plate and butt welding processes under similar heat inputs to verify:

1. that experiments may be duplicated under reasonably similar conditions to give repeatable results;

2. to compare butt and bead-on-plate welds for similarities and differences;

to compare strains in both top and bottom of the plates to study the importance of bending strains as compared with transverse and longitudinal strains;

4. to observe transient principal strain magnitudes and directions;

5. to measure residual stress/strain distributions

in the longitudinal and transverse directions;

6. to measure the deflection of the two half plates in a butt welding process under tack welded conditions;

7. to present longitudinal and transverse strains for computational technique verification, and;

8. to collect and present in usable form available physical and mechanical temperature dependent data for use in the computer analysis.

Standard strain gages will be utilized which may not exceed 400°F. Since the material properties in the heat affected zone (HAZ) are not fully known or understood and the high temperature strain gages have proven unreliable (6, 7) in part because of temperature compensation data and in part by the lack of material properties data within the HAZ, strain measurements will be beyond the HAZ.

II: MATERIAL BEHAVIOR

A. General:

A new finite element program to study residual stresses and metal movement is presently being developed by M.I.T.'s Department of Ocean Engineering concurrent with this thesis. Since an attempt is being made here to provide material properties for and consistent with this new program, a brief and simple formulation of the tangent stiffness technique, incremental stress strain relationship, and thermal loading terms is provided for the sole purpose of demonstrating the importance of temperature dependency. Then, material properties consistent with this formulation are presented for 6061 aluminum alloy in the T6 and T651 condition, the material utilized for the experiments presented in Chapter III.

B. Mathematical Formulation:

The most common finite element approach to plasticity problems in welding has been the Tangent Stiffness Approach. The problem is first solved elastically for the general loads. Then the elastic limit loads are determined by scaling down the given loads until the element with the maximum equivalent stress is just reached. The differences between the given loads and the elastic limit loads are then

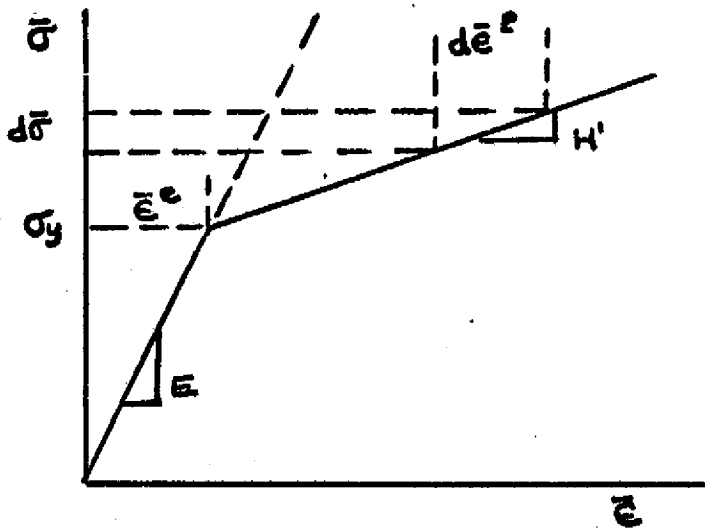

Figure 2: Equivalent Stress and Strain (14,pp 20)

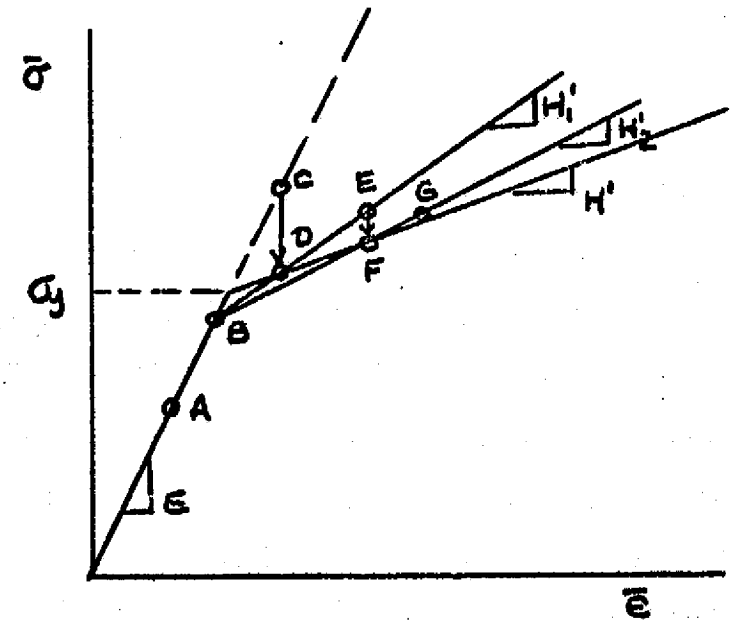

Figure 3: Iteration Process to Bring Back the Stress Point on to the $\bar{\sigma}$-$\bar{\varepsilon}$ curve with H'. The element in the transition region starts out at point B as elastic. The elastic increment BC of the element for the prescribed load increment dP is first calculated. The stress point corresponding to C should be D on the stress-strain curve. Using the modulus corresponding to BD, the increment BF for dP is next calculated. This process may be repeated until the solution converges (17, pp 300,303).

divided into a predetermined number of loading increments. The problem is then solved including plasticity for each element. When an element becomes plastic, the tangent stiffness approach is used to determine an effective elasto-plastic stiffness for that element. In this approach, the Prandtl-Reuss relation and the plastic modulus are combined with the elastic stress-strain relations to produce an incremental stress-strain relation which includes the effects of plasticity. These incremental relations depend upon the instantaneous stress levels in each element (14, pp. 4 - 5).

In general,

$$\underset{\sim}{d\sigma} = \underset{\sim}{E_t}\ \underset{\sim}{d\varepsilon} \qquad (2)$$

where $\underset{\sim}{E_t}$ is the tangent modulus coefficient. $\underset{\sim}{E_t}$ has an elastic term and a plastic term. The plastic term is zero if no yielding takes place. Then, $\underset{\sim}{E_t}$ may be used to establish the tangent stiffness array $\underset{\sim}{K_n}$ for each element,

$$\underset{\sim}{K_n} = \int_{\text{Volume}} \underset{\sim}{B_n^t}\ \underset{\sim}{E_t}\ \underset{\sim}{B_n}\ d\ (\text{Volume}) \qquad (3)$$

where $\underset{\sim}{B_n}$ defines the strain displacement relationships. Thus, where loading is applied in increments, the structure stiffness array may be found at each stage of loading by evaluating each element's tangent stiffness (21, pp. 12 - 13).

The incremental pseudo-thermal loading term likewise

becomes

$$\underset{\sim}{dP_n} = \int_{\text{Volume}} \underset{\sim}{B_n^t}\, \underset{\sim}{E_t}\, \underset{\sim}{d\varepsilon_t}\, d\,(\text{Volume}) \tag{4}$$

where $\underset{\sim}{d\varepsilon_t}$ is the thermal strain caused by the welding process. Summed over the entire structure, one obtains:

$$\underset{\sim}{K}\,\underset{\sim}{dU} = \underset{\sim}{dP} \tag{5}$$

$$\underset{\sim}{dU} = \underset{\sim}{K^{-1}}\,\underset{\sim}{dP} \tag{6}$$

$$\underset{\sim}{d\varepsilon} = \underset{\sim}{B^t}\,\underset{\sim}{dU} \tag{7}$$

$$\underset{\sim}{d\sigma} = \underset{\sim}{E_t}\,\underset{\sim}{B^t}\,\underset{\sim}{dU} \tag{8}$$

To determine the tangent modulus coefficient related to equation (2), one must consider the following relations:*

Prandtl-Reuss Flow Rule:

$$\underset{\sim}{d\varepsilon^p} = \frac{\partial \bar{\sigma}}{\partial \underset{\sim}{\sigma}}\, d\bar{\varepsilon}^p \tag{9}$$

Yielding Surface Behavior:

$$d\bar{\sigma} = \frac{\partial \bar{\sigma}}{\partial \underset{\sim}{\sigma}}^T\, \underset{\sim}{d\sigma} \tag{10}$$

Material Behavior:

$$\bar{\sigma} = \bar{\sigma}_o + E_t^p\, \bar{\varepsilon}_p = \bar{\sigma}_o + H'\bar{\varepsilon}_p \tag{11}$$

$$d\bar{\sigma} = E_t^p\, d\bar{\varepsilon}_p = H'\, d\bar{\varepsilon}_p \tag{12}$$

Utilizing equations (9) - (12) and recalling that

---

* The p and e superscripts refer to plastic and elastic respectively.

$$\underset{\sim}{d\sigma} = \underset{\sim}{D}\underset{\sim}{d\varepsilon}^{e} = \underset{\sim}{D}\,(\underset{\sim}{d\varepsilon} - \underset{\sim}{d\varepsilon}^{p}) \qquad (13)$$

where $\underset{\sim}{d\varepsilon}$ is the total incremental strain and $\underset{\sim}{D}$ is given in Equation (24) for the plane stress situation, one arrives at the following relationship:

$$\underset{\sim}{d\sigma} = \left\{ \underset{\sim}{D} - \underset{\sim}{D}\frac{\partial\bar{\sigma}}{\partial\underset{\sim}{\sigma}} \left[\frac{\frac{\partial\bar{\sigma}}{\partial\underset{\sim}{\sigma}}^{T} \underset{\sim}{D}}{H^{1} + \frac{\partial\bar{\sigma}}{\partial\underset{\sim}{\sigma}}^{T} \underset{\sim}{D} \frac{\partial\bar{\sigma}}{\partial\underset{\sim}{\sigma}}} \right] \right\} \underset{\sim}{d\varepsilon} \qquad (14)$$

This reduces to equation (2) where the quantity in $\{\ \}$ is the tangent modulus coefficient. This is consistent with reference (17, pp. 310).

If we assume plane stress conditions and consider the equivalent stress for Von Mises' isotropic material,

$$\bar{\sigma}^{2} = \sigma_x^{2} - \sigma_x\sigma_y + \sigma_y^{2} + 3\tau_{xy}^{2} \qquad (15)$$

Differentiating,

$$d\bar{\sigma} = \frac{1}{2\bar{\sigma}} \left[(2\sigma_x - \sigma_y)\, d\sigma_x + (2\sigma_y - \sigma_x)\, d\sigma_y + 6\tau_{xy} d\tau_{xy} \right] \qquad (16)$$

This may be rewritten in matrix form as

$$d\bar{\sigma} = \frac{1}{\bar{\sigma}}\, \underset{\sim}{\sigma}^{T} \begin{bmatrix} 1 & -\frac{1}{2} & 0 \\ -\frac{1}{2} & 1 & 0 \\ 0 & 0 & 3 \end{bmatrix} \underset{\sim}{d\sigma} \qquad (17)$$

or

$$d\bar{\sigma} = \frac{1}{\bar{\sigma}}\, \underset{\sim}{\sigma}^{T}\, \underset{\sim}{F}\, \underset{\sim}{d\sigma} \qquad (18)$$

where

$$\underset{\sim}{\sigma} = \begin{bmatrix} \sigma_x \\ \sigma_y \\ \tau_{xy} \end{bmatrix} \quad (19) \qquad \underset{\sim}{d\sigma} = \begin{bmatrix} d\sigma_x \\ d\sigma_y \\ d\tau_{xy} \end{bmatrix} \quad (20)$$

Comparing equations (10) and (18), we see that

$$\frac{\partial \bar{\sigma}}{\partial \underset{\sim}{\sigma}}^T = \frac{1}{\bar{\sigma}} \underset{\sim}{\sigma}^T \underset{\sim}{F} \quad (21)$$

Transposing,

$$\frac{\partial \bar{\sigma}}{\partial \underset{\sim}{\sigma}} = \frac{1}{\bar{\sigma}} \underset{\sim}{F}^T \underset{\sim}{\sigma} = \frac{1}{\bar{\sigma}} \underset{\sim}{F}\, \underset{\sim}{\sigma} \quad (22)$$

Substituting the previous relationships into equation (14) we arrive at

$$\underset{\sim}{d\sigma} = \left[\underset{\sim}{D} - \frac{\underset{\sim}{D}\,\underset{\sim}{F}\,\underset{\sim}{\sigma}\,\underset{\sim}{\sigma}^T\,\underset{\sim}{F}\,\underset{\sim}{D}}{\bar{\sigma}^2 H' + \underset{\sim}{\sigma}^T\,\underset{\sim}{F}\,\underset{\sim}{D}\,\underset{\sim}{F}\,\underset{\sim}{\sigma}} \right] \underset{\sim}{d\varepsilon} \quad (23)$$

for a two dimensional, plane stress, isotropic case, with the Von Mises' yield criterion where

$$\underset{\sim}{D} = \frac{E}{1 - \nu^2} \begin{bmatrix} 1 & \nu & 0 \\ 0 & 1 & 0 \\ 0 & 0 & \frac{1-\nu}{2} \end{bmatrix} \quad (24)$$

$$\underset{\sim}{F} = \begin{bmatrix} 1 & -\frac{1}{2} & 0 \\ -\frac{1}{2} & 1 & 0 \\ 0 & 0 & 3 \end{bmatrix} \quad (25)$$

$$\bar{\sigma}^2 = \sigma_x^2 - \sigma_x\sigma_y + \sigma_y^2 + 3\tau_{xy}^2 \quad (15)$$

Equation (23) is but a simple example of the more complex general case. The important point to note here is that E, $\bar{\sigma}$, and H' are functions of temperature and this makes quite complex even the most simple of welding problem examples.

In the previous study at the Massachusetts Institute of Technology, Andrews (14, pp. 25) assumed the simplest model possible for the nodal force matrix, i.e., that of a constant temperature of each element. In this case, the nodal force matrix for each increment becomes

$$\underset{\sim}{dP}_n = \int_{\text{Volume}} (\underset{\sim}{B}^T_n \underset{\sim}{E}_t \underset{\sim}{d\varepsilon}_t) \, d\,(\text{Volume}) \qquad (4)$$

$$\underset{\sim}{d\varepsilon}_t = \Delta T \begin{bmatrix} \alpha \\ \alpha \\ 0 \end{bmatrix}$$

where

ΔT = average temperature change of element

α = coefficient of linear thermal expansion

If the element in question is plastic, the tangent stiffness matrix is used. Masubuchi and Iwaki (13, pp. 9) assumed a much more complex loading function which accounted for the equivalent nodal forces due to the dependency of the coefficient of thermal expansion and Young's modulus on temperature. The plastic terms additionally took the temperature dependency of the yield surface into account. Yielding is complex. It can occur during the heating stage

and also in the subsequent cooling stage since some elements can be stressed to their yield point in the reverse direction. Yamada (17, pp. 298) assumed the same simplified type of expression as equation (4) in his study of thermal stresses due to rapid heating. As in the case of the incremental stress-strain relation, the important point to note is that in varying degrees of difficulty, the loading term is dependent upon E, $\bar{\sigma}$, and α which are in turn dependent upon temperature.

The temperature distribution, uncoupled from the mechanical problem just described, may be approximated by classical, finite difference, or finite element techniques (9-11, 13, 14, 18, 20, 24-30). In terms of the conductivity tensor, κ, the general representation of the anisotropic heterogeneous continuum is

$$\rho c \frac{dT}{dt} = \nabla \cdot (\kappa \cdot \nabla T) + U''' \qquad (25)$$

where ρ is the density, c is the specific heat, κ is the thermal conductivity, and U''' is the heat generation per unit volume (23, pp. 29, 44-45). Fourier's law applied to the boundary conditions provides

$$q = -\kappa \cdot \nabla T \qquad (26)$$

where q is the heat flux normal to the boundary surface. If the continuum is isotropic, these vector equations reduce to the familiar

$$\rho c \frac{dT}{dt} = \nabla \cdot (\kappa \nabla T) + U''' \tag{27}$$

$$q = -\kappa \nabla T \tag{28}$$

Equation (27) may be reduced to

$$\rho c \frac{dT}{dt} = \nabla \kappa \cdot \nabla T + \kappa \nabla^2 T + U''' \tag{29}$$

If κ is a function of space only, equation (29) is linear. On the other hand, where κ depends on temperature alone,

equation (29) may be modified to:

$$\rho c \frac{dT}{dt} = \frac{dU}{dT} (\nabla T)^2 + \kappa \nabla^2 T + U''' \qquad (30)$$

which is nonlinear. For homogeneous isotropic continua κ is constant and equation (29) reduces to

$$\frac{dT}{dt} = a\nabla^2 T + \frac{U'''}{\rho c} \qquad (31)$$

where a is the thermal diffusivity. Since ρ, c, and κ are functions of temperature, the welding problem becomes highly nonlinear. Coupled with phase changes, this problem becomes even more complex.

C. Material Properties:

As discussed in Section B, tabulation of the material properties as a function of temperature is of prime importance. This information is difficult to obtain and often simply is not available. In this experimental work, alloy 6061 in the T651 Condition is utilized. It is one of the most versatile of the wrought, heat treatable aluminum alloys. An understanding of the behavior of this common, relatively inexpensive material during welding and heat treating may also contribute to the understanding of the behavior of quenched and tempered steels such as HY-80 and HY-130 currently in use today. 6061 is readily welded by all methods and has excellent weldability characteristics.

The plate used in this experiment has a Federal Specification of QQA-250/11.

1. Composition (31, Code 3206, pp. 1)

	Percent	
	Min.	Max.
Chromium	0.15	0.35
Copper	0.15	0.40
Iron	-	0.7
Magnesium	0.8	1.2
Manganese	-	0.15
Silicon	0.40	0.8
Titanium	-	0.15
Zinc	-	0.25
Other impurities		
each	-	0.05
total	-	0.15
Aluminum	Balance	

TABLE 1: Composition of 6061 Aluminum Alloy

2. Heat Treatment (31, Code 3206, pp. 1)

Annealed (0 Condition): Heat to 775°F for 2 to 6 hours, cool at 50°F per hour maximum to 500°F. The rate of subsequent cooling is unimportant.

T4 Condition: Solution heat treat to 970°F, water quench, and naturally age at room temperature to a substantially stable condition.

T6 Condition: Solution heat treat to 970°F, water quench, artificially age by precipitation heat treatment at 320°F for 16 to 20 hours or 350°F 6 to 10 hours and

air cool.

T651/T451 Condition: Same as the T6/T4 Condition followed by a 1 1/2 to 3 percent permanent set stretch stress relief prior to any precipitation heat treatment.

The soft, as quenched 0 Condition can be preserved by refrigeration in order to minimize springback and increase the general ease of forming operations. Maximum holding times which will preserve the formability of this condition are shown in Table 2 (31, Code 3206, pp. 3).

Temperature °F	R.T.	32	20
Time	2 hours	2 days	7 days +

TABLE 2: Holding Times for 6061 in 0 Condition

3. Specified Mechanical Properties (31, Code 3206, pp. 2)

TABLE 3: Specified Mechanical Properties.

Condition	0	T4, T451	T6, T651
Thickness - in.	0.250	0.250	0.250
Ultimate Stress in Tension min. ksi	22	30	42
0.2% Offset Yield Stress in Tension min - ksi	12	16	35
Ultimate Elongation 2 inch min - %	18	16 - 18	6 - 10
Ultimate Shear Stress Typical - ksi	12	24	30

4. Mechanical Properties:

In welding aluminum, it must be remembered that the metal in the area of the weld will be in an annealed condition after welding. There will be a corresponding loss of strength unless heat treatment is done after welding. Welding does not always reduce the strength of the heat treated alloys to that of the fully annealed condition because there is some air quenching of the metal as it cools (32, pp. 6.33). Table 4 (32, pp. 6.34) demonstrates this effect for the type of filler metal utilized in this experiment.

Filler Wire	Specified minimum tensile strength of base plate in ksi.	Average tensile strength across weld in ksi.	Average bend free elongation %
	Not heat treated after welding		
4043	42.0	27.2	16.0
	Heat treated and aged after welding		
4043	42.0	43.5	11.0

TABLE 4: Strength and Ductility of Welded Butt Joints in Aluminum (TIG and GMA with argon).

Brungraber and Nelson (33) report that 6061 alloy may be heated up to 550°F by butt welding without appreciably affecting the mechanical properties of the base plate. They further report that for thicknesses less than one

inch, the distance from the center of the weld to the edge of the heat affected zone (HAZ) may be predicted as:

$$b_h = 0.6t + 0.00059 \frac{EI}{Vt} \qquad (32)$$

where E has units of volts, I amperes, V inches per minute, and t (thickness) inches. As an example, for E = 20., I = 240., t = .25 and V = 32.16, EI/Vt = 597 watt - min/in^2, and b_h = .50 inch. The extent of the fusion zone may depend somewhat on the parameter EI/Vt but it is governed primarily by the thickness t of the plate and the geometry of the edge preparation.

Figures 4 through 10 provide mechanical properties at both room temperature and elevated temperatures. Figure 4 provides typical tension and compression stress strain curves for the experimental plate. Figure 5 provides the average stress strain curves for varying temperatures from room temperature to 700°F based on a half hour exposure to the temperature in question. This may or may not be a valid approximation for the welding problem, but it is the only information currently available. Figure 6 shows the effect of this temperature on the 0.2% offset yield stress. This may be approximated as the cubic polynomial given in Table 5. Figure 7 demonstrates the effect of the half hour soak temperature on Young's

modulus. This curve was generated from Figure 5. Its cubic approximation is listed in Table 5.

Figure 8 shows the room temperature tangent modulus at various stress levels. Its straight line approximation is

$$H' \times 10^{-3}(\text{ksi}) = 0.917\sigma\ (\text{ksi}) + 38.064 \tag{33}$$

The highest stress level shown on this figure is 40.7 ksi. This equates to $H' = 0.746 \times 10^{+3}$ ksi and may be utilized effectively for constant strain hardening. Figure 9 represents an estimate of the temperature effects on the tangent modulus. If one assumes that

$$H'(T°F) \propto E(T°F) \tag{34}$$

then

$$H'(T°F) = \frac{H'(R.T.) \times E(T°F)}{E(R.T.)} \tag{35}$$

Masubuchi and Andrews (11) define the constant strain hardening parameter for their one-dimensional computer program as

$$H' = mE \tag{36}$$

From the above equations,

$$m = H'/E = H'(T°F)/E(T°F) = 0.0742 \tag{37}$$

This is the first such value ever determined for their

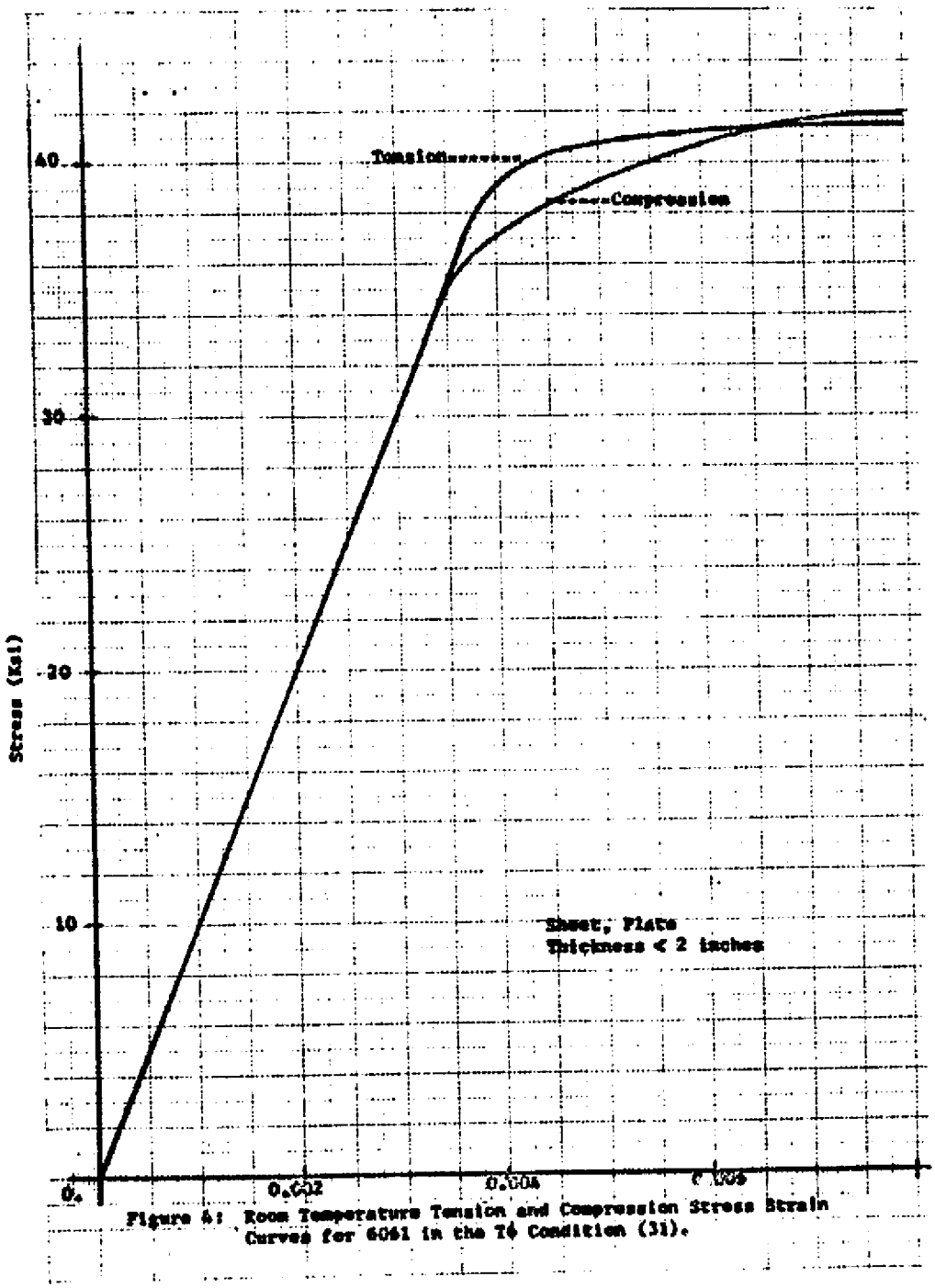

Figure 4: Room Temperature Tension and Compression Stress Strain Curves for 6061 in the T6 Condition (31).

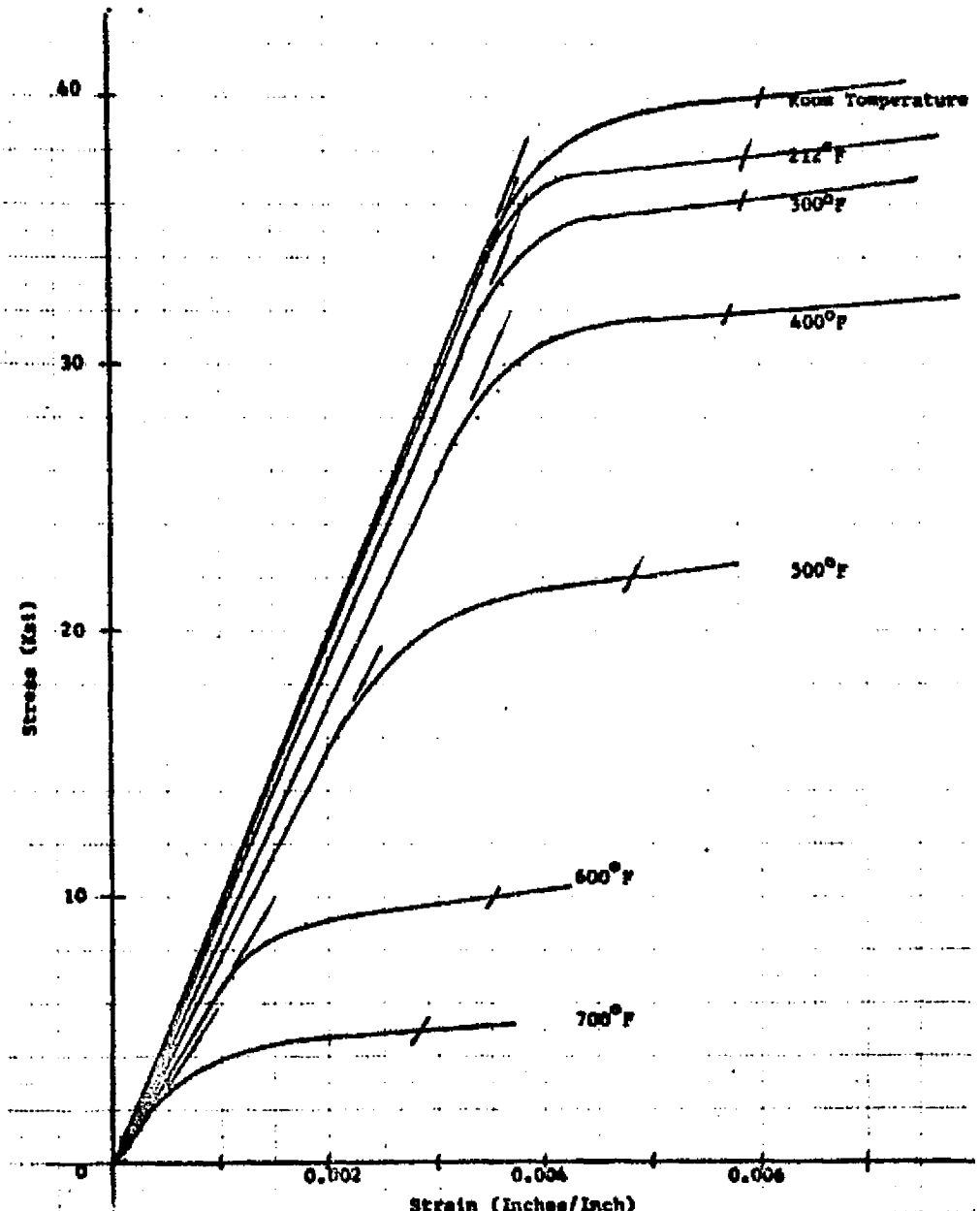

Figure 5: Stress Strain Curves for 6061 in T6 Condition after 0.5 Hour at Temperature (31,32)

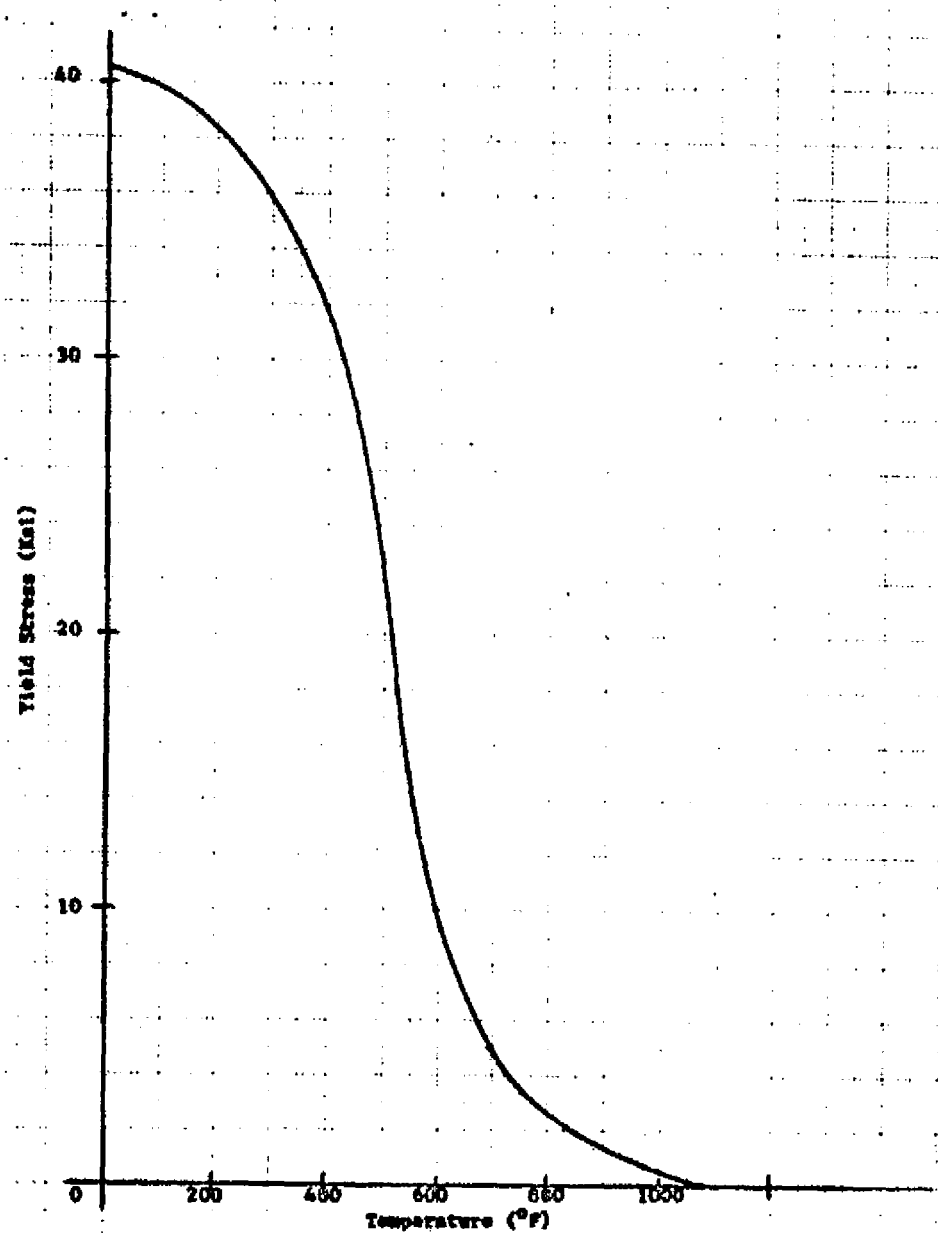

Figure 6: Effect of Temperature on 0.2% Off-set Yield Stress for 6061 in T6 Condition. (31,32)

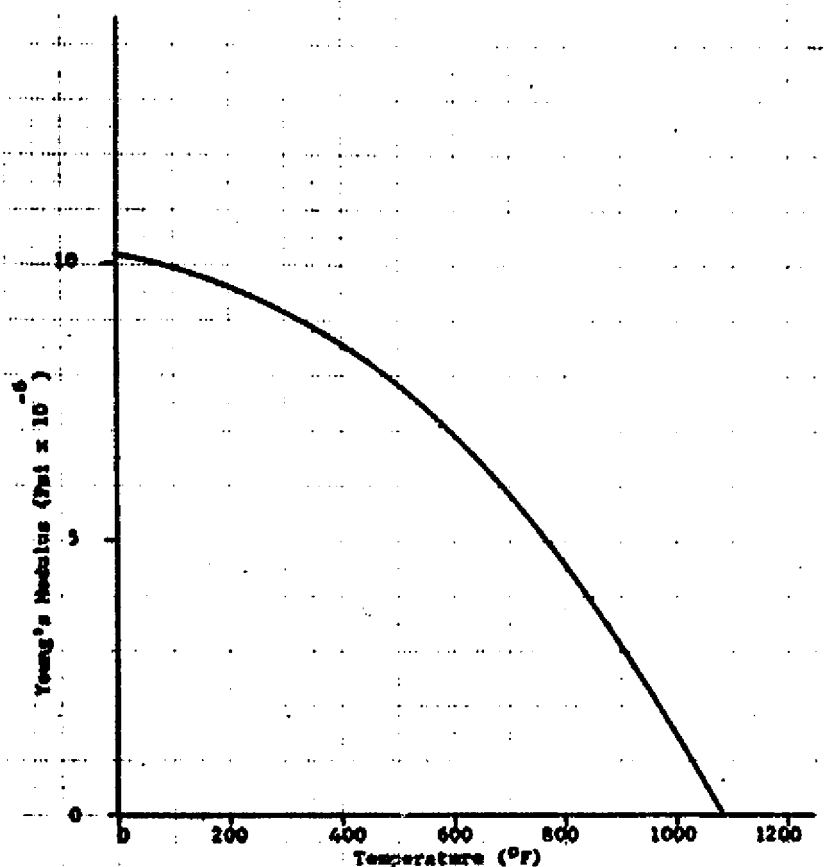

Figure 7: Estimated Effect of Temperature on Young's Modulus for 6061 in T6 Condition (31,32).

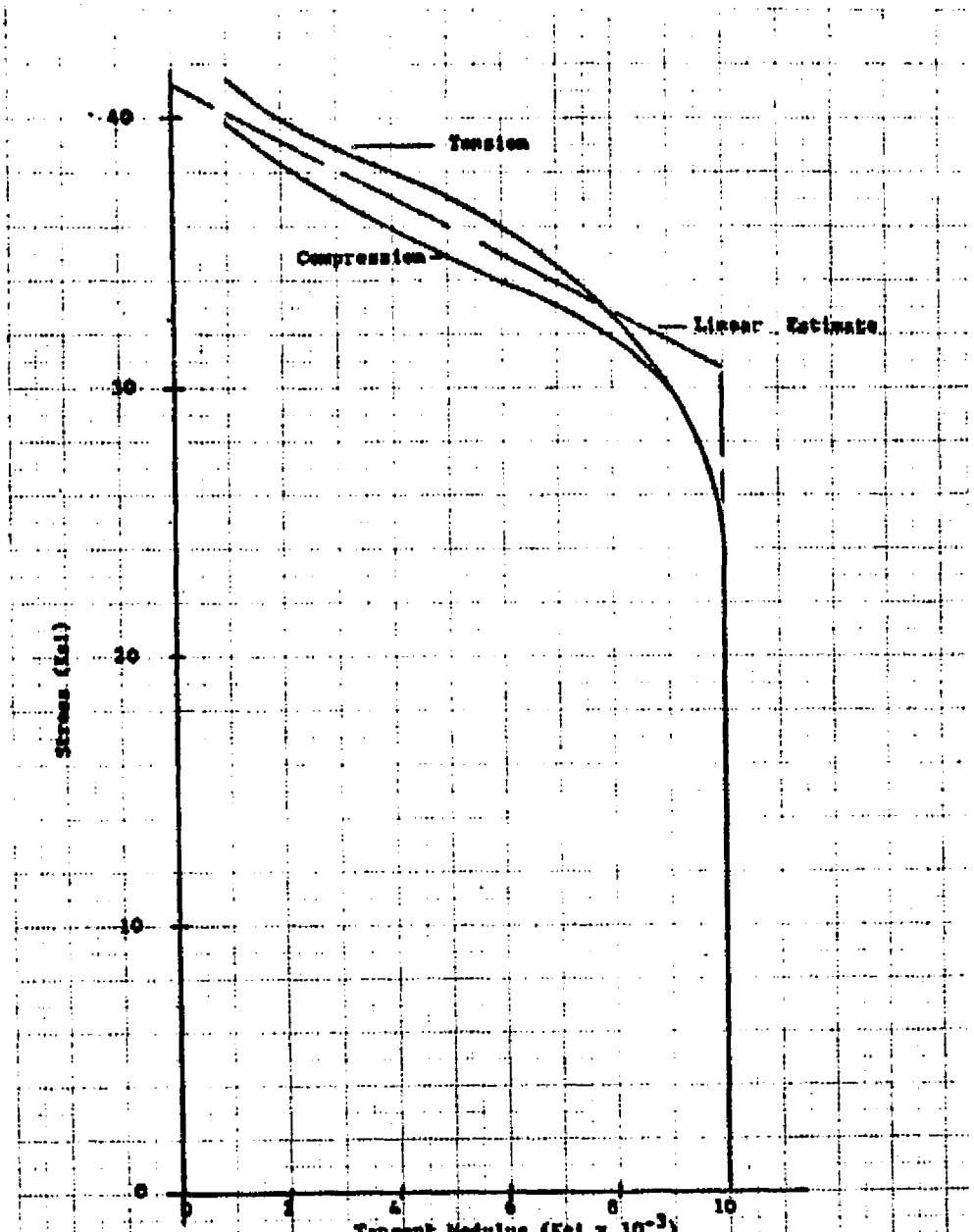

Figure 81 Tangent Modulus Curves for 6061 Sheet and Plate in T6 Condition. Thickness < 2 Inches. (31)

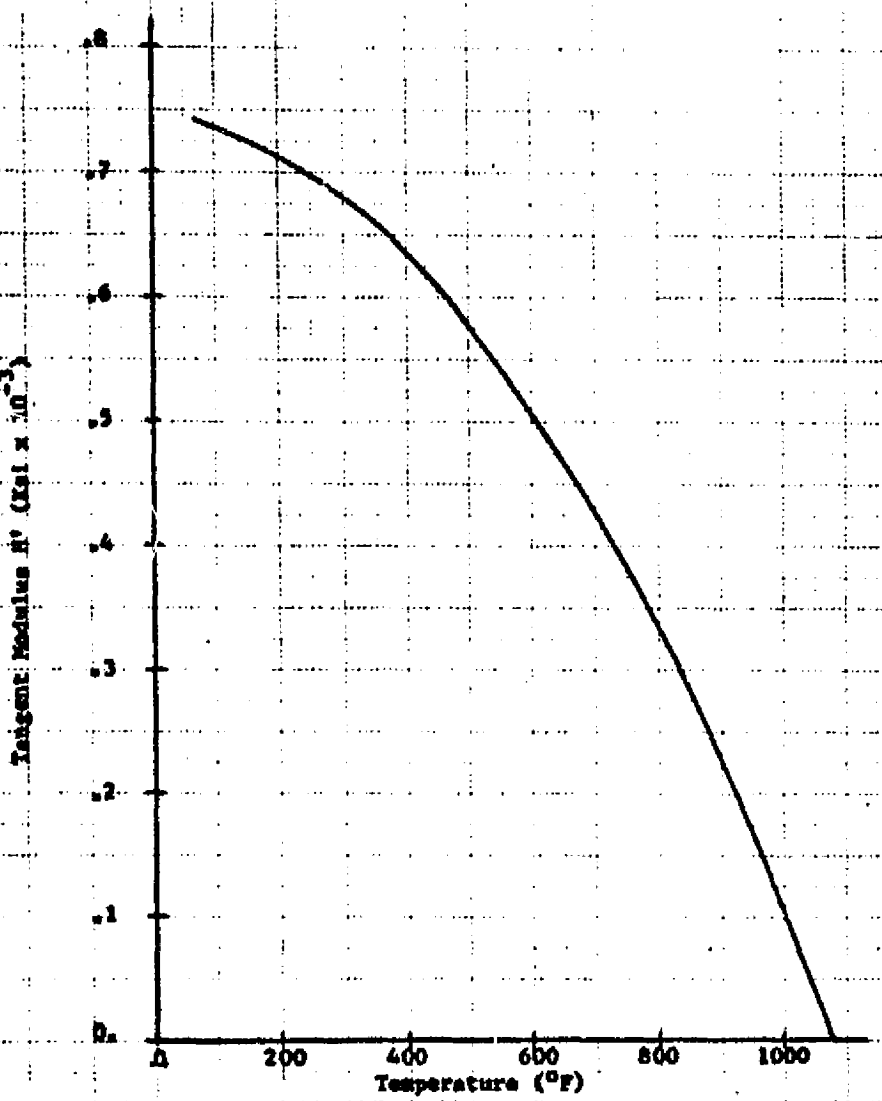

Figure 9: Tangent Modulus for 6061 in the T6 Condition Based on a Half Hour Exposure at Working Temperature (32).

FUNCTION:	RANGE	a	b	c	d
σ_y(T)Ksi	$0 \leq T^\circ F \leq 500$	0.4050000E 02	-0.7480200E-02	0.2589636E-04	-0.1698679E-06
σ_y(T)Ksi	$500 \leq T^\circ F \leq 1080$	0.1840897E 03	-0.5656120E 00	0.5837074E-03	-0.2016852E-06
E(T)x10^{-6}Psi	$0 \leq T^\circ F \leq 1080$	0.1020000E 02	-0.1817137E-02	-0.4810746E-05	-0.2084789E-08
H'(T)x10^{-3}Ksi	$0 \leq T^\circ F \leq 1080$	0.7520000E 00	-0.1240664E-03	-0.4036978E-06	-0.1168005E-09
α_T(T)Microstrain/$^\circ$F	$0 \leq T^\circ F \leq 500$	0.1219000E 02	0.9464994E-02	-0.1169593E-04	0.1049988E-07
α_T(T)Microstrain/$^\circ$F	$500 \leq T^\circ F \leq 1080$	0.1409189E 02	-0.6089211E-03	0.7212205E-05	-0.2243820E-08
$\bar{\alpha}_T$(T)Microstrain/$^\circ$F	$0 \leq T^\circ F \leq 600$	0.1241000E 02	0.4283324E-02	-0.2624947E-05	0.1041599E-08
$\bar{\alpha}_T$(T)Microstrain/$^\circ$F	$600 \leq T^\circ F \leq 1080$	0.1332638E 02	0.1167117E-02	0.4798676E-06	0.2805547E-09
ρ(T) Lb_m/in^3	$0 \leq T^\circ F \leq 300$	0.9800000E-01	-0.7683365E-05	0.1200050E-07	-0.1166804E-10
ρ(T) Lb_m/in^3	$300 \leq T^\circ F \leq 1080$	0.9760000E-01	-0.3875000E-05		
C(T)x10^{-2}Btu/HrFt$^\circ$F	$0 \leq T^\circ F \leq 500$	0.2161000E 00	0.1197828E-03	-0.1859963E-06	0.1816616E-09
C(T)x10^{-2}Btu/HrFt$^\circ$F	$500 \leq T^\circ F \leq 1080$	0.2018934E 00	0.1561132E-03	-0.1503752E-06	0.7874967E-10
H'(σ)x10^{-3}Ksi	$30.8 \leq \sigma$(Ksi) ≤ 40.7	0.3806400E 02	-0.9170000E 00		

Table 5: Summary of Mechanical and Physical Properties for Computer Simulation of 6061 T6 Aluminum Alloy in the Form $F(x) = a + bx + cx^2 + dx^3$. Use Caution in Reducing the Number of Significant Figures Given for the Coefficients at High Temperatures.

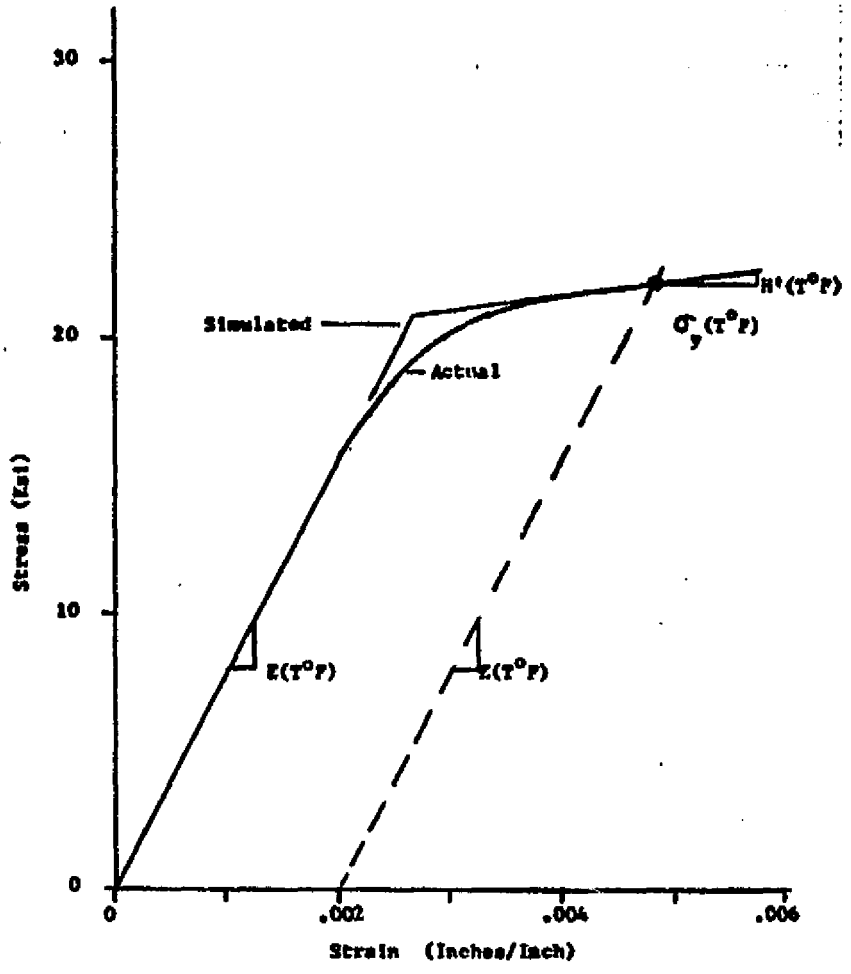

Figure 10: Simulation of Tensile Properties at Various Temperatures after 0.5 Hour at Temperature. In this example T°F is 500°F.

program.

Figure 10 also demonstrates a computer algorithm for the tensile properties at various temperatures based on the half hour soak. To determine this approximate value, proceed as follows:

a. Determine σ_y(T°F) from Table 5 or Figure 6.

b. Determine E(T°F) from Table 5 or Figure 7.

c. Determine H'(T°F) from equation (35) and Table 5 or Figure 9.

d. Plot σ_y(T°F) at 0.2% offset.

e. Draw line through point d above with slope H'(T°F).

f. Connect line in e above with line through origin with slope E(T°F).

5. Physical Properties

Figures 11 through 14 show the effect of temperature on the coefficient and mean coefficient of linear expansion α, density ρ, thermal conductivity κ, and specific heat C. The coefficient of linear expansion shown in Figure 11 is based on empirical equations for high purity aluminum and alloy constants provided by reference (35). The alloy constant for 6061 T0 is 0.990, i.e., 0.990 α (pure aluminum) = α (alloy). The value of this constant for heat treated tempers is approximately 0.015 greater. With these tempers, application is restricted to temper-

atures which do not appreciably exceed those used in the final aging treatments (320-350°F). The basic alloy constant is limited to temperatures below 600°F. Figure 11 is extrapolated past 600°F to the melting point. Figure 12 provides an estimate of density provided by reference (36) extrapolated to the melting point. Figure 13 provides an estimate of thermal conductivity. Reference (37, Volume II, Part 2, pp. 769) provides thermal conductivity information of 6000 series aluminum alloys from 300 to 650°K. A linear relationship was plotted parallel to this data passing through the one data point provided by reference (38). Reference (37) (Volume I, pp. 11) listed the specific heat-temperature relationship for pure aluminum. A parallel relationship (39, pp. 180) passing through the data point provided by reference (31, Code 3206, pp. 1) resulted in the estimated data shown in Figure 14.

These physical values may be approximated by the cubic polynomials given in Table 5 for computer simulation. Appendix A lists the computer program for determining the coefficients given in Table 5 and for testing these coefficients in 10°F increments.

Table 6 summarizes the physical and mechanical properties of 6061 T6 in the form utilized by Masubuchi and Andrews (11) in their one-dimensional program.

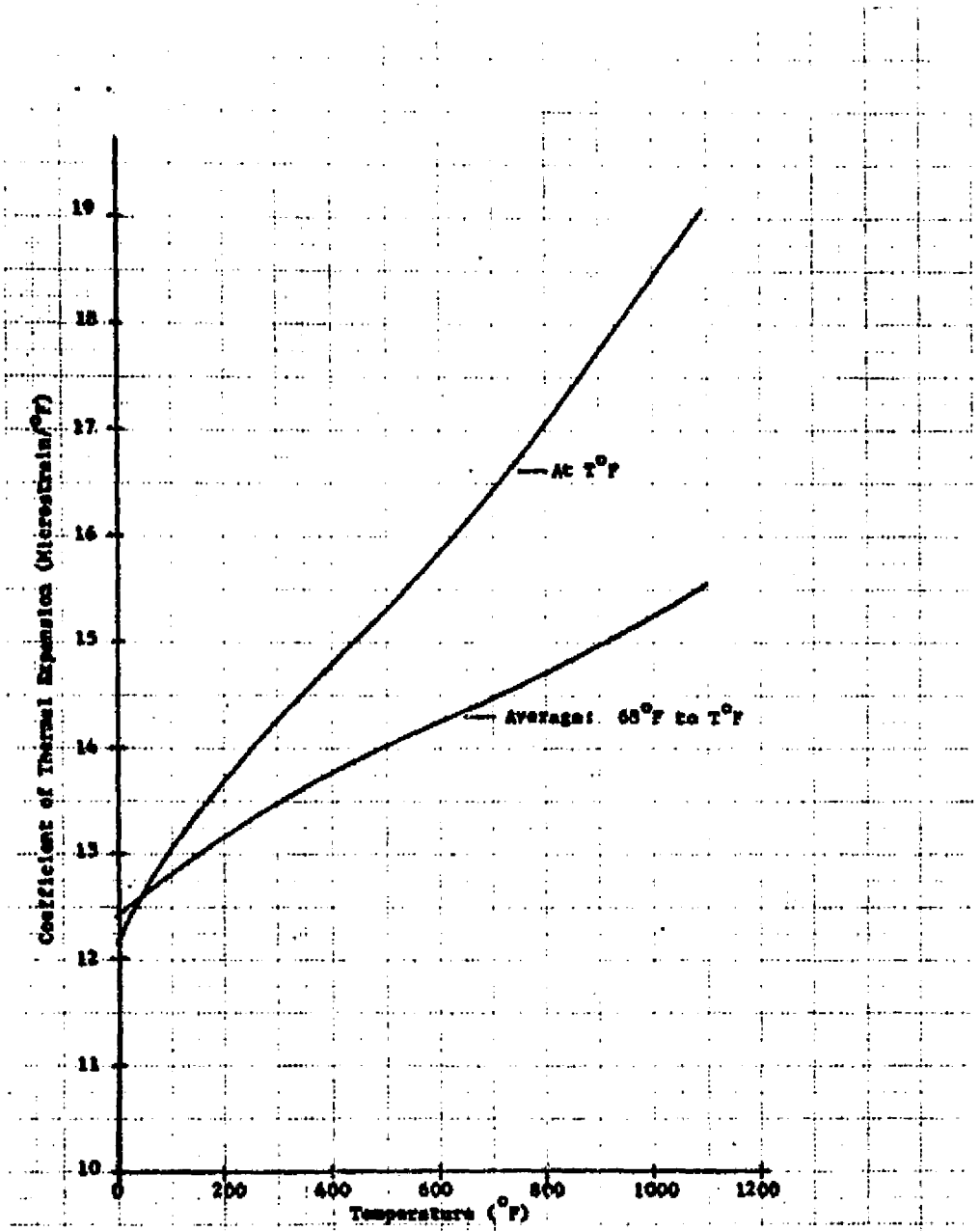

Figure 11: Coefficient of Thermal Expansion for 6061 (35).

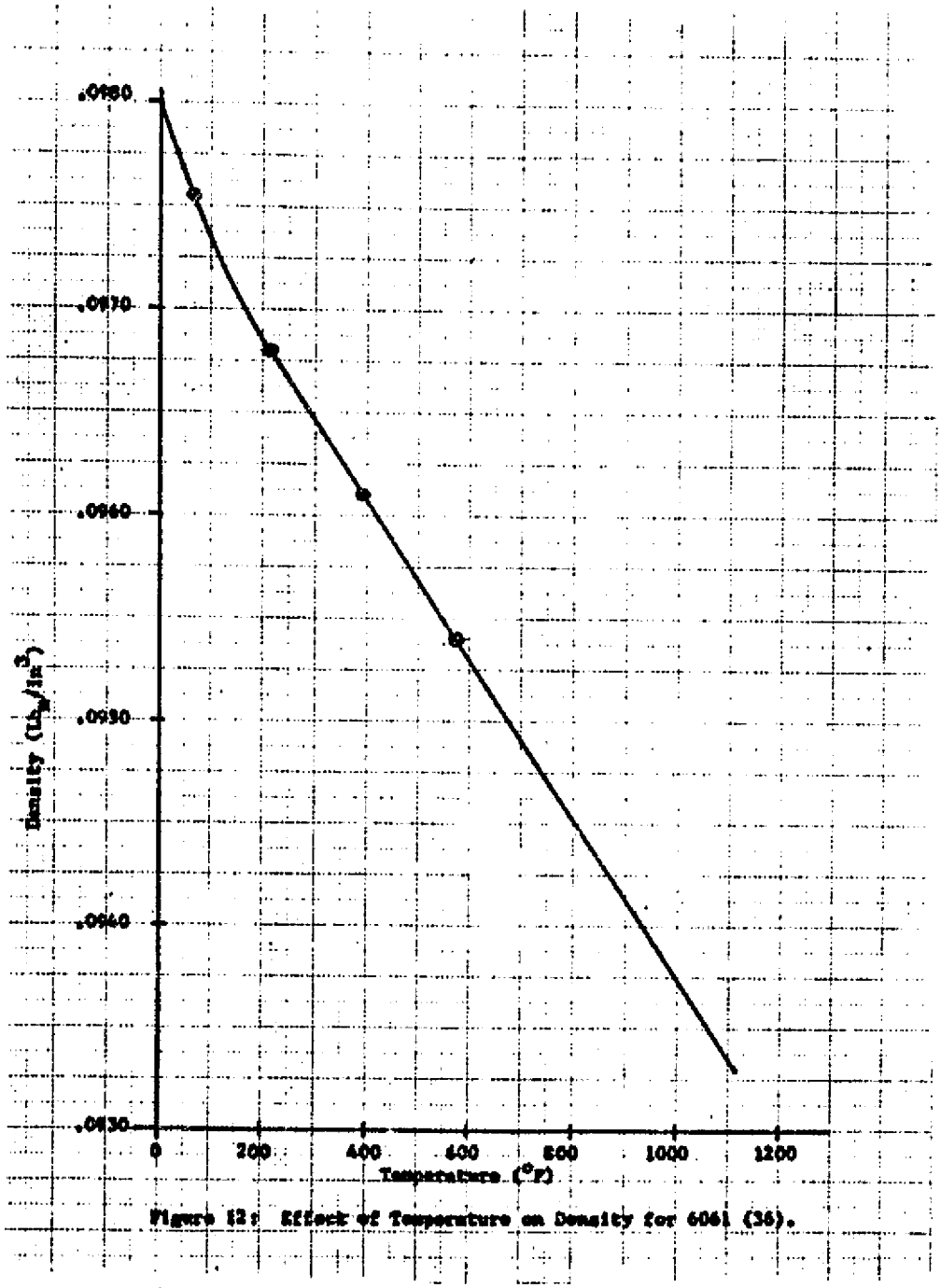

Figure 12: Effect of Temperature on Density for 6061 (36).

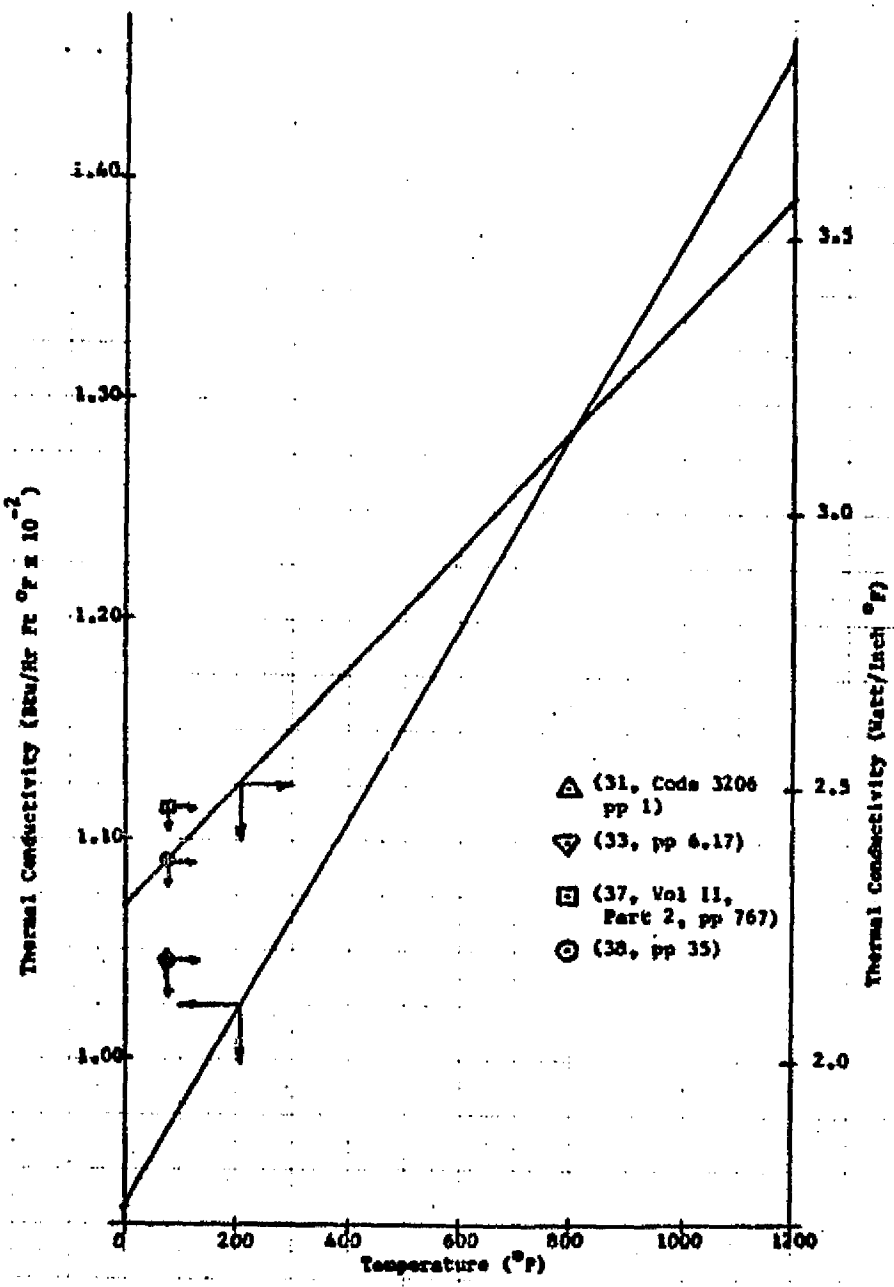

Figure 13: Estimated Effect of Temperature on Thermal Conductivity for 6061 in T6 Condition.

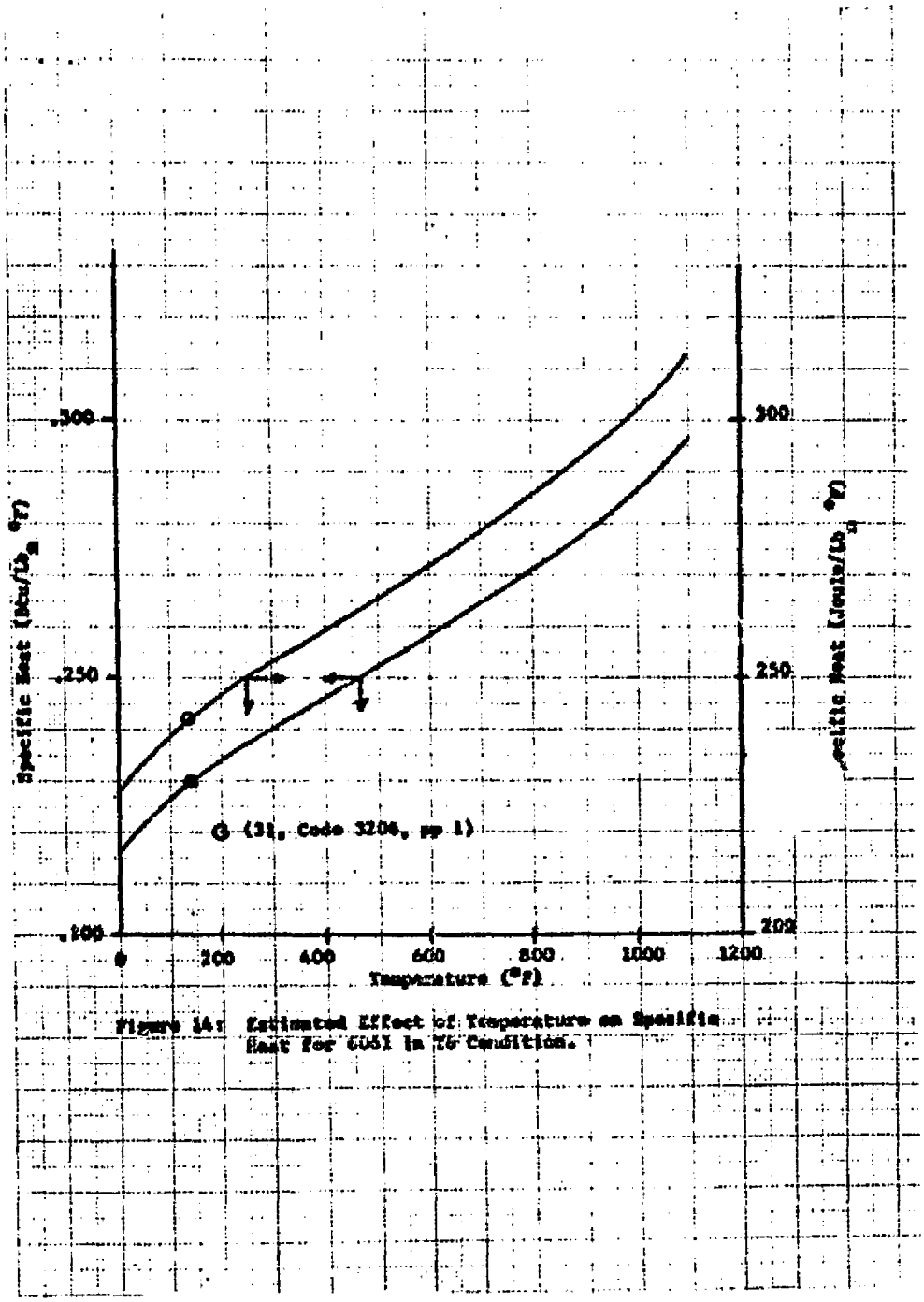

Figure 14: Estimated Effect of Temperature on Specific Heat for 6061 in T6 Condition.

T	°F	0.0	100.0	200.0	300.0	400.0	500.0	600.0	700.0	800.0	1080.0
K	Watt/In°F	2.280	2.389	2.497	2.603	2.712	2.838	2.925	3.062	3.142	3.572
C	Joule/Lb_m°F	227.7	238.2	246.5	253.0	259.0	265.2	271.6	278.1	285.4	310.0
ρ	Lb_m/In^3	0.098	0.097	0.097	0.096	0.096	0.096	0.095	0.095	0.094	0.093
E	$x10^{-6}$ Psi	10.18	9.94	9.60	9.15	8.58	7.83	6.93	5.85	4.60	0.00
σ_y	Ksi	40.50	39.80	38.38	36.00	31.70	22.00	9.60	5.00	2.60	0.00
α_T	Microstrain/°F	12.19	13.03	13.67	14.26	14.78	15.31	15.85	16.43	17.06	19.02
m	-----	0.0742	0.0742	0.0742	0.0742	0.0742	0.0742	0.0742	0.0742	0.0742	0.0742

Table 6: Summary of Mechanical and Physical Properties for 6061 T6 Aluminum Alloy.

III: PROCEDURES

A. Scope of the Research:

A series of six experiments measuring temperature and strain changes during welding was performed. System models representing constrained bead-on-plate and butt joints were constructed from 6061 aluminum alloy in the T6 condition. Welding procedures were utilized which offered full penetration with minimum heat input. This allowed strain gage locations as close to the weld line as possible without exceeding the 400°F maximum allowable gage temperature limitation.

B. Selection of Parameters:

The aluminum selected for this investigation was picked because of its easy availability and wide use in the marine and aeronautical industries. It develops its strength from its heat treatment. The 0.250 inch plate thickness used in this study was determined by availability, past experimental work, ease of handling, and an interest in approaching a two-dimensional problem, yet minimizing the extent of bending and buckling. The joint design for the butt welds used in this experiment (straight) was selected for simplicity and ease of preparation. Steel backing plates were utilized below the weld and at

the clamped ends of the plates to provide support and distributed clamping and yet minimize heat conduction effects. Each specimen was clamped at its edges to a 0.500 inch mild steel bed plate which resisted deformation.

The size of the test plates was set at a nominal 18 by 30 inches to provide essentially steady state conditions at strain gage locations, and to approach the temperature distribution of an infinite plate.

The weld process used was semi-automatic Gas Metal-Arc (GMA or MIG). It allows control of weld variables, reduces operator error, and fosters repeatability. No preheating was necessary.

C. Strain Measurement by Electric Resistance Strain Gages:

The fundamental concept of strain gage operation is that certain conductors exhibit a change in electrical resistance with a change in strain. Gages designed according to this principle are attached to test materials whose strains are then monitored by measuring resistance variations across the gage. In the case of welding thermal strains, the observed resistance change, ΔR, is made up of:

$$\Delta R = \Delta R_1(\epsilon_e) + \Delta R_2(\epsilon_p) + \Delta R_3(\alpha T) + \Delta R_4(T)$$

where

$\Delta R_1(\varepsilon_e)$ = the resistance change corresponding to elastic mechanical strain, ε_e, from which stresses can be computed.

$\Delta R_2(\varepsilon_p)$ = the resistance change corresponding to plastic mechanical strain, ε_p, if it exists.

$\Delta R_3(\alpha T)$ = the resistance change corresponding to temperature induced thermal strain, αT.

$\Delta R_4(T)$ = the resistance change caused by thermoelectric effects in the gage itself.

While it is not presently possible to discriminate between the two mechanical strains, ε_e and ε_p, $\Delta R_3(\alpha T)$ and $\Delta R_4(T)$ can be separated out by physical temperature compensation of the strain gage material coupled with empirical calculation. For this investigation, α_T for the gage was approximately 13.0 microstrain/°F. The $\Delta R_4(T)$ and the difference between gage α_T and base plate α_T will then generate an error. To compute this error, a test gage of the type and lot used in the experiment is mounted on a small sample of 2024 aluminum alloy by the gage manufacturer. The sample is then heated at equilibrium until a curve of "apparent strain" vs. temperature is obtained to the operating temperature range. The gage readings recorded in the weld experiments can then be corrected by subtracting out the apparent strain

value corresponding to temperatures observed at the gage location. Figures 16 and 17 show this factory provided information for the individual gages and rosettes respectively. In each case, the curves have been reduced by the factory to fourth order polynomials yielding microstrain for ease in computer calculation.

Gage:

$$EAP = -69.36 + 2.07T - 2.02 \times 10^{-2}T^2 + 5.39 \times 10^{-5}T^3 - 3.27 \times 10^{-8}T^4 \quad (38)$$

Rosettes:

$$EAP = -60.68 + 2.22T - 2.40 \times 10^{-2}T^2 + 7.05 \times 10^{-5}T^3 - 5.59 \times 10^{-8}T^4 \quad (39)$$

Since 6061 T6 has a greater coefficient of thermal expansion than the 2024 T4 test plate, a correction to these polynomials has been made. This correction was calculated as follows:

In general,

$$\text{Thermal Strain} = \int_{T_1}^{T_2} \alpha(T)\, dT \quad (40)$$

From reference (35),

$$\alpha_{6061} = C_{6061}\, \alpha \text{ pure Al.} = .99\, \alpha \text{ pure Al.} \quad (41)$$

$$\alpha_{2024} = C_{2024}\, \alpha \text{ pure Al.} = .97\, \alpha \text{ pure Al.} \quad (42)$$

$$\alpha \text{ pure Al.} = \frac{\alpha_{6061}}{.99} \quad (43)$$

$$\Delta EAP = \int_{T_1}^{T_2} (C_{6061} - C_{2024})\, \alpha_{\text{pure Al.}}(T)\, dT \quad (44)$$

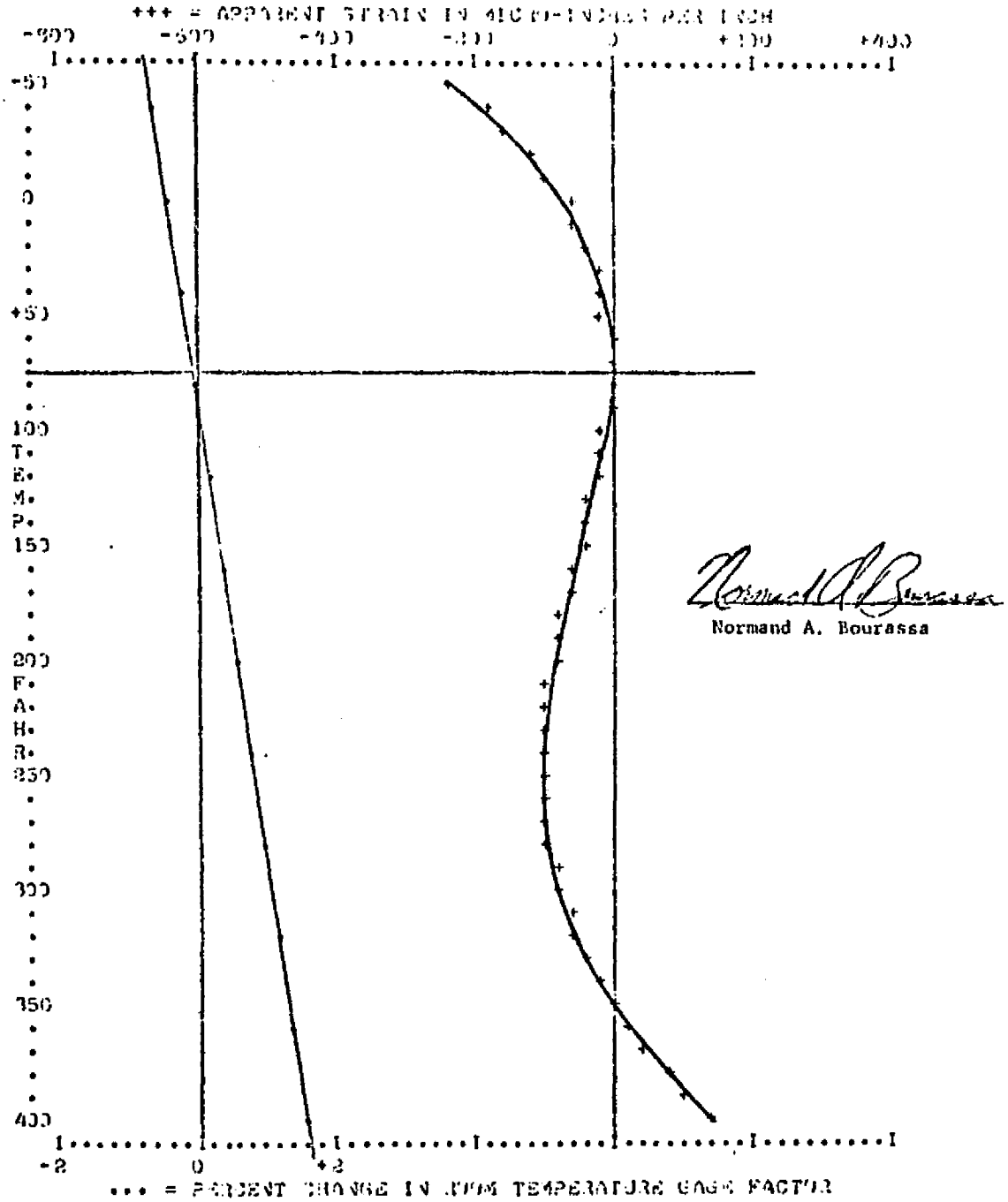

Normand A. Bourassa

Figure 16: Apparent Strain Correction for EAE-25-12S13L Strain Gages Utilized in this Study.

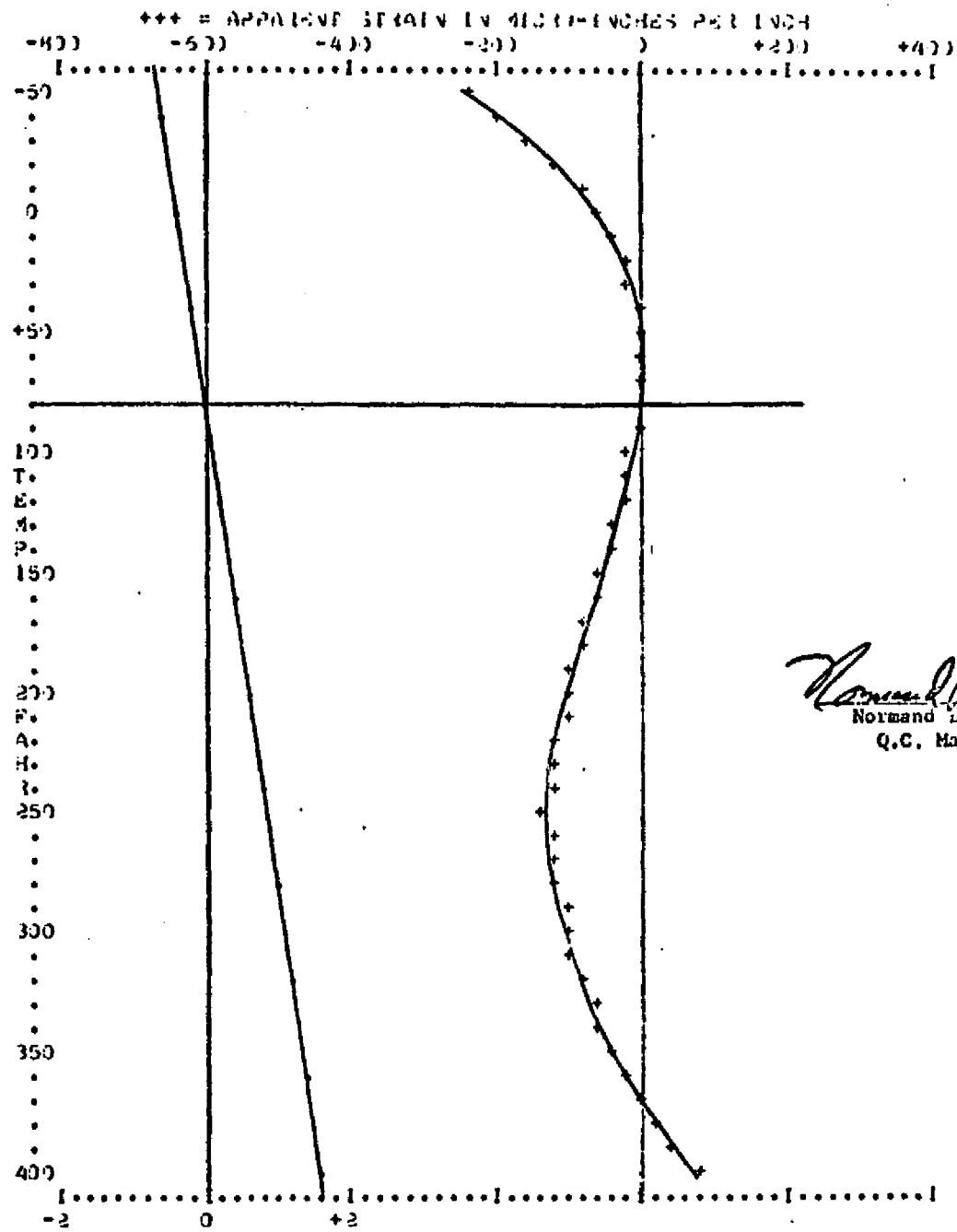

Normand Bourassa
Q.C. Manager

Figure 17: Apparent Strain Correction for FAER-18RB-12S13-ET Strain Gage Rosettes Utilised in this Study.

$$\Delta EAP = \int_{T_1}^{T_2} \left(\frac{.20}{.99}\right) \left(\alpha_{6061}(T)\right) dT \qquad (45)$$

Integrating the polynomial given in Table 5 for $\alpha_{6061}(T)$, $0 \leq T \leq 400°F$, between 77°F and T°F yields the following apparent strain correction for both gages and rosettes:

$$\Delta EAP = -19.4979 + .2463T + .9561 \times 10^{-4}T^2 - .7879 \times 10^{-7}T^3 + .5303 \times 10^{-10}T^4 \qquad (46)$$

Equation (46) must be added to equations (38) and (39) to obtain true apparent strain corrections. The true apparent strain is then subtracted from the actual strain to provide true mechanical strains.

Strain gages manufactured in the form of rosettes provide as many as three independent readings in three directions at a single location. This is enough to completely describe the two-dimensional strain state at that location (41, 42, 43) and is discussed in the next chapter.

D. Description of Apparatus:

1. Test Plates: A description of the test specimens is summarized in Figures 18 through 22 which provide dimensions and gage locations. Devices (1) through (12) were dynamically measured during welding. Gages (21) through (25) were statically measured before and after

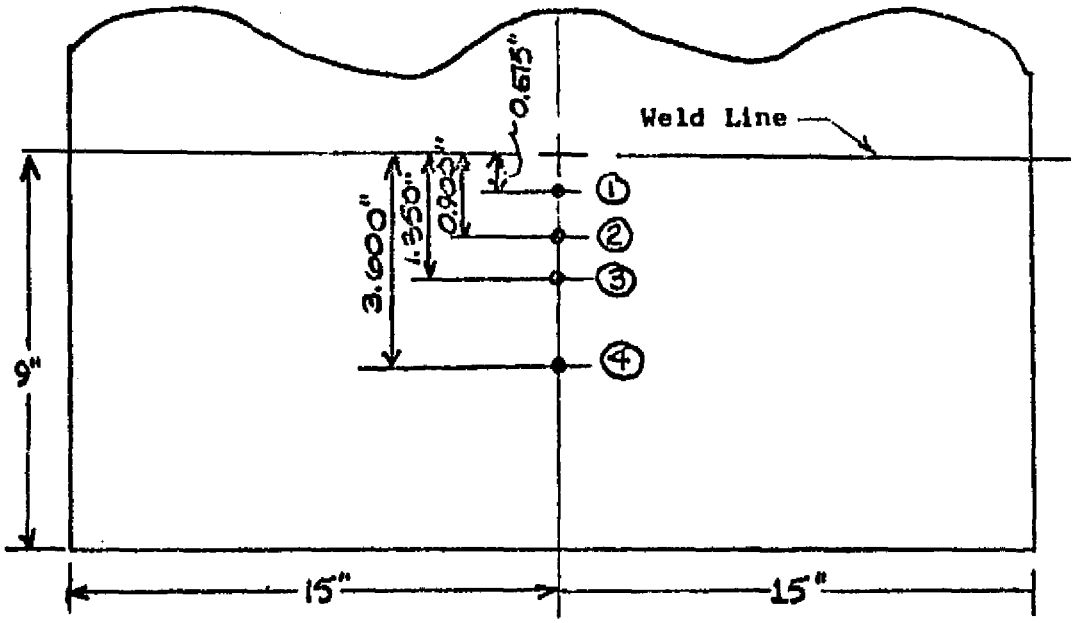

Figure 18: Test No. 1 and Test No. 2 (Butt and Bead-on-Plate Welds Respectively) Measuring Temperature Distribution.

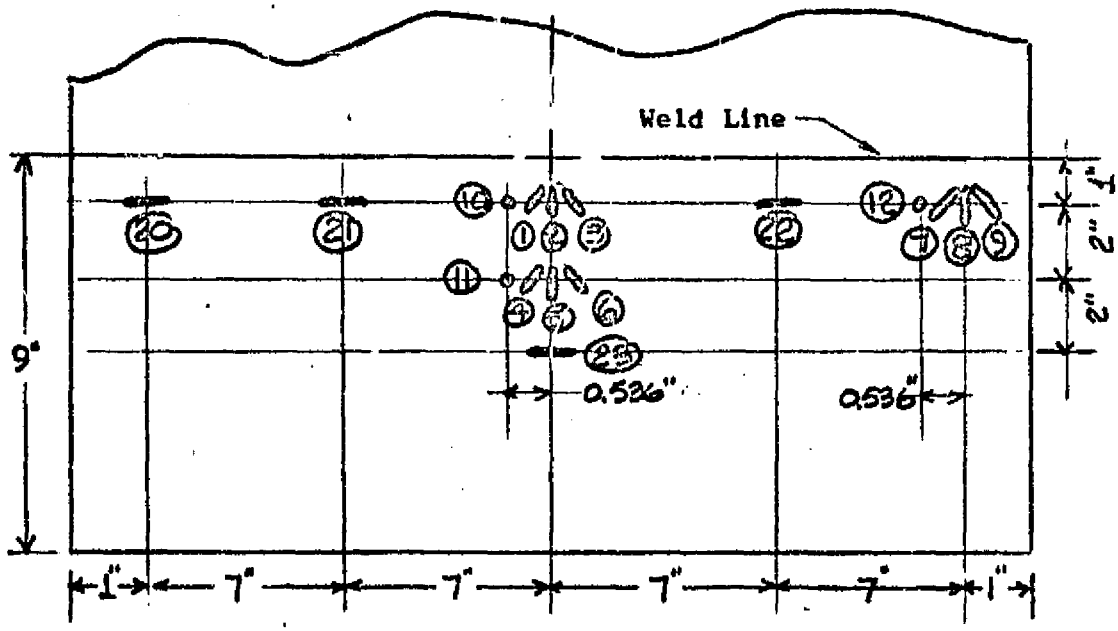

Figure 19: Test No. 3 (Bead-on-Plate Weld) Measuring Temperature Distribution and Strains.

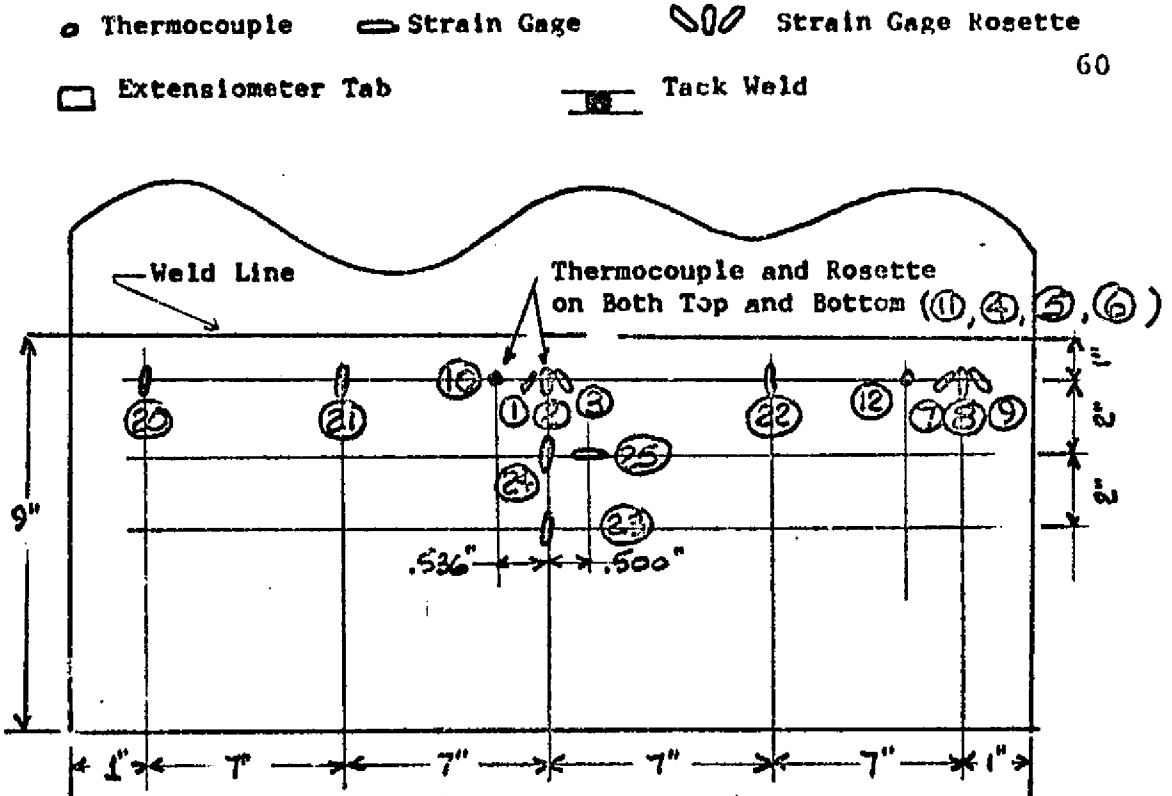

Figure 20: Test No. 4 (Bead-on-Plate Weld) Measuring Temperature Distribution and Strains.

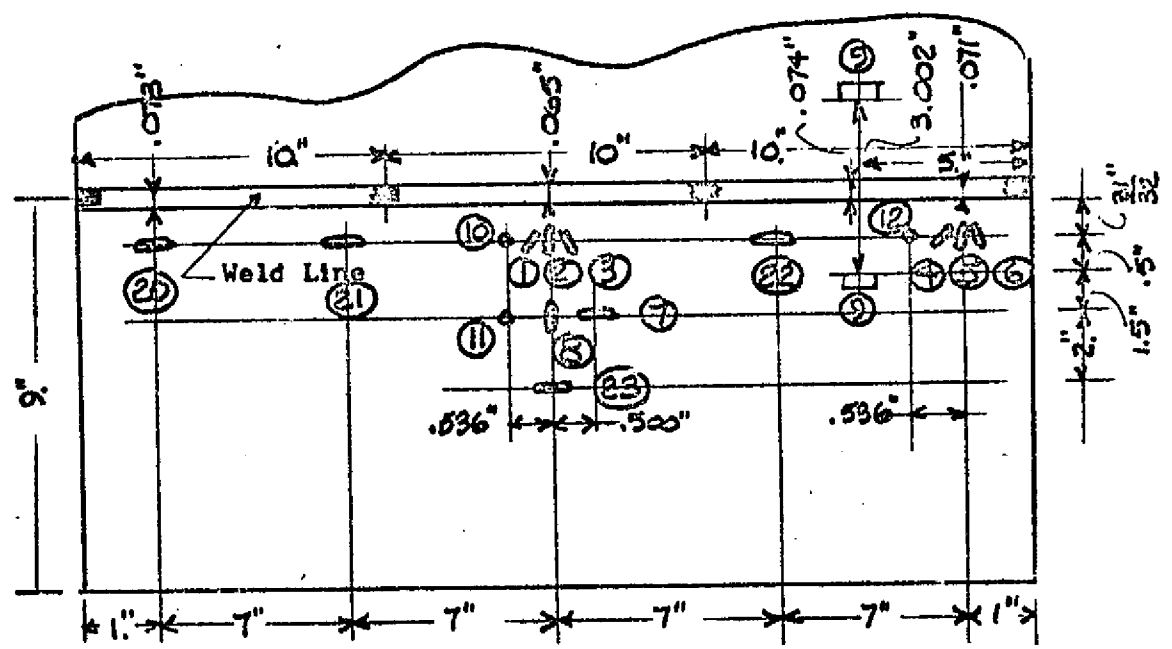

Figure 21: Test No. 5 (Butt Weld) Measuring Temperature Distribution, Strains, and Extension of Root Gap.

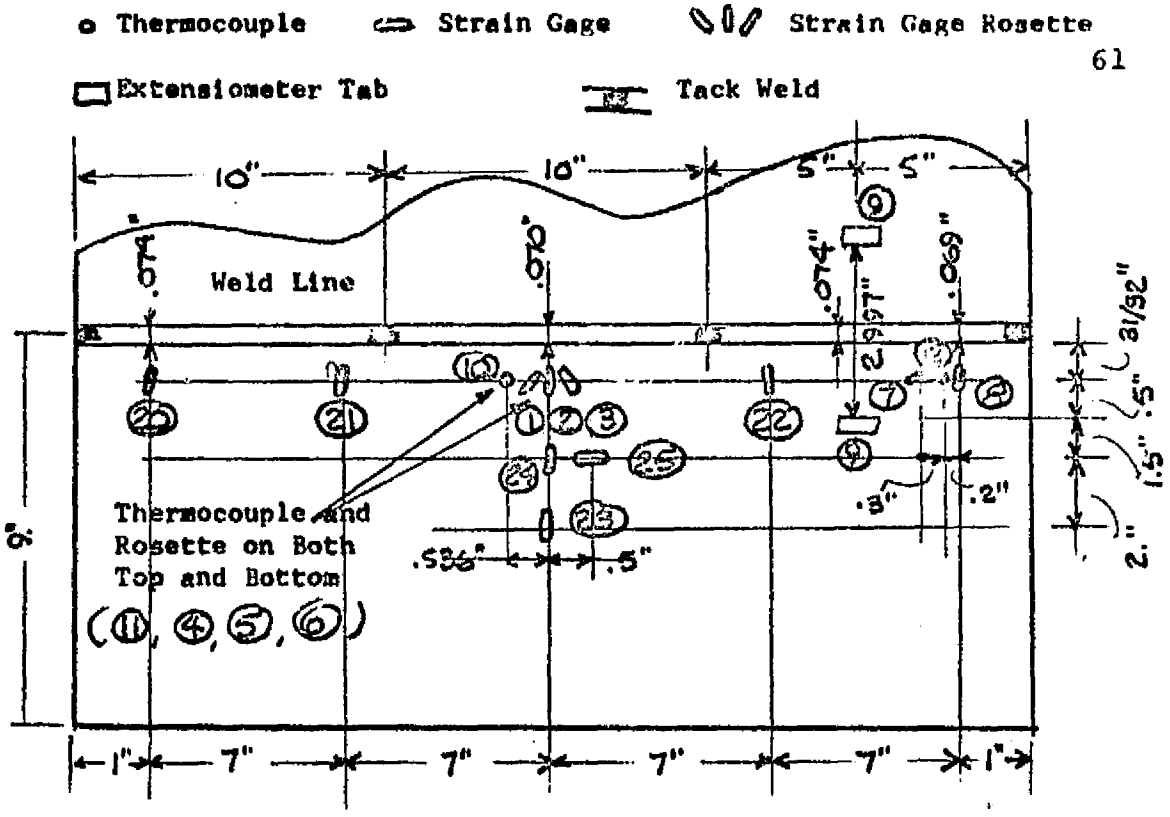

Figure 22: Test No. 6 (Butt Weld) Measuring Temperature Distribution, Strains, and Extension of Root Gap.

welding. The arrangement of constraining clamps is shown in Figure 23.

2. Sensors and Instrumentation:

a. Strain Gages. Two types of gages were used in this investigation: SR-4 foil 45° rosettes and SR-4 foil single element gages. Gage properties were as follows:

Gage	SR-4 Rosette	SR-4 Gage
Designation	FAER-18RB-12S13-ET	FAE-25-12S13L
Manufacturer	BLH Electronics	BLH Electronics
Grid Length (in.)	3/16	1/4
Grid Width (in.)	0.90	0.13
Overall Length (in.)	0.280	0.35
Overall Width (in.)	0.540	0.13
Temperature Range	-50 to +400°F	-50 to +400°F
Resistance	120.	120.
Gage Factor	2.03	2.07
Cement	EPY-600	EPY-600
Protective Covering	BLH Barrier-C	BLH Barrier-C

b. Temperature Sensors: All temperature sensors used were Chromel/Alumel thermocouples made from Leads and Northrup No. 28 wires. Each thermocouple was spot-welded onto the test specimen and protected by No. 33 Sauereisen Sealing Cement. Each was

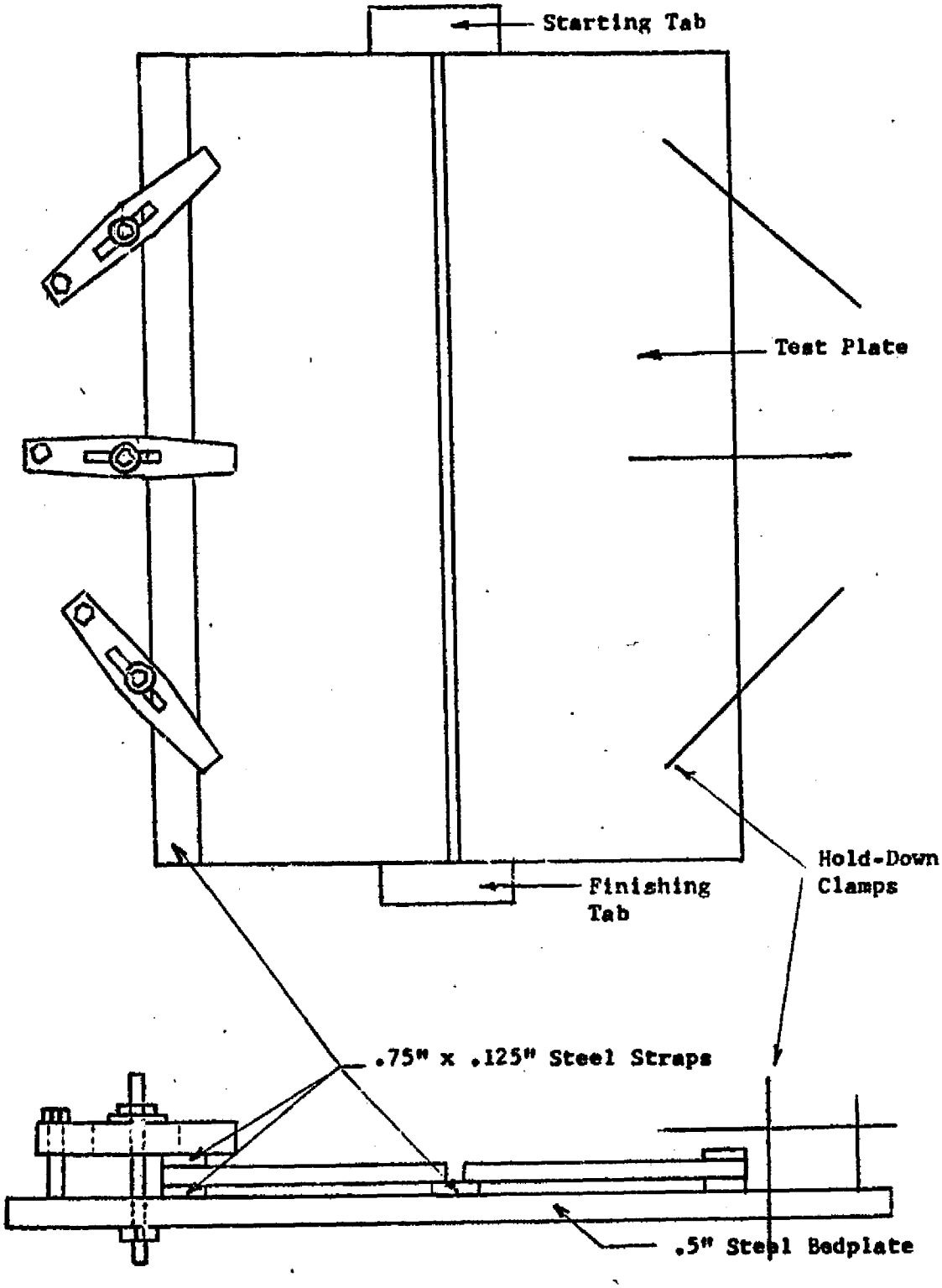

Figure 23: Constraining Equipment

located 0.536 inch (1 second of arc travel) ahead of the strain gage mid-axis.

c. Instrumentation. Strain gages were connected into a Potentiometric Circuit (Half-Wheatstone Bridge), balanced and calibrated as indicated schematically in Figure 24. Thermocouples were referenced to a 32°F ice-bath and calibrated as indicated in Figure 25. Both circuits were fed into a Honeywell continuous-recording, 12-channel Visicorder. When the raw data was actually read off the recorder tape, some traces were delayed or advanced with respect to others. This was done to correct for the finite difference in position along the weld line of the thermocouples (1 second) and strain rosette elements ($\pm$ 1/3 second).

This produces the effect of a simultaneous strain and temperature reading at the strain gage location. Timing was accomplished by means of an electric stop watch as well as a timer integral to the Visicorder. Static strain measurements were taken with a Budd Instrument Division Model P-350 strain indicator.

d. Extensiometer. Figure 26 shows a sketch of the extensiometer utilized in Tests 5 and 6. Strain

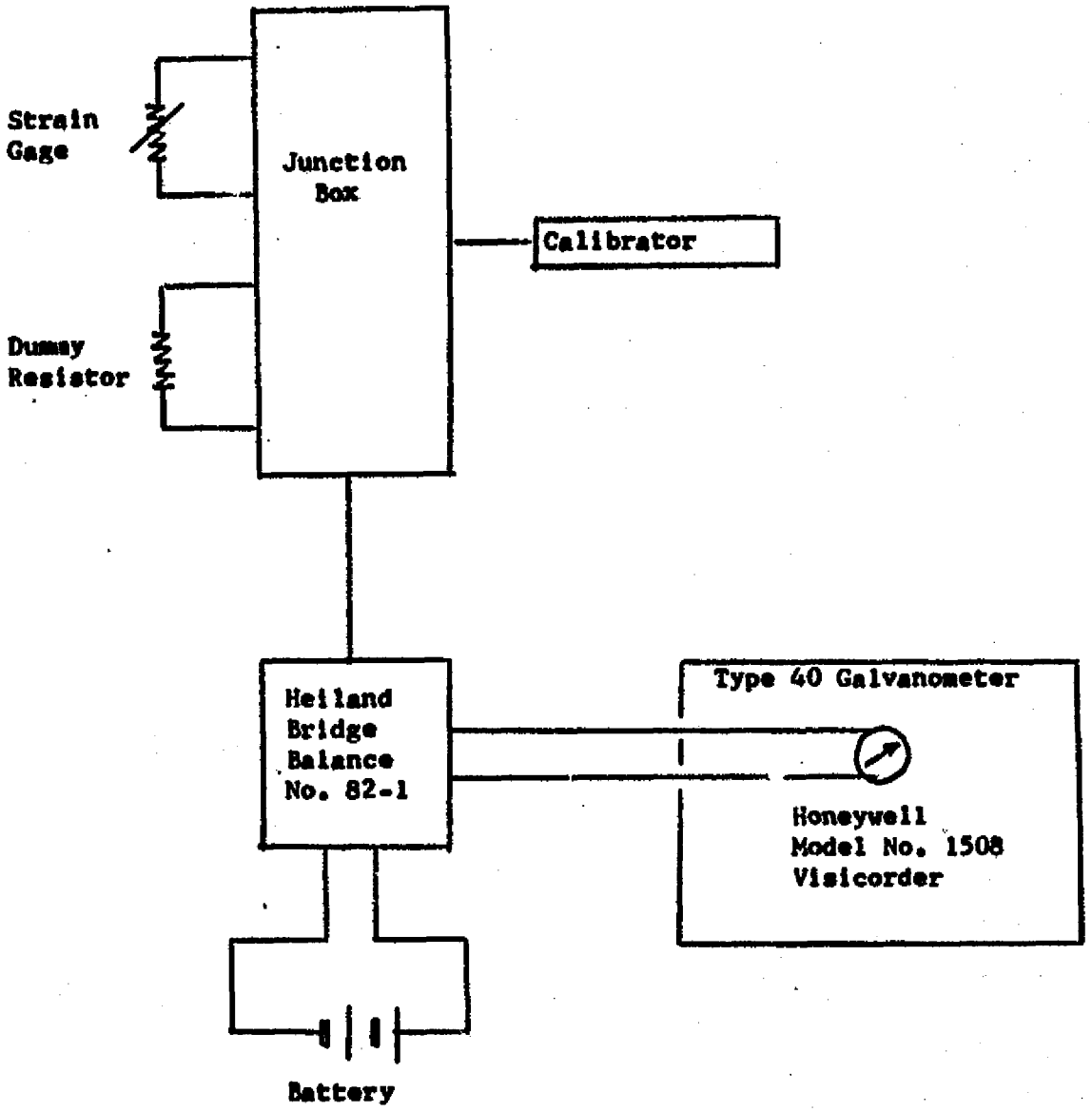

Figure 24: Strain Gage Instrumentation Circuit (7.)

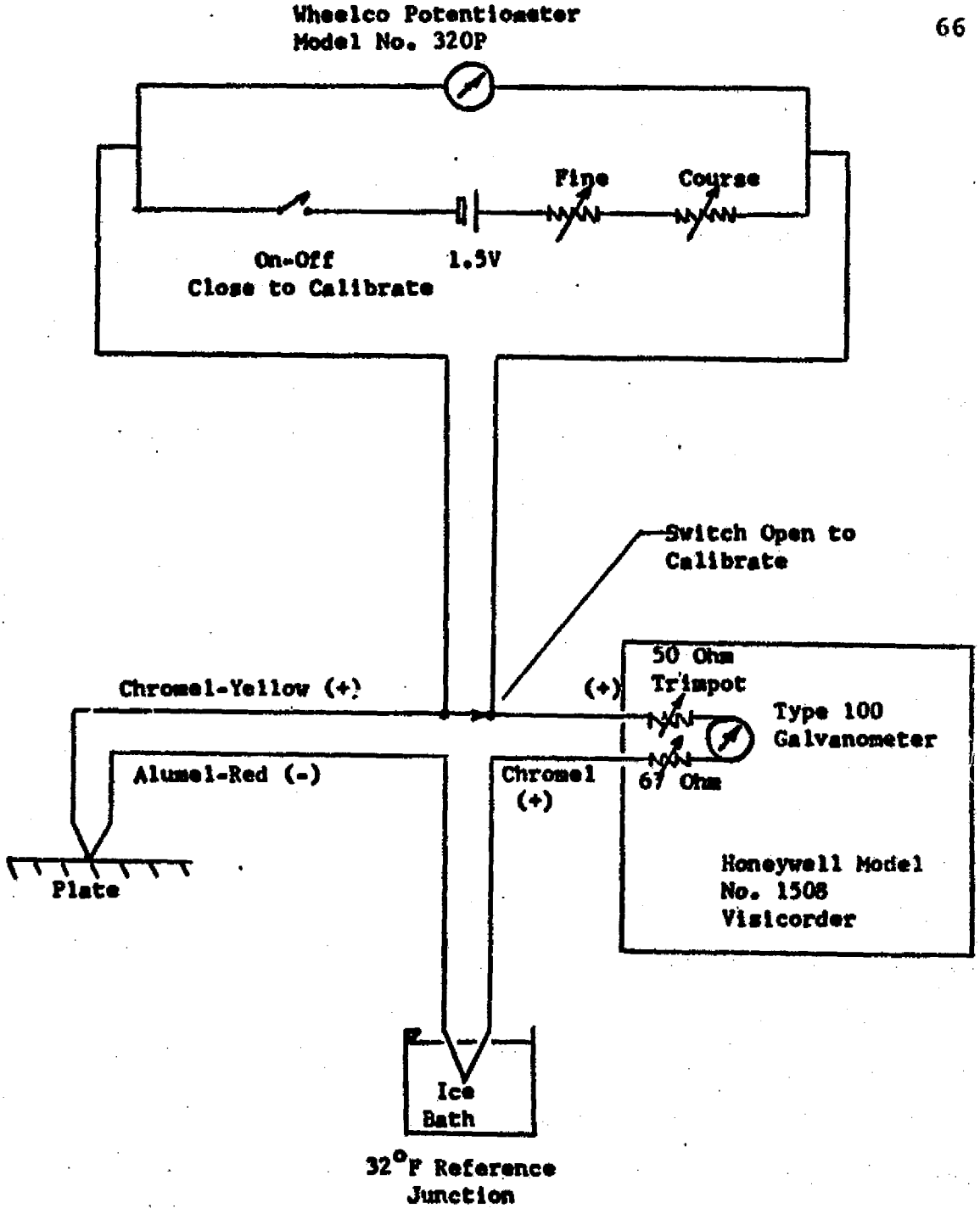

Figure 25: Thermocouple Instrumentation Circuit (7).

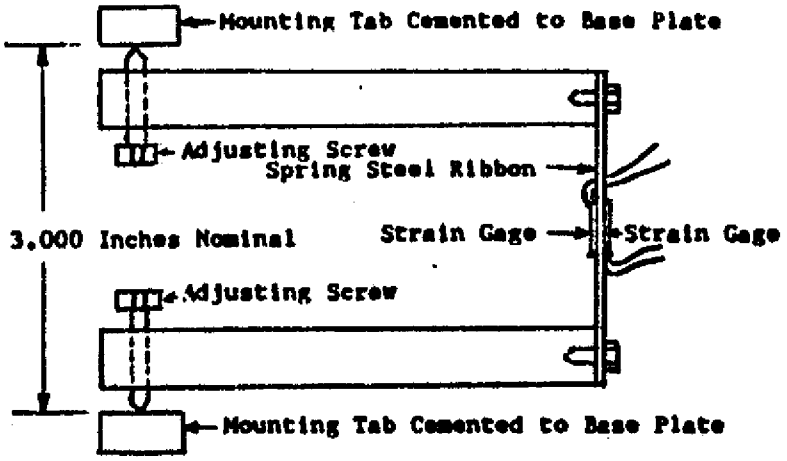

Figure 26: Extensiometer. The Adjusting Screws are Set So That the Spring Holds Extensiometer Firmly in Place.

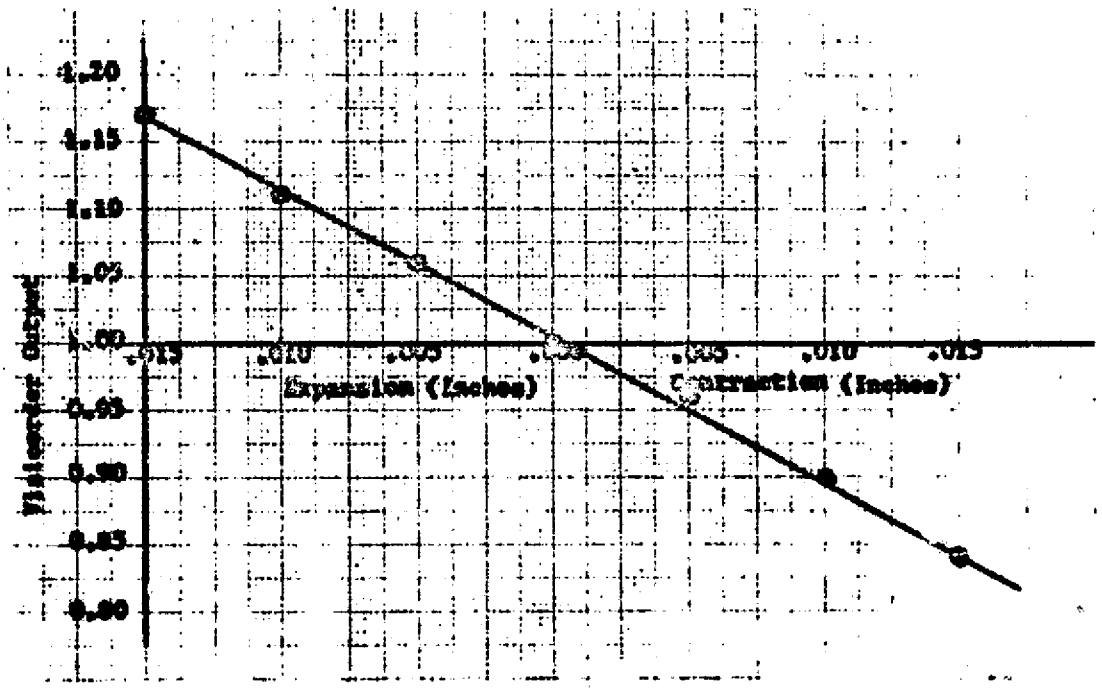

Figure 27: Extensiometer Calibration Curve. 0.000 Inches Represents an Extensiometer Gap of 3.00 Inches.

gages were located on both sides of a spring steel ribbon and connected into adjacent legs of the resistance network circuit described in paragraph c. above. The net effect of such a set-up is to double the bending sensitivity and null the stretching sensitivity. Figure 27 provides the calibration curve for the Visacorder referenced to actual dimensional changes in inches. The extensiometer and its mounting tabs may be seen in the photographs in Figures 28 through 31. It was pulled back away from the torch to prevent damage when the arc past the mounting tabs. Once the torch was safely clear, it was set back in place to observe weld shrinkage. It is noted that the mounting tabs were cemented in place with EPY 600 Cement vice bolting or welding to minimize local straining of the base plate.

3. Welding Equipment and Conditions: Welding conditions are summarized in Tables 7 and 8. The welding machine utilized was manufactured by the Linde Division of Union Carbide Corporation and consisted of a type HW-16 GMA torch, a SVI-300 power supply, and associated governor, carriage and wire feed mechanisms. Travel speed, arc voltage, amperage and arc length were present to the same value for all experiments. Some fluctuations of amperage did exist when the geometry of the weld changed from

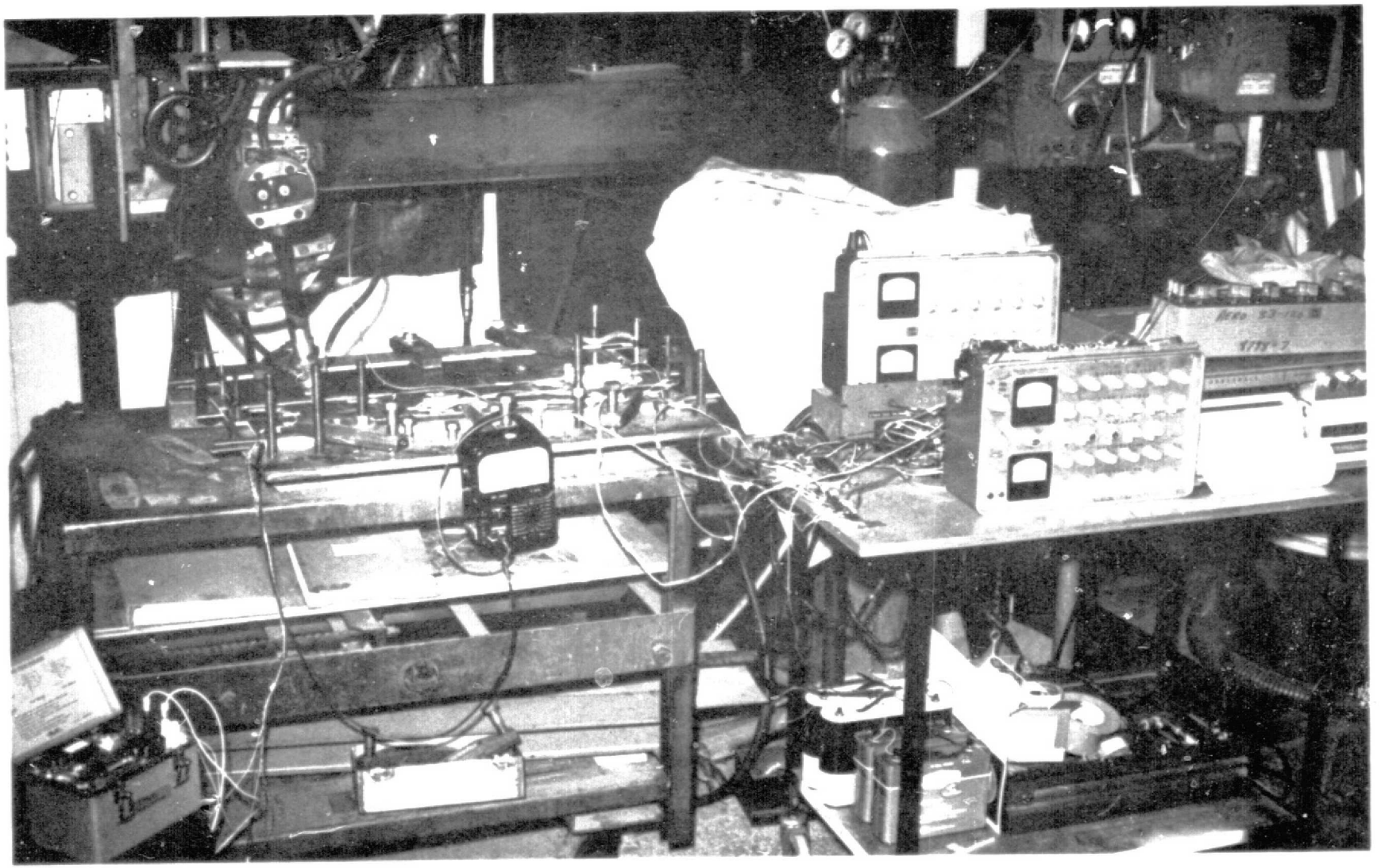

Figure 28: Overview of Experimental Equipment Showing Instrumentation and Recorder.

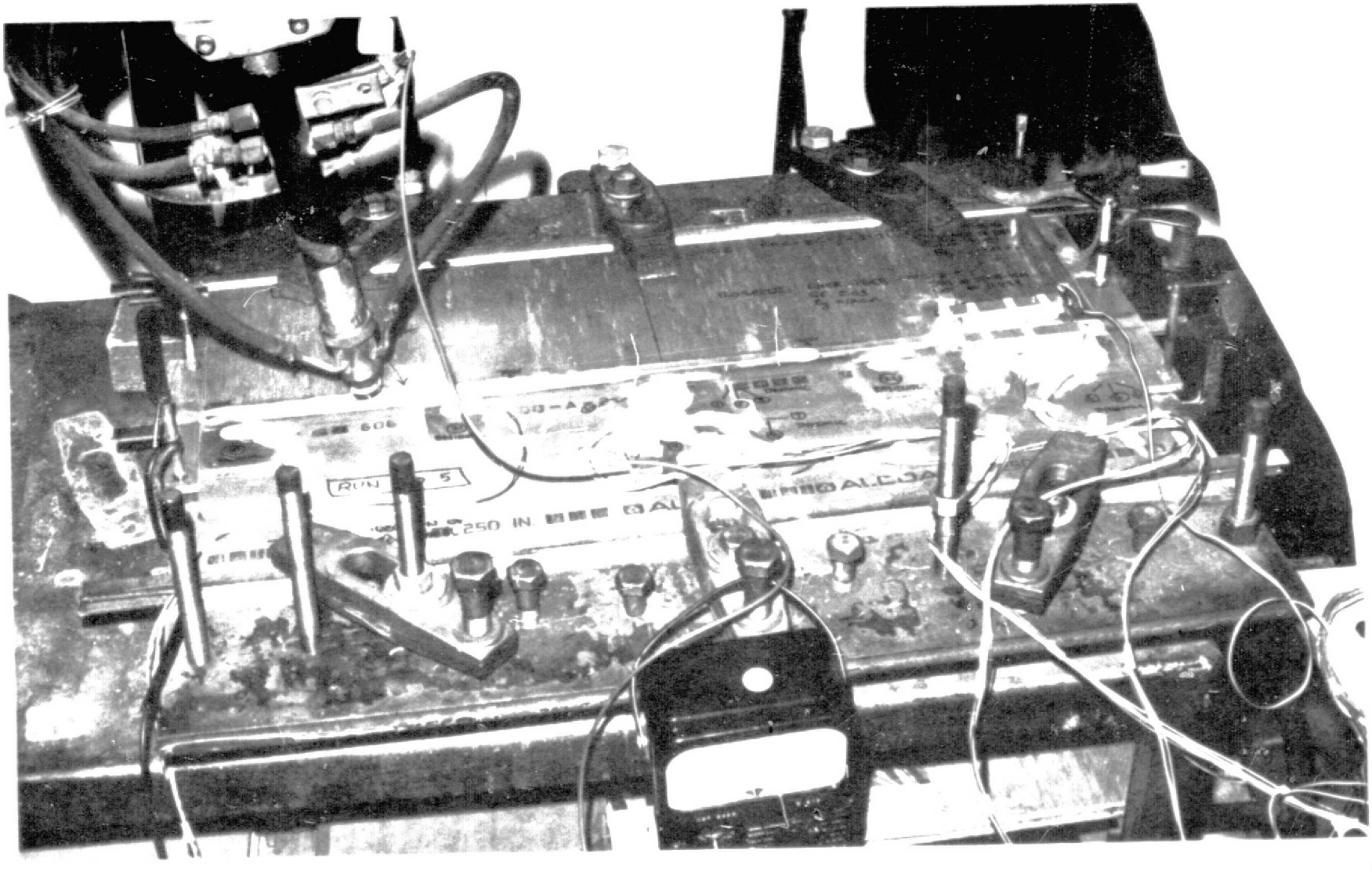

Figure 29: Plate Instrumented and Clamped Under Welding Torch.

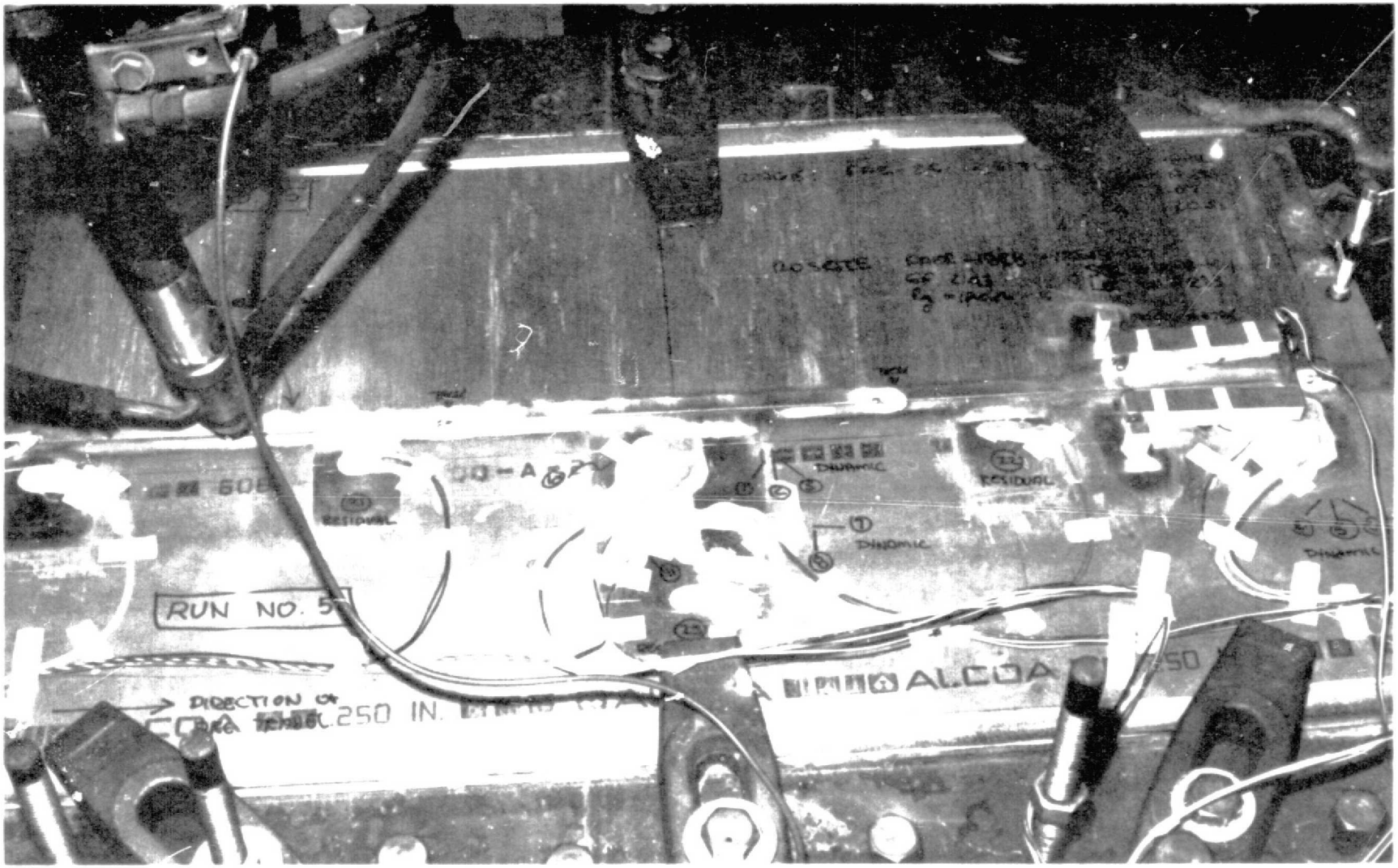

Figure 30: Plate Instrumented and Clamped Under Welding Torch.

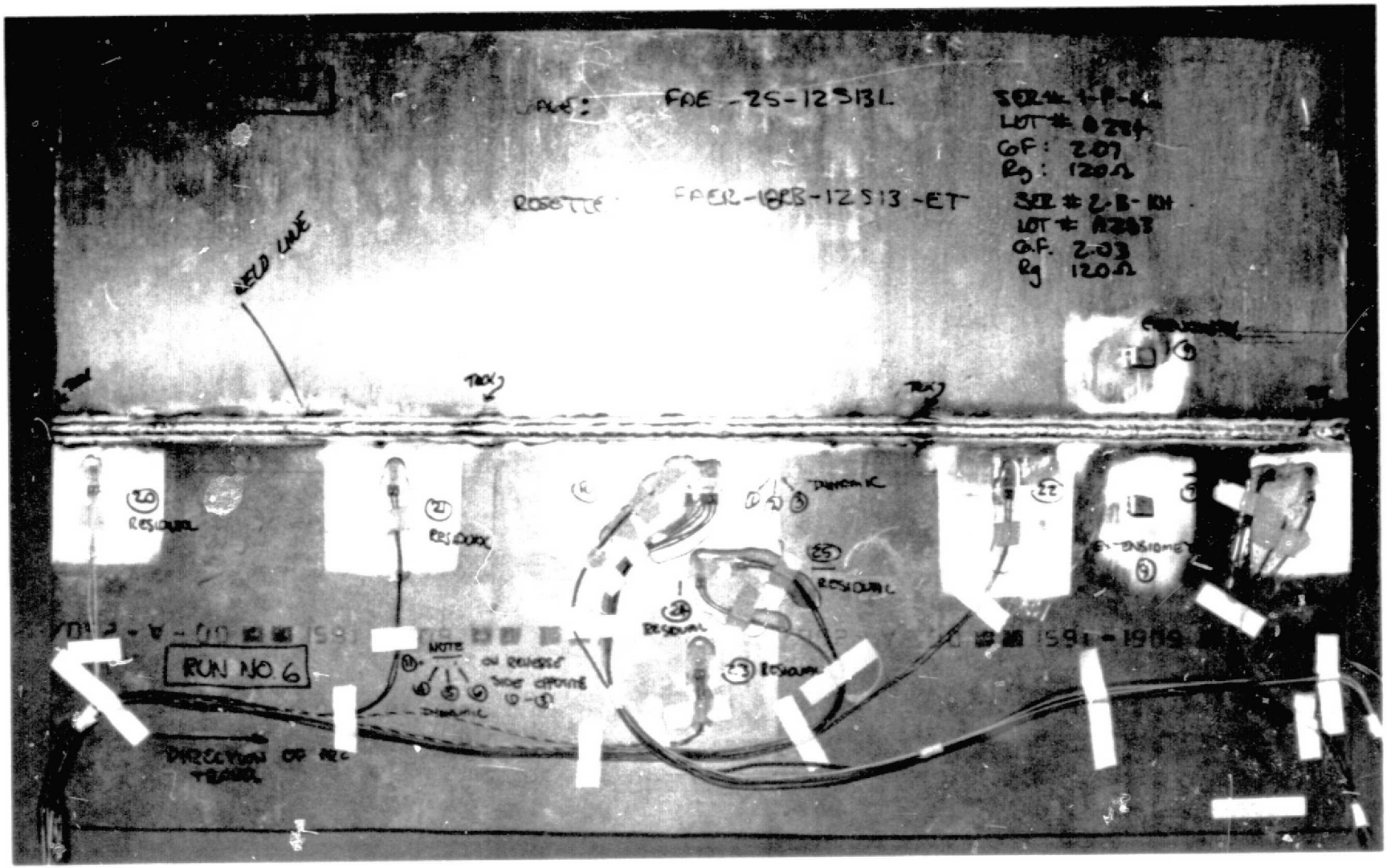

Figure 31: Sample Plate Instrumented and Welded.

bead-on-plate to butt. Wire feed is a functin of the other variables and was maintained by the machine automatically. Figures 29 through 31 are photographs of the actual equipment set-up.

E. Experimental Procedures:

The experimental operation is shown schematically in Figure 32. The test plate was instrumented and clamped into place. The welding machine was lined up with the joint and positioned over the run-off tab at the left end of the backing plate. Welding speed, arc voltage and amperage were pre-set. The visicorder was actuated and an arc was struck on the backing plate. As the welding torch crossed from starting tab to plate, the timer was started. The Visicorder output was marked when the arc passed the center strain gage location. When the welding bead reached the run-off tab at the right end of the plate, the arc was extinguished and the plate allowed to cool. Thr recorder continued to monitor the gages until the plate cooled to ambient temperature. After cooling, the plate was released from its clamp, and the new strains recorded either with the recorder or the Budd Instrument.

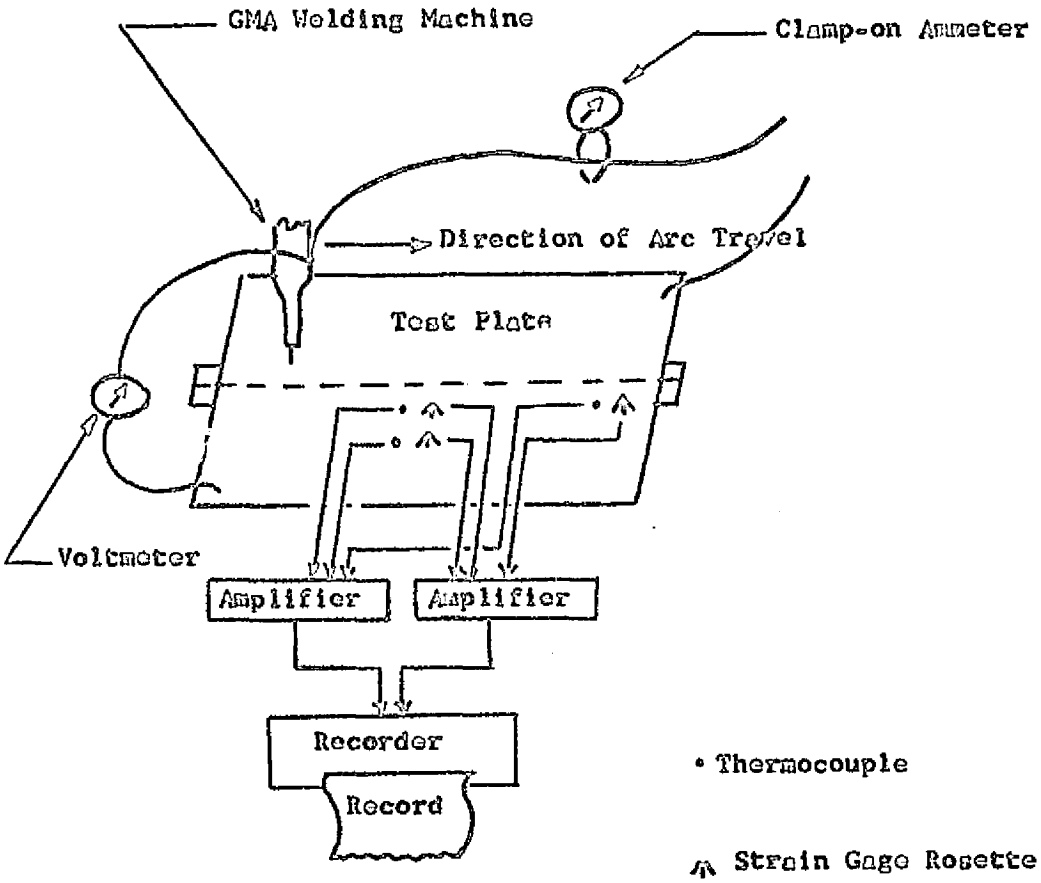

Figure 32: Schematic of Apparatus and Procedure. (7)

IV: DATA DEDUCTION

A. General:

At any point on a free (unloaded) surface of a solid, it is necessary to know three independent quantities in order to specify the state of stress completely. These quantities are the magnitudes of two principal stresses, σ_1, and σ_2, and their directions, ϕ or $(\phi + 90°)$, with respect to some reference. For isotropic elastic materials, these values can be calculated from strains measured on the surface at the point in question, and since three independent quantities are to be determined, it will be necessary to make three independent measurements of strain (42, pp. G2-03).

B. Strain Calculations:

Equation 47 describes the relationship for general strains for a three-element rosette shown in Figure 33.

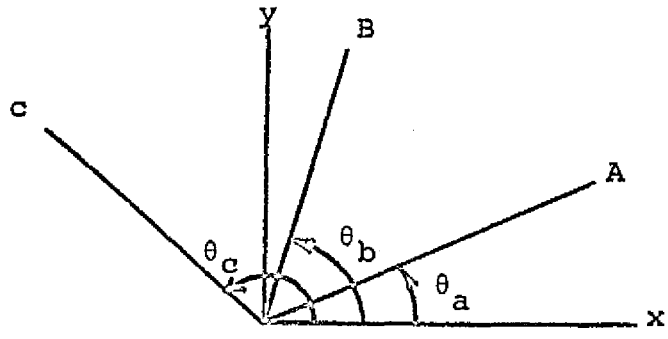

Figure 33

$$\begin{bmatrix} \varepsilon_a \\ \varepsilon_b \\ \varepsilon_c \end{bmatrix} = \begin{bmatrix} \cos^3\theta_a & \sin^2\theta_a & \sin\theta_a \cos\theta_a \\ \cos^2\theta_b & \sin^2\theta_b & \sin\theta_b \cos\theta_b \\ \cos^2\theta_c & \sin^2\theta_c & \sin\theta_c \cos\theta_c \end{bmatrix} \begin{bmatrix} \varepsilon_x \\ \varepsilon_y \\ \gamma_{xy} \end{bmatrix} \quad (47)$$

In the special case of a three-element 45° rectangular rosette shown in Figure 34,

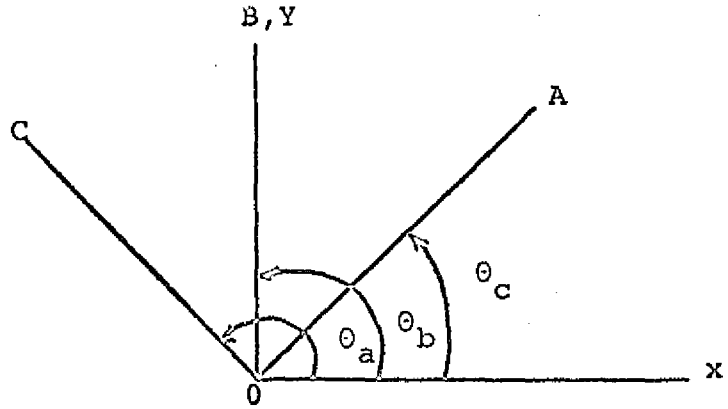

Figure 34

Equation (47) reduces to

$$\begin{bmatrix} \varepsilon_a \\ \varepsilon_b \\ \varepsilon_c \end{bmatrix} = \frac{1}{2} \begin{bmatrix} 1 & 1 & 1 \\ 0 & 2 & 0 \\ 1 & 1 & -1 \end{bmatrix} \begin{bmatrix} \varepsilon_x \\ \varepsilon_y \\ \gamma_{xy} \end{bmatrix} \quad (48)$$

Solving Equation (48) for ε_x, ε_y, and γ_{xy},

$$\begin{bmatrix} \varepsilon_x \\ \varepsilon_y \\ \gamma_{xy} \end{bmatrix} = \begin{bmatrix} 1 & -1 & 1 \\ 0 & 1 & 0 \\ 1 & 0 & -1 \end{bmatrix} \begin{bmatrix} \varepsilon_a \\ \varepsilon_b \\ \varepsilon_c \end{bmatrix} \quad (49)$$

The Mohr's Circle for this special case is shown in Figure 35.

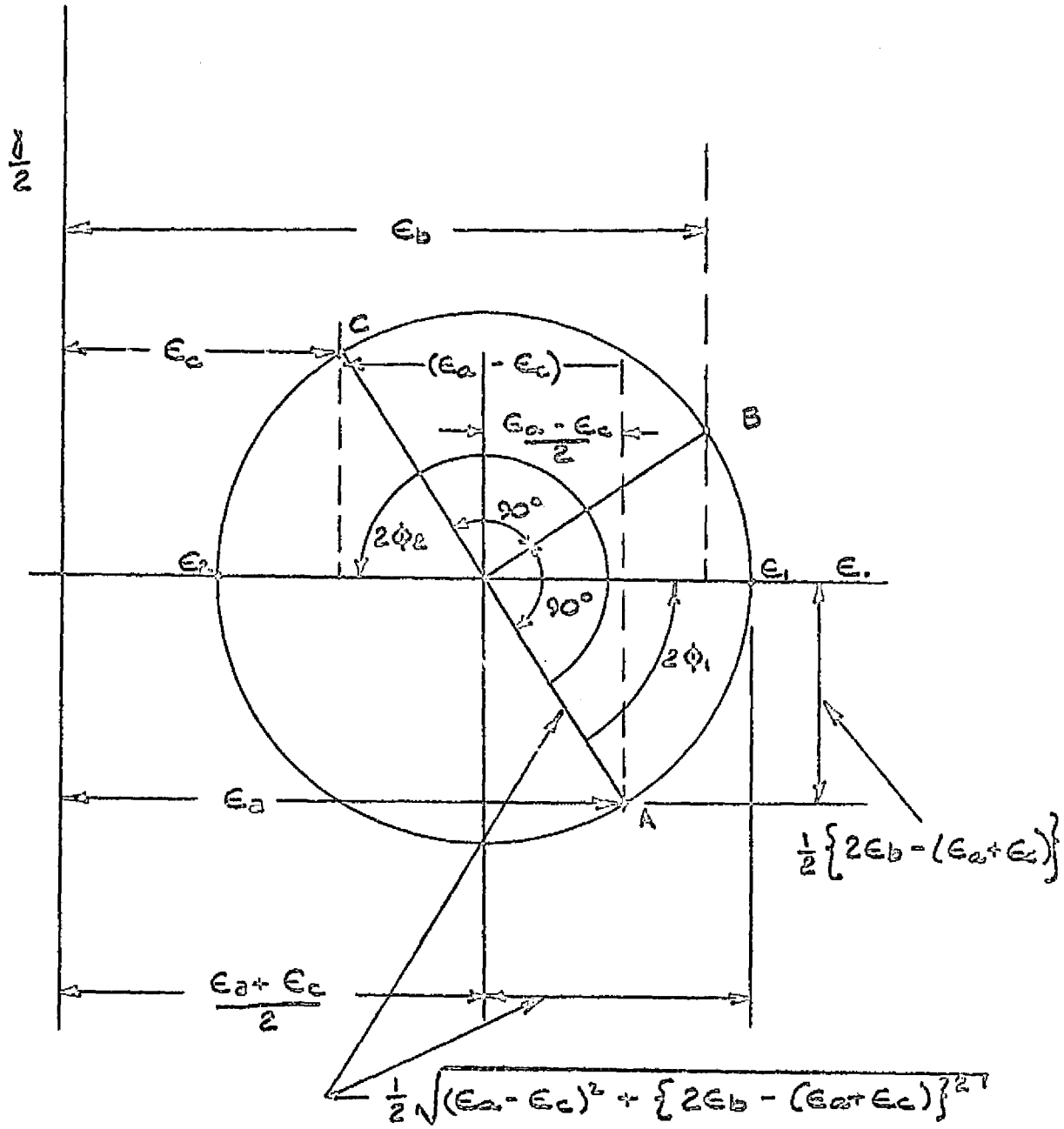

Figure 35: Mohr's Circle for the Rectangular Rosette With Three Observations of Strain (42, pp. G2-12).

Principal strains are

$$\varepsilon_1 = \left(\frac{\varepsilon_x + \varepsilon_y}{2}\right) + \frac{1}{2}\sqrt{(\varepsilon_x - \varepsilon_y)^2 + \gamma_{xy}^2} \qquad (50)$$

$$\varepsilon_2 = \left(\frac{\varepsilon_x + \varepsilon_y}{2}\right) - \frac{1}{2}\sqrt{(\varepsilon_x - \varepsilon_y)^2 + \gamma_{xy}^2} \qquad (51)$$

where ϕ is defined as the angle of one of the principal axes with respect to the axis of reference. Mathematically,

$$\text{Tan } 2\phi = \frac{\gamma_{xy}}{\varepsilon_x - \varepsilon_y} \qquad (52)$$

In the literature, there is considerable confusion concerning ϕ and which principal axis it defines. Murray (42, pp. G2-11, 15) offers a consistent method for dealing with this problem. If ϕ_1 is defined as the angle measured (positive in the anti-clockwise direction) from the positive OA axis of the strain rosette to the positive O1 axis which corresponds to the direction of ε_1, the algebraically largest principal strain, then:

Rule 1. When $\varepsilon_b > \frac{\varepsilon_a + \varepsilon_c}{2}$, then $0° < \phi_1 < 90°$ (53)

Rule 2. When $\varepsilon_b < \frac{\varepsilon_a + \varepsilon_c}{2}$, then $-90° < \phi < 0°$ (54)

Rule 3. When $\varepsilon_b = \frac{\varepsilon_a + \varepsilon_c}{2}$ (55)

and (a) $\varepsilon_a > \varepsilon_c$, then $\varepsilon_a = \varepsilon_1$ and $\phi_1 = 0°$ (55a)

or (b) $\varepsilon_a < \varepsilon_c$, then $\varepsilon_a = \varepsilon_2$ and $\phi_1 = \pm 90°$ (55b)

Rules 1 through 3 are defined with axis OA as the reference. To convert to the situation consistent with this investigation, axis OA is +45° (anti-clockwise) from the x-axis.

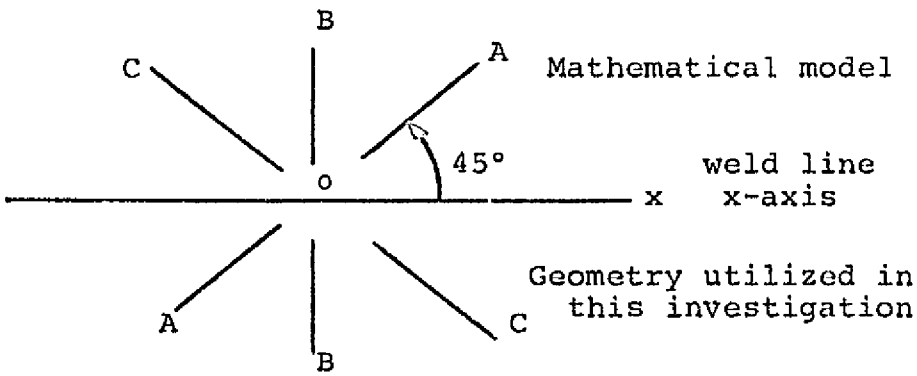

Figure 36

$$\phi_x = \phi_1 + 45° \qquad (56)$$

The geometry utilized in this investigation reduces to that of the mathematical model if the axes are kept consistent with Figure 36.

C. Stress Calculations:

This investigation yields mechanical strains. The automatic temperature compensating feature of the strain gage coupled with the apparent strain correction removes the thermal strain effect. Stresses must be determined by total strain.

$$\varepsilon_{mech} + \varepsilon_{thermal} = \varepsilon_{total} \qquad (57)$$

where

$$\varepsilon_{thermal} = \int_{T_1}^{T_2} \alpha(T)\, dT \tag{40}$$

For general two-dimensional stress calculations,

$$\sigma_x = \frac{E}{1 - \nu^2} \left(\varepsilon_{x_{total}} + \nu \varepsilon_{y_{total}}\right) \tag{58}$$

$$\sigma_y = \frac{E}{1 - \nu^2} \left(\varepsilon_{y_{total}} + \nu \varepsilon_{x_{total}}\right) \tag{59}$$

$$\sigma_1 = \frac{E}{1 - \nu^2} \left(\varepsilon_{1_{total}} + \nu \varepsilon_{2_{total}}\right) \tag{60}$$

$$\sigma_2 = \frac{E}{1 - \nu^2} \left(\varepsilon_{2_{total}} + \nu \varepsilon_{1_{total}}\right) \tag{61}$$

For this particular configuration,

$$\gamma_{xy_{mech}} = \varepsilon_a - \varepsilon_c = \gamma_{xy_{total}} \tag{62}$$

$$\tau_{xy} = G\gamma_{xy} = \frac{E}{2(1 + \nu)} \gamma_{xy} \tag{63}$$

ν is Poisson's ratio. Nominally, $\nu \approx .333$ for aluminum. ν will probably change with temperature, but should not exceed a maximum value of .500 in the weld puddle because of volume consideration when melted (at .500, there will be no volume change).

Stress calculations are dependent upon $E(T)$ and $\alpha(T)$ assuming ν is relatively independent of temperature. These

values may be determined from Table 5 in Chapter II. The values of $E(T)$ given assumes that the value from a half-hour soak approximates that from welding.

D. Determination of Plastic Conditions:

Masubuchi (43) theorizes that the region in the vicinity of the weld has undergone plastic deformation when the invarient I is larger than the value of yield stress, where,

$$I = (\sigma_x^2 - \sigma_x\sigma_y + \sigma_y^2 + 3\tau_{xy}^2)^{1/2} \qquad (64)$$

This value was derived from the second stress deviator tensor invariant J_2 (44, pp. 41) which for a two-dimensional situation is reduced to

$$J_2 = \frac{1}{3}(\sigma_x^2 - \sigma_x\sigma_y + \sigma_y^2 + 3\tau_{xy}^2) = \frac{1}{3}I^2 \qquad (65)$$

The Distortion Energy Theory (Von Mises' Yield Criterion) at the yield point in simple tension (44, pp. 75) predicts that

$$J_2 = \frac{1}{3}\bar{\sigma}^2 \qquad (66)$$

Equating Equations (65) and (66)

$$J_2 = \frac{1}{3}I^2 = \frac{1}{3}\bar{\sigma}^2 \qquad (67)$$

or

$$I = \bar{\sigma} = \sqrt{3J_2} \qquad (68)$$

Therefore, a check to see if plastic conditions exist would occur is that

$$\frac{I\ (T)}{\bar{\sigma}\ (T)} \geq 1.0 \qquad (69)$$

It is important to note that any single component of the stress field in Equation (65) may be greater than the yield stress in simple tension without having yield occur.

Again, the yield stress is determined from Table 5 in Chapter II.

E. Data Reduction Program:

Appendix B lists the basic program utilized for rosettes in this investigation. It is modified slightly to suit other geometries (rosettes in different locations) or slightly different welding conditions. Input cards are listed as comment cards in the main program and samples are shown in the appendix. In the case where all strains are zero or equal, the program defaults to $\phi_x = 90°$. For example, if at time = 0.0 the strains are initialized to zero, the resulting ϕ_x at time = 0.0 is meaningless. In the case where initial strains at time = 0.0 are not zero, the program will reference all succeeding strains to their initial value. Single element strain gage data may be processed by this same program to provide temperature compensation.

V RESULTS:

A. General Trends:

Figures 37 through 59 graphically present part of the experimental data tabulated in Appendix C. Table 7 discusses the particular problems and parameters associated with each test. Several effects are discussed below:

1. Arc Efficiency. Figures 37 through 40 show the temperature distributions for Test No. 1 and 2, and also the one dimensional computer analysis results for $\eta = 0.70$ and 0.75. The $\eta = 0.75$ curve seems to fit the data best. This efficiency factor includes all heat loss effects associated with the heat generation and cooling. The tail of the experimental temperature distribution is higher than the computer analysis because, geometrically, the experimental plates are not infinite and cool slower than the computer model.

2. Placement of Strain Gages. Figure 41 shows the transverse temperature distribution based on Figures 37 through 40. In general, the peak temperature predicted at transverse locations are supported by the testing shown in Figures 42 through 44. Figure 41 provides an effective technique for positioning strain gages to prevent damage or exceeding their temperature compensation limits.

Test Number	I Amperes	V Volts	v Inch/Sec.	Heat Input Joules/Inch	Comment
1.	230	20	0.536	8582	Butt weld to measure temperature distribution only. Immediately opposite thermocouple line arc burned a deep crater in the weld. Temperature distribution at 0.675 inch reflects problem. During last quarter of run, arc cut more plate than it welded. More tacks are required, i.e., shift from 2 to 4.
2.	220	20	0.536	8209	Bead-on-plate to measure temperature distribution only
3.	240	19	0.536	8507	Bead-on-plate to measure temperature distribution and strains. Sensitivity of Visicorder set low.
4.	240	19	0.536	8507	Bead-on-plate to measure temperature distribution and strains. Strain readings in the vicinity of the arc on all rosettes appeared erratic. Strains were much higher than expected.
5.	250	19	0.536	8862	Butt weld to measure temperature distribution and strains.
6.	250	19	0.536	8862	Butt weld to measure temperature distribution and strains. Gages 4 and 5 failed after arc passed by in vicinity of highest strains at 30+ seconds. At 42 seconds, Visicorder paper ran out and all remaining data was lost.

Table 7: Summary of Welding Conditions for Each Test

Test Number	I: Amperes	V: Volts	v: in./min	t: inches	EI/vt: Watt-min/in^2	b_h inches
1.	230	20	32.16	.250	572.14	0.488
2.	220	20	32.16	.250	547.26	0.473
3.	240	19	32.16	.250	567.16	0.485
4.	240	19	32.16	.250	567.16	0.485
5.	250	19	32.16	.250	590.80	0.499
6.	250	19	32.16	.250	590.80	0.499

TABLE 8: Summary of Extent of HAZ (b_h)

3. Butt vs. Bead-on-plate Characteristics. Figures 41 through 44 provide temperature distribution data for the tests with strain gages installed and Figures 45 through 51 provide data on transverse and longitudinal strain distributions resulting from these tests. Ideally, a butt weld becomes more and more like a bead-on-plate weld for multipass situations. One would hope for a two dimensional model which could cover both cases. Unfortunately, Figures 43 and 44 show a different inicial temperature distribution for bead-on-plate and butt welds. This implies that for the plate thickness utilized in this study, the two types of weld will behave somewhat differently in the way of thermally-induced strains, moments, and distortions. The bead-on-plate weld is not a two dimensional situation, but the butt weld clearly is. Figures 45, 46, 48, and 49 seem to agree with this observation for strains, since bottom bead-on-plate values do not match the top ones. The higher transverse strains for Test No. 4 are noted, but not fully explained. The strains were eratic at their peak values as if the plate was slipping in its constraint.

4. Correlation Between Experiments. In general, there is not much correlation between residual strains from experiment to experiment. This problem has been noted at MIT with previous experiments and is again noted here in the various strain distributions. An effort to find a

means of correlation was made by looking at the angle between the largest principal strain and the x-axis (ϕ_x). This data is shown in Figures 52 through 55. There seems to be little correlation in the residual strain region other than that the major strains are either close to the x or the y axis. Along the edge of the panel, however, the test data consistently show a ϕ_x which implies loading by shear.

Figures 56 through 58 provide a much more successful means of correlation. The ratio of the invariant described in Equation (64) to the temperature dependent uniaxial yield stress from Table 5 is plotted with respect to time. For residual conditions, there appears to be very good correlation between the "state of stress" composed of all stress components from test to test. In addition, when the value of this ratio exceeds 1.0, a yielding situation exists, and plastic deformation occurs.

The static residual strain measurements made during this study offered such a wide and inconsistent variety of values that they were not included. One possible reason for this is that the position of the strain gages one inch away from the centerline of the plate may have been near the region in Figure 1-4, where the stress distribution went through a zero point with a large slope . Hence, a minor variation in stress could imply large positive or negative

variations in strain.

5. Extensiometer. The extensiometer results are plotted in Figure 59. Initial measurements vary from experiment to experiment because of the difficulty of placing the holding tabs in the exact same position. However, it is interesting to note that for the two situations presented here, once the weld was filled in the vicinity of the extensiometer, the extensions became a measurement of transverse shrinkage and were similar in both tests. Test No. 1 utilized two tack welds at the ends of the plate, and the arc became unstable as a result of metal movement in the center. All subsequent tests utilized four equally spaced tacks, so the plates were essentially rigid except in the immediate region of the arc.

B. Accuracy of the Experimental Model and Instrumentation:

1. The Physical Model. As mentioned previously, the plate geometry, level of constraint, and welding procedures are considered to be representative of ship fabrication processes. However, the means of constraining the panels is unsatisfactory because of evidence of slipping. Considerable difficulty was experienced in cementing the strain gages to the model. The best cement still remains

EPY-600 because it offers a lower curing temperature. However, pressure must be applied to the gage while the cement is curing, making this an extremely critical stage in model production.

2. Data Reduction Calculations. The temperature compensation has been previously discussed. However, in the strain distributions presented, there is a strange fluctuation in the results in the vicinity of the arc immediately before the thermal strains take off. It is of the opinion of this author that this is in part, if not all, due to temperature compensation techniques and represents only an "apparent strain". In any case, it is a minor effect and relatively unimportant.

3. Instrumentation. The Visacorder output was scaled initially in Test No. 4 to 1200 microstrain/inch and for later tests at 500 to 600 microstrain/inch. The reading accuracy is well within the 5% instrument accuracy estimated by technicians aiding in this study.

4. Welding Machine. The welding machine utilized in this study leaves much to be desired. The speed drive appears not to give a uniform arc velocity although the time to span the full plate length seems to be consistent. The voltmeter and ammeter on the power supply have never been calibrated and a clamp-on ammeter and separate

voltmeter had to be utilized as a result. The meters on the actual welding machine controls are either inoperative or way out of calibration. There is no screen over the tip of the torch which prevents back splatter from fouling the automatic filler metal feed system. Luckily, the wire jams which occurred as a result were on the starting tabs and the expensive test plates were not ruined.

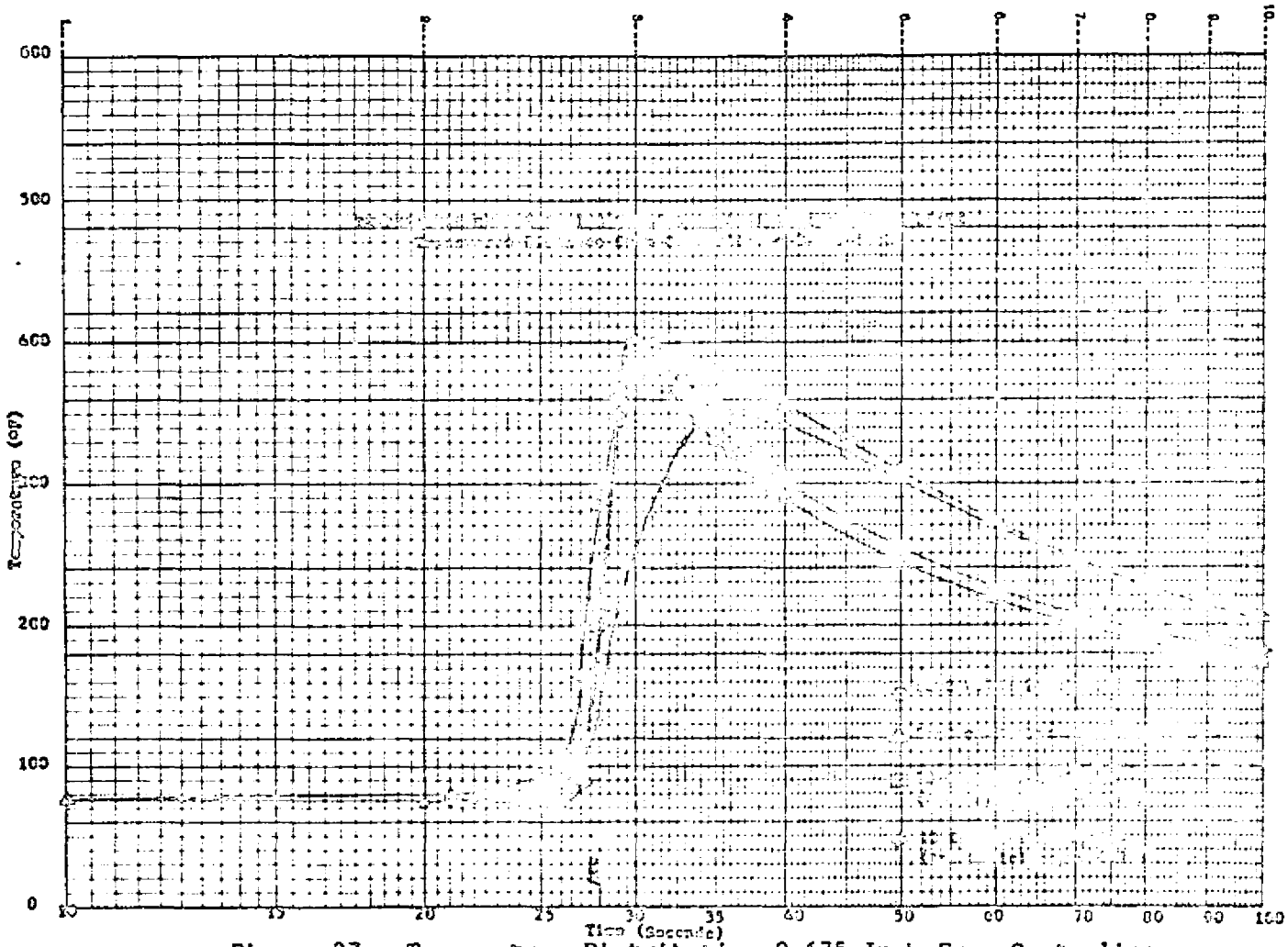

Figure 37: Temperature Distribution 0.675 Inch From Centerline.

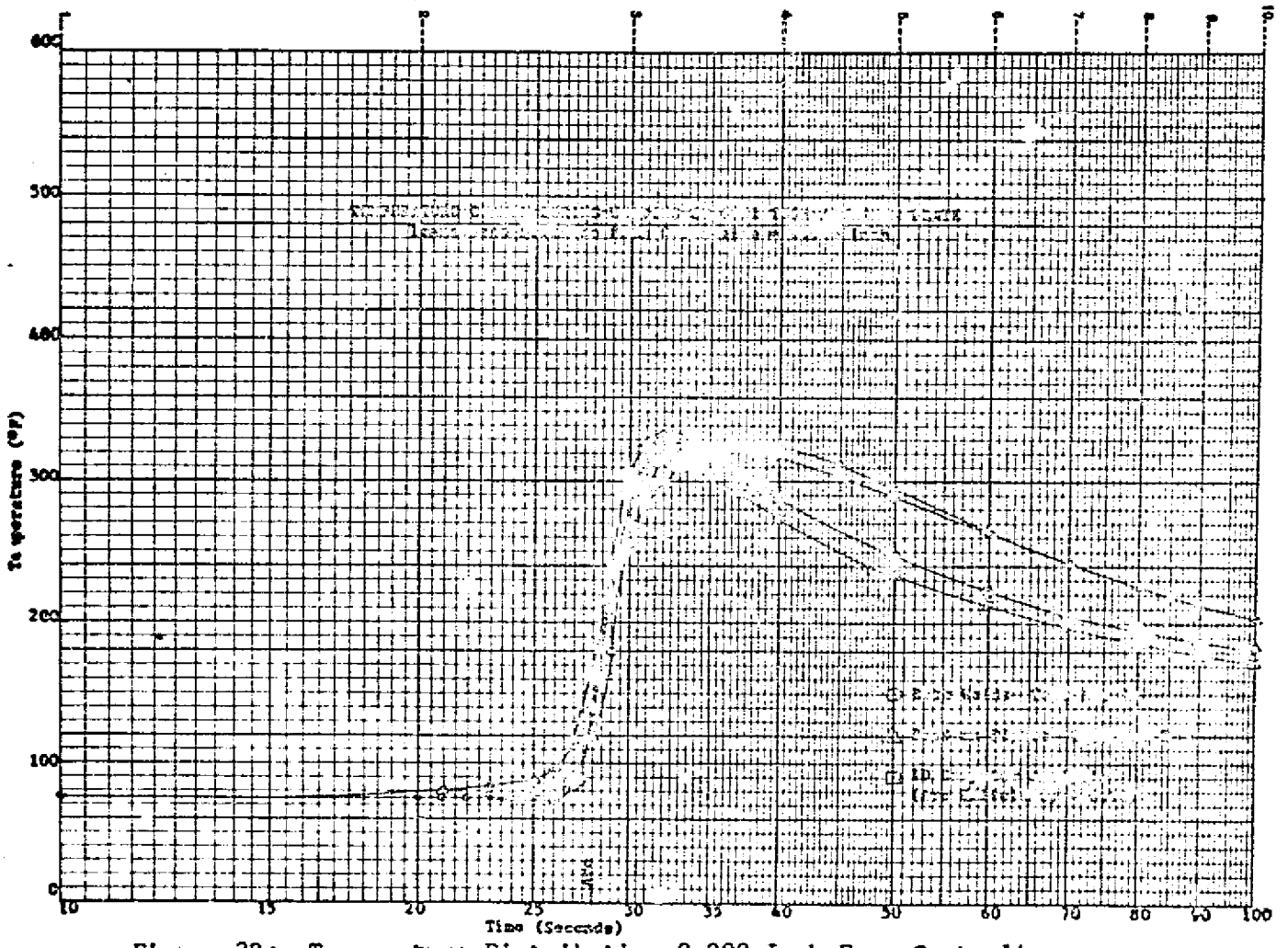

Figure 38: Temperature Distribution 0.900 Inch From Centerline.

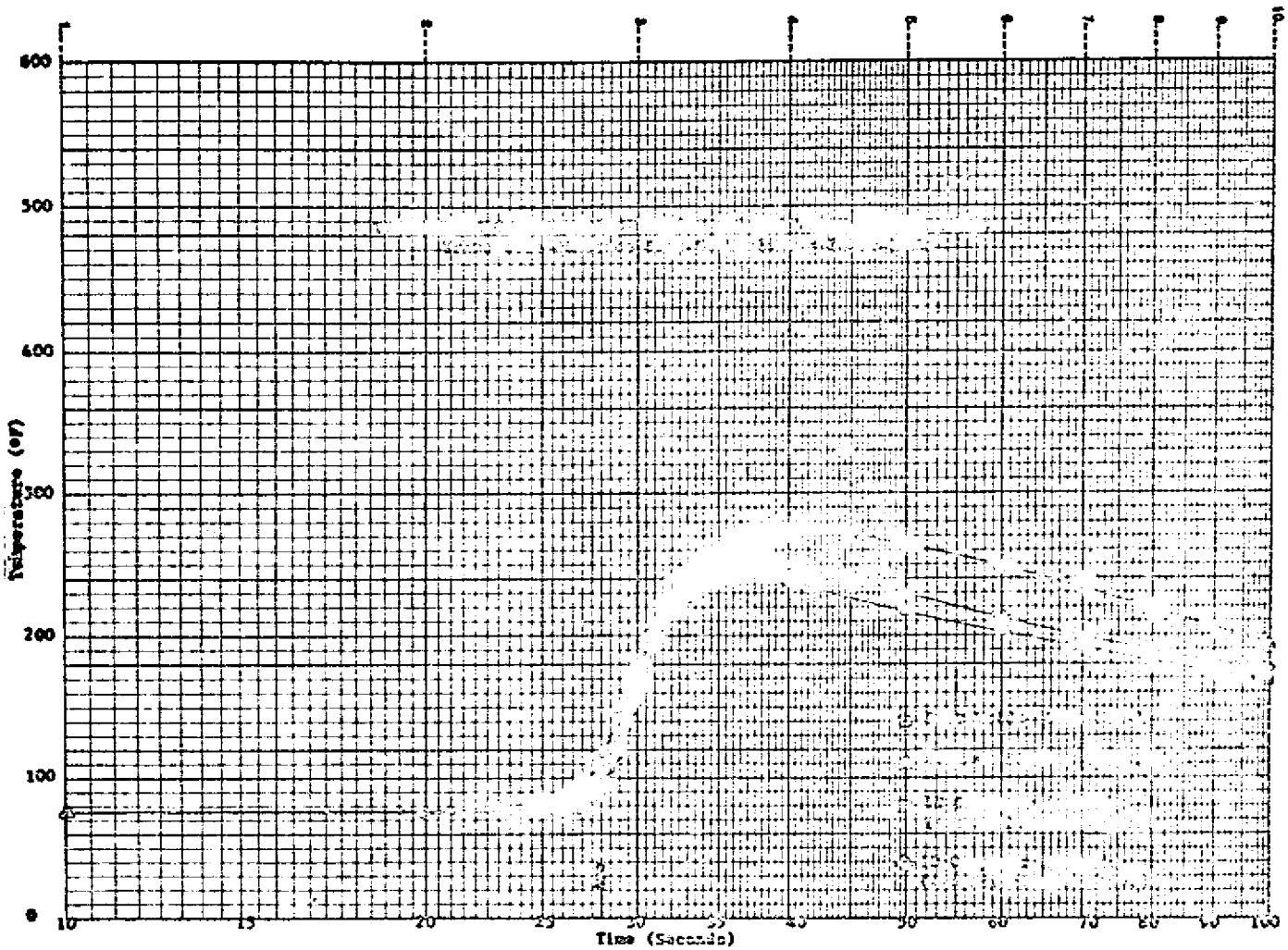

Figure 39: Temperature Distribution 1.350 Inch From Centerline.

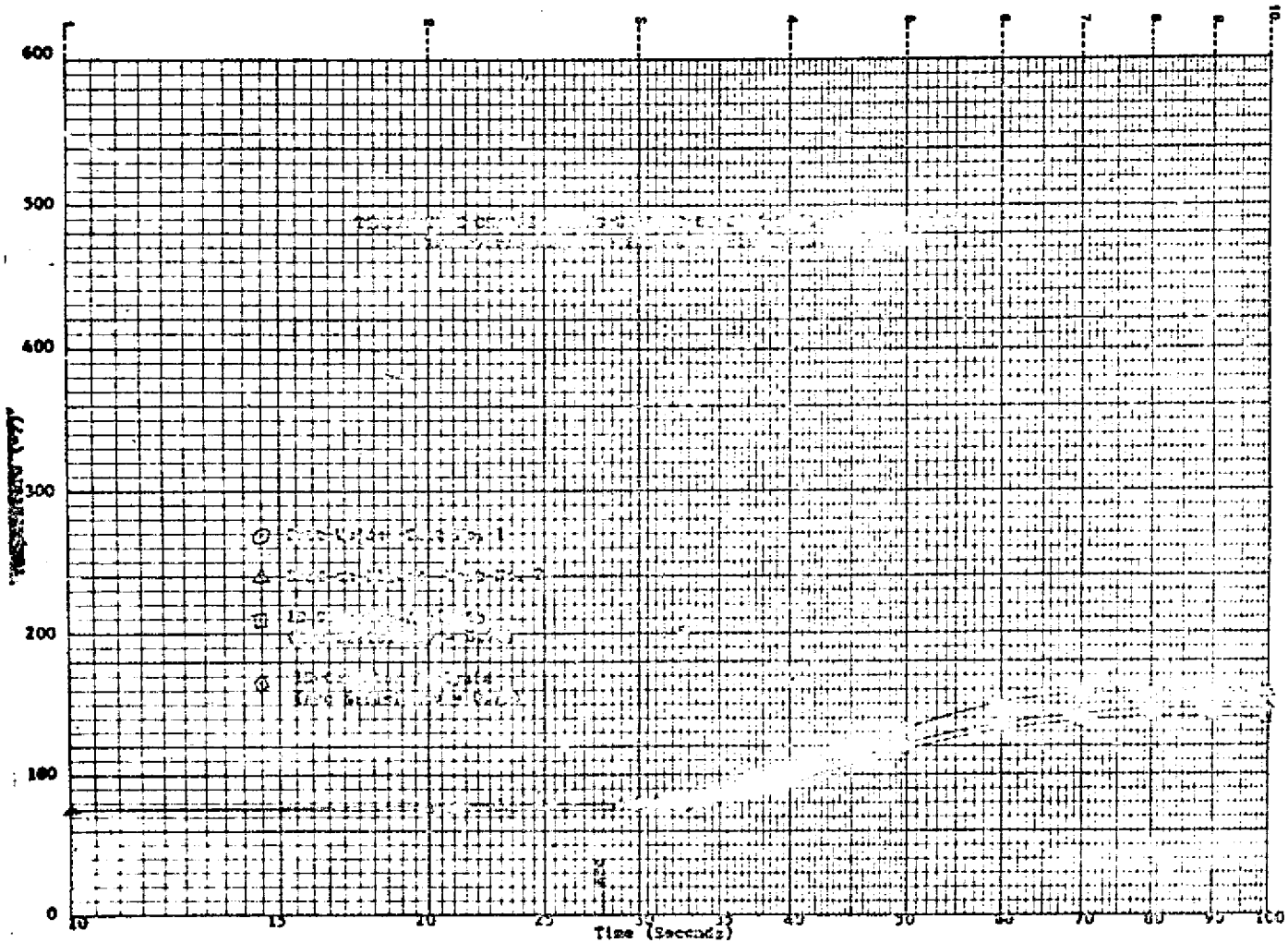

Figure 40: Temperature Distribution 3.600 Inches From Centerline.

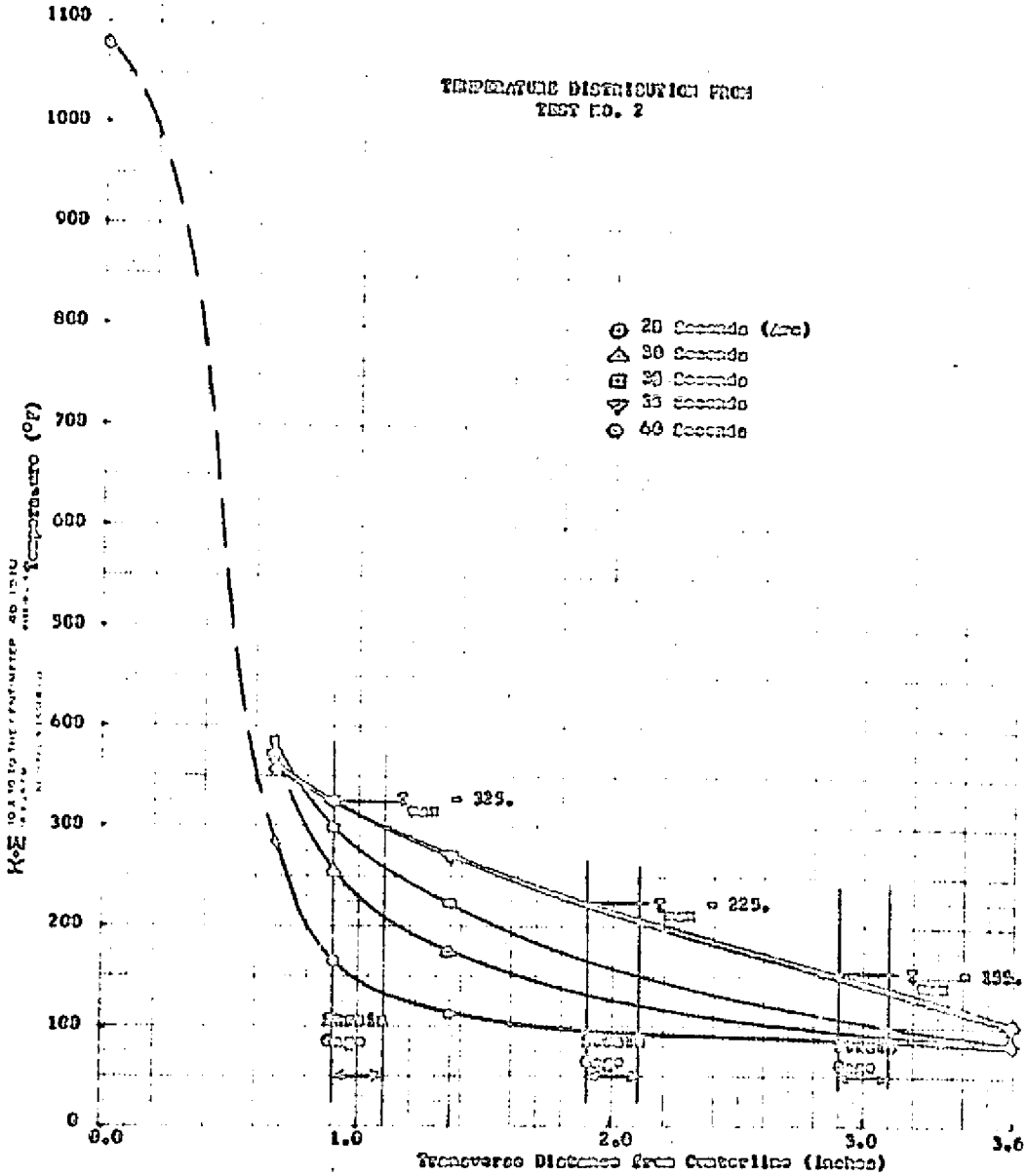

Figure 61: Transverse Temperature Distribution.

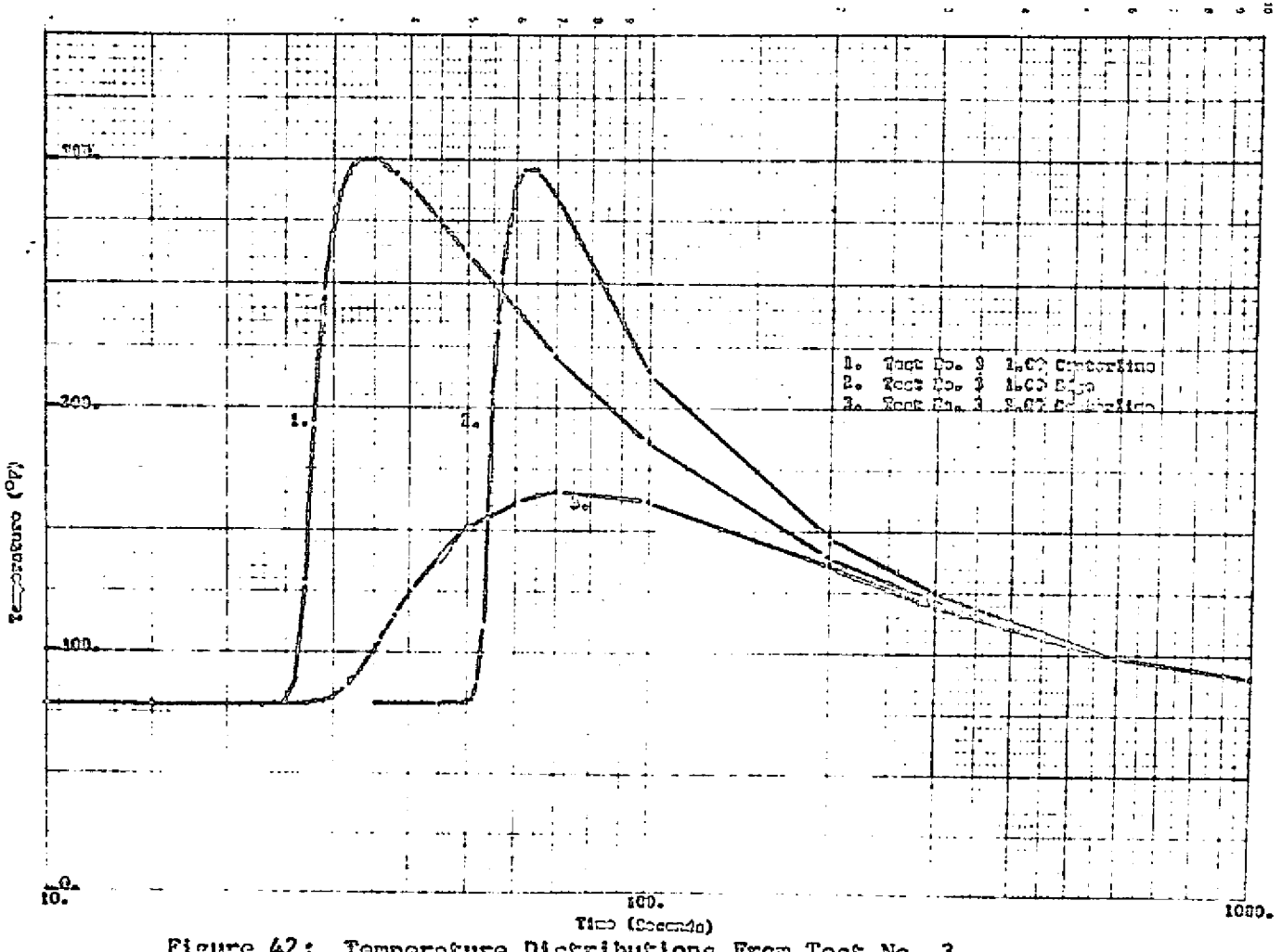

Figure 42: Temperature Distributions From Test No. 3.

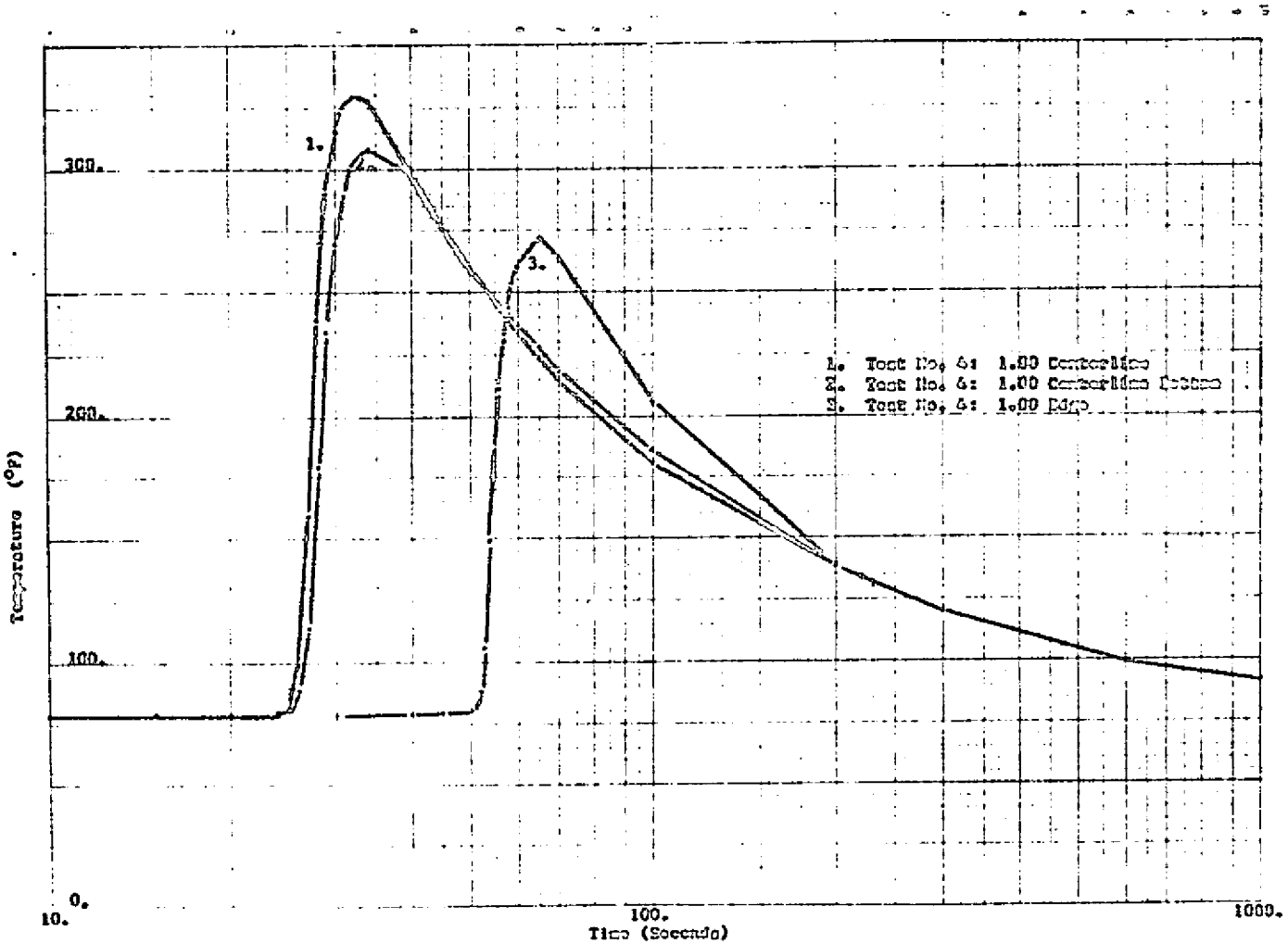

Figure 43: Temperature Distributions From Test No. 4.

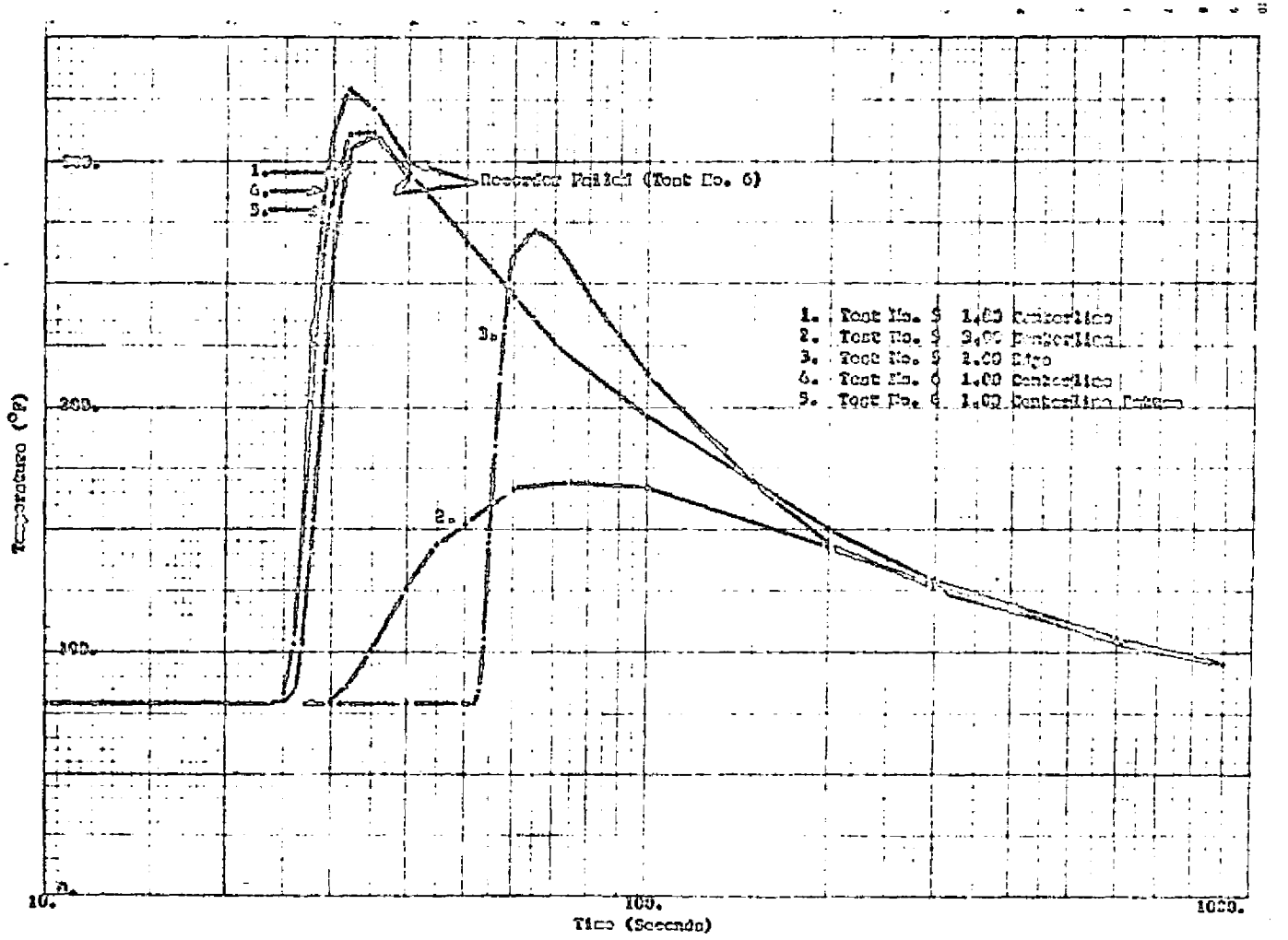

Figure 44: Temperature Distributions From Test No. 5 And 6.

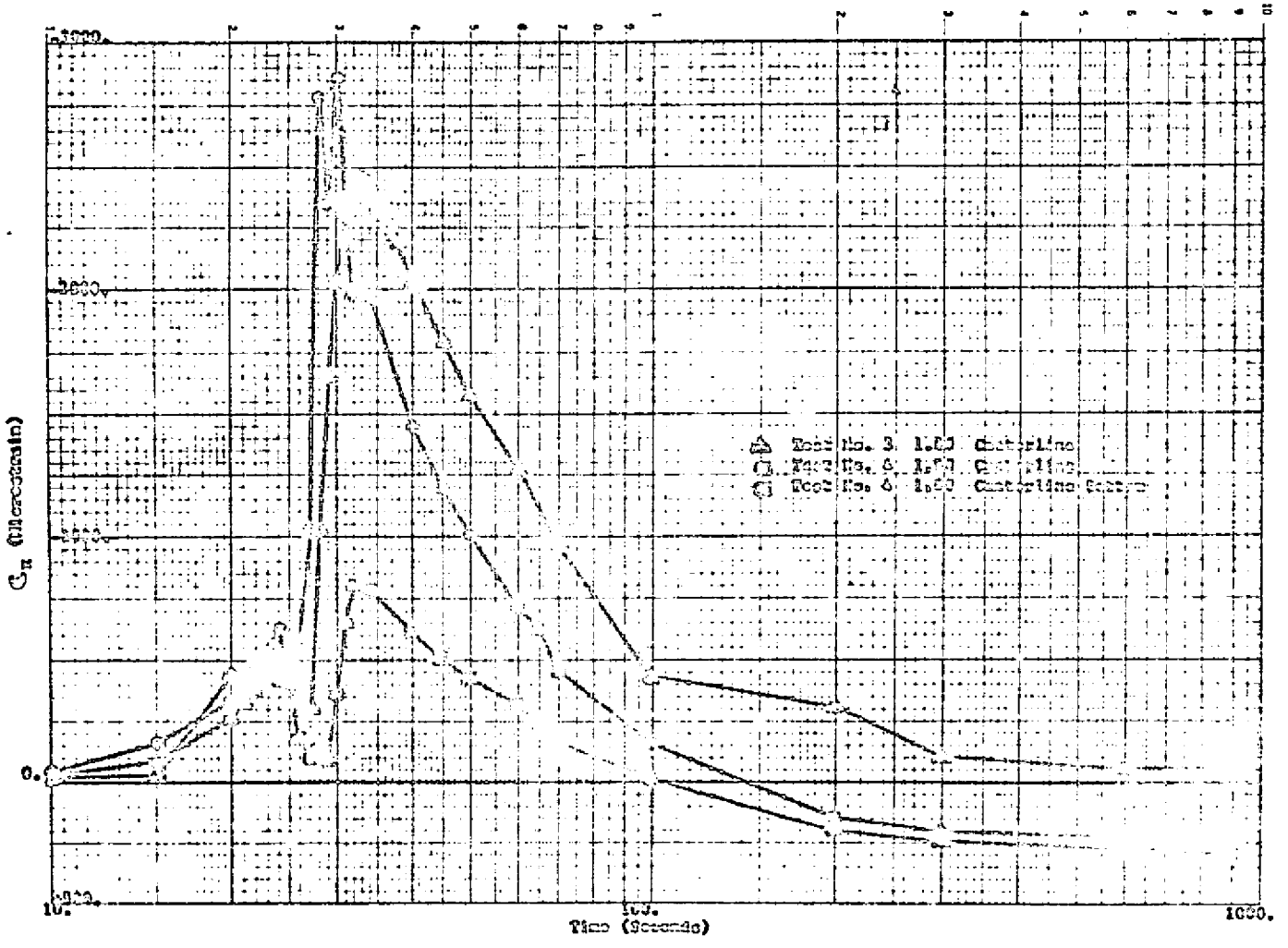

Figure 45: Longitudinal Strain Distributions.

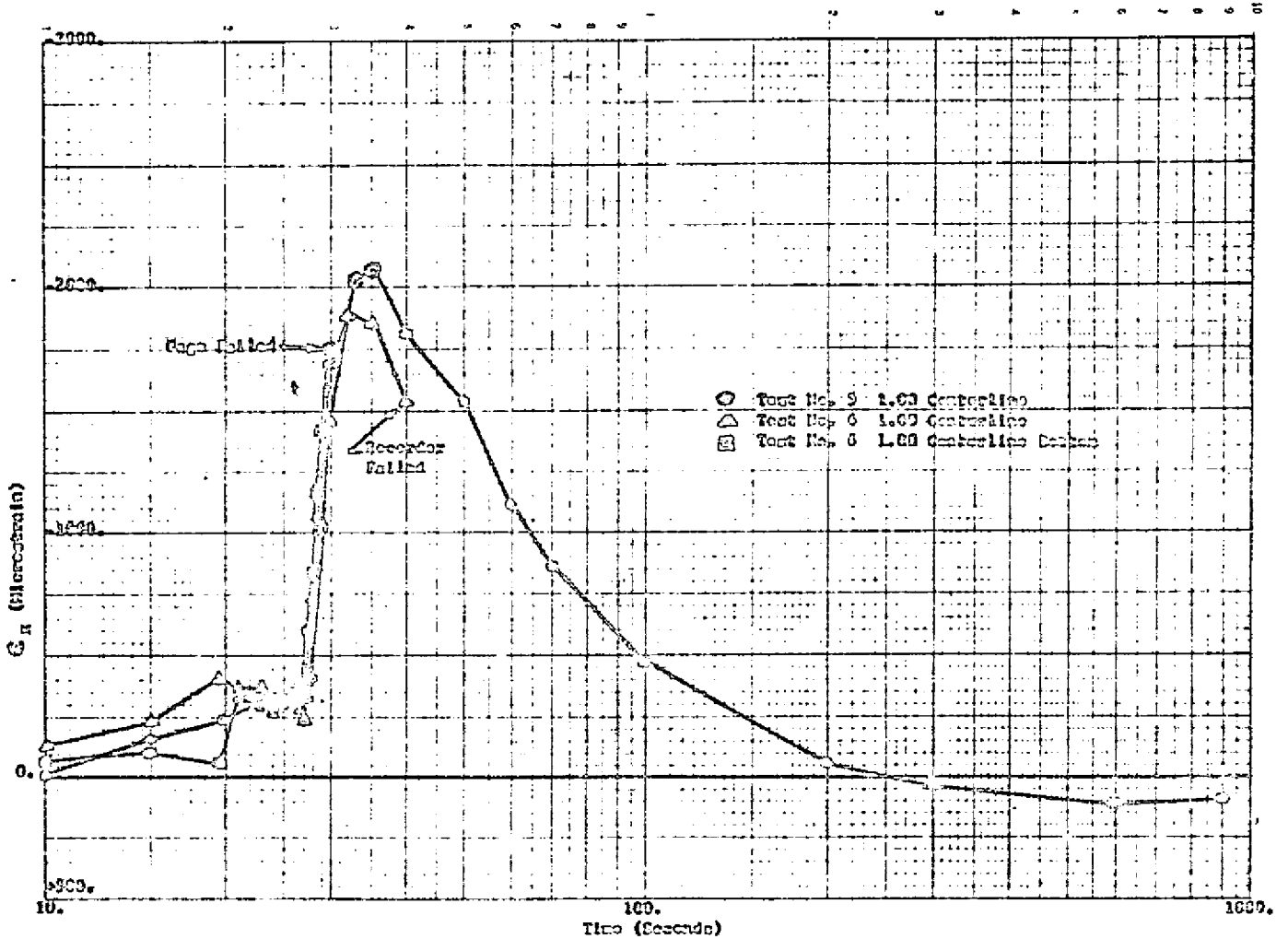

Figure 46: Longitudinal Strain Distributions.

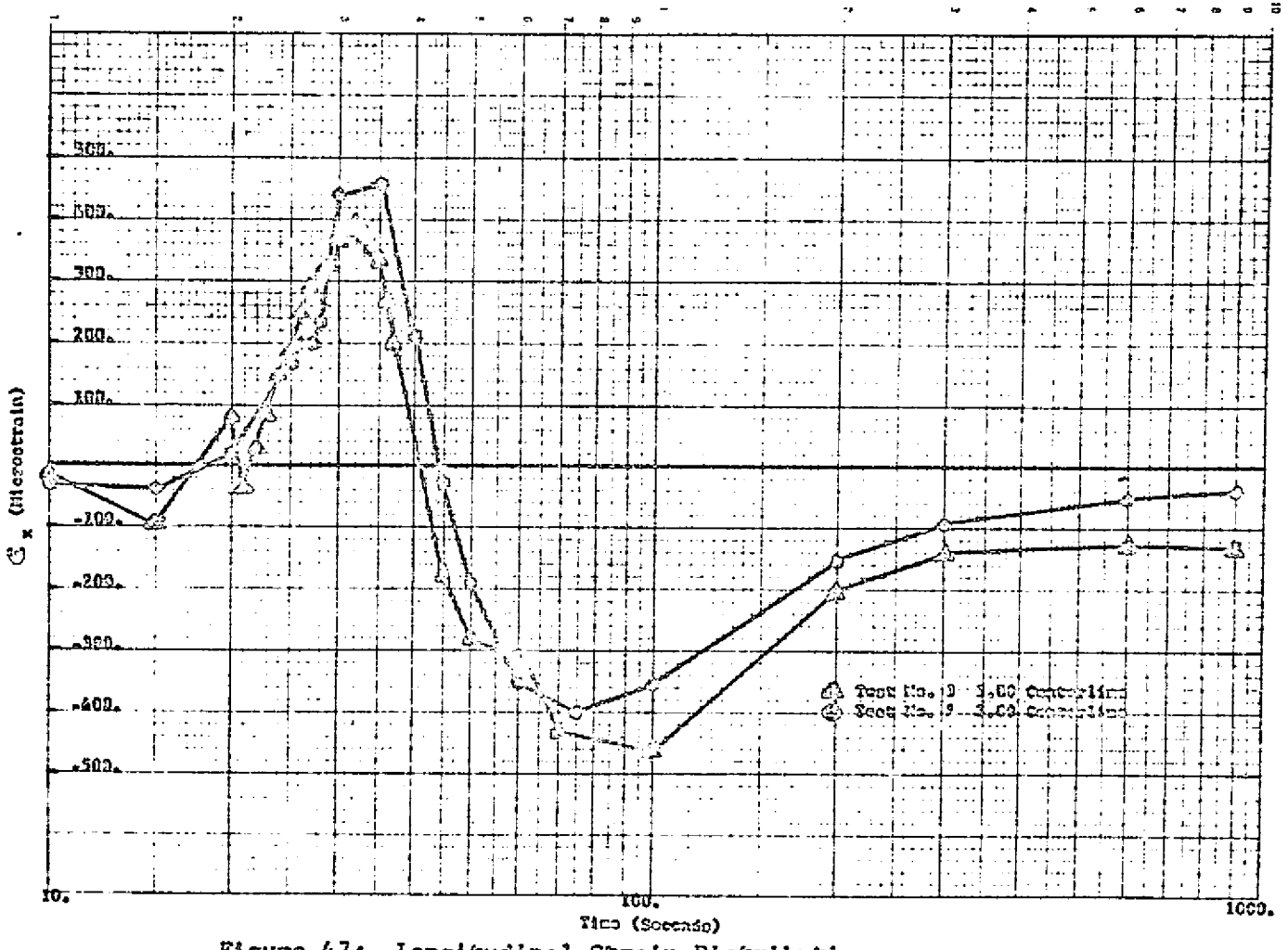

Figure 47: Longitudinal Strain Distributions.

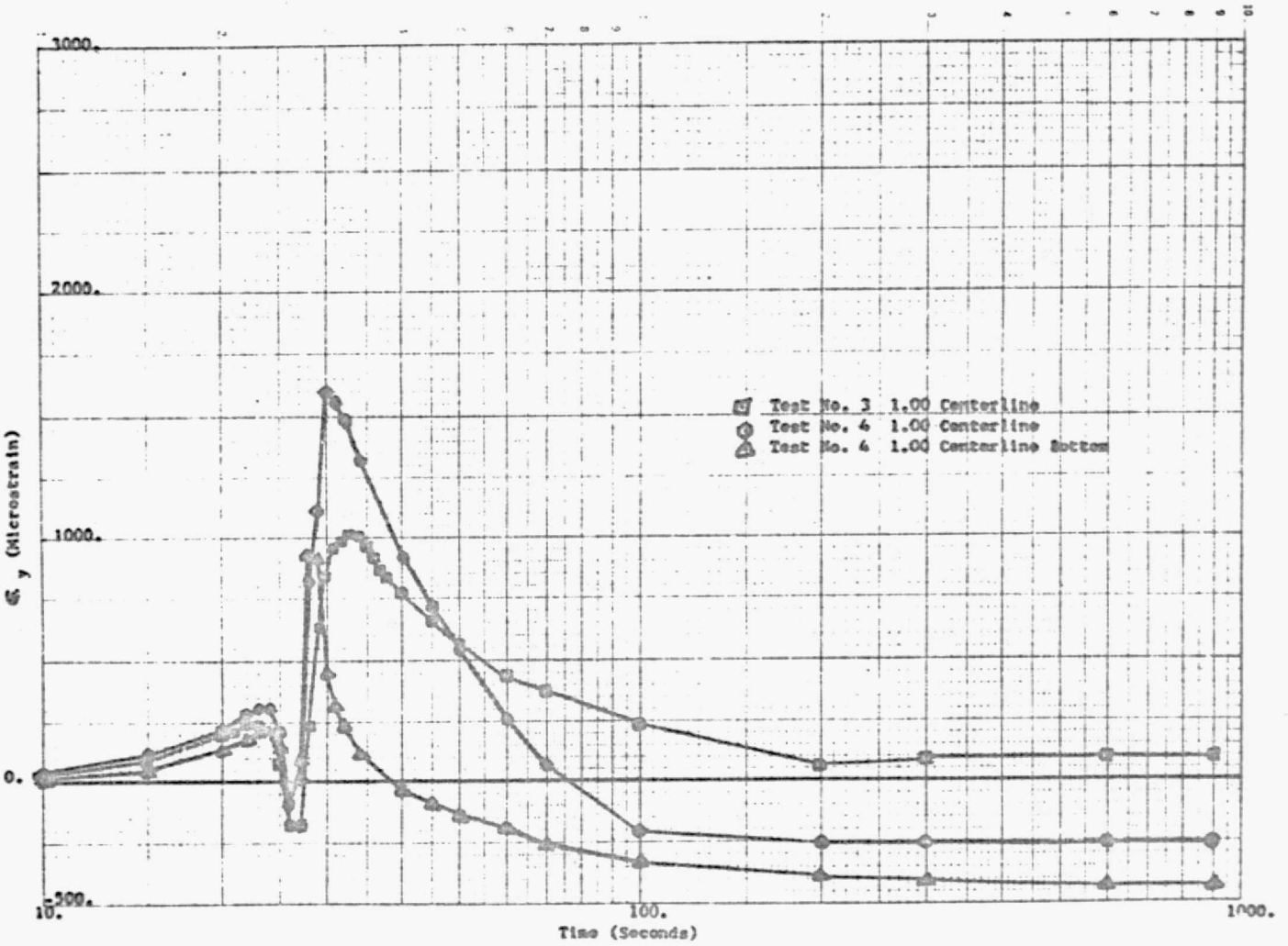

Figure 48: Transverse Strain Distributions.

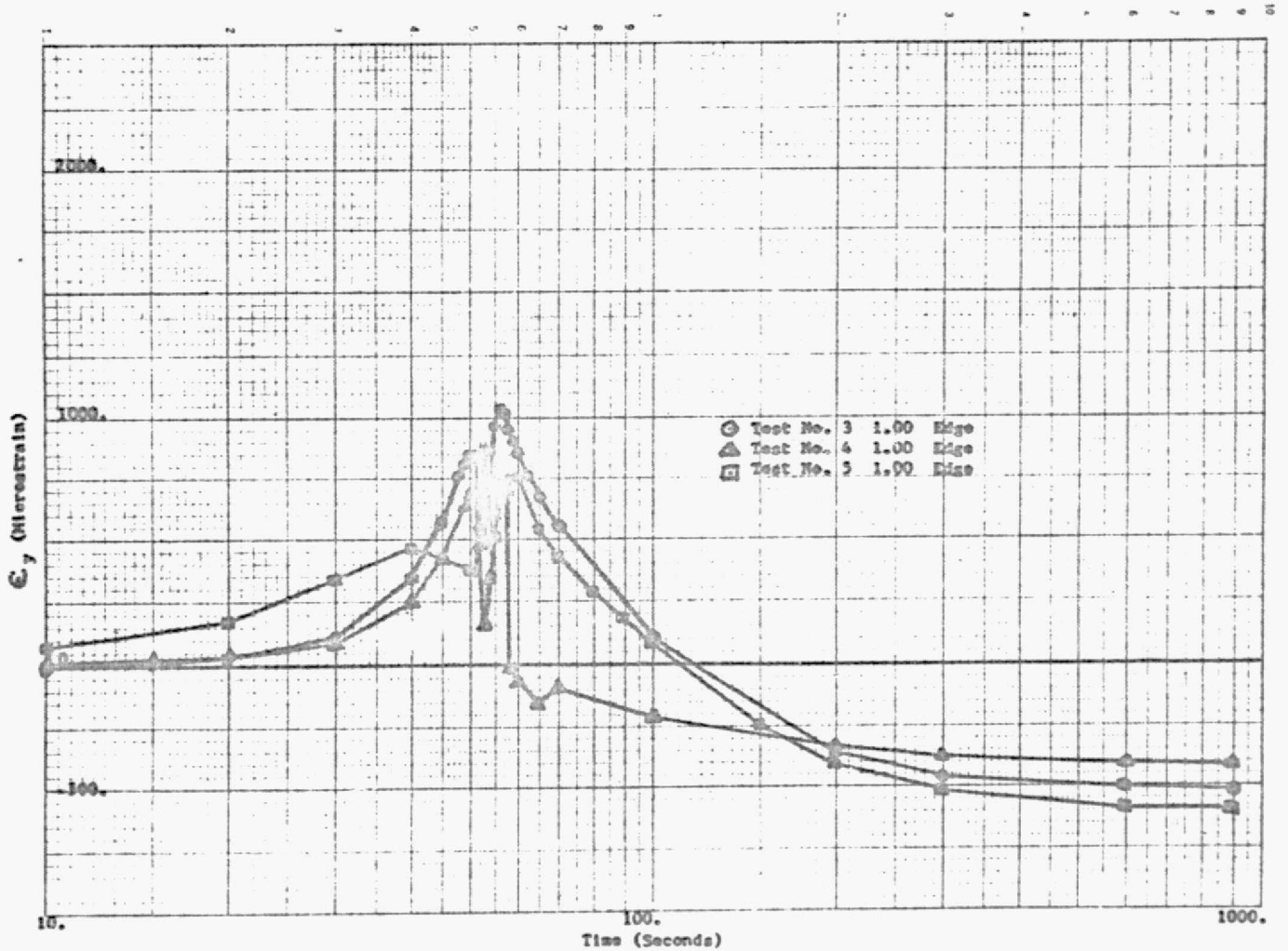

Figure 49: Transverse Strain Distributions.

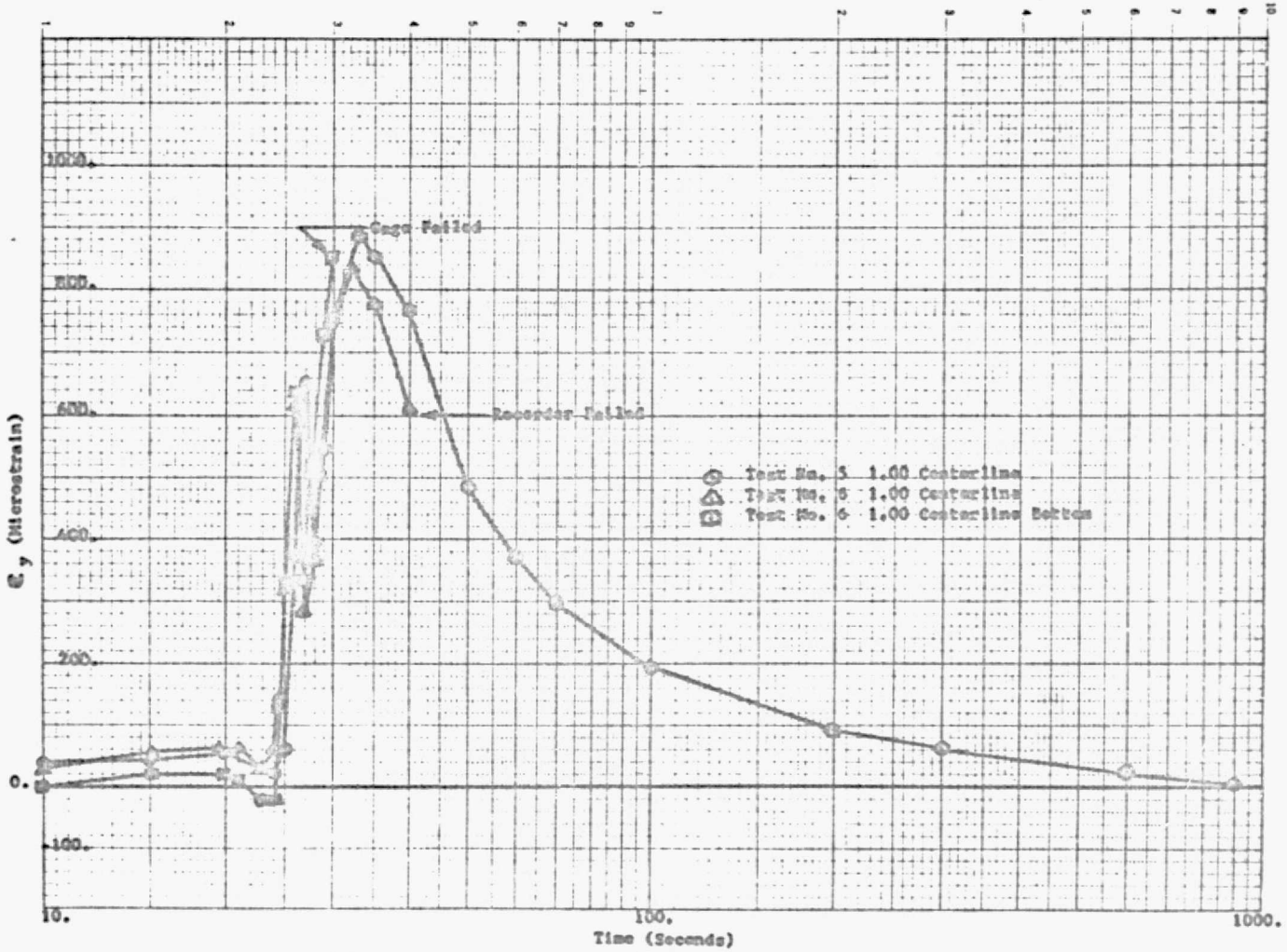

Figure 50: Transverse Strain Distributions.

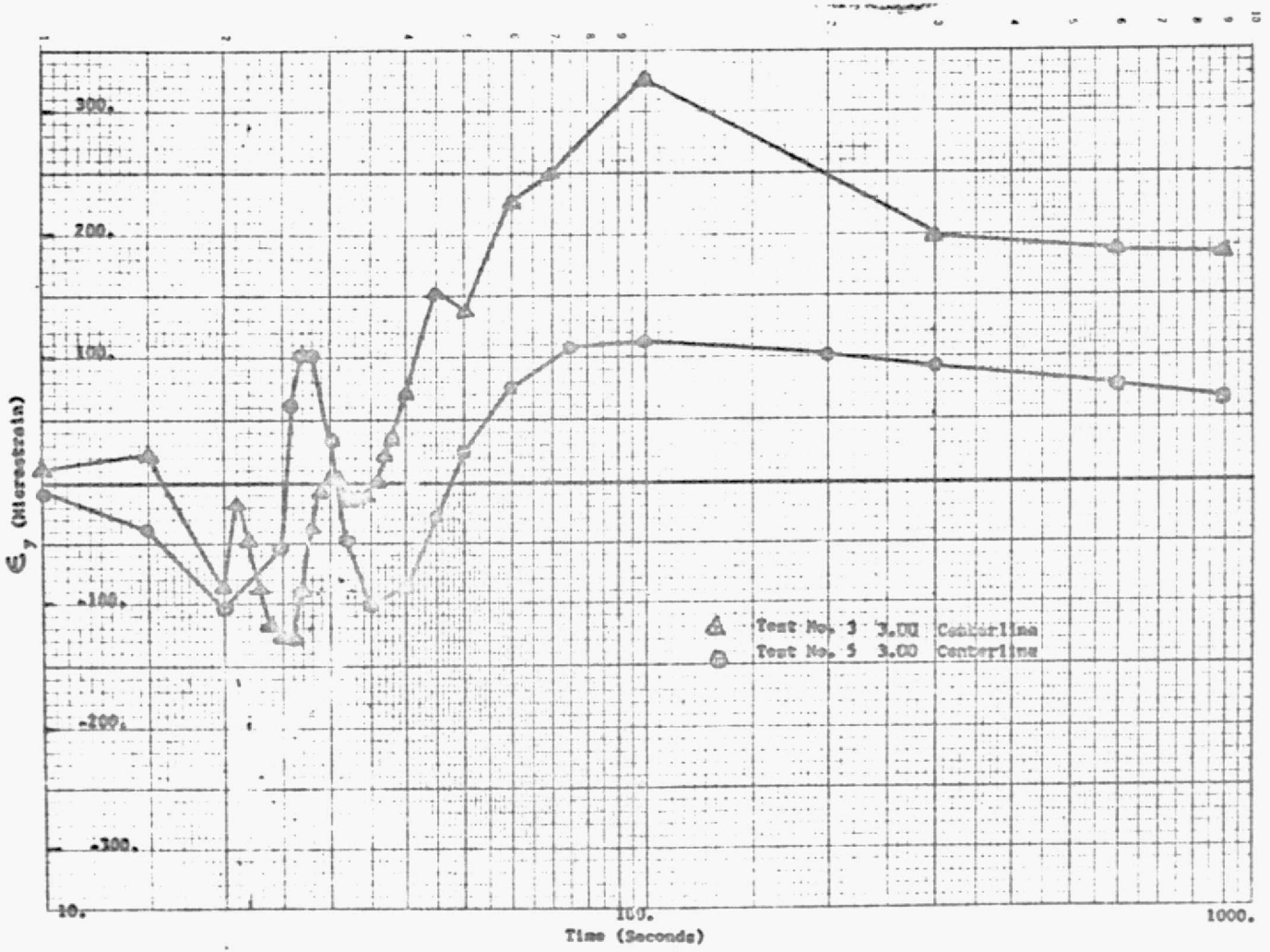

Figure 51: Transverse Strain Distributions.

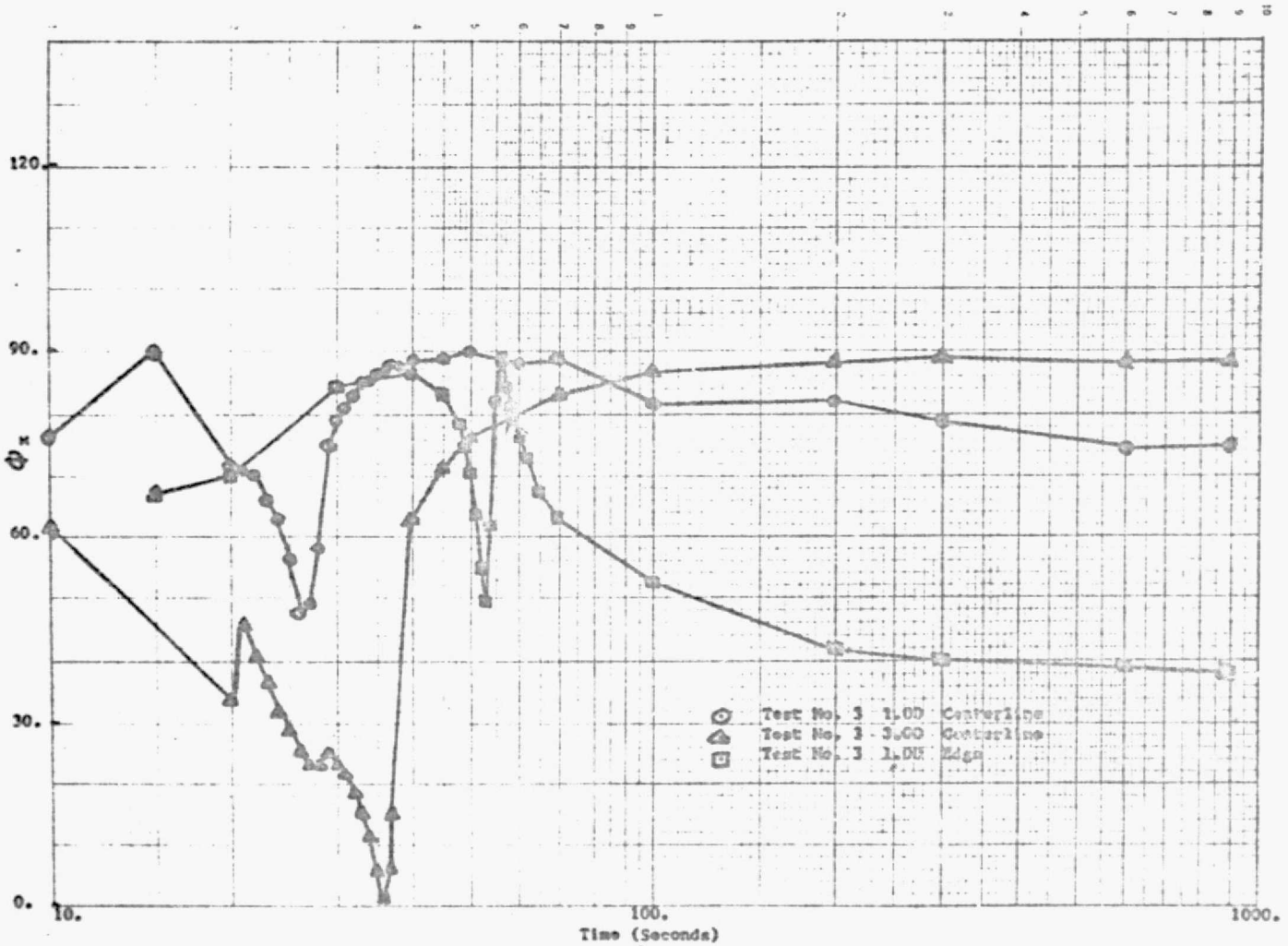

Figure 52: Φ_x Distributions.

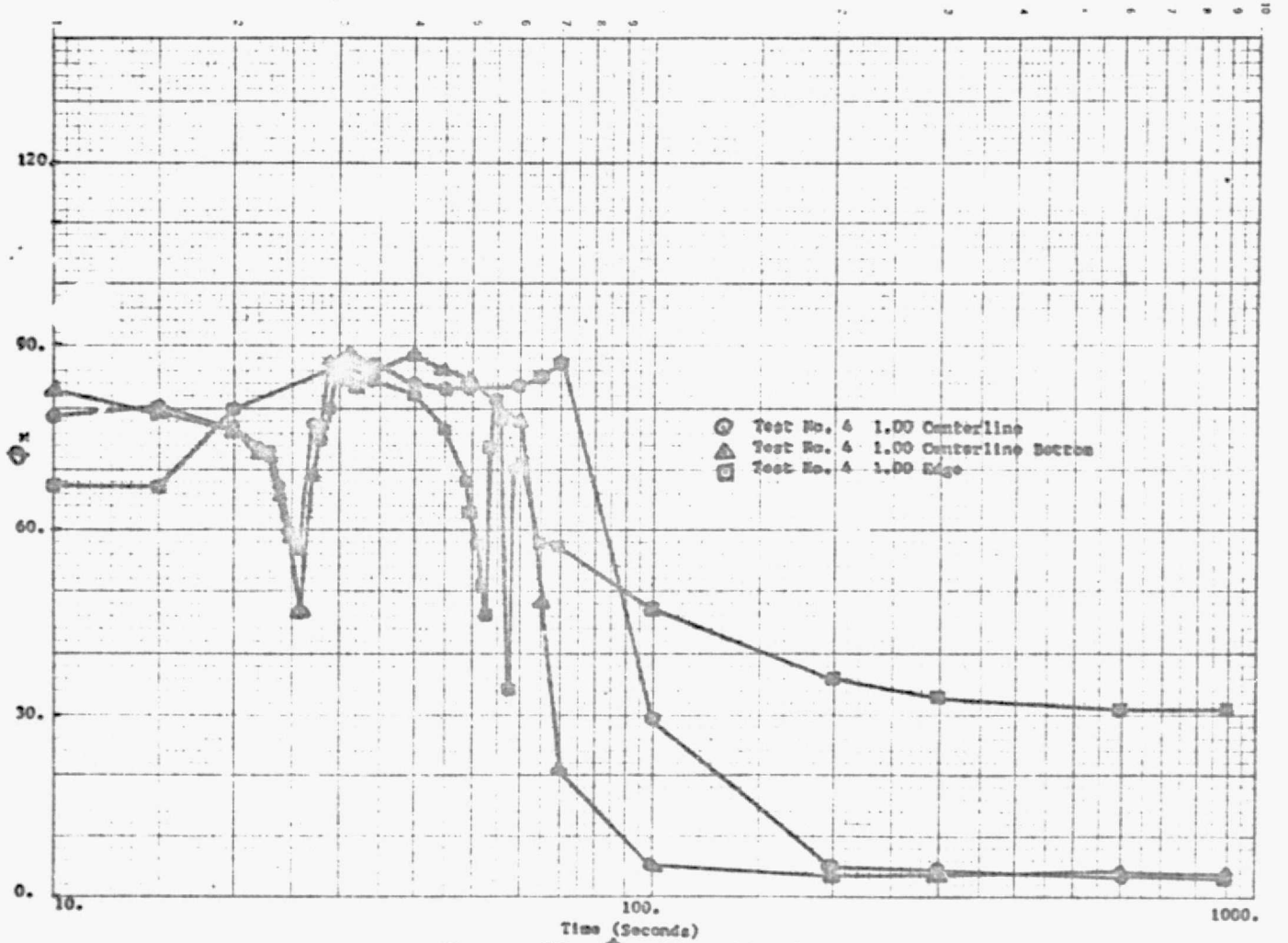

Figure 53: Φ_x Distributions.

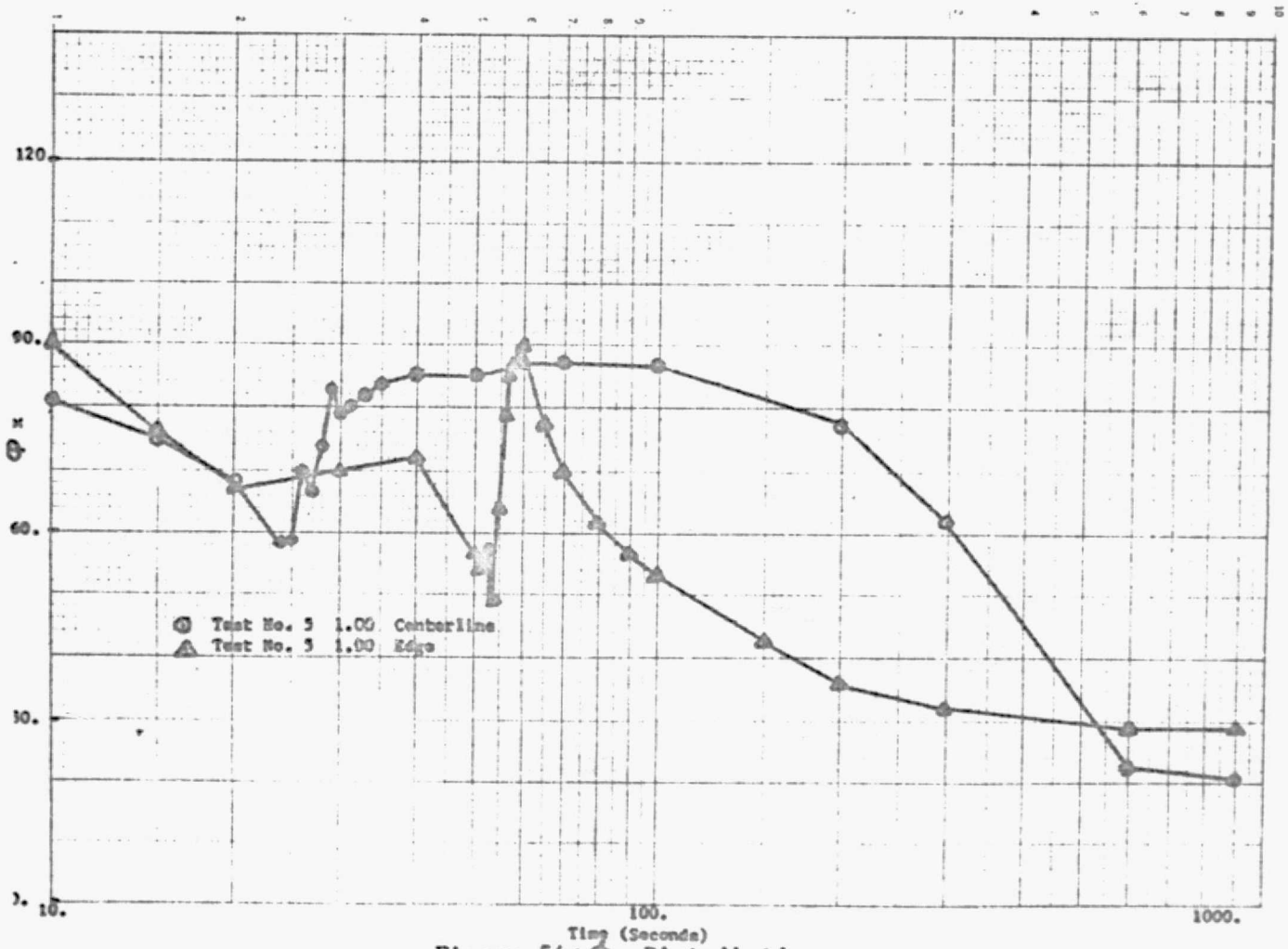

Figure 54: ϕ_x Distributions.

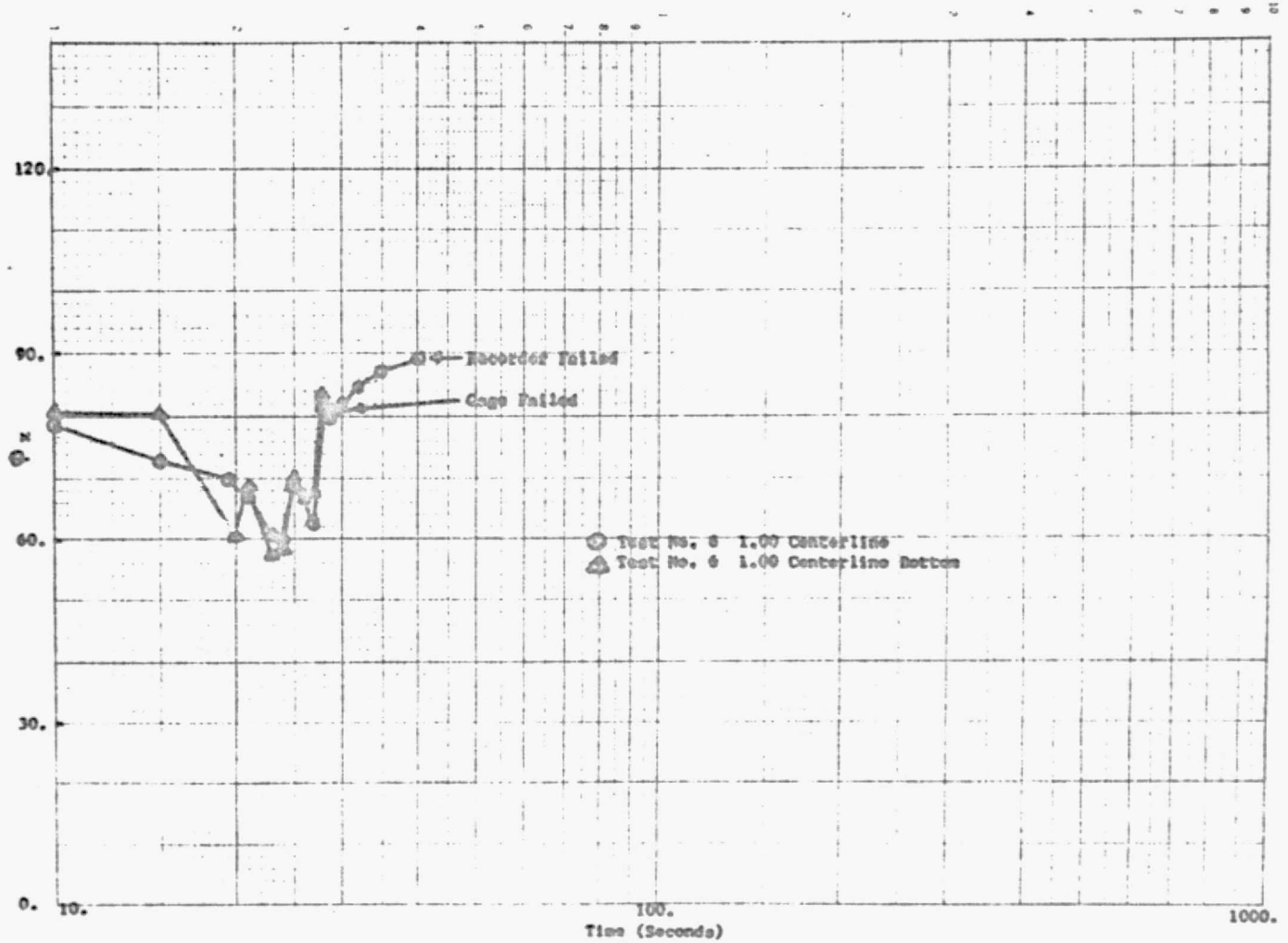

Figure 55: Φ_x Distributions.

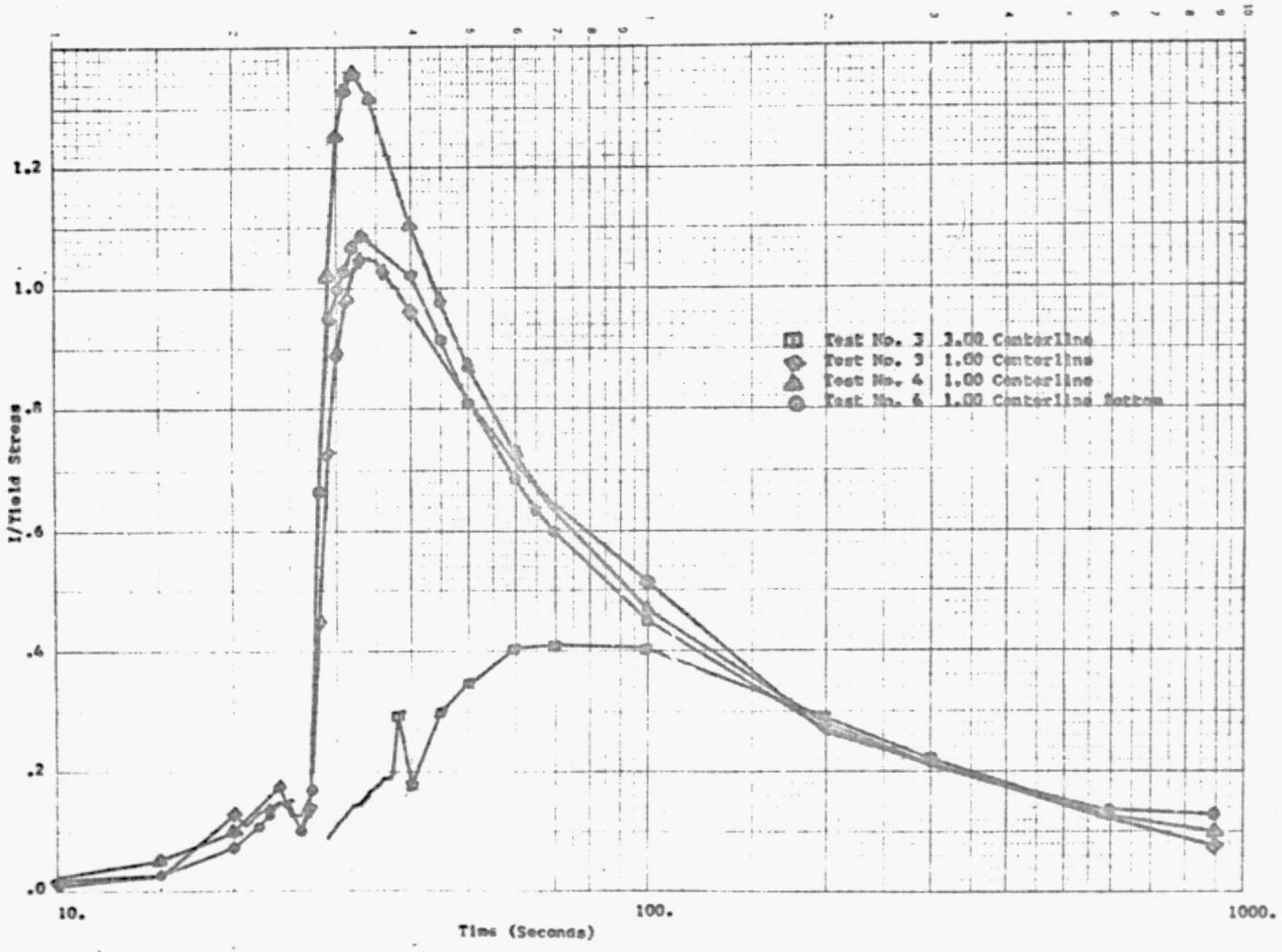

Figure 56: I / σ_y Distributions.

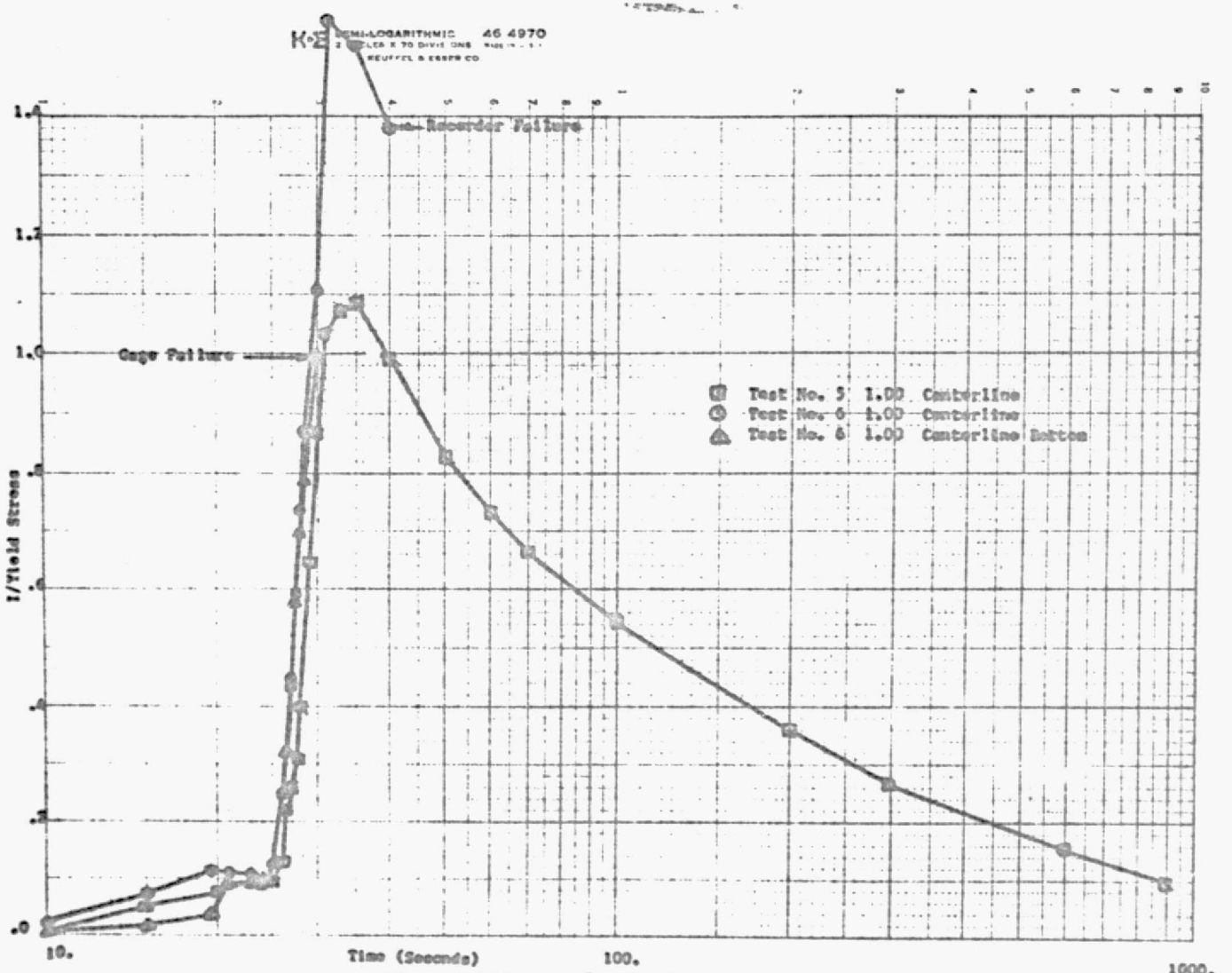

Figure 57: I/σ_y Distributions.

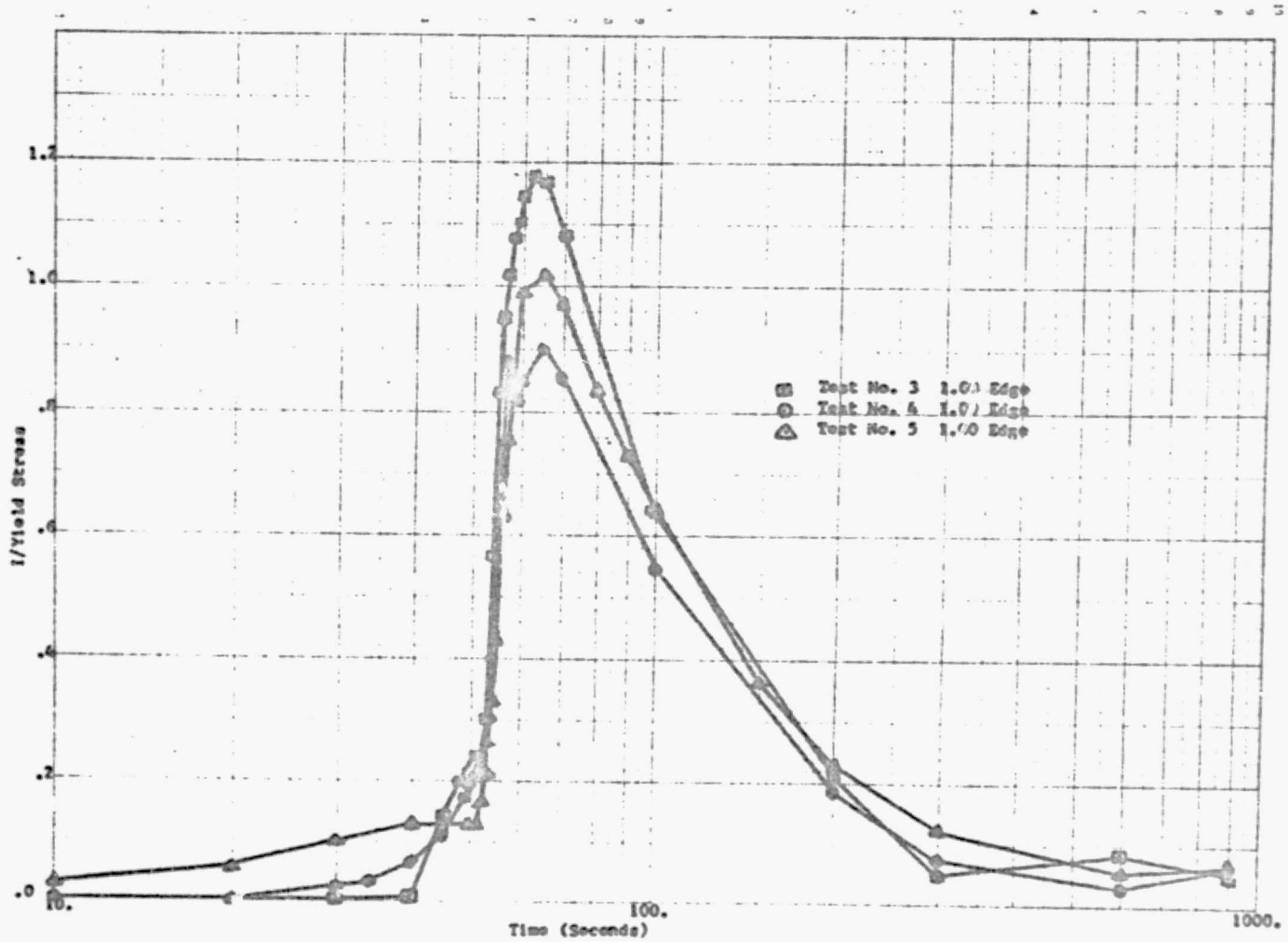

Figure 58: I / σ_y Distributions.

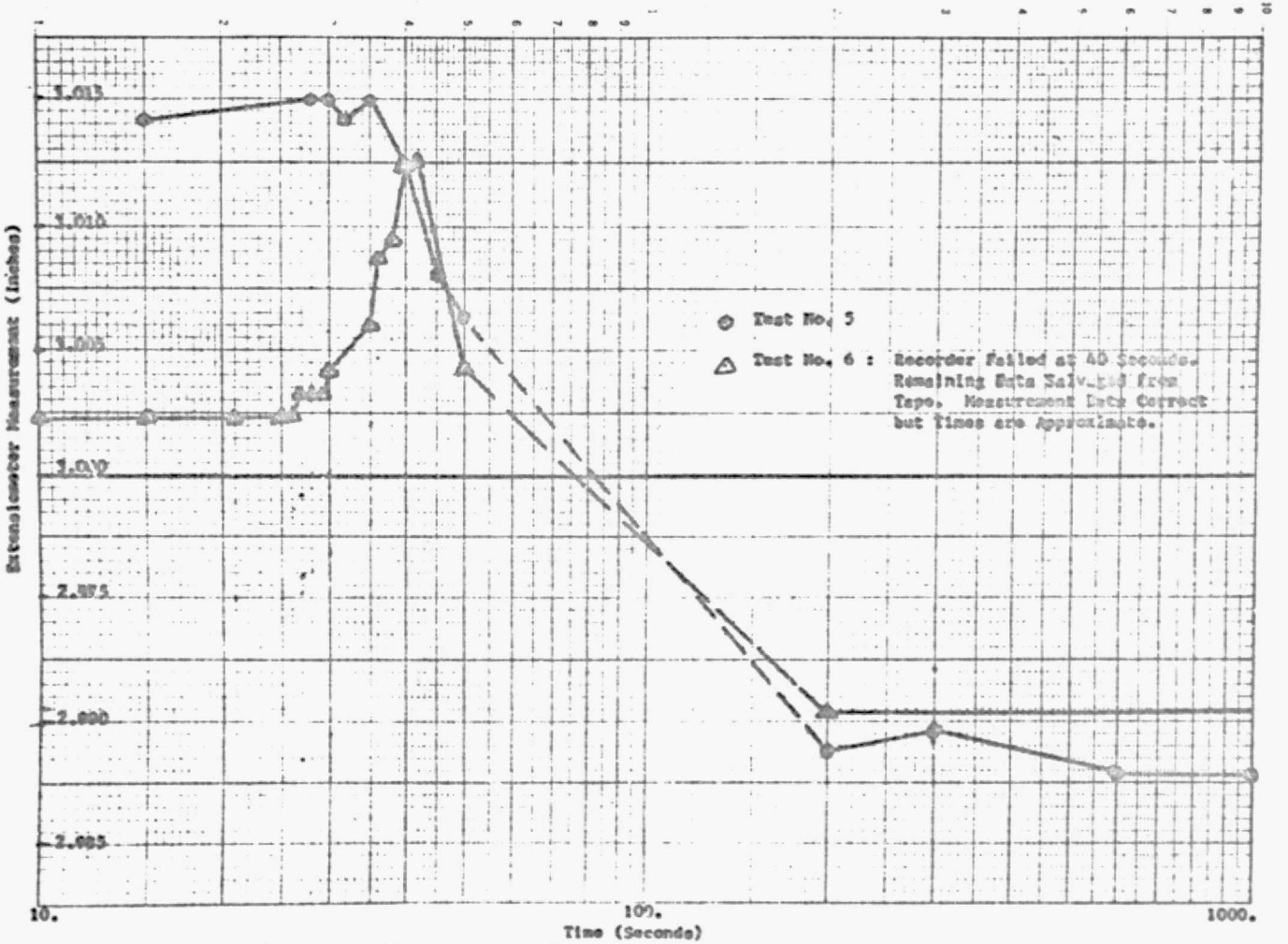

Figure 59: Butt Weld Extensiometer Measurements.

VI RECOMMENDATIONS:

1. The small number of tests performed in this study should be expanded into more tests, ultimately with plates of varying thicknesses. Data reduction from the Visacorder strip charts is difficult and time-consuming. If a large number of test are run, it becomes almost imperative that some form of direct digital output be utilized to provide punched tapes or cards compatible with MIT's IBM computer system. Multipass tests likewise require this capability. Welding is a statistical process, so the larger the basis of data the better the results will be. Obviously, there are serious questions of financial and manpower resources available, so the trade-off of more experiments vs. better data must be seriously considered.

2. More bead-on-plate tests which record top and bottom strain and temperature distributions are needed to verify a two dimensional approximation.

3. The welding machine utilized by this study should be carefully inspected and the discrepancies noted in Chapter V remedied, or another machine must be found.

4. A "V" or "J" weld preparation should be considered for butt welding thicker plates.

5. Smaller strain gages should be utilized to allow easier application and closer positioning to the weld. This sacrifices the larger area for averaging measurements, however. Multiple-element gages should be of the stacked variety to eliminate time corrections for individual elements, and make data reduction simpler. Gages such as BLH Electronics' FABR-12-12SX13ET (stacked, three-element 45°, 0.12 inch gage length), FABX-12-12S13ET (stacked, two-element, 90°, 0.12 inch gage length), or FAER-06RB-S13ET (three-element, 45°, .0625 inch gage length) or equivalent Micro-Measurements, Inc. gages should be utilized.

6. If time permits, an independent check of apparent strain corrections is recommended to verify factory data. This may be accomplished by cementing a gage to a sample test plate and heating it in an oven.

7. High temperature strain gages should again be considered to see if they are any more reliable than reported previously by Klein (7).

8. The test plate mounting assembly should be modified to allow bolting vice clamping of the plate boundaries. This may be done simply by drilling and tapping the bed plate currently in use, and will eliminate any slipping from taking place.

9. Further use of the extensiometer is not recommended. It costs one channel on the Visacorder and causes the loss of a rosette (12 channels are available: 3 rosettes and 3 thermocouples, or 2 rosettes, 2 single-element gages, the extensiometer and 3 thermocouples). This author feels that there is more to be learned at present from the "state of stress" than from shrinkage measurements. However, if continued use of the extensiometer is desired, two more gages should be installed to double its sensitivity.

10. Continued basic research is needed to provide better physical and mechanical properties for a larger variety of structural materials.

```
// 'JON J. BRYAN',CLASS=L,REGION=128K
/*MITID USER=(M10004,8940,,    )
/*SKI STANDARD
/*MAIN TIME=2,LINES=2,CARDS=2
//  EXEC WATFIV
//G.SYSIN DD *
$JOB            BRYAN,NOSUBCHK,LIBLIST,TIME=1,PAGES=20
C      CURVE FITTING PROGRAM UTILIZING A CUBIC POLYNOMIAL.
C      TABLES OF T, F(T) READ IN.
C      POLYNOMIAL COEFFICIENTS READ OUT IN E15.7 FORMAT.
       DIMENSION T(4),F(4),B(4),A(4,4),P(4)
       DO 999 L=1,13
       READ(5,100)T
       READ(5,100)F
  100  FORMAT(4F10.3)
       WRITE(6,95)
   95  FORMAT(20X,'TEMPERATURE FUNCTION TABLE OF ORIGINAL DATA
      1FOLLOWS:'//)
       WRITE(6,96)T
   96  FORMAT(5X,'TEMPERATURE',4X,4(F10.3,5X),//)
       WRITE(6,97)F
   97  FORMAT(5X,'FUNCTION F(T)',2X,4(F10.3,5X),//)
       DO 1 J=1,4
       X=T(J)
       A(J,1)=1.0
       A(J,2)=X
       A(J,3)=X**2
       A(J,4)=X**3
    1  CONTINUE
C      COEFFICIENT MATRIX A(I,J) NOW ESTABLISHED.
       B(1)=F(1)
       B(2)=F(2)
       B(3)=F(3)
       B(4)=F(4)
       CALL SIMQ(A,B,4,KS)
C      SOLUTION VECTOR READ OUT AS B(I).  A(I,J) IS DESTROYED.
```

```
C       SING VALUE KS:  0 IMPLIES NORMAL SOLUTION; 1 IMPLIES SINGULAR SET
C       OF EQUATIONS.
        WRITE(6,98)
 98     FORMAT(5X,'SING VALUE KS=0 IMPLIES NORMAL SOLUTION.  KS=1 IMPLIES
       1SINGULAR SET OF EQUATIONS.',///)
        WRITE(6,99) KS
 99     FORMAT(5X,'SING VALUE KS = ',I3///)
        WRITE(6,101)
 101    FORMAT(5X,'P(I)=A(0) + A(1)*I + ..... +A(J)*I**J',////)
        DO 2 J=1,4
        K=J-1
        WRITE(6,102) K,B(J)
 102    FORMAT(5X,'A(',I3,')=',5X,E15.7///)
 2      CONTINUE
        WRITE(7,103)B
 103    FORMAT(4E15.7)
 999    CONTINUE
        CALL EXIT
        END
$ENTRY
0.0          77.0         300.0        500.0
40.5         40.0         36.0         22.0
500.0        700.0        1000.0       1080.0
22.0         5.0          0.5          0.0
0.0          77.0         500.0        1080.0
10.2         10.6         7.85         0.0
0.0          400.0        800.0        1080.0
10.2         8.57         4.60         0.0
0.0          77.0         600.0        1080.0
0.752        0.740        0.507        0.000
77.0         400.0        700.0        1080.0
0.752        0.638        0.427        0.0
0.0          100.0        300.0        500.0
12.19        13.33        14.26        15.31
500.0        700.0        900.0        1080.0
15.31        16.43        17.75        19.32
```

```
0.0          200.0        400.0        600.0
12.41        13.17        13.77        14.26
600.0        750.0        900.0        1080.0
14.26        14.59        14.97        15.50
0.0          100.0        200.0        300.0
9.80         9.734        9.685        9.646
0.0          100.0        300.0        500.0
2.161        2.204        2.402        2.522
500.0        700.0        900.0        1080.0
2.522        2.645        2.760        2.543
$STOP.
/*
```

```
// 'JON J. BRYAN',CLASS=F,REGION=128K
/*MAIN USER=(M10034,0940,,    )
/*SKI STANDARD
/*MAIN TIME=2,LINES=5
//  EXEC WATFIV
//G.SYSIN DD *
$JOB            BRYAN,TIME=1
C      FUNCTION GENERATOR TO TEST POLYNOMIAL COEFFICIENTS.
C      TEST RUNS FROM 0 TO 108 DEGREES FAHRENHEIT.
C      COEFFICIENTS READ IN WITH 4E15.7 FORMAT.
       DIMENSION B(4),T(110),P(110)
       DO 999 L=1,13
       READ(5,100)B
  100  FORMAT(4E15.7)
       WRITE(6,103)
  103  FORMAT(30X,'TEMPERATURE FUNCTION TABLE FOLLOWS:'//)
       DO 1 J=1,109
       T(J)=(J-1)*1.
       X=T(J)
       P(J)=B(1)+B(2)*X+B(3)*X**2+B(4)*X**3
       WRITE(6,106) T(J),P(J)
  106  FORMAT(5X,'IF T = ',F10.3,5X,'THEN F(T) APPROXIMATED =',F10.3/)
    1  CONTINUE
  999  CONTINUE
       CALL EXIT
       END
$ENTRY
  0.4000000E 02 -0.7480200E-02  0.2589436E-04 -0.1698679E-06
  0.1840897E 03 -0.5056120E 00  0.5837074E-03 -0.2016852E-06
  0.1020000E 02 -0.2337847E-02 -0.3124401E-05 -0.3199794E-08
  0.1020000E 02 -0.1817137E-02 -0.4810746E-05 -0.2084789E-08
  0.7520000E 00 -0.1240664E-05 -0.4636978E-06 -0.1168005E-09
  0.7648185E 00 -0.1320357E-03 -0.4406592E-06 -0.3592053E-10
  0.1219000E 02  0.9464994E-02 -0.1169993E-04  0.1049988E-07
  0.1409139E 02 -0.6086211E-03  0.7212205E-05 -0.2243020E-06
  0.1241000E 02  0.4283524E-02 -0.2624947E-05  0.1041597E-05
```

```
 0.1552e030E 02  0.11671178E-02  0.4790e676E-0E  0.e805947E-09
 0.9e000000E 01 -0.7e63365E-03  0.1290059E-05 -0.1166804E-08
 0.2161e000E 01  0.1197628E-02 -0.1859963E-05  0.1e16e16E-08
 0.e0184e4E 01  0.1501152E-02 -0.1503752E-05  0.7874907E-09
$SIUP
/*
```

```
// 'JON J. BRYAN',CLASS=B,REGION=128K
/*MITID USER=(M10004,PS4C,,    )
/*SRI STANDARD
/*MAIN TIME=2,LINES=5
/*FORMAT PR,DDNAME=FT06F001,FORMS=THESIS,OVFL=ON,COPIES=2
//  EXEC WATFIV
//C.SYSIN DD *
$JOB            BRYAN,TIME=1,PAGES=20
C      DATA REDUCTION COMPUTATION
C      WELDING STRAIN-TEMPERATURE VARIATION: EXPERIMENATAL RESULTS.
C      INPUT CARDS TO THIS PROGRAM ARE:
C      CARD 1: NUMBER OF GAGES, VOLTS, AMPS (I5,2F6.0)
C      CARD 2:  COEFFICIENTS FOR COEFFICIENT OF THERMAL EXPANSION
C      POLYNOMIAL (4E15.7)
C      CARD 3:  COEFFICIENTS FOR YOUNG'S MODULUS POLYNOMIAL (4F15.7).
C      CARD 4:  COEFFICIENTS FOR YIELD STRESS (4F15.7).
C      CARD 5:  POISSON'S RATIO (F10.3)
C      CARD 6: STRAIN DATA: TIME: TEMP GAGE 1, TEMP GAGE 2, TEMP GAGE 3:
C              STRAIN, GAGE 1, LEG A, B, C: GAGE 2, LEG A,B, C:
C              GAGE 3, LEG A, B, C. (F8.0, 12F6.2)
C      CARD 7,8,9 ETC.  SAME TYPE OF DATA AS CARD 6.
C      UNITS:  COEFFICIENT OF THERMAL EXPANSION:  MICROSTRAIN/DEGREE
C      FAHRENHEIT:  YOUNGS MODULUS:  PSI: YIELD STRESS: KSI: STRAINS:
C      MICROSTRAIN.
       REAL NU
       INTEGER GAGE
       DIMENSION T(99),SZERO(99,3),STRN(99,3),S(99,3)
       DIMENSION EX(99),EY(99),GXY(99),E1(99),E2(99)
       DIMENSION PHIX(99)
       DIMENSION A(4),E(4),Y(4),ETHO(3), SIGX(3),SIGY(3),TAUXY(3),X4(3)
       DIMENSION Y1(3),X5(3)
       READ(5,50)GAGE,VOLTS,AMPS
   50  FORMAT(I5,2F6.0)
       J=GAGE
       WRITE(6,100)
  100  FORMAT(13X,'WELDING STRAIN ROSETTE DATA: EXPERIMENTAL RESULTS'/
```

```
     15X,'*************************************************************
     2*'///)
      WRITE(6,101)
  101 FORMAT(18X,'TEST NUMBER 4:  BEAD-ON-PLATE'/)
      WRITE(6,110)VOLTS,AMPS
  110 FORMAT(18X,'ALUMINUM ALLOY 6061 IN T651 CONDITION'/18X,'THICKNESS
     1= 0.250 INCHES'/18X,'GMA WELD PROCESS'/18X,'ARC VOLTAGE = ',F6.0/
     2 18X,'AMPERES = ',F6.0/18X'SPEED OF TRAVEL = 32.16 INCHES/MINUTE')
      WRITE(6,111)
  111 FORMAT(18X,'4043 FILLER METAL:  0.0625 INCH DIAMETER'/18X,
     2'UNITS OF STRAIN = MICROSTRAIN'//)
      WRITE(6,112)
  112 FORMAT(33X,'CAUTION',//18X,'TEMP = 0.00 COMPUTATIONS REPRESENT'/
     218X,'BLANK SPACES ON INPUT CARDS ARE'/19X,
     3'MEANINGLESS.  IGNORE ALL SUCH COMPUTATIONS.'///)
      WRITE(6,120)
  120 FORMAT(28X,'TRANSVERSE DISTANCE FROM WELD IN INCHES'//
     210X,'TIME',18X,'1.00',12X,'1.00',12X,'1.00'/
     38X,'(SECONDS)',11X,'(CENTERLINE)',4X,'(BOTTOM C/L)',
     46X,'(EDGE)'////)
      READ(5,91)A
      READ(5,91)E
      READ(5,91)Y
   91 FORMAT(4E15.7)
      READ(5,92)NU
   92 FORMAT(F10.3)
C     READ IN ROSETTE DATA: TIME, TEMP, STRAINS A,B AND C.
    1 READ(5,140,END=999) TIME,(T(K),K=1,J),((S(K,L),L=1,3),K=1,J)
  140 FORMAT(F8.0,12F6.2)
      IF(TIME.GT.0.)GO TO 3
      DO 6 II=1,J
      ETHC(II)=A(1)*T(II)+A(2)*T(II)**2/2.+A(3)*T(II)**3/3.+A(4)*T(II)
     1**4/4.
      DO 7 KK=1,3
    7 SZERO(II,KK)=S(II,KK)
    6 CONTINUE
```

```
  3     DO 8 JJ=1,J
C       TEMPERATURE COMPENSATION FOR FAER-18RB-12S13-FT LOT NO. A283
C       GAGES ON 2024-T4 ALUMINUM TEST PLATE.
        ASTR=-60.68+2.22*T(JJ)-2.40E-2*T(JJ)**2+7.05E-5*T(JJ)**3
       1-5.59E-8*T(JJ)**4
        ASTR1=-19.4979+.2463*T(JJ)+.9561E-4*T(JJ)**2-.7979E-7*T(JJ)**3
       1+.5303E-10*T(JJ)**4
        ASTR=ASTR+ASTR1
        IF(TIME.EQ.0.) GO TO 11
        DO 9 KK=1,3
  9     STRN(JJ,KK)=  S(JJ,KK)-SZERO(JJ,KK)-ASTR
        GO TO 13
 11     DO 12 KK=1,3
 12     STRN(JJ,KK)=S(JJ,KK)-ASTR
 13     CONTINUE
C       STRAINS ARE NOW TEMPERATURE COMPENSATED.
        CALL STRAIN(STRN(JJ,1),STRN(JJ,2),STRN(JJ,3),EX(JJ),EY(JJ),GXY(JJ)
       2,E1(JJ),E2(JJ),PHIX(JJ))
        CALL STRESS(EX(JJ),EY(JJ),GXY(JJ),ETHO(JJ),A,E,Y,T(JJ),NL,
       1SIGX(JJ),SIGY(JJ),TAUXY(JJ),X4(JJ),Y1(JJ),X5(JJ))
  8     CONTINUE
        WRITE(6,160)TIME,(T(K),K=1,J),((S(K,L),K=1,J),L=1,3),((STRN(K,L),K
       2=1,J),L=1,3),(EX(K),K=1,J),(EY(K),K=1,J),(GXY(K),K=1,J),(E1(K),K=1
       3,J),(E2(K),K=1,J),(PHIX(K),K=1,J)
 160    FORMAT(6X,F8.2/5X,'TEMPERATURE(DEG.FAHR)',3(F10.2,6X)/
       25X,'STRAIN A. (MEAS)',5X,3(F10.2,6X)/
       35X,'STRAIN B. (MEAS)',5X,3(F10.2,6X)/
       45X,'STRAIN C. (MEAS)',5X,3(F10.2,6X)/
       55X,'STRAIN A. (MECH)',5X,3(F10.2,6X)/
       65X,'STRAIN B. (MECH)',5X,3(F10.2,6X)/
       75X,'STRAIN C. (MECH)',5X,3(F10.2,6X)/
       85X,'STRAIN X. (MECH)',5X,3(F10.2,6X)/
       95X,'STRAIN Y. (MECH)',5X,3(F10.2,6X)/
       15X,'GAMMA XY. (MECH)',5X,3(F10.2,6X)/
       25X,'PRIN.STR.1. (" )',5X,3(F10.2,6X)/
       35X,'PRIN.STR.2. (" )',5X,3(F10.2,6X)/
```

```
     45X,'PHI X (DEGREES)',6X,3(F10.2,6X))
      WRITE(6,161) (SIGX(K),K=1,J),(SIGY(K),K=1,J),(TAUXY(K),K=1,J),
     1(Y1(K),K=1,J),(X4(K),K=1,J),(X5(K),K=1,J)
  161 FORMAT(5X,'SIGMA XX (KSI)',7X,3(F10.2,6X)/
     15X,'SIGMA YY (KSI)',7X,3(F10.2,6X)/
     25X,'TAU XY   (KSI)',7X,3(F10.2,6X)/
     35X,'YIELD STRESS (KSI)',3X,3(F10.2,6X)/
     45X,'I (KSI)',14X,3(E10.4,6X)/
     55X,'I/YIELD STRESS',7X,3(E10.4,6X)///)
      GO TO 1
  999 CALL EXIT
      END
      SUBROUTINE STRAIN(EA,EB,EC,EX,EY,GXY,E1,E2,PHIX)
C     THIS SUBROUTINE CALCULATES STRAINS ALONG THE X, Y AND PRINCIPAL
C     AXES; THE SHEAR ANGLE GAMMA XY; AND PHIX, THE ANGLE BETWEEN THE
C     X AXIS AND THE AXIS OF THE LARGEST PRINCIPAL STRAIN.
C     CALCULATIONS ARE BASED ON THE RECTANGULAR ROSETTE WITH THREE
C     OBSERVATIONS OF STRAIN.
C     PHI1 IS DEFINED AS THE ANGLE MEASURED POSITIVE IN THE ANTI-
C     CLOCKWISE DIRECTION FROM THE POSITIVE OA AXIS OF THE STRAIN
C     ROSETTE TO THE POSITIVE O1 AXIS WHICH CORRESPONDS TO THE DIRECTION
C     OF THE LARGEST PRINCIPAL STRAIN.
C     COMPUTATIONS, OTHER THAN PHI, UTILIZE AXIS OX AS THE REFERENCE
C     AXIS.
C     THE ANGLE BETWEEN THE X AXIS AND THE OA AXIS = 45 DEGREES.
      EX=EA-EB+EC
      EY=EB
      GXY=EA-EC
      A=EX+EY
      B=EX-EY
      C=SQRT(B**2+GXY**2)
      E1=.5*(A+C)
      E2=.5*(A-C)
      B1=EA-EC
      B2=EA+EC
      B3=2.*EB-B2
```

```
      IF(B1.EQ.0.)GO TO 6
      PHI1=ABS(.5*ATAN(B3/B1))
      GO TO 7
    6 PHI1=3.1416/4.
    7 CONTINUE
      D=.5*(EA+EC)
      IF(FB.GT.0)GO TO 1
      IF(FB.LT.0)GO TO 2
      IF(EA.GT.EC)GO TO 3
      IF(EA.LT.EC)GO TO 4
    1 PHI2=+PHI1
      GO TO 5
    2 PHI2=-PHI1
      GO TO 5
    3 PHI2=0.0
      GO TO 5
    4 PHI2=+3.1416/2.
    5 PHI3=PHI2*180./3.1416
      PHIX=PHI3+45.0
C     45 DEGREE CORRECTION IS MADE TO BRING THE REFERENCE AXIS
C     FROM CA TO X.
      RETURN
      END
      SUBROUTINE STRESS (FX,EY,GXY,ETHO,A,E,Y,T,NU,SIGX,SIGY,TAUXY,
     1X4,Y1,X5)
      REAL NU
      DIMENSION A(4),E(4),Y(4)
C     AT THIS POINT, THERMAL STRAINS ARE CALCULATED ASSUMING ISOTROPIC
C     MATERIAL.
      ETHT=A(1)*T+A(2)*T**2/2.+A(3)*T**3/3.+A(4)*T**4/4.
      ETH=ETHT-ETHO
C     AT THIS POINT, TOTAL STRAINS ARE CALCULATED.
      EXT=EX+ETH
      EYT=EY+ETH
      E1=E(1)+E(2)*T+E(3)*T**2+E(4)*T**3
C     E1 IS YOUNG'S MODULUS AT TEMPERATURE T.
```

Intentionally Left Blank

```
      X1=1.0E-3*E1/(1.-NU**2)
      X2=1.0E-3*E1/(2*(1.+NU))
      SIGX=X1*(EXT+NU*EYT)
      SIGY=X1*(EYT+NU*EXT)
      TAUXY=X2*GXY
C     UNITS OF STRESS ARE NOW IN KSI.   YOUNG'S MODULUS WAS READ IN
C     AS PSI * E-6 AND STRAINS WERE IN TERMS OF MICRO STRAIN.  X1 AND
C     X2 HAVE BEEN CORRECTED BY E-3 TO CONVERT PSI TO KSI.
      X3=(SIGX**2-SIGX*SIGY+SIGY**2+3.*TAUXY)
      X31=ABS(X3)
      X4=SQRT(X31)
C     K4 IS MASUBUCHI'S STRESS INVARIANT IN UNITS OF KSI.
      Y1=Y(1)+Y(2)*T+Y(3)*T**2+Y(4)*T**3
C     Y1 IS YIELD STRESS AT TEMPERATURE T IN UNITS OF KSI.
      X5=X4/Y1
C     X5 IS THE PLASTICITY CONDITION RATIO BASED ON MASUBUCHI'S STRESS
C     INVARIANT.  WHEN IT IS E.T. OR G.T. 1.0 PLASTIC STRAINING HAS
C     OCCURRED.
      RETURN
      END
```

```
$ENTRY
    3 19.0  240.0
  C.1219000E 02  0.9464994E-02 -0.1169993E-04  0.1049988E-07
  C.1020000E 02 -0.1817137E-02 -0.4810746E-05 -0.2084789E-08
  C.4050000E 02 -0.7480200E-02  0.2589436E-04 -0.1698679E-06
.333
0.      78.   78.   78.   0.    0.    0.    0.    0.    0.    0.    0.    0.
10.     78.   79.   78.   15.   40.   -20.  5.    20.   -5.   10.   15.   15.
15.     79.   79.   78.   25.   115.  -75.  5.    45.   -45.  10.   20.   20.
20.     79.   79.   78.   80.   220.  -200. 35.   135.  -165. 20.   30.   20.
22.     79.   79.         150.  285.  -335. 95.   185.  -290.
23.     79.   79.         215.  300.  -465. 155.  210.  -415.
24.     80.   79.         315.  300.  -645. 275.  220.  -585.
25.     82.   81.         435.  200.  -650. 465.  145.  -830.
26.     98.   88.         250.  -100. -950. 560.  -90.  -840.
27.     159.  114.        -790. -25.  -310. -105. 85.   75.
28.     239.  179.        -2095.745.  -10.  80.   875.  590.
29.     290.  234.        -1290.1060. -55.  375.  835.  285.
30.     316.  269.  78.   -1050.1575. -255. -55.  385.  5.    50.   95.   40.
31.     326.  288.        -470. 1550. -325. -320. 265.  -135.
32.     328.  302.        -110. 1480. -400. -440. 195.  -205.
34.     327.  308.  78.   -165. 1315. -500. -430. 90.   -295. 75.   130.  50.
40.     297.  298.  78.   -65.  865.  -565. -355. -80.  -385. 150.  250.  75.
45.     277.  278.  79.   -80.  645.  -530. -335. -160. -390. 310.  420.  80.
                  80.                                        625.  640.  -75.
49.
50.     260.  259.  80.   -130. 460.  -490. -330. -215. -385. 820.  680.  -220.
                  82.                                        1090. 680.  -505.
51.
                  88.                                        1365. 470.  -875.
52.
                  106.                                       880.  145.  -645.
53.
                  148.                                       235.  310.  -30.
54.
                  186.                                       50.   540.  275.
55.
                  212.                                       -135. 640.  345.
56.
                  230.                                       270.  610.  185.
57.
                  244.                                       -155. -110. -5.
58.
                  253.                                       -365. -110. -135.
59.
60.     237.  234.  260.  -200. 175.  -415. -310. -275. -365. -365. -140. -170.
```

65.	228.	224.	272.	-255.	75.	-380.	-300.	-320.	-345.	-470.	-220.	-135.
70.	219.	215.	263.	-245.	-10.	-295.	-240.	-340.	-335.	-535.	-165.	-35.
100.	186.	181.	206.	-280.	-265.	-205.	-200.	-380.	-255.	-540.	-280.	-55.
200.	138.	137.	139.	-120.	-285.	-45.	-85.	-410.	-155.	-485.	-365.	-130.
300.	120.	121.	119.	-80.	-275.	-10.	-50.	-420.	-140.	-475.	-390.	-170.
600.	99.	99.	99.	-50.	-265.	5.	-35.	-435.	-135.	-470.	-410.	-215.
900.	92.	92.	90.	-40.	-260.	10.	-25.	-435.	-125.	-475.	-415.	-225.
1200.	88.	88.	87.	-40.	-265.	5.	-80.	-425.	-130.	-480.	-420.	-240.

$STOP
/*

WELDING STRAIN ROSETTE DATA: EXPERIMENTAL RESULTS

TEST NUMBER 3: BEAD-ON-PLATE

ALUMINUM ALLOY 6061 IN T651 CONDITION
THICKNESS = 0.250 INCHES
GMA WELD PROCESS
ARC VOLTAGE = 19.
AMPERES = 240.
SPEED OF TRAVEL = 37.16 INCHES/MINUTE
4043 FILLER METAL: 0.0625 INCH DIAMETER
UNITS OF STRAIN = MICROSTRAIN

CAUTION

TEMP = 0.00 COMPUTATIONS REPRESENT
BLANK SPACES ON INPUT CARDS AND ARE
MEANINGLESS. IGNORE ALL SUCH COMPUTATIONS.

TIME (SECONDS)	TRANSVERSE DISTANCE FROM WELD IN INCHES 1.00 (CENTERLINE)	1.00 (CENTERLINE)	1.00 (EDGE)
0.00			
TEMPERATURE(DEG.FAHR)	78.00	78.00	78.00
STRAIN A, (MEAS)	0.00	0.00	0.00
STRAIN B, (MEAS)	0.00	0.00	0.00
STRAIN C, (MEAS)	0.00	0.00	0.00
STRAIN A, (MECH)	1.00	1.00	1.00
STRAIN B, (MECH)	1.00	1.00	1.00
STRAIN C, (MECH)	1.00	1.00	1.00
STRAIN X, (MECH)	1.00	1.00	1.00
STRAIN Y, (MECH)	1.00	1.00	1.00
GAMMA XY, (MECH)	0.00	0.00	0.00
PRIN.STR.1, (*)	1.00	1.00	1.00
PRIN.STR.2, (*)	1.00	1.00	1.00
PHI X (DEGREES)	90.00	90.00	90.00
SIGMA XX (KSI)	0.00	0.00	0.00
SIGMA YY (KSI)	0.00	0.00	0.00
TAU XY (KSI)	0.00	0.00	0.00
YIELD STRESS (KSI)	37.00	37.00	37.00
1 (KSI)	0.29615-01	0.29615-01	0.29615-01
1/YIELD STRESS	0.71035-03	0.71035-03	0.71035-03

WELDING STRAIN ROSETTE DATA: EXPERIMENTAL RESULTS

TEST NUMBER 4: BEAD-ON-PLATE

ALUMINUM ALLOY 6061 IN T651 CONDITION
THICKNESS = 0.250 INCHES
GMA WELD PROCESS
ARC VOLTAGE = 19.
AMPERES = 240.
SPEED OF TRAVEL = 37.16 INCHES/MINUTE
4043 FILLER METAL: 0.0625 INCH DIAMETER
UNITS OF STRAIN = MICROSTRAIN

CAUTION

TEMP = 0.00 COMPUTATIONS REPRESENT
BLANK SPACES ON INPUT CARDS AND ARE
MEANINGLESS. IGNORE ALL SUCH COMPUTATIONS.

TIME (SECONDS)	TRANSVERSE DISTANCE FROM WELD IN INCHES 1.00 (CENTERLINE)	1.00 (BOTTOM C/L)	1.00 (EDGE)
0.00			
TEMPERATURE(DEG.FAHR)	78.00	78.00	78.00
STRAIN A, (MEAS)	0.00	0.00	0.00
STRAIN B, (MEAS)	0.00	0.00	0.00
STRAIN C, (MEAS)	0.00	0.00	0.00
STRAIN A, (MECH)	1.00	1.00	1.00
STRAIN B, (MECH)	1.00	1.00	1.00
STRAIN C, (MECH)	1.00	1.00	1.00
STRAIN X, (MECH)	1.00	1.00	1.00
STRAIN Y, (MECH)	1.00	1.00	1.00
GAMMA XY, (MECH)	0.00	0.00	0.00
PRIN.STR.1, (*)	1.00	1.00	1.00
PRIN.STR.2, (*)	1.00	1.00	1.00
PHI X (DEGREES)	90.00	90.00	90.00
SIGMA XX (KSI)	0.00	0.00	0.00
SIGMA YY (KSI)	0.00	0.00	0.00
TAU XY (KSI)	0.00	0.00	0.00
YIELD STRESS (KSI)	37.00	37.00	37.00
1 (KSI)	0.29615-01	0.29615-01	0.29615-01
1/YIELD STRESS	0.71035-03	0.71035-03	0.71035-03

10.00

TEMPERATURE(DEG.FAHR)	79.00	77.33	79.00
STRAIN A. (MEAS)	15.00	30.00	0.00
STRAIN B. (MEAS)	30.00	20.00	0.00
STRAIN C. (MEAS)	-15.00	-30.00	0.00
STRAIN A. (MECH)	16.89	31.99	1.89
STRAIN B. (MECH)	31.89	21.99	1.89
STRAIN C. (MECH)	-13.11	-28.11	1.89
STRAIN X. (MECH)	-28.11	-13.11	1.89
STRAIN Y. (MECH)	31.89	21.99	1.89
GAMMA XY. (MECH)	30.00	60.00	0.00
PRIN.STR.1. (P)	35.43	37.97	1.89
PRIN.STR.2. (P)	-31.65	-36.24	1.89
PHI X (DEGREES)	76.72	61.84	90.00
SIGMA XX (KSI)	-0.23	-0.32	0.09
SIGMA YY (KSI)	0.25	-0.02	0.03
TAU XY (KSI)	0.11	0.23	0.00
YIELD STRESS (KSI)	39.99	40.00	39.99
T (KSI)	0.7015E 00	0.9791E 00	0.2941E-01
T/YIELD STRESS	0.1754E-01	0.2195E-01	0.7355E-03

15.00

TEMPERATURE(DEG.FAHR)	79.00	79.00	79.00
STRAIN A. (MEAS)	30.00	60.00	0.00
STRAIN B. (MEAS)	90.00	60.00	15.00
STRAIN C. (MEAS)	30.00	-100.00	15.00
STRAIN A. (MECH)	31.89	61.99	1.89
STRAIN B. (MECH)	91.89	61.99	16.89
STRAIN C. (MECH)	31.89	-98.11	16.89
STRAIN X. (MECH)	-28.11	-98.11	1.89
STRAIN Y. (MECH)	91.89	61.89	16.89
GAMMA XY. (MECH)	0.00	140.00	-15.00
PRIN.STR.1. (P)	91.89	79.99	16.91
PRIN.STR.2. (P)	-28.11	-127.11	-1.27
PHI X (DEGREES)	90.00	67.50	67.50
SIGMA XX (KSI)	0.03	-0.05	0.09
SIGMA YY (KSI)	0.03	0.10	0.00
TAU XY (KSI)	0.00	0.53	-0.04
YIELD STRESS (KSI)	39.99	39.99	39.99
T (KSI)	0.9171E 00	0.1609E 01	0.3779E 00
T/YIELD STRESS	0.2293E-01	0.4024E-01	0.9449E-02

20.00

TEMPERATURE(DEG.FAHR)	79.00	79.00	79.00
STRAIN A. (MEAS)	120.00	210.00	-135.00
STRAIN B. (MEAS)	210.00	-90.00	30.00
STRAIN C. (MEAS)	-960.00	-225.00	15.00
STRAIN A. (MECH)	121.89	211.89	-133.11
STRAIN B. (MECH)	211.89	-91.11	31.89
STRAIN C. (MECH)	-158.11	-218.11	14.89
STRAIN X. (MECH)	-648.11	91.89	-148.11

10.00

TEMPERATURE(DEG.FAHR)	78.00	79.00	79.00
STRAIN A. (MEAS)	15.00	5.00	10.00
STRAIN B. (MEAS)	40.00	20.00	15.00
STRAIN C. (MEAS)	-20.00	-5.00	15.00
STRAIN A. (MECH)	16.89	6.99	11.89
STRAIN B. (MECH)	41.89	21.99	16.89
STRAIN C. (MECH)	-18.11	-3.07	16.89
STRAIN X. (MECH)	-43.11	-18.02	11.89
STRAIN Y. (MECH)	41.89	21.98	16.89
GAMMA XY. (MECH)	35.00	10.00	-5.00
PRIN.STR.1. (P)	45.35	22.60	17.02
PRIN.STR.2. (P)	-46.57	-18.63	10.85
PHI X (DEGREES)	78.81	82.09	67.50
SIGMA XX (KSI)	-0.23	0.07	0.29
SIGMA YY (KSI)	0.31	0.37	0.24
TAU XY (KSI)	0.13	0.06	-0.02
YIELD STRESS (KSI)	39.99	39.99	39.99
T (KSI)	0.8377E 00	0.4821E 00	0.8951E-01
T/YIELD STRESS	0.2095E-01	0.1205E-01	0.2239E-02

15.00

TEMPERATURE(DEG.FAHR)	79.00	79.00	79.00
STRAIN A. (MEAS)	25.00	5.00	10.00
STRAIN B. (MEAS)	115.00	45.00	30.00
STRAIN C. (MEAS)	-75.00	-45.00	30.00
STRAIN A. (MECH)	26.99	6.99	11.89
STRAIN B. (MECH)	116.99	46.99	31.89
STRAIN C. (MECH)	-73.02	-43.02	31.89
STRAIN X. (MECH)	-163.02	-83.02	11.89
STRAIN Y. (MECH)	116.98	46.98	31.89
GAMMA XY. (MECH)	100.00	50.00	-10.00
PRIN.STR.1. (P)	125.44	51.62	33.06
PRIN.STR.2. (P)	-171.44	-87.66	9.92
PHI X (DEGREES)	90.17	79.48	67.50
SIGMA XX (KSI)	-1.21	-0.57	0.22
SIGMA YY (KSI)	0.03	0.41	0.29
TAU XY (KSI)	0.38	0.19	-0.04
YIELD STRESS (KSI)	39.99	39.99	39.99
T (KSI)	0.2116E 01	0.1134E 01	0.2101E 00
T/YIELD STRESS	0.5292E-01	0.2837E-01	0.5253E-02

20.00

TEMPERATURE(DEG.FAHR)	79.00	79.00	79.00
STRAIN A. (MEAS)	90.00	35.00	20.00
STRAIN B. (MEAS)	220.00	135.00	30.00
STRAIN C. (MEAS)	-200.00	-165.00	30.00
STRAIN A. (MECH)	81.99	36.99	21.89
STRAIN B. (MECH)	221.99	136.99	31.89
STRAIN C. (MECH)	-198.02	-163.02	21.89
STRAIN X. (MECH)	-338.02	-253.02	11.89

STRAIN Y, (MECH)	211.99	-99.11	31.99
GAMMA XY, (MECH)	490.00	490.00	-150.00
PRIN.STR.1, (*)	289.93	228.38	59.24
PRIN.STR.2, (*)	-575.15	-234.39	-175.24
PHI X (DEGREES)	71.00	56.21	70.10
SIGMA XX (KSI)	-6.26	0.59	-1.55
SIGMA YY (KSI)	0.71	-0.69	-0.20
TAU XY (KSI)	1.81	1.62	-0.56
YIELD STRESS (KSI)	39.99	39.99	39.99
I (KSI)	0.62935 01	0.24665 01	0.66775 00
I/YIELD STRESS	0.13015 01	0.61665-01	0.16705-01

21.00

TEMPERATURE(DEG.FAHR)	78.00	78.00	
STRAIN A, (MEAS)	157.00	230.00	
STRAIN B, (MEAS)	210.00	-10.00	
STRAIN C, (MEAS)	-270.00	-280.00	
STRAIN A, (MECH)	151.89	231.89	
STRAIN B, (MECH)	211.89	-9.11	
STRAIN C, (MECH)	-268.11	-258.11	
STRAIN X, (MECH)	-329.11	-19.11	
STRAIN Y, (MECH)	211.89	-9.11	
GAMMA XY, (MECH)	420.00	400.00	
PRIN.STR.1, (*)	289.96	231.96	
PRIN.STR.2, (*)	-430.16	-259.16	
PHI X (DEGREES)	71.06	45.58	
SIGMA XX (KSI)	-2.03	-0.73	
SIGMA YY (KSI)	1.14	-0.16	
TAU XY (KSI)	1.58	1.96	
YIELD STRESS (KSI)	39.99	39.99	
I (KSI)	0.42288 01	0.23615 01	
I/YIELD STRESS	0.10575 00	0.59025-01	

22.00

TEMPERATURE(DEG.FAHR)	78.00	78.00	
STRAIN A, (MEAS)	180.00	250.00	
STRAIN B, (MEAS)	240.00	-50.00	
STRAIN C, (MEAS)	-375.00	-270.00	
STRAIN A, (MECH)	181.99	251.99	
STRAIN B, (MECH)	241.99	-48.11	
STRAIN C, (MECH)	-373.11	-269.11	
STRAIN X, (MECH)	-433.11	31.99	
STRAIN Y, (MECH)	241.99	-48.11	
GAMMA XY, (MECH)	555.00	530.00	
PRIN.STR.1, (*)	361.37	254.95	
PRIN.STR.2, (*)	-532.55	-271.17	
PHI X (DEGREES)	70.29	40.63	
SIGMA XX (KSI)	-2.98	0.13	
SIGMA YY (KSI)	1.10	-0.67	
TAU XY (KSI)	2.09	1.74	
YIELD STRESS (KSI)	39.99	39.99	
I (KSI)	0.52615 01	0.26915 01	

STRAIN Y, (MECH)	271.99	136.38	71.89
GAMMA XY, (MECH)	280.00	200.00	0.00
PRIN.STR.1, (*)	355.03	160.59	71.89
PRIN.STR.2, (*)	-371.07	-296.62	11.89
PHI X (DEGREES)	76.72	76.72	90.00
SIGMA XX (KSI)	-2.78	-2.26	0.25
SIGMA YY (KSI)	1.43	0.75	0.40
TAU XY (KSI)	1.05	0.75	0.00
YIELD STRESS (KSI)	39.99	39.99	39.99
I (KSI)	0.41145 01	0.21005 01	0.35605 00
I/YIELD STRESS	0.10295 00	0.77535-01	0.89035-02

22.00

TEMPERATURE(DEG.FAHR)	78.00	78.00	
STRAIN A, (MEAS)	150.00	95.00	
STRAIN B, (MEAS)	285.00	185.00	
STRAIN C, (MEAS)	-335.00	-290.00	
STRAIN A, (MECH)	151.99	96.98	
STRAIN B, (MECH)	286.99	196.98	
STRAIN C, (MECH)	-333.02	-288.02	
STRAIN X, (MECH)	-469.02	-378.02	
STRAIN Y, (MECH)	286.98	196.98	
GAMMA XY, (MECH)	485.02	395.02	
PRIN.STR.1, (*)	352.15	246.33	
PRIN.STR.2, (*)	-539.20	-437.37	
PHI X (DEGREES)	72.64	72.96	
SIGMA XX (KSI)	-4.01	-3.17	
SIGMA YY (KSI)	1.47	0.88	
TAU XY (KSI)	1.83	1.45	
YIELD STRESS (KSI)	39.99	39.99	
I (KSI)	0.45695 01	0.44085 01	
I/YIELD STRESS	0.11395 00	0.11025 00	

23.00

TEMPERATURE(DEG.FAHR)	78.00	78.00	
STRAIN A, (MEAS)	215.00	155.00	
STRAIN B, (MEAS)	305.00	210.00	
STRAIN C, (MEAS)	-465.00	-415.00	
STRAIN A, (MECH)	216.98	156.98	
STRAIN B, (MECH)	301.98	211.98	
STRAIN C, (MECH)	-463.02	-413.02	
STRAIN X, (MECH)	-563.02	-468.02	
STRAIN Y, (MECH)	301.98	211.98	
GAMMA XY, (MECH)	530.00	570.00	
PRIN.STR.1, (*)	421.25	315.63	
PRIN.STR.2, (*)	-667.28	-571.67	
PHI X (DEGREES)	70.67	70.91	
SIGMA XX (KSI)	-6.85	-6.39	
SIGMA YY (KSI)	1.56	0.91	
TAU XY (KSI)	2.04	2.14	
YIELD STRESS (KSI)	39.99	39.99	
I (KSI)	0.56805 01	0.53805 01	

T/YIELD STRESS	0.13158E 00	0.62038E-01

23.00		
TEMPERATURE(DEG.FAHR)	79.00	79.00
STRAIN A. (MEAS)	270.00	280.00
STRAIN B. (MEAS)	240.00	-90.00
STRAIN C. (MEAS)	-480.00	-290.00
STRAIN A. (MECH)	271.99	281.99
STRAIN B. (MECH)	241.99	-89.11
STRAIN C. (MECH)	-478.02	-289.11
STRAIN X. (MECH)	-469.02	91.89
STRAIN Y. (MECH)	241.99	-89.11
GAMMA XY. (MECH)	750.00	570.00
PRIN.STR.1. (E)	406.54	294.70
PRIN.STR.2. (E)	-612.59	-300.59
PHI X (DEGREES)	66.31	96.70
SIGMA XX (KSI)	-3.95	0.59
SIGMA YY (KSI)	1.24	-0.67
TAU XY (KSI)	2.82	2.14
YIELD STRESS (KSI)	39.99	39.99
I (KSI)	0.5522E 01	0.2768E 01
I/YIELD STRESS	0.1381E 00	0.6921E-01

24.00		
TEMPERATURE(DEG.FAHR)	79.00	79.00
STRAIN A. (MEAS)	345.00	290.00
STRAIN B. (MEAS)	210.00	-120.00
STRAIN C. (MEAS)	-630.00	-260.00
STRAIN A. (MECH)	346.99	291.89
STRAIN B. (MECH)	211.99	-119.11
STRAIN C. (MECH)	-628.02	-258.11
STRAIN X. (MECH)	-493.02	151.89
STRAIN Y. (MECH)	211.99	-119.11
GAMMA XY. (MECH)	976.00	560.00
PRIN.STR.1. (E)	441.07	323.74
PRIN.STR.2. (E)	-742.11	-289.46
PHI X (DEGREES)	62.93	31.09
SIGMA XX (KSI)	-4.57	1.27
SIGMA YY (KSI)	0.73	-0.76
TAU XY (KSI)	3.67	2.07
YIELD STRESS (KSI)	39.99	39.99
I (KSI)	0.6987E 01	0.3040E 01
I/YIELD STRESS	0.1496E 00	0.7602E-01

25.00		
TEMPERATURE(DEG.FAHR)	79.00	79.00
STRAIN A. (MEAS)	455.00	290.00
STRAIN B. (MEAS)	30.00	-130.00
STRAIN C. (MEAS)	-835.00	-230.00
STRAIN A. (MECH)	447.00	291.99

T/YIELD STRESS	0.1603E 00	0.1368E 00

26.00		
TEMPERATURE(DEG.FAHR)	80.00	79.00
STRAIN A. (MEAS)	315.00	275.00
STRAIN B. (MEAS)	300.00	220.00
STRAIN C. (MEAS)	-645.00	-585.00
STRAIN A. (MECH)	317.09	276.99
STRAIN B. (MECH)	302.09	221.99
STRAIN C. (MECH)	-642.91	-583.02
STRAIN X. (MECH)	-627.91	-628.12
STRAIN Y. (MECH)	302.09	221.99
GAMMA XY. (MECH)	940.00	860.00
PRIN.STR.1. (E)	505.39	417.53
PRIN.STR.2. (E)	-831.21	-723.57
PHI X (DEGREES)	67.05	65.55
SIGMA XX (KSI)	-5.56	-6.93
SIGMA YY (KSI)	1.44	0.71
TAU XY (KSI)	3.61	3.23
YIELD STRESS (KSI)	39.99	39.99
I (KSI)	0.7194E 01	0.5165E 01
I/YIELD STRESS	0.1799E 00	0.1542E 00

25.00		
TEMPERATURE(DEG.FAHR)	82.00	81.00
STRAIN A. (MEAS)	635.00	465.00
STRAIN B. (MEAS)	200.00	145.00
STRAIN C. (MEAS)	-850.00	-830.00
STRAIN A. (MECH)	637.37	667.22
STRAIN B. (MECH)	202.37	147.22
STRAIN C. (MECH)	-647.63	-727.78
STRAIN X. (MECH)	-612.63	-507.78
STRAIN Y. (MECH)	202.37	147.22
GAMMA XY. (MECH)	1095.00	1295.00
PRIN.STR.1. (E)	513.46	545.73
PRIN.STR.2. (E)	-729.72	-905.83
PHI X (DEGREES)	59.77	58.41
SIGMA XX (KSI)	-3.12	-4.58
SIGMA YY (KSI)	1.51	0.33
TAU XY (KSI)	4.09	4.87
YIELD STRESS (KSI)	39.97	39.97
I (KSI)	0.5376E 01	0.6105E 01
I/YIELD STRESS	0.1345E 00	0.1528E 00

26.00		
TEMPERATURE(DEG.FAHR)	99.00	89.00
STRAIN A. (MEAS)	250.00	560.00
STRAIN B. (MEAS)	-100.00	-90.00
STRAIN C. (MEAS)	-950.00	-940.00
STRAIN A. (MECH)	256.93	563.62

STRAIN A. (MECH)	92.09	-128.07
STRAIN C. (MECH)	-827.91	-229.07
STRAIN X. (MECH)	-467.91	191.93
STRAIN Y. (MECH)	92.09	-129.07
GAMMA XY. (MECH)	1290.09	529.93
PRIN.STR.1. (M)	521.33	337.77
PRIN.STR.2. (M)	-877.14	-277.33
PHI X (DEGREES)	56.36	29.39
SIGMA XX (KSI)	-6.37	1.98
SIGMA YY (KSI)	-0.26	-0.53
TAU XY (KSI)	4.85	1.56
YIELD STRESS (KSI)	39.99	39.99
I (KSI)	0.5669E 01	0.3284E 01
I/YIELD STRESS	0.1417E 00	0.8167E-01

24.00		
TEMPERATURE(DEG.FAHR)	99.00	79.00
STRAIN A. (MEAS)	360.00	290.00
STRAIN B. (MEAS)	-180.00	-130.00
STRAIN C. (MEAS)	-960.00	-170.00
STRAIN A. (MECH)	363.88	291.99
STRAIN B. (MECH)	-174.12	-129.11
STRAIN C. (MECH)	-978.12	-168.11
STRAIN X. (MECH)	-294.12	251.89
STRAIN Y. (MECH)	-174.12	-129.11
GAMMA XY. (MECH)	1200.00	663.00
PRIN.STR.1. (M)	366.89	267.77
PRIN.STR.2. (M)	-939.11	-236.66
PHI X (DEGREES)	47.85	25.33
SIGMA XX (KSI)	-1.86	2.36
SIGMA YY (KSI)	-0.96	-1.50
TAU XY (KSI)	4.50	1.71
YIELD STRESS (KSI)	39.99	39.99
I (KSI)	0.4013E 01	0.2415E 01
I/YIELD STRESS	0.1005E 00	0.6038E-01

27.00		
TEMPERATURE(DEG.FAHR)	130.00	79.00
STRAIN A. (MEAS)	-690.00	300.00
STRAIN B. (MEAS)	-300.00	-90.00
STRAIN C. (MEAS)	-210.00	-100.00
STRAIN A. (MECH)	-395.22	301.99
STRAIN B. (MECH)	-275.22	-99.11
STRAIN C. (MECH)	-185.22	-98.11
STRAIN X. (MECH)	-305.22	291.99
STRAIN Y. (MECH)	-275.22	-99.11
GAMMA XY. (MECH)	-210.00	400.00
PRIN.STR.1. (M)	-184.16	377.75
PRIN.STR.2. (M)	-396.29	-175.87
PHI X (DEGREES)	49.07	23.29
SIGMA XX (KSI)	5.65	2.96
SIGMA YY (KSI)	5.87	0.19

STRAIN A. (MECH)	-93.07	-86.99
STRAIN C. (MECH)	-[illegible].07	-836.99
STRAIN X. (MECH)	-573.07	-186.99
STRAIN Y. (MECH)	-93.07	-86.99
GAMMA XY. (MECH)	1200.00	1470.00
PRIN.STR.1. (M)	394.53	565.69
PRIN.STR.2. (M)	-903.07	-839.17
PHI X (DEGREES)	56.31	47.04
SIGMA XX (KSI)	-7.37	-7.69
SIGMA YY (KSI)	0.81	0.76
TAU XY (KSI)	4.49	5.35
YIELD STRESS (KSI)	39.96	39.93
I (KSI)	0.5055E 01	0.6024E 01
I/YIELD STRESS	0.1269E 00	0.1509E 00

27.00		
TEMPERATURE(DEG.FAHR)	150.00	114.00
STRAIN A. (MEAS)	-790.00	-195.00
STRAIN B. (MEAS)	-25.00	85.00
STRAIN C. (MEAS)	-310.00	75.00
STRAIN A. (MECH)	-745.01	-90.22
STRAIN B. (MECH)	13.99	90.78
STRAIN C. (MECH)	-265.01	80.78
STRAIN X. (MECH)	-1030.01	-100.22
STRAIN Y. (MECH)	13.99	90.78
GAMMA XY. (MECH)	-690.00	-180.00
PRIN.STR.1. (M)	72.96	134.37
PRIN.STR.2. (M)	-1182.27	-136.75
PHI X (DEGREES)	77.79	69.01
SIGMA XX (KSI)	4.37	6.22
SIGMA YY (KSI)	12.09	7.71
TAU XY (KSI)	-1.76	-0.67
YIELD STRESS (KSI)	39.29	39.73
I (KSI)	0.1034E 02	0.6937E 01
I/YIELD STRESS	0.2632E 00	0.1746E 00

28.00		
TEMPERATURE(DEG.FAHR)	239.00	179.00
STRAIN A. (MEAS)	-2005.00	80.00
STRAIN B. (MEAS)	745.00	875.00
STRAIN C. (MEAS)	-10.00	590.00
STRAIN A. (MECH)	-2917.99	136.08
STRAIN B. (MECH)	822.01	933.09
STRAIN C. (MECH)	67.01	648.09
STRAIN X. (MECH)	-2772.99	-146.92
STRAIN Y. (MECH)	822.01	933.08
GAMMA XY. (MECH)	-2085.00	-510.00
PRIN.STR.1. (M)	1102.46	990.24
PRIN.STR.2. (M)	-3053.42	-204.10
PHI X (DEGREES)	74.94	77.35
SIGMA XX (KSI)	4.06	21.24
SIGMA YY (KSI)	25.58	29.10

TAU XY (KSI)	-0.79	1.59
YIELD STRESS (KSI)	39.99	39.99
I (KSI)	0.5555E 01	0.2445E 01
I/YIELD STRESS	0.1389E 00	0.6113E-01

28.00

TEMPERATURE(DEG.FAHR)	191.00	79.00
STRAIN A, (MEAS)	-1045.00	320.00
STRAIN B, (MEAS)	191.00	-61.00
STRAIN C, (MEAS)	151.00	-53.10
STRAIN A, (MECH)	-1030.19	321.00
STRAIN B, (MECH)	946.81	-98.10
STRAIN C, (MECH)	916.81	-68.10
STRAIN X, (MECH)	-1031.19	311.00
STRAIN Y, (MECH)	946.81	-99.00
GAMMA XY, (MECH)	-1915.00	391.00
PRIN.STR.1, (P)	497.01	301.86
PRIN.STR.2, (P)	-1777.20	-117.67
PHI X (DEGREES)	59.19	21.31
SIGMA XX (KSI)	11.41	3.57
SIGMA YY (KSI)	33.65	3.06
TAU XY (KSI)	-4.49	1.30
YIELD STRESS (KSI)	39.99	39.99
I (KSI)	0.1755E 02	0.7702E 01
I/YIELD STRESS	0.4515E 00	0.1925E-01

29.00

TEMPERATURE(DEG.FAHR)	247.00	79.00
STRAIN A, (MEAS)	-1245.00	351.00
STRAIN B, (MEAS)	565.00	-10.00
STRAIN C, (MEAS)	40.00	-47.00
STRAIN A, (MECH)	-1149.34	351.00
STRAIN B, (MECH)	531.66	-3.00
STRAIN C, (MECH)	134.66	-38.00
STRAIN X, (MECH)	-1661.34	321.00
STRAIN Y, (MECH)	631.66	-8.00
GAMMA XY, (MECH)	-1335.00	391.00
PRIN.STR.1, (P)	806.21	412.42
PRIN.STR.2, (P)	-1935.21	-93.44
PHI X (DEGREES)	75.19	24.00
SIGMA XX (KSI)	15.06	3.71
SIGMA YY (KSI)	37.22	1.31
TAU XY (KSI)	-4.47	1.47
YIELD STRESS (KSI)	39.99	39.99
I (KSI)	0.2345E 02	0.9962E 01
I/YIELD STRESS	0.5865E 00	0.2491E-01

30.00

TEMPERATURE(DEG.FAHR)	273.00	91.00	79.00
STRAIN A, (MEAS)	-1245.00	391.00	45.00

TAU XY (KSI)	-7.40	-1.84
YIELD STRESS (KSI)	37.87	39.99
I (KSI)	0.2783E 02	0.2565E 02
I/YIELD STRESS	0.7227E 01	0.6655E 00

29.00

TEMPERATURE(DEG.FAHR)	290.00	234.00
STRAIN A, (MEAS)	-1290.00	374.00
STRAIN B, (MEAS)	1067.00	435.00
STRAIN C, (MEAS)	-55.00	295.00
STRAIN A, (MECH)	-1237.20	452.11
STRAIN B, (MECH)	1117.80	917.11
STRAIN C, (MECH)	-7.20	787.11
STRAIN X, (MECH)	-2357.20	-97.89
STRAIN Y, (MECH)	1117.80	912.11
GAMMA XY, (MECH)	-1235.00	99.00
PRIN.STR.1, (P)	1219.56	914.11
PRIN.STR.2, (P)	-2458.96	-99.99
PHI X (DEGREES)	80.19	87.65
SIGMA XX (KSI)	19.24	31.94
SIGMA YY (KSI)	43.23	30.13
TAU XY (KSI)	-6.27	0.37
YIELD STRESS (KSI)	35.37	37.99
I (KSI)	0.3731E 02	0.1605E 02
I/YIELD STRESS	0.1054E 01	0.4459E 00

30.00

TEMPERATURE(DEG.FAHR)	316.00	260.00	79.00
STRAIN A, (MEAS)	-1059.00	-55.00	60.00
STRAIN B, (MEAS)	1575.00	395.00	95.00
STRAIN C, (MEAS)	-255.00	5.00	63.00
STRAIN A, (MECH)	-1027.49	13.15	51.80
STRAIN B, (MECH)	1597.58	453.15	95.80
STRAIN C, (MECH)	-247.49	73.15	61.80
STRAIN X, (MECH)	-2857.49	-366.85	-7.11
STRAIN Y, (MECH)	1597.58	453.15	94.80
GAMMA XY, (MECH)	-795.00	-40.00	10.00
PRIN.STR.1, (P)	1633.77	466.95	97.14
PRIN.STR.2, (P)	-2893.60	-367.94	-9.34
PHI X (DEGREES)	84.84	87.91	87.14
SIGMA XX (KSI)	20.60	33.02	0.33
SIGMA YY (KSI)	50.86	30.55	1.33
TAU XY (KSI)	-2.71	-0.21	0.04
YIELD STRESS (KSI)	35.36	37.96	39.99
I (KSI)	0.4421E 02	0.1701E 02	0.1017E 01
I/YIELD STRESS	0.1250E 01	0.4479E 00	0.2543E-01

31.00

TEMPERATURE(DEG.FAHR)	326.00	239.00	
STRAIN A, (MEAS)	-470.00	-220.00	

STRAIN A, (MEAS)	780.00	0.00	195.00
STRAIN C, (MEAS)	-75.00	-15.00	15.00
STRAIN A, (MECH)	-1179.56	387.22	65.89
STRAIN B, (MECH)	866.44	7.22	104.89
STRAIN C, (MECH)	-4.56	-7.78	16.89
STRAIN X, (MECH)	-2033.56	372.22	-49.11
STRAIN Y, (MECH)	866.44	7.22	136.89
GAMMA XY, (MECH)	-1173.00	390.00	27.00
PRIN.STR.1, (M)	960.77	456.02	128.27
PRIN.STR.2, (M)	-2167.85	-41.57	-44.60
PHI X (DEGREES)	79.05	23.25	84.36
SIGMA XX (KSI)	18.21	6.38	-2.09
SIGMA YY (KSI)	38.31	2.00	1.04
TAU XY (KSI)	-4.01	1.47	0.18
YIELD STRESS (KSI)	36.06	30.97	10.00
I (KSI)	0.33075 02	0.46500 01	0.13365 01
I/YIELD STRESS	0.95675 00	0.11665 00	0.13365 01

	11.00		
TEMPERATURE(DEG.FAHR)	273.00	94.00	
STRAIN A, (MEAS)	-1765.00	570.00	
STRAIN B, (MEAS)	915.00	0.00	
STRAIN C, (MEAS)	-210.00	30.00	
STRAIN A, (MECH)	-1199.39	372.22	
STRAIN B, (MECH)	963.61	7.22	
STRAIN C, (MECH)	-156.39	12.22	
STRAIN X, (MECH)	-2215.39	382.22	
STRAIN Y, (MECH)	963.61	7.22	
GAMMA XY, (MECH)	-1935.00	350.00	
PRIN.STR.1, (M)	1060.22	454.44	
PRIN.STR.2, (M)	-2334.00	-60.00	
PHI X (DEGREES)	81.21	21.21	
SIGMA XX (KSI)	13.75	5.69	
SIGMA YY (KSI)	41.63	2.63	
TAU XY (KSI)	-3.51	1.35	
YIELD STRESS (KSI)	36.66	30.00	
I (KSI)	0.35965 02	0.51575 01	
I/YIELD STRESS	0.98075 00	0.17915 00	

	22.00		
TEMPERATURE(DEG.FAHR)	297.00	99.00	
STRAIN A, (MEAS)	-1170.00	360.00	
STRAIN B, (MEAS)	945.00	-20.00	
STRAIN C, (MEAS)	-330.00	30.00	
STRAIN A, (MECH)	-1124.00	341.67	
STRAIN B, (MECH)	990.01	-16.39	
STRAIN C, (MECH)	-294.00	33.62	
STRAIN X, (MECH)	-2390.00	293.62	
STRAIN Y, (MECH)	990.01	-36.38	
GAMMA XY, (MECH)	-960.00	310.00	
PRIN.STR.1, (M)	1042.17	445.43	
PRIN.STR.2, (M)	-2451.35	-69.38	

STRAIN A, (MEAS)	1550.00	265.00	
STRAIN C, (MEAS)	-525.00	-135.00	
STRAIN A, (MECH)	-462.42	-265.39	
STRAIN B, (MECH)	1557.58	319.61	
STRAIN C, (MECH)	-317.42	-80.39	
STRAIN X, (MECH)	-2337.42	-665.39	
STRAIN Y, (MECH)	1557.58	319.61	
GAMMA XY, (MECH)	-145.00	-195.00	
PRIN.STR.1, (M)	1568.93	398.72	
PRIN.STR.2, (M)	-2399.76	-674.00	
PHI X (DEGREES)	89.03	86.68	
SIGMA XX (KSI)	27.45	9.63	
SIGMA YY (KSI)	53.82	40.45	
TAU XY (KSI)	-0.68	-0.66	
YIELD STRESS (KSI)	36.03	36.66	
I (KSI)	0.46605 02	0.17695 02	
I/YIELD STRESS	0.13365 01	0.10795 01	

	33.00		
TEMPERATURE(DEG.FAHR)	329.00	399.00	
STRAIN A, (MEAS)	-110.00	-440.00	
STRAIN B, (MEAS)	1490.00	195.00	
STRAIN C, (MEAS)	-405.00	-205.00	
STRAIN A, (MECH)	-195.64	-300.58	
STRAIN B, (MECH)	1494.36	235.42	
STRAIN C, (MECH)	-335.64	-164.58	
STRAIN X, (MECH)	-1995.64	-799.58	
STRAIN Y, (MECH)	1494.36	235.42	
GAMMA XY, (MECH)	720.00	-235.00	
PRIN.STR.1, (M)	1600.61	249.55	
PRIN.STR.2, (M)	-1991.69	-812.75	
PHI X (DEGREES)	87.61	83.69	
SIGMA XX (KSI)	31.13	14.43	
SIGMA YY (KSI)	54.59	41.54	
TAU XY (KSI)	0.98	-0.71	
YIELD STRESS (KSI)	34.84	35.32	
I (KSI)	0.47665 02	0.18655 02	
I/YIELD STRESS	0.13625 01	0.10705 01	

	44.00		
TEMPERATURE(DEG.FAHR)	337.00	398.00	78.00
STRAIN A, (MEAS)	-145.00	-445.00	75.00
STRAIN B, (MEAS)	1515.00	90.00	130.00
STRAIN C, (MEAS)	-500.00	-295.00	50.00
STRAIN A, (MECH)	-159.00	-296.77	74.99
STRAIN B, (MECH)	1520.00	129.23	131.99
STRAIN C, (MECH)	-474.00	-261.77	51.99
STRAIN X, (MECH)	-1974.00	-791.77	-7.11
STRAIN Y, (MECH)	1520.00	129.23	131.99
GAMMA XY, (MECH)	335.00	-135.00	95.00
PRIN.STR.1, (M)	1529.47	129.23	132.04
PRIN.STR.2, (M)	-1982.51	-784.78	-4.26

PHI X (DEGREES)	83.06	18.55
SIGMA XX (KSI)	19.65	6.90
SIGMA YY (KSI)	42.98	3.27
TAU XY (KSI)	-2.89	1.16
YIELD STRESS (KSI)	36.11	39.93
I (KSI)	0.3715E 02	0.5768E 01
I/YIELD STRESS	0.1029E 01	0.1445E 00

35.00

TEMPERATURE(DEG.FAHR)	300.00	91.00
STRAIN A. (MEAS)	-1093.00	293.00
STRAIN B. (MEAS)	975.00	-29.00
STRAIN C. (MEAS)	-450.00	50.00
STRAIN A. (MECH)	-1297.33	204.66
STRAIN B. (MECH)	1017.67	-15.54
STRAIN C. (MECH)	-407.33	44.45
STRAIN X. (MECH)	-2462.33	374.44
STRAIN Y. (MECH)	1017.67	-15.54
GAMMA XY. (MECH)	-433.33	237.00
PRIN.STR.1. (M)	1045.95	405.34
PRIN.STR.2. (M)	-2489.61	-64.93
PHI X (DEGREES)	84.97	15.74
SIGMA XX (KSI)	19.67	6.67
SIGMA YY (KSI)	41.55	3.76
TAU XY (KSI)	-2.17	0.96
YIELD STRESS (KSI)	36.03	39.91
I (KSI)	0.3763E 02	0.6630E 01
I/YIELD STRESS	0.1047E 01	0.1663E 00

34.00

TEMPERATURE(DEG.FAHR)	300.00	94.00
STRAIN A. (MEAS)	-1035.00	240.00
STRAIN B. (MEAS)	960.00	-30.00
STRAIN C. (MEAS)	-435.00	40.00
STRAIN A. (MECH)	-962.33	246.16
STRAIN B. (MECH)	1002.67	-13.96
STRAIN C. (MECH)	-469.33	96.16
STRAIN X. (MECH)	-2417.33	356.15
STRAIN Y. (MECH)	1002.67	-13.96
GAMMA XY. (MECH)	-510.00	150.00
PRIN.STR.1. (M)	1071.59	370.79
PRIN.STR.2. (M)	-2436.24	-29.47
PHI X (DEGREES)	85.76	11.03
SIGMA XX (KSI)	20.04	7.43
SIGMA YY (KSI)	43.55	4.66
TAU XY (KSI)	-1.75	0.56
YIELD STRESS (KSI)	36.03	39.87
I (KSI)	0.3769E 02	0.8630E 01
I/YIELD STRESS	0.1047E 01	0.1663E 00

PHI X (DEGREES)	87.10	85.74	14.75
SIGMA XX (KSI)	33.83	35.28	7.66
SIGMA YY (KSI)	52.81	41.69	1.69
TAU XY (KSI)	1.13	-0.46	0.00
YIELD STRESS (KSI)	36.00	35.42	39.89
I (KSI)	0.4590E 02	0.3873E 02	0.1417E 01
I/YIELD STRESS	0.1917E 01	0.1085E 01	0.3553E-01

40.00

TEMPERATURE(DEG.FAHR)	293.00	208.00	98.00
STRAIN A. (MEAS)	-45.00	-355.00	350.00
STRAIN B. (MEAS)	855.00	-80.00	350.00
STRAIN C. (MEAS)	-545.00	-385.00	75.00
STRAIN A. (MECH)	-17.00	-317.15	151.83
STRAIN B. (MECH)	910.01	-35.15	351.83
STRAIN C. (MECH)	-517.00	-345.15	78.00
STRAIN X. (MECH)	-1449.01	-615.15	-73.11
STRAIN Y. (MECH)	910.01	-35.15	351.83
GAMMA XY. (MECH)	500.00	33.33	95.00
PRIN.STR.1. (M)	937.17	-36.32	361.01
PRIN.STR.2. (M)	-1476.20	-615.56	-75.13
PHI X (DEGREES)	34.09	88.52	13.32
SIGMA XX (KSI)	32.14	34.70	7.49
SIGMA YY (KSI)	45.49	39.63	2.75
TAU XY (KSI)	1.72	2.13	0.29
YIELD STRESS (KSI)	36.11	36.03	39.69
I (KSI)	0.3903E 02	0.3636E 02	0.1441E 01
I/YIELD STRESS	0.1110E 01	0.1029E 01	0.3633E-01

45.00

TEMPERATURE(DEG.FAHR)	277.00	278.00	79.00
STRAIN A. (MEAS)	-80.00	-335.00	310.00
STRAIN B. (MEAS)	445.00	-165.00	430.00
STRAIN C. (MEAS)	-530.00	-360.00	90.00
STRAIN A. (MECH)	-16.76	-277.66	311.68
STRAIN B. (MECH)	700.24	-97.66	491.68
STRAIN C. (MECH)	-486.76	-327.66	8.01
STRAIN X. (MECH)	-1191.76	-537.66	-71.33
STRAIN Y. (MECH)	700.24	-97.66	491.68
GAMMA XY. (MECH)	450.00	65.00	310.00
PRIN.STR.1. (M)	736.82	-95.41	465.83
PRIN.STR.2. (M)	-1218.34	-536.17	-45.73
PHI X (DEGREES)	33.36	84.19	24.61
SIGMA XX (KSI)	27.57	32.13	1.44
SIGMA YY (KSI)	40.75	34.91	4.85
TAU XY (KSI)	1.57	2.19	0.34
YIELD STRESS (KSI)	36.03	36.03	39.69
I (KSI)	0.3617E 02	0.3343E 02	0.4553E 01
I/YIELD STRESS	0.1004E 01	0.9278E 00	0.1153E 01

35.00

TEMPERATURE(DEG.FAHR)	300.00	100.00
STRAIN A. (MEAS)	-939.00	190.00
STRAIN B. (MEAS)	915.00	-20.00
STRAIN C. (MEAS)	-525.00	170.00
STRAIN A. (MECH)	-887.33	197.76
STRAIN B. (MECH)	957.67	-12.24
STRAIN C. (MECH)	-497.33	127.76
STRAIN X. (MECH)	-2327.33	337.76
STRAIN Y. (MECH)	957.67	-12.24
GAMMA XY. (MECH)	-405.00	70.00
PRIN.STR.1. (")	970.11	341.22
PRIN.STR.2. (")	-2339.76	-15.71
PHI X (DEGREES)	86.49	5.66
SIGMA XX (KSI)	20.81	8.00
SIGMA YY (KSI)	43.40	5.39
TAU XY (KSI)	-1.19	0.26
YIELD STRESS (KSI)	36.00	39.84
E (KSI)	C.3784E 02	0.711RE 01
E/YIELD STRESS	C.1043E 01	0.1787E 00

36.00

TEMPERATURE(DEG.FAHR)	299.00	106.00
STRAIN A. (MEAS)	-915.00	130.00
STRAIN B. (MEAS)	870.00	-10.00
STRAIN C. (MEAS)	-570.00	120.00
STRAIN A. (MECH)	-871.23	149.52
STRAIN B. (MECH)	913.77	9.52
STRAIN C. (MECH)	-526.23	130.52
STRAIN X. (MECH)	-2411.23	270.52
STRAIN Y. (MECH)	913.77	9.52
GAMMA XY. (MECH)	-345.00	10.00
PRIN.STR.1. (")	922.97	270.41
PRIN.STR.2. (")	-2920.43	9.43
PHI X (DEGREES)	82.95	1.06
SIGMA XX (KSI)	20.66	8.45
SIGMA YY (KSI)	42.81	5.41
TAU XY (KSI)	-1.19	0.04
YIELD STRESS (KSI)	36.04	39.97
E (KSI)	C.3705E 02	0.7649E 01
E/YIELD STRESS	C.1029E 01	0.1922E 00

37.00

TEMPERATURE(DEG.FAHR)	296.00	110.00
STRAIN A. (MEAS)	-860.00	90.00
STRAIN B. (MEAS)	825.00	10.00
STRAIN C. (MEAS)	-600.00	120.00
STRAIN A. (MECH)	-793.05	92.57
STRAIN B. (MECH)	871.95	22.57
STRAIN C. (MECH)	-553.05	132.57
STRAIN X. (MECH)	-2214.05	202.57
STRAIN Y. (MECH)	871.95	22.57

49.00

TEMPERATURE(DEG.FAHR)		90.00
STRAIN A. (MEAS)		695.00
STRAIN B. (MEAS)		640.00
STRAIN C. (MEAS)		-75.00
STRAIN A. (MECH)		677.09
STRAIN B. (MECH)		667.09
STRAIN C. (MECH)		-72.91
STRAIN X. (MECH)		-87.91
STRAIN Y. (MECH)		667.09
GAMMA XY. (MECH)		790.00
PRIN.STR.1. (")		742.79
PRIN.STR.2. (")		-228.69
PHI X (DEGREES)		88.10
SIGMA XX (KSI)		1.81
SIGMA YY (KSI)		7.29
TAU XY (KSI)		2.63
YIELD STRESS (KSI)		39.98
E (KSI)		0.7155E 01
E/YIELD STRESS		0.1793E 00

50.00

TEMPERATURE(DEG.FAHR)	260.00	259.00	90.00
STRAIN A. (MEAS)	-190.00	-330.00	820.00
STRAIN B. (MEAS)	460.00	215.00	690.00
STRAIN C. (MEAS)	-490.00	-385.00	-220.00
STRAIN A. (MECH)	-57.64	257.36	872.09
STRAIN B. (MECH)	532.36	-142.64	692.09
STRAIN C. (MECH)	-417.64	-317.64	-217.91
STRAIN X. (MECH)	-1007.64	-427.64	-77.91
STRAIN Y. (MECH)	532.36	-142.64	692.09
GAMMA XY. (MECH)	360.00	55.00	1040.00
PRIN.STR.1. (")	553.17	-139.61	966.14
PRIN.STR.2. (")	-1028.40	-429.85	-361.96
PHI X (DEGREES)	83.49	84.54	87.08
SIGMA XX (KSI)	25.77	29.29	7.37
SIGMA YY (KSI)	36.54	31.29	7.79
TAU XY (KSI)	1.75	0.19	3.91
YIELD STRESS (KSI)	37.37	37.35	39.99
E (KSI)	C.3257E 02	0.3035E 02	0.7777E 01
E/YIELD STRESS	C.8718E 00	0.8126E 00	0.1945E 00

51.00

TEMPERATURE(DEG.FAHR)	87.00
STRAIN A. (MEAS)	1090.00
STRAIN B. (MEAS)	895.00
STRAIN C. (MEAS)	-505.00
STRAIN A. (MECH)	1092.37
STRAIN B. (MECH)	882.37
STRAIN C. (MECH)	-512.63
STRAIN X. (MECH)	-92.63
STRAIN Y. (MECH)	692.37

GAMMA XY, (MECH)	-240.01	-40.00	
PRIN.STR.1, (")	776.63	204.77	
PRIN.STR.2, (")	-2222.71	-90.35	
PHI X (DEGREES)	97.79	6.26	
SIGMA XX (KSI)	20.91	8.54	
SIGMA YY (KSI)	47.20	7.70	
TAU XY (KSI)	-0.83	-0.15	
YIELD STRESS (KSI)	36.15	38.76	
I (KSI)	0.3651E 02	0.7926E 01	
I/YIELD STRESS	0.1010E 01	0.1993E 00	

38.00			
TEMPERATURE(DEG.FAHR)	294.00	115.00	
STRAIN A, (MEAS)	-840.00	400.00	
STRAIN B, (MEAS)	795.00	20.00	
STRAIN C, (MEAS)	-600.00	320.00	
STRAIN A, (MECH)	-791.03	415.35	
STRAIN B, (MECH)	841.97	35.35	
STRAIN C, (MECH)	-551.03	135.35	
STRAIN X, (MECH)	-2186.03	515.35	
STRAIN Y, (MECH)	841.97	35.35	
GAMMA XY, (MECH)	-247.00	240.00	
PRIN.STR.1, (")	968.72	553.79	
PRIN.STR.2, (")	-2192.77	-2.40	
PHI X (DEGREES)	97.76	15.13	
SIGMA XX (KSI)	20.77	11.04	
SIGMA YY (KSI)	41.68	9.47	
TAU XY (KSI)	-0.83	1.04	
YIELD STRESS (KSI)	36.22	39.73	
I (KSI)	0.3604E 02	0.1191E 02	
I/YIELD STRESS	0.9955E 00	0.2997E 00	

40.00			
TEMPERATURE(DEG.FAHR)	283.00	121.00	78.00
STRAIN A, (MEAS)	-765.00	-430.00	135.00
STRAIN B, (MEAS)	720.00	50.00	345.00
STRAIN C, (MEAS)	-603.00	120.00	75.00
STRAIN A, (MECH)	-710.39	-370.79	136.89
STRAIN B, (MECH)	774.61	70.21	346.89
STRAIN C, (MECH)	-545.39	160.21	76.89
STRAIN X, (MECH)	-2030.39	-390.79	-133.11
STRAIN Y, (MECH)	774.61	70.21	346.89
GAMMA XY, (MECH)	-165.00	-520.00	60.00
PRIN.STR.1, (")	922.03	209.24	360.24
PRIN.STR.2, (")	-2032.82	-661.81	-136.98
PHI X (DEGREES)	88.22	63.09	86.44
SIGMA XX (KSI)	21.04	5.57	-0.20
SIGMA YY (KSI)	40.46	9.14	3.41
TAU XY (KSI)	-0.57	-1.03	0.23
YIELD STRESS (KSI)	36.44	39.46	39.99
I (KSI)	0.3502E 02	0.6939E 01	0.3611E 01
I/YIELD STRESS	0.9613E 00	0.1759E 00	0.9029E-01

GAMMA XY, (MECH)	1595.00	
PRIN.STR.1, (")	1191.53	
PRIN.STR.2, (")	-591.79	
PHI X (DEGREES)	57.96	
SIGMA XX (KSI)	2.29	
SIGMA YY (KSI)	8.11	
TAU XY (KSI)	5.99	
YIELD STRESS (KSI)	39.97	
I (KSI)	0.8396E 01	
I/YIELD STRESS	0.2101E 00	

52.00		
TEMPERATURE(DEG.FAHR)	99.00	
STRAIN A, (MEAS)	1365.00	
STRAIN B, (MEAS)	470.00	
STRAIN C, (MEAS)	-875.00	
STRAIN A, (MECH)	1368.67	
STRAIN B, (MECH)	473.67	
STRAIN C, (MECH)	-871.38	
STRAIN X, (MECH)	91.67	
STRAIN Y, (MECH)	473.67	
GAMMA XY, (MECH)	2260.00	
PRIN.STR.1, (")	1390.99	
PRIN.STR.2, (")	-911.74	
PHI X (DEGREES)	50.68	
SIGMA XX (KSI)	3.97	
SIGMA YY (KSI)	7.35	
TAU XY (KSI)	8.49	
YIELD STRESS (KSI)	39.97	
I (KSI)	0.[illegible]E 01	
I/YIELD STRESS	0.[illegible]E 00	

53.00		
TEMPERATURE(DEG.FAHR)	1[illegible].00	
STRAIN A, (MEAS)	[illegible].35	
STRAIN B, (MEAS)	145.33	
STRAIN C, (MEAS)	-645.00	
STRAIN A, (MECH)	890.57	
STRAIN B, (MECH)	155.57	
STRAIN C, (MECH)	-[illegible].65	
STRAIN X, (MECH)	100.57	
STRAIN Y, (MECH)	155.57	
GAMMA XY, (MECH)	1[illegible].00	
PRIN.STR.1, (")	891.91	
PRIN.STR.2, (")	-[illegible].54	
PHI X (DEGREES)	44.[illegible]	
SIGMA XX (KSI)	7.13	
SIGMA YY (KSI)	7.53	
TAU XY (KSI)	[illegible].49	
YIELD STRESS (KSI)	[illegible].80	
I (KSI)	[illegible].84[illegible] 01	
I/YIELD STRESS	[illegible].21[illegible] 00	

65.00

TEMPERATURE(DEG.FAHR)	275.00	149.00	70.00
STRAIN A, (MEAS)	-675.00	-170.00	270.00
STRAIN B, (MEAS)	630.00	120.00	570.00
STRAIN C, (MEAS)	-595.00	80.00	90.00
STRAIN A, (MECH)	-610.63	-139.36	271.89
STRAIN B, (MECH)	564.57	151.64	571.99
STRAIN C, (MECH)	-590.63	111.64	91.99
STRAIN X, (MECH)	-1795.43	-179.36	-206.11
STRAIN Y, (MECH)	664.57	151.64	571.99
GAMMA XY, (MECH)	-93.00	-250.00	180.00
PRIN.STR.1, (P)	665.79	193.44	587.14
PRIN.STR.2, (P)	-1796.35	-229.36	-218.36
PHI X (DEGREES)	88.65	71.63	88.63
SIGMA XX (KSI)	20.69	10.57	-3.33
SIGMA YY (KSI)	37.84	13.30	5.67
TAU XY (KSI)	-9.71	-0.97	0.69
YIELD STRESS (KSI)	35.97	35.69	39.53
I (KSI)	0.33815 02	0.11865 02	0.55445 01
I/YIELD STRESS	0.88008 00	0.33025 00	0.14065 00

41.00

TEMPERATURE(DEG.FAHR)	70.00
STRAIN A, (MEAS)	465.00
STRAIN B, (MEAS)	745.00
STRAIN C, (MEAS)	15.00
STRAIN A, (MECH)	466.98
STRAIN B, (MECH)	764.99
STRAIN C, (MECH)	14.99
STRAIN X, (MECH)	-293.02
STRAIN Y, (MECH)	764.99
GAMMA XY, (MECH)	453.01
PRIN.STR.1, (P)	913.16
PRIN.STR.2, (P)	-339.02
PHI X (DEGREES)	70.47
SIGMA XX (KSI)	-3.12
SIGMA YY (KSI)	7.74
TAU XY (KSI)	1.69
YIELD STRESS (KSI)	39.00
I (KSI)	0.8154E 01
I/YIELD STRESS	0.2043E 00

49.00

TEMPERATURE(DEG.FAHR)	70.00
STRAIN A, (MEAS)	570.00
STRAIN B, (MEAS)	810.00
STRAIN C, (MEAS)	-75.00
STRAIN A, (MECH)	571.99
STRAIN B, (MECH)	811.99

54.00

TEMPERATURE(DEG.FAHR)	168.00
STRAIN A, (MEAS)	295.00
STRAIN B, (MEAS)	310.00
STRAIN C, (MEAS)	-30.00
STRAIN A, (MECH)	272.27
STRAIN B, (MECH)	347.27
STRAIN C, (MECH)	7.27
STRAIN X, (MECH)	-67.73
STRAIN Y, (MECH)	347.27
GAMMA XY, (MECH)	265.00
PRIN.STR.1, (P)	395.97
PRIN.STR.2, (P)	-106.67
PHI X (DEGREES)	73.72
SIGMA XX (KSI)	14.09
SIGMA YY (KSI)	17.11
TAU XY (KSI)	3.98
YIELD STRESS (KSI)	39.41
I (KSI)	0.1560E 02
I/YIELD STRESS	0.4033E 00

55.00

TEMPERATURE(DEG.FAHR)	195.00
STRAIN A, (MEAS)	530.00
STRAIN B, (MEAS)	540.00
STRAIN C, (MEAS)	975.00
STRAIN A, (MECH)	182.19
STRAIN B, (MECH)	692.19
STRAIN C, (MECH)	337.19
STRAIN X, (MECH)	-157.81
STRAIN Y, (MECH)	692.19
GAMMA XY, (MECH)	-225.00
PRIN.STR.1, (P)	618.56
PRIN.STR.2, (P)	-169.37
PHI X (DEGREES)	81.70
SIGMA XX (KSI)	21.39
SIGMA YY (KSI)	26.78
TAU XY (KSI)	-3.07
YIELD STRESS (KSI)	39.91
I (KSI)	0.2445E 02
I/YIELD STRESS	0.6234E 00

56.00

TEMPERATURE(DEG.FAHR)	212.00
STRAIN A, (MEAS)	-175.00
STRAIN B, (MEAS)	660.00
STRAIN C, (MEAS)	965.00
STRAIN A, (MECH)	-51.49
STRAIN B, (MECH)	713.51

STRAIN C. (MECH)			-22.02
STRAIN X. (MECH)			-913.02
STRAIN Y. (MECH)			811.98
GAMMA XY. (MECH)			645.00
PRIN.STR.1. (")			907.47
PRIN.STR.2. (")			-398.91
PHI X (DEGREES)			77.09
SIGMA XX (KSI)			-0.22
SIGMA YY (KSI)			8.17
TAU XY (KSI)			2.42
YIELD STRESS (KSI)			19.99
T (KSI)			0.87475 01
T/YIELD STRESS			0.21995 00

50.00			
TEMPERATURE(DEG.FAHR)	261.00	151.00	30.00
STRAIN A. (MEAS)	-595.01	-217.00	735.00
STRAIN B. (MEAS)	405.00	153.00	840.00
STRAIN C. (MEAS)	-570.00	40.00	-225.00
STRAIN A. (MECH)	-513.06	-170.61	737.09
STRAIN B. (MECH)	566.06	189.39	843.09
STRAIN C. (MECH)	-604.06	79.39	-222.91
STRAIN X. (MECH)	-1579.06	-293.61	-377.91
STRAIN Y. (MECH)	566.06	189.39	843.09
GAMMA XY. (MECH)	-15.00	-250.00	560.00
PRIN.STR.1. (")	566.99	229.56	1013.91
PRIN.STR.2. (")	-1579.06	-311.79	-459.63
PHI X (DEGREES)	89.80	76.00	70.30
SIGMA XX (KSI)	20.02	11.79	-0.15
SIGMA YY (KSI)	35.00	15.16	3.65
TAU XY (KSI)	-7.05	-0.00	3.61
YIELD STRESS (KSI)	37.29	19.38	10.99
T (KSI)	0.30435 02	0.13665 02	0.83245 01
T/YIELD STRESS	0.81750 00	0.70595 00	0.75335 00

51.00			
TEMPERATURE(DEG.FAHR)			91.00
STRAIN A. (MEAS)			1005.00
STRAIN B. (MEAS)			840.00
STRAIN C. (MEAS)			-480.00
STRAIN A. (MECH)			1037.22
STRAIN B. (MECH)			842.22
STRAIN C. (MECH)			-477.78
STRAIN X. (MECH)			-312.78
STRAIN Y. (MECH)			842.22
GAMMA XY. (MECH)			1485.00
PRIN.STR.1. (")			1205.37
PRIN.STR.2. (")			-675.92
PHI X (DEGREES)			63.94
SIGMA XX (KSI)			9.23
SIGMA YY (KSI)			3.91
TAU XY (KSI)			5.59

STRAIN C. (MECH)			419.51
STRAIN X. (MECH)			-356.49
STRAIN Y. (MECH)			713.51
GAMMA XY. (MECH)			-480.00
PRIN.STR.1. (")			766.97
PRIN.STR.2. (")			-437.96
PHI X (DEGREES)			77.97
SIGMA XX (KSI)			7.39
SIGMA YY (KSI)			13.07
TAU XY (KSI)			-1.79
YIELD STRESS (KSI)			19.99
T (KSI)			0.23995 02
T/YIELD STRESS			0.75195 00

37.00			
TEMPERATURE(DEG.FAHR)			230.00
STRAIN A. (MEAS)			270.00
STRAIN B. (MEAS)			630.00
STRAIN C. (MEAS)			195.00
STRAIN A. (MECH)			946.96
STRAIN B. (MECH)			696.96
STRAIN C. (MECH)			361.96
STRAIN X. (MECH)			-79.04
STRAIN Y. (MECH)			696.96
GAMMA XY. (MECH)			85.00
PRIN.STR.1. (")			699.29
PRIN.STR.2. (")			-81.41
PHI X (DEGREES)			96.83
SIGMA XX (KSI)			23.61
SIGMA YY (KSI)			14.07
TAU XY (KSI)			0.30
YIELD STRESS (KSI)			34.94
T (KSI)			0.19605 02
T/YIELD STRESS			0.89435 00

58.00			
TEMPERATURE(DEG.FAHR)			344.00
STRAIN A. (MEAS)			-195.00
STRAIN B. (MEAS)			-11[illegible]
STRAIN C. (MEAS)			-5[illegible]
STRAIN A. (MECH)			-79.47
STRAIN B. (MECH)			-11[illegible]
STRAIN C. (MECH)			71.53
STRAIN X. (MECH)			9[illegible]
STRAIN Y. (MECH)			-9[illegible]
GAMMA XY. (MECH)			-1[illegible]
PRIN.STR.1. (")			7[illegible]
PRIN.STR.2. (")			-9[illegible]
PHI X (DEGREES)			54.1[illegible]
SIGMA XX (KSI)			31.76
SIGMA YY (KSI)			31.91
TAU XY (KSI)			-7.51

YIELD STRESS (KSI)	39.97
I (KSI)	[illegible]
I/YIELD STRESS	[illegible]

52.00	
TEMPERATURE(DEG.FAHR)	86.00
STRAIN A, (MEAS)	1200.00
STRAIN B, (MEAS)	645.00
STRAIN C, (MEAS)	-750.00
STRAIN A, (MECH)	1193.14
STRAIN B, (MECH)	648.14
STRAIN C, (MECH)	-746.86
STRAIN X, (MECH)	-171.86
STRAIN Y, (MECH)	648.14
GAMMA XY, (MECH)	2040.00
PRIN.STR.1, (")	1359.99
PRIN.STR.2, (")	-913.68
PHI X (DEGREES)	55.09
SIGMA XX (KSI)	2.97
SIGMA YY (KSI)	8.46
TAU XY (KSI)	7.66
YIELD STRESS (KSI)	39.94
I (KSI)	[illegible]
I/YIELD STRESS	[illegible]

53.00	
TEMPERATURE(DEG.FAHR)	109.00
STRAIN A, (MEAS)	1210.00
STRAIN B, (MEAS)	465.00
STRAIN C, (MEAS)	-555.00
STRAIN A, (MECH)	1212.04
STRAIN B, (MECH)	477.04
STRAIN C, (MECH)	-562.96
STRAIN X, (MECH)	102.04
STRAIN Y, (MECH)	477.04
GAMMA XY, (MECH)	1755.00
PRIN.STR.1, (")	1223.54
PRIN.STR.2, (")	-556.46
PHI X (DEGREES)	49.61
SIGMA XX (KSI)	0.02
SIGMA YY (KSI)	12.05
TAU XY (KSI)	6.54
YIELD STRESS (KSI)	39.77
I (KSI)	[illegible]
I/YIELD STRESS	[illegible]

54.00	
TEMPERATURE(DEG.FAHR)	156.00
STRAIN A, (MEAS)	855.00
STRAIN B, (MEAS)	[illegible]

YIELD STRESS (KSI)	37.75
I (KSI)	[illegible]
I/YIELD STRESS	[illegible]

59.00	
TEMPERATURE(DEG.FAHR)	253.00
STRAIN A, (MEAS)	-365.00
STRAIN B, (MEAS)	-110.00
STRAIN C, (MEAS)	-135.00
STRAIN A, (MECH)	-290.31
STRAIN B, (MECH)	-35.31
STRAIN C, (MECH)	-60.31
STRAIN X, (MECH)	-315.31
STRAIN Y, (MECH)	-35.31
GAMMA XY, (MECH)	-330.00
PRIN.STR.1, (")	5.97
PRIN.STR.2, (")	-356.49
PHI X (DEGREES)	79.30
SIGMA XX (KSI)	29.75
SIGMA YY (KSI)	31.71
TAU XY (KSI)	-0.91
YIELD STRESS (KSI)	37.51
I (KSI)	[illegible]
I/YIELD STRESS	[illegible]

60.00			
TEMPERATURE(DEG.FAHR)	237.00	236.00	240.00
STRAIN A, (MEAS)	-290.00	-310.00	-365.00
STRAIN B, (MEAS)	175.00	-275.00	-140.00
STRAIN C, (MEAS)	-415.00	-365.00	-170.00
STRAIN A, (MECH)	-122.91	-232.95	-291.64
STRAIN B, (MECH)	257.09	-197.09	-67.64
STRAIN C, (MECH)	-337.91	-287.99	-97.64
STRAIN X, (MECH)	-717.91	-322.89	-327.64
STRAIN Y, (MECH)	252.09	-197.89	-67.64
GAMMA XY, (MECH)	215.00	55.00	-195.00
PRIN.STR.1, (")	263.93	-192.10	-91.63
PRIN.STR.2, (")	-724.76	-328.67	-355.65
PHI X (DEGREES)	99.77	78.13	71.30
SIGMA XX (KSI)	23.59	25.60	30.83
SIGMA YY (KSI)	33.45	24.49	33.63
TAU XY (KSI)	0.76	0.20	-0.69
YIELD STRESS (KSI)	37.02	37.99	37.32
I (KSI)	[illegible]	[illegible]	[illegible]
I/YIELD STRESS	[illegible]	[illegible]	[illegible]

65.00			
TEMPERATURE(DEG.FAHR)	229.00	224.00	229.00
STRAIN A, (MEAS)	-255.00	-300.00	-470.00
STRAIN B, (MEAS)	75.00	-320.00	-290.00

STRAIN C, (MEAS)	-390.00	-365.00	-135.00
STRAIN A, (MECH)	-178.23	-229.74	-493.56
STRAIN B, (MECH)	151.77	-243.74	-153.56
STRAIN C, (MECH)	-397.23	-368.74	-65.56
STRAIN X, (MECH)	-633.23	-248.74	-318.56
STRAIN Y, (MECH)	151.77	-743.76	-153.56
GAMMA XY, (MECH)	175.00	65.00	-335.03
PRIN.STR.1, (P)	156.71	-223.69	-40.36
PRIN.STR.2, (P)	-639.18	-268.88	-477.37
PHI X (DEGREES)	85.48	48.17	58.11
SIGMA XX (KSI)	22.43	24.36	33.76
SIGMA YY (KSI)	28.31	24.60	33.90
TAU XY (KSI)	7.45	0.16	-1.17
YIELD STRESS (KSI)	38.13	38.21	34.65
I (KSI)	0.25605 03	0.24390E 03	0.33205 03
I/YIELD STRESS	0.67135 01	0.63825 01	0.80055 01

70.00

TEMPERATURE(DEG.FAHR)	219.01	215.39	213.00
STRAIN A, (MEAS)	-245.01	-241.99	-535.00
STRAIN B, (MEAS)	-10.01	-340.99	-145.01
STRAIN C, (MEAS)	-295.01	-335.99	-35.01
STRAIN A, (MECH)	-165.67	-145.64	-493.91
STRAIN B, (MECH)	65.33	-245.64	-33.89
STRAIN C, (MECH)	-215.67	-243.64	76.11
STRAIN X, (MECH)	-454.67	-160.64	-313.89
STRAIN Y, (MECH)	65.33	-745.64	-33.89
GAMMA XY, (MECH)	50.00	65.00	-535.00
PRIN.STR.1, (P)	66.53	-142.74	53.63
PRIN.STR.2, (P)	-455.87	-243.04	-401.27
PHI X (DEGREES)	87.25	71.17	57.87
SIGMA XX (KSI)	22.33	23.55	31.17
SIGMA YY (KSI)	27.05	22.70	32.95
TAU XY (KSI)	5.13	0.14	-1.75
YIELD STRESS (KSI)	35.33	38.40	33.33
I (KSI)	0.24615 03	0.23235 03	0.31065 03
I/YIELD STRESS	0.69635 01	0.60435 01	0.85965 01

100.00

TEMPERATURE(DEG.FAHR)	186.01	181.99	179.00
STRAIN A, (MEAS)	-235.01	-231.99	-525.00
STRAIN B, (MEAS)	-245.01	-330.99	-135.01
STRAIN C, (MEAS)	-295.01	-335.99	-35.01
STRAIN A, (MECH)	-217.67	-140.64	-483.91
STRAIN B, (MECH)	-277.67	-339.64	-323.89
STRAIN C, (MECH)	-165.67	-145.64	76.11
STRAIN X, (MECH)	-157.67	-154.64	-243.89
STRAIN Y, (MECH)	-337.67	-330.64	-330.89
GAMMA XY, (MECH)	-75.00	50.00	-425.00
PRIN.STR.1, (P)	-136.43	-13.27	17.17
PRIN.STR.2, (P)	-226.11	-321.17	-401.16
PHI X (DEGREES)	75.63	5.11	1.06

SIGMA XX (KSI)	-17.73	-19.73	33.59
SIGMA YY (KSI)	-13.73	-15.73	39.99
TAU XY (KSI)	0.00	0.00	-0.21
YIELD STRESS (KSI)	40.50	40.50	37.97
I (KSI)	0.1379E 02	0.1373E 02	0.7693E 02
I/YIELD STRESS	0.3390E 00	0.3350E 00	0.9535E 00

SIGMA XX (KSI)	19.92	18.49	71.16
SIGMA YY (KSI)	17.99	16.27	71.49
TAU XY (KSI)	-0.27	0.29	-1.75
YIELD STRESS (KSI)	39.01	39.99	38.57
I (KSI)	0.1916E 02	0.1750E 02	0.2117E 03
I/YIELD STRESS	0.4661E 00	0.4490E 00	0.5489E 03

57.00	
TEMPERATURE(DEG.FAHR)	254.33
STRAIN A. (MEAS)	30.00
STRAIN B. (MEAS)	545.00
STRAIN C. (MEAS)	745.00
STRAIN A. (MECH)	139.41
STRAIN B. (MECH)	1019.41
STRAIN C. (MECH)	419.41
STRAIN X. (MECH)	-465.59
STRAIN Y. (MECH)	1019.41
GAMMA XY. (MECH)	-315.00
PRIN.STR.1. (*)	1035.61
PRIN.STR.2. (*)	-511.79
PHI X (DEGREES)	34.13
SIGMA XX (KSI)	31.74
SIGMA YY (KSI)	42.42
TAU XY (KSI)	-1.11
YIELD STRESS (KSI)	37.69
I (KSI)	0.1917E 02
I/YIELD STRESS	0.5101E 01

200.00			
TEMPERATURE(DEG.FAHR)	139.00	137.00	139.00
STRAIN A. (MEAS)	-120.00	-95.00	-685.00
STRAIN B. (MEAS)	-285.00	-410.00	-965.00
STRAIN C. (MEAS)	-45.00	-155.00	-130.00
STRAIN A. (MECH)	-69.75	-55.45	-454.06
STRAIN B. (MECH)	-254.75	-380.45	-934.06
STRAIN C. (MECH)	-14.75	-125.45	-99.06
STRAIN X. (MECH)	150.25	139.55	-219.06
STRAIN Y. (MECH)	-254.75	-380.45	-934.06
GAMMA XY. (MECH)	-75.00	70.00	-355.00
PRIN.STR.1. (*)	153.69	291.66	-99.08
PRIN.STR.2. (*)	-258.20	-388.66	-453.34
PHI X (DEGREES)	5.25	3.44	16.01
SIGMA XX (KSI)	12.33	12.21	9.13
SIGMA YY (KSI)	7.33	7.02	7.28
TAU XY (KSI)	-0.23	0.26	-1.31
YIELD STRESS (KSI)	38.51	38.53	38.56
I (KSI)	0.1109E 02	0.1077E 02	0.7695E 01
I/YIELD STRESS	0.2808E 00	0.2734E 00	0.1954E 00

58.00	
TEMPERATURE(DEG.FAHR)	270.00
STRAIN A. (MEAS)	-120.00
STRAIN B. (MEAS)	885.00
STRAIN C. (MEAS)	960.00
STRAIN A. (MECH)	-53.40
STRAIN B. (MECH)	959.60
STRAIN C. (MECH)	427.60
STRAIN X. (MECH)	-577.40
STRAIN Y. (MECH)	559.60
GAMMA XY. (MECH)	-690.00
PRIN.STR.1. (*)	999.36
PRIN.STR.2. (*)	-414.16
PHI X (DEGREES)	31.39
SIGMA XX (KSI)	33.59
SIGMA YY (KSI)	44.23
TAU XY (KSI)	-1.69
YIELD STRESS (KSI)	37.69
I (KSI)	0.1956E 02
I/YIELD STRESS	0.1079E 01

400.00			
TEMPERATURE(DEG.FAHR)	120.00	121.00	114.33
STRAIN A. (MEAS)	-90.00	-50.33	-476.33
STRAIN B. (MEAS)	-275.00	-430.00	-393.33
STRAIN C. (MEAS)	-10.00	-140.00	-173.33
STRAIN A. (MECH)	-61.66	-21.04	-466.33
STRAIN B. (MECH)	-256.66	-401.04	-333.33
STRAIN C. (MECH)	8.34	-121.04	-153.33
STRAIN X. (MECH)	233.34	268.96	-233.33
STRAIN Y. (MECH)	-256.66	-401.04	-333.33
GAMMA XY. (MECH)	-75.00	93.00	-333.33
PRIN.STR.1. (*)	305.00	262.36	-133.33
PRIN.STR.2. (*)	-253.31	-404.14	-471.66
PHI X (DEGREES)	4.33	3.04	31.04
SIGMA XX (KSI)	9.66	9.69	6.33
SIGMA YY (KSI)	6.00	6.77	7.33
TAU XY (KSI)	-0.24	0.33	-1.33
YIELD STRESS (KSI)	38.67	38.67	38.67
I (KSI)	0.9229E 01	0.8977E 01	0.2693E 01
I/YIELD STRESS	0.2074E 00	0.2112E 00	0.7529E-01

59.00

600.00

TEMPERATURE(DEG.FAHR)	200.00
STRAIN A. (MEAS)	-260.00
STRAIN B. (MEAS)	960.00
STRAIN C. (MEAS)	375.00
STRAIN A. (MECH)	-178.99
STRAIN B. (MECH)	591.10
STRAIN C. (MECH)	436.10
STRAIN X. (MECH)	-641.99
STRAIN Y. (MECH)	971.10
GAMMA XY. (MECH)	-615.00
PRIN.STR.1. (P)	547.05
PRIN.STR.2. (P)	-717.05
PHI X (DEGREES)	20.15
SIGMA XX (KSI)	34.45
SIGMA YY (KSI)	45.15
TAU XY (KSI)	-2.14
YIELD STRESS (KSI)	34.71
I (KSI)	1.69815 02
I/YIELD STRESS	9.1812F 01

60.00

TEMPERATURE(DEG.FAHR)	260.00	160.30	230.00
STRAIN A. (MEAS)	-650.00	-220.00	-330.00
STRAIN B. (MEAS)	360.00	180.00	810.00
STRAIN C. (MEAS)	-555.00	40.00	435.00
STRAIN A. (MECH)	-373.06	-172.05	-276.29
STRAIN B. (MECH)	434.94	227.05	863.71
STRAIN C. (MECH)	-475.06	87.05	489.71
STRAIN X. (MECH)	-1291.06	-312.05	-651.29
STRAIN Y. (MECH)	436.94	227.05	863.71
GAMMA XY. (MECH)	105.00	-265.00	-765.00
PRIN.STR.1. (P)	439.56	256.77	554.91
PRIN.STR.2. (P)	-1290.65	-347.41	-742.33
PHI X (DEGREES)	88.24	77.14	76.60
SIGMA XX (KSI)	18.69	13.60	35.94
SIGMA YY (KSI)	30.93	17.56	46.37
TAU XY (KSI)	0.37	-0.05	-2.65
YIELD STRESS (KSI)	37.85	30.75	54.40
I (KSI)	2.27005 02	1.15965 02	2.41575 01
I/YIELD STRESS	6.71335 00	3.40415 00	3.11555 01

65.00

TEMPERATURE(DEG.FAHR)	295.00
STRAIN A. (MEAS)	-650.00
STRAIN B. (MEAS)	770.00
STRAIN C. (MEAS)	510.00
STRAIN A. (MECH)	-497.35
STRAIN B. (MECH)	744.95
STRAIN C. (MECH)	554.95
STRAIN X. (MECH)	-613.05
STRAIN Y. (MECH)	744.95
GAMMA XY. (MECH)	-540.00

TEMPERATURE(DEG.FAHR)	90.00	90.00	90.00
STRAIN A. (MEAS)	-50.00	-35.00	-470.00
STRAIN B. (MEAS)	-255.00	-435.00	-410.00
STRAIN C. (MEAS)	5.00	-135.00	-215.00
STRAIN A. (MECH)	-42.66	-27.66	-469.66
STRAIN B. (MECH)	-247.66	-427.66	-402.66
STRAIN C. (MECH)	12.34	-127.66	-237.66
STRAIN X. (MECH)	227.34	272.34	-267.66
STRAIN Y. (MECH)	-247.66	-427.66	-402.66
GAMMA XY. (MECH)	-55.00	130.00	-255.00
PRIN.STR.1. (P)	228.83	275.80	-190.80
PRIN.STR.2. (P)	-259.33	-441.33	-479.63
PHI X (DEGREES)	3.24	4.07	31.05
SIGMA XX (KSI)	5.65	5.52	-0.44
SIGMA YY (KSI)	2.32	0.20	-1.45
TAU XY (KSI)	-0.21	0.37	-0.05
YIELD STRESS (KSI)	39.85	39.85	39.85
I (KSI)	0.49986F 01	0.54687F 01	3.10956F 01
I/YIELD STRESS	0.12545 00	0.1372F 00	0.7768F-01

500.00

TEMPERATURE(DEG.FAHR)	90.00	90.00	90.00
STRAIN A. (MEAS)	-40.00	-25.00	-475.00
STRAIN B. (MEAS)	-260.00	-435.00	-415.00
STRAIN C. (MEAS)	10.00	-125.00	-205.00
STRAIN A. (MECH)	-35.33	-20.33	-470.84
STRAIN B. (MECH)	-255.33	-430.33	-410.84
STRAIN C. (MECH)	14.77	-120.33	-220.84
STRAIN X. (MECH)	234.77	280.77	-270.84
STRAIN Y. (MECH)	-255.33	-430.33	-410.84
GAMMA XY. (MECH)	-50.00	100.00	-250.00
PRIN.STR.1. (P)	234.04	278.72	-206.95
PRIN.STR.2. (P)	-254.60	-433.60	-436.72
PHI X (DEGREES)	3.91	3.05	31.26
SIGMA XX (KSI)	4.30	4.35	-2.37
SIGMA YY (KSI)	0.77	-1.06	-3.35
TAU XY (KSI)	-0.17	0.37	-0.04
YIELD STRESS (KSI)	39.90	39.90	39.91
I (KSI)	0.49195 01	0.50795 01	0.24675 01
I/YIELD STRESS	0.12056 00	0.1273F 00	0.6185F-01

1200.00

TEMPERATURE(DEG.FAHR)	90.00	90.00	90.00
STRAIN A. (MEAS)	-40.00	-50.00	-480.00
STRAIN B. (MEAS)	-245.00	-425.00	-400.00
STRAIN C. (MEAS)	5.00	-130.00	-240.00
STRAIN A. (MECH)	-38.39	-78.38	-476.67
STRAIN B. (MECH)	-261.33	-421.38	-416.63
STRAIN C. (MECH)	9.62	-124.38	-234.63
STRAIN X. (MECH)	233.62	213.62	-296.63
STRAIN Y. (MECH)	-261.33	-421.38	-416.63
GAMMA XY. (MECH)	-45.00	50.00	-240.00

PRIN.STR.1. (*)			517.63
PRIN.STR.2. (*)			-744.50
PHI X (DEGREES)			72.59
SIG X XX (KSI)			37.13
SIGMA YY (KSI)			44.64
TAU XY (KSI)			-3.31
YIELD STRESS (KSI)			38.15
I (KSI)			0.63575 02
I/YIELD STRESS			0.11795 01

45.00

TEMPERATURE(DEG.FAHR)			206.00
STRAIN A. (MEAS)			-595.00
STRAIN B. (MEAS)			630.00
STRAIN C. (MEAS)			615.00
STRAIN A. (MECH)			-538.05
STRAIN B. (MECH)			675.95
STRAIN C. (MECH)			661.95
STRAIN X. (MECH)			-559.05
STRAIN Y. (MECH)			674.95
GAMMA XY. (MECH)			-1230.00
PRIN.STR.1. (*)			521.15
PRIN.STR.2. (*)			-797.25
PHI X (DEGREES)			67.85
SIGMA XX (KSI)			37.44
SIGMA YY (KSI)			45.61
TAU XY (KSI)			-4.13
YIELD STRESS (KSI)			38.15
I (KSI)			0.42175 02
I/YIELD STRESS			0.11075 01

70.00

TEMPERATURE(DEG.FAHR)	221.00	144.00	295.00
STRAIN A. (MEAS)	-360.00	-220.00	-751.00
STRAIN B. (MEAS)	300.00	200.00	495.00
STRAIN C. (MEAS)	-377.00	-60.00	675.00
STRAIN A. (MECH)	-286.24	-177.24	-692.82
STRAIN B. (MECH)	375.76	269.76	552.18
STRAIN C. (MECH)	-316.24	-19.24	732.18
STRAIN X. (MECH)	-974.24	-611.24	-812.82
STRAIN Y. (MECH)	375.76	269.76	52.18
GAMMA XY. (MECH)	30.00	-180.00	00
PRIN.STR.1. (*)	335.01	250.05	19
PRIN.STR.2. (*)	-976.42	-639.59	.82
PHI X (DEGREES)	90.36	93.39	61.79
SIGMA XX (KSI)	18.23	13.14	35.49
SIGMA YY (KSI)	27.99	18.16	49.87
TAU XY (KSI)	3.11	-0.59	-4.04
YIELD STRESS (KSI)	38.29	38.19	38.54
I (KSI)	0.24564 02	0.16185 02	0.39515 02
I/YIELD STRESS	0.64115 00	0.41785 00	0.10415 01

PRIN.STR.1. (*)	236.66	219.59	-222.47
PRIN.STR.2. (*)	-267.40	-422.36	-490.79
PHI X (DEGREES)	2.69	2.23	31.72
SIGMA XX (KSI)	3.58	2.89	-3.16
SIGMA YY (KSI)	-0.13	-1.99	-4.06
TAU XY (KSI)	-0.17	0.19	-0.90
YIELD STRESS (KSI)	38.03	38.03	38.03
I (KSI)	0.39935 01	0.47665 01	0.33055 01
I/YIELD STRESS	0.89675-01	0.12535 00	0.87775-01

100.00			
TEMPERATURE(DEG.FAHR)	187.00	162.00	215.00
STRAIN A. (MEAS)	-60.00	-160.00	-1070.00
STRAIN B. (MEAS)	180.00	280.00	30.00
STRAIN C. (MEAS)	-255.00	-70.00	645.00
STRAIN A. (MECH)	2.69	-112.95	-945.44
STRAIN B. (MECH)	242.69	327.05	104.36
STRAIN C. (MECH)	-192.31	-22.95	719.36
STRAIN X. (MECH)	-432.31	-467.95	-390.64
STRAIN Y. (MECH)	242.69	327.05	104.36
GAMMA XY. (MECH)	195.00	-90.00	-1665.00
PRIN.STR.1. (")	256.49	299.61	767.31
PRIN.STR.2. (")	-446.12	-465.50	-973.58
PHI X (DEGREES)	91.04	86.75	52.32
SIGMA XX (KSI).	17.14	12.32	23.04
SIGMA YY (KSI)	22.04	18.11	26.14
TAU XY (KSI)	3.71	-0.33	-5.97
YIELD STRESS (KSI)	39.90	39.75	38.40
T (KSI)	0.2010E 02	0.1599E 02	0.2439E 02
T/YIELD STRESS	0.5167E 00	0.4073E 00	0.6351E 00

200.00			
TEMPERATURE(DEG.FAHR)	140.00	136.00	148.00
STRAIN A. (MEAS)	-210.00	-40.00	-1110.00
STRAIN B. (MEAS)	30.00	170.00	-405.00
STRAIN C. (MEAS)	-105.00	-20.00	480.00
STRAIN A. (MECH)	-179.34	-11.14	-1072.73
STRAIN B. (MECH)	61.66	198.86	-367.73
STRAIN C. (MECH)	-73.36	8.86	517.27
STRAIN X. (MECH)	-319.36	-201.14	-187.73
STRAIN Y. (MECH)	61.66	198.86	-367.73
GAMMA XY. (MECH)	-105.00	-20.00	-1590.00
PRIN.STR.1. (")	68.85	199.11	522.35
PRIN.STR.2. (")	-370.57	-201.39	-1077.81
PHI X (DEGREES)	92.18	88.57	41.77
SIGMA XX (KSI)	8.74	9.72	10.10
SIGMA YY (KSI)	11.51	12.67	8.77
TAU XY (KSI)	-0.39	-1.07	-5.86
YIELD STRESS (KSI)	39.49	39.53	39.41
T (KSI)	0.1035E 02	0.1148E 02	0.8529E 01
T/YIELD STRESS	0.2620E 00	0.2903E 00	0.2164E 00

300.00			
TEMPERATURE(DEG.FAHR)	127.00	120.00	135.00
STRAIN A. (MEAS)	15.00	0.00	-1119.00
STRAIN B. (MEAS)	75.00	170.00	-435.00
STRAIN C. (MEAS)	-60.00	10.00	420.00
STRAIN A. (MECH)	34.58	18.34	-1088.51
STRAIN B. (MECH)	94.58	189.34	-459.51
STRAIN C. (MECH)	-40.42	28.34	441.49

STRAIN X. (MECH)	-100.42	-141.66	-188.51
STRAIN Y. (MECH)	94.59	188.34	-459.51
GAMMA XY. (MECH)	75.00	-10.00	-1530.00
PRIN.STR.1. (")	101.54	188.41	453.31
PRIN.STR.2. (")	-107.39	-141.74	-1100.33
PHI X (DEGREES)	79.49	89.13	40.00
SIGMA XX (KSI)	7.74	7.24	5.29
SIGMA YY (KSI)	9.19	9.79	3.29
TAU XY (KSI)	0.29	-0.04	-5.69
YIELD STRESS (KSI)	39.64	39.69	39.84
I (KSI)	0.86095 01	0.87275 01	0.30975 01
I/YIELD STRESS	0.21705 00	0.21995 00	0.77815-01

600.00

TEMPERATURE(DEG.FAHR)	99.00	99.00	99.00
STRAIN A. (MEAS)	60.00	10.00	-1095.00
STRAIN B. (MEAS)	90.00	190.00	-510.00
STRAIN C. (MEAS)	-30.00	30.00	405.00
STRAIN A. (MECH)	67.34	17.34	-1087.66
STRAIN B. (MECH)	97.34	187.34	-502.66
STRAIN C. (MECH)	-22.66	37.34	417.34
STRAIN X. (MECH)	-52.66	-132.66	-172.66
STRAIN Y. (MECH)	97.34	187.34	-502.66
GAMMA XY. (MECH)	90.00	-20.00	-1530.00
PRIN.STR.1. (")	109.80	187.65	430.27
PRIN.STR.2. (")	-65.13	-132.98	-1105.60
PHI X (DEGREES)	74.52	89.21	39.80
SIGMA XX (KSI)	3.84	3.27	0.25
SIGMA YY (KSI)	4.96	5.67	-2.22
TAU XY (KSI)	0.34	-0.07	-5.61
YIELD STRESS (KSI)	39.85	39.85	39.85
I (KSI)	0.46145 01	0.49045 01	0.33635 01
I/YIELD STRESS	0.11585 00	0.12315 00	0.84425-01

900.00

TEMPERATURE(DEG.FAHR)	91.00	92.00	91.00
STRAIN A. (MEAS)	60.00	10.00	-1095.00
STRAIN B. (MEAS)	90.00	190.00	-535.00
STRAIN C. (MEAS)	-30.00	30.00	405.00
STRAIN A. (MECH)	64.46	14.77	-1090.54
STRAIN B. (MECH)	94.46	184.77	-520.54
STRAIN C. (MECH)	-25.54	34.77	409.46
STRAIN X. (MECH)	-55.54	-135.23	-160.54
STRAIN Y. (MECH)	94.46	184.77	-520.54
GAMMA XY. (MECH)	90.00	-20.00	-1530.00
PRIN.STR.1. (")	106.92	185.08	420.76
PRIN.STR.2. (")	-68.01	-135.54	-1111.84
PHI X (DEGREES)	74.52	89.21	39.25
SIGMA XX (KSI)	3.24	1.88	-1.74
SIGMA YY (KSI)	3.37	4.29	-3.94
TAU XY (KSI)	0.34	-0.07	-5.62
YIELD STRESS (KSI)	39.91	39.91	39.91

E (KSI)	0.3136E 01	0.3684E 01	0.2171E 01
E/YIELD STRESS	0.7860E-01	0.9234E-01	0.5439E-01

1200.00

TEMPERATURE(DEG.FAHR)	97.00	86.00	97.00
STRAIN X, (MICS)	65.00	10.00	-1110.00
STRAIN Y, (MICS)	75.00	173.00	-540.00
STRAIN Z, (MICS)	-65.00	30.00	390.00
STRAIN X, (MICH)	69.37	13.69	-1106.63
STRAIN Y, (MICH)	79.37	173.69	4536.63
STRAIN Z, (MICH)	-61.63	33.69	393.37
STRAIN XY, (MICH)	-71.63	-126.38	-174.63
STRAIN YZ, (MICH)	79.37	173.62	-536.63
GAMMA XY, (MICH)	30.00	-20.00	-1500.00
PRIN.STR.1, (")	90.83	173.95	414.67
PRIN.STR.2, (")	-94.17	-126.71	-1127.93
OCT X (DEGREES)	74.67	89.07	38.25
SIGMA XX (KSI)	1.23	1.16	-2.24
SIGMA YY (KSI)	2.35	3.41	-4.96
TAU XY (KSI)	0.36	-0.11	-5.43
YIELD STRESS (KSI)	39.93	39.93	39.93
E (KSI)	0.3376E 01	0.3986E 01	0.1267E 01
E/YIELD STRESS	0.5690E-01	0.7435E-01	0.3176E-01

CORE USAGE OBJECT CODE= 9480 BYTES, ARRAY AREA= 6480 BYTES, TOTAL AREA AVAILABLE= 26720 BYTES

COMPILE TIME= 0.37 SEC, EXECUTION TIME= 0.97 SEC. WATFIV - VERSION 1 LEVEL 2 AUGUST 1970 DATE= 73/121

ORIGINAL PAGE IS
OF POOR QUALITY

WELDING STRAIN ROSETTE DATA: EXPERIMENTAL RESULTS

****

TEST NUMBER 5: BUTT WELD

ALUMINUM ALLOY 6061 IN T651 CONDITION
THICKNESS = 0.250 INCHES
GMA WELD PROCESS
ARC VOLTAGE = 19.
AMPERES = 250.
SPEED OF TRAVEL = 32.16 INCHES/MINUTE
4043 FILLER METAL: 0.0625 INCH DIAMETER
UNITS OF STRAIN = MICROSTRAIN

CAUTION

TEMP = 0.00 COMPUTATIONS REPRESENT
BLANK SPACES ON INPUT CARDS AND ARE
MEANINGLESS. IGNORE ALL SUCH COMPUTATIONS.

TRANSVERSE DISTANCE FROM WELD IN INCHES

TIME (SECONDS)	1.00 (CENTERLINE)	1.00 (EDGE)	BLANK (BLANK)
0.00			
TEMPERATURE(DEG.FAHR)	78.00	78.00	
STRAIN A. (MEAS)	-10.00	-72.00	
STRAIN B. (MEAS)	-4.00	-111.00	
STRAIN C. (MEAS)	36.00	11.00	
STRAIN A. (MECH)	-8.11	-70.11	
STRAIN B. (MECH)	-2.11	-109.11	
STRAIN C. (MECH)	37.89	12.89	
STRAIN X. (MECH)	31.89	51.89	
STRAIN Y. (MECH)	-2.11	-109.11	
GAMMA XY. (MECH)	-46.00	-83.00	
PRIN.STR.1. (")	43.49	61.96	
PRIN.STR.2. (")	-13.71	-119.18	
PHI X (DEGREES)	26.77	13.64	
SIGMA XX (KSI)	0.35	0.18	
SIGMA YY (KSI)	0.10	-1.04	
TAU XY (KSI)	-0.17	-0.31	
YIELD STRESS (KSI)	39.99	39.99	
I (KSI)	0.6480E 00	0.5905E 00	
I/YIELD STRESS	0.1620E-01	0.1476E-01	

WELDING STRAIN ROSETTE DATA: EXPERIMENTAL RESULTS

****

TEST NUMBER 6: BUTT WELD

ALUMINUM ALLOY 6061 IN T651 CONDITION
THICKNESS = 0.250 INCHES
GMA WELD PROCESS
ARC VOLTAGE = 19.
AMPERES = 250.
SPEED OF TRAVEL = 32.16 INCHES/MINUTE
4043 FILLER METAL: 0.0625 INCH DIAMETER
UNITS OF STRAIN = MICROSTRAIN

CAUTION

TEMP = 0.00 COMPUTATIONS REPRESENT
BLANK SPACES ON INPUT CARDS AND ARE
MEANINGLESS. IGNORE ALL SUCH COMPUTATIONS.

TRANSVERSE DISTANCE FROM WELD IN INCHES

TIME (SECONDS)	1.00 (CENTERLINE)	[illegible]	BLANK (BLANK)
0.00			
TEMPERATURE(DEG.FAHR)	78.00	78.00	
STRAIN A. (MEAS)	0.00	59.00	
STRAIN B. (MEAS)	0.00	19.00	
STRAIN C. (MEAS)	63.00	9.00	
STRAIN A. (MECH)	1.89	[illegible]	
STRAIN B. (MECH)	1.59	[illegible]	
STRAIN C. (MECH)	64.89	[illegible]	
STRAIN X. (MECH)	64.89	[illegible]	
STRAIN Y. (MECH)	1.89	[illegible]	
GAMMA XY. (MECH)	-63.00	[illegible]	
PRIN.STR.1. (")	77.44	[illegible]	
PRIN.STR.2. (")	-11.16	6.73	
PHI X (DEGREES)	22.50	29.52	
SIGMA XX (KSI)	0.74	0.65	
SIGMA YY (KSI)	0.27	0.43	
TAU XY (KSI)	-0.24	0.19	
YIELD STRESS (KSI)	39.99	39.99	
I (KSI)	0.5509E 00	0.9455E 00	
I/YIELD STRESS	0.1348E-01	0.2364E-01	

10.00		
TEMPERATURE(DEG.FAHR)	78.00	78.00
STRAIN A. (MEAS)	-10.00	-84.00
STRAIN B. (MEAS)	32.00	-39.00
STRAIN C. (MEAS)	54.00	-1.00
STRAIN A. (MECH)	1.89	-10.11
STRAIN B. (MECH)	37.89	73.89
STRAIN C. (MECH)	19.99	-10.11
STRAIN X. (MECH)	-16.11	-94.11
STRAIN Y. (MECH)	37.89	73.89
GAMMA XY. (MECH)	-18.00	0.00
PRIN.STR.1. (")	39.35	73.89
PRIN.STR.2. (")	-17.57	-94.11
PHI X (DEGREES)	80.78	90.00
SIGMA XX (KSI)	-0.04	-0.78
SIGMA YY (KSI)	0.37	0.48
TAU XY (KSI)	-0.07	0.00
YIELD STRESS (KSI)	39.99	39.99
I (KSI)	0.2292E 00	0.1105E 01
I/YIELD STRESS	0.5732E-02	0.2763E-01

15.00		
TEMPERATURE(DEG.FAHR)	78.00	
STRAIN A. (MEAS)	-10.00	
STRAIN B. (MEAS)	38.00	
STRAIN C. (MEAS)	-84.00	
STRAIN A. (MECH)	1.89	
STRAIN B. (MECH)	43.89	
STRAIN C. (MECH)	-118.11	
STRAIN X. (MECH)	-160.11	
STRAIN Y. (MECH)	43.89	
GAMMA XY. (MECH)	120.00	
PRIN.STR.1. (")	60.23	
PRIN.STR.2. (")	-176.45	
PHI X (DEGREES)	74.77	
SIGMA XX (KSI)	-1.64	
SIGMA YY (KSI)	-0.11	
TAU XY (KSI)	0.45	
YIELD STRESS (KSI)	39.99	
I (KSI)	0.1971E 01	
I/YIELD STRESS	0.4928E-01	

20.00		
TEMPERATURE(DEG.FAHR)	78.00	78.00
STRAIN A. (MEAS)	38.00	96.00
STRAIN B. (MEAS)	50.00	63.00
STRAIN C. (MEAS)	-204.00	-43.00
STRAIN A. (MECH)	49.89	169.89
STRAIN B. (MECH)	55.89	175.89
STRAIN C. (MECH)	-238.11	-52.11
STRAIN X. (MECH)	-244.11	-58.11

10.00		
TEMPERATURE(DEG.FAHR)	78.00	78.00
STRAIN A. (MEAS)	-18.00	11.00
STRAIN B. (MEAS)	30.00	19.00
STRAIN C. (MEAS)	-27.00	-15.00
STRAIN A. (MECH)	-10.11	-46.11
STRAIN B. (MECH)	31.89	1.89
STRAIN C. (MECH)	-30.11	-22.11
STRAIN X. (MECH)	-136.11	-70.11
STRAIN Y. (MECH)	31.89	1.89
GAMMA XY. (MECH)	72.00	-24.00
PRIN.STR.1. (")	39.28	3.84
PRIN.STR.2. (")	-143.50	-72.06
PHI X (DEGREES)	78.40	80.78
SIGMA XX (KSI)	-1.42	-0.78
SIGMA YY (KSI)	-0.15	-0.24
TAU XY (KSI)	0.27	-0.09
YIELD STRESS (KSI)	39.99	39.99
I (KSI)	0.1620E 01	0.4607E 00
I/YIELD STRESS	0.4051E-01	0.1152E-01

15.00		
TEMPERATURE(DEG.FAHR)	78.00	79.00
STRAIN A. (MEAS)	6.00	-7.00
STRAIN B. (MEAS)	54.00	37.00
STRAIN C. (MEAS)	-123.00	-15.00
STRAIN A. (MECH)	7.89	-64.02
STRAIN B. (MECH)	55.89	19.98
STRAIN C. (MECH)	-184.11	-22.02
STRAIN X. (MECH)	-232.11	-130.02
STRAIN Y. (MECH)	55.89	19.98
GAMMA XY. (MECH)	192.00	-42.00
PRIN.STR.1. (")	84.96	23.99
PRIN.STR.2. (")	-261.18	-109.43
PHI X (DEGREES)	73.15	80.78
SIGMA XX (KSI)	-2.41	-0.93
SIGMA YY (KSI)	-0.24	0.02
TAU XY (KSI)	0.72	-0.16
YIELD STRESS (KSI)	39.99	39.99
I (KSI)	0.2728E 01	0.6365E 00
I/YIELD STRESS	0.6821E-01	0.1592E-01

20.00		
TEMPERATURE(DEG.FAHR)	78.00	79.00
STRAIN A. (MEAS)	24.00	107.00
STRAIN B. (MEAS)	60.00	37.00
STRAIN C. (MEAS)	-312.00	-87.00
STRAIN A. (MECH)	25.89	49.98
STRAIN B. (MECH)	61.89	19.98
STRAIN C. (MECH)	-376.11	-94.02
STRAIN X. (MECH)	-412.11	-64.02

STRAIN Y. (MECH)	55.89	175.89
GAMMA XY. (MECH)	288.00	222.00
PRIN.STR.1. (")	113.82	220.17
PRIN.STR.2. (")	-302.04	-102.39
PHI X (DEGREES)	68.08	68.25
SIGMA XX (KSI)	-2.54	0.01
SIGMA YY (KSI)	-0.29	1.77
TAU XY (KSI)	1.08	0.84
YIELD STRESS (KSI)	39.99	39.99
I (KSI)	0.3012E 01	0.2369E 01
I/YIELD STRESS	0.7531E-01	0.5924E-01

24.00

TEMPERATURE(DEG.FAHR)	78.00
STRAIN A. (MEAS)	170.00
STRAIN B. (MEAS)	14.00
STRAIN C. (MEAS)	-456.00
STRAIN A. (MECH)	181.89
STRAIN B. (MECH)	19.89
STRAIN C. (MECH)	-490.11
STRAIN X. (MECH)	-328.11
STRAIN Y. (MECH)	19.89
GAMMA XY. (MECH)	672.00
PRIN.STR.1. (")	224.27
PRIN.STR.2. (")	-532.49
PHI X (DEGREES)	58.69
SIGMA XX (KSI)	-3.63
SIGMA YY (KSI)	-1.01
TAU XY (KSI)	2.53
YIELD STRESS (KSI)	39.99
I (KSI)	0.4253E 01
I/YIELD STRESS	0.1064E 00

25.00

TEMPERATURE(DEG.FAHR)	80.00
STRAIN A. (MEAS)	200.00
STRAIN B. (MEAS)	56.00
STRAIN C. (MEAS)	-408.00
STRAIN A. (MECH)	212.09
STRAIN B. (MECH)	62.09
STRAIN C. (MECH)	-441.91
STRAIN X. (MECH)	-291.91
STRAIN Y. (MECH)	62.09
GAMMA XY. (MECH)	654.00
PRIN.STR.1. (")	256.92
PRIN.STR.2. (")	-486.74
PHI X (DEGREES)	59.21
SIGMA XX (KSI)	-2.67
SIGMA YY (KSI)	-0.01
TAU XY (KSI)	2.46
YIELD STRESS (KSI)	39.98
I (KSI)	0.3806E 01

STRAIN Y. (MECH)	61.89	19.98
GAMMA XY. (MECH)	432.00	144.00
PRIN.STR.1. (")	132.05	61.34
PRIN.STR.2. (")	-405.37	-135.37
PHI X (DEGREES)	69.65	60.15
SIGMA XX (KSI)	-4.42	-0.45
SIGMA YY (KSI)	-0.55	0.18
TAU XY (KSI)	1.51	0.54
YIELD STRESS (KSI)	39.99	39.99
I (KSI)	0.4208E 01	0.1354E 01
I/YIELD STRESS	0.1052E 00	0.3386E-01

I/YIELD STRESS	0.9519E-01

26.00

TEMPERATURE(DEG.FAHR)	83.00
STRAIN A. (MEAS)	302.00
STRAIN B. (MEAS)	368.00
STRAIN C. (MEAS)	-246.00
STRAIN A. (MECH)	314.54
STRAIN B. (MECH)	374.54
STRAIN C. (MECH)	-279.46
STRAIN X. (MECH)	-339.46
STRAIN Y. (MECH)	374.54
GAMMA XY. (MECH)	594.00
PRIN.STR.1. (")	681.93
PRIN.STR.2. (")	-446.85
PHI X (DEGREES)	70.12
SIGMA XX (KSI)	-1.45
SIGMA YY (KSI)	3.91
TAU XY (KSI)	2.23
YIELD STRESS (KSI)	39.96
I (KSI)	0.5458E 01
I/YIELD STRESS	0.1366E 00

28.50

TEMPERATURE(DEG.FAHR)	98.00
STRAIN A. (MEAS)	488.00
STRAIN B. (MEAS)	584.00
STRAIN C. (MEAS)	-264.00
STRAIN A. (MECH)	534.93
STRAIN B. (MECH)	594.93
STRAIN C. (MECH)	-293.07
STRAIN X. (MECH)	-383.17
STRAIN Y. (MECH)	594.93
GAMMA XY. (MECH)	798.00
PRIN.STR.1. (")	737.06
PRIN.STR.2. (")	-525.20
PHI X (DEGREES)	70.39
SIGMA XX (KSI)	1.79
SIGMA YY (KSI)	9.11
TAU XY (KSI)	2.95
YIELD STRESS (KSI)	39.86
I (KSI)	0.8680E 01
I/YIELD STRESS	0.2229E 00

27.00

TEMPERATURE(DEG.FAHR)	103.00
STRAIN A. (MEAS)	650.00
STRAIN B. (MEAS)	638.00
STRAIN C. (MEAS)	-384.00
STRAIN A. (MECH)	669.08

I/YIELD STRESS	0.1152E 00	0.9607E-01

24.00

TEMPERATURE(DEG.FAHR)	79.00	79.00
STRAIN A. (MEAS)	215.00	215.00
STRAIN B. (MEAS)	60.00	37.00
STRAIN C. (MEAS)	-417.00	-405.00
STRAIN A. (MECH)	211.98	157.98
STRAIN B. (MECH)	61.98	19.98
STRAIN C. (MECH)	-478.02	-[illegible]
STRAIN X. (MECH)	-328.02	-274.02
STRAIN Y. (MECH)	61.98	19.98
GAMMA XY. (MECH)	690.00	570.00
PRIN.STR.1. (")	263.28	193.66
PRIN.STR.2. (")	-529.31	-447.69
PHI X (DEGREES)	59.74	56.04
SIGMA XX (KSI)	-3.27	-2.62
SIGMA YY (KSI)	-0.34	-0.61
TAU XY (KSI)	2.59	2.14
YIELD STRESS (KSI)	39.99	39.99
I (KSI)	0.4163E 01	0.3611E 01
I/YIELD STRESS	0.1040E 00	0.9031E-01

24.50

TEMPERATURE(DEG.FAHR)	79.00	83.00
STRAIN A. (MEAS)	268.00	245.00
STRAIN B. (MEAS)	144.00	145.00
STRAIN C. (MEAS)	-339.00	-405.00
STRAIN A. (MECH)	289.96	188.09
STRAIN B. (MECH)	145.98	126.09
STRAIN C. (MECH)	-403.02	-411.91
STRAIN X. (MECH)	-256.02	-351.91
STRAIN Y. (MECH)	145.98	126.09
GAMMA XY. (MECH)	690.00	600.00
PRIN.STR.1. (")	344.26	272.28
PRIN.STR.2. (")	-454.30	-496.09
PHI X (DEGREES)	60.11	64.53
SIGMA XX (KSI)	-2.15	-3.10
SIGMA YY (KSI)	0.88	0.51
TAU XY (KSI)	2.39	2.26
YIELD STRESS (KSI)	39.99	39.98
I (KSI)	0.3873E 01	0.4206E 01
I/YIELD STRESS	0.9689E-01	0.1052E 00

25.00

TEMPERATURE(DEG.FAHR)	83.00	83.00
STRAIN A. (MEAS)	298.00	329.00
STRAIN B. (MEAS)	318.00	343.00
STRAIN C. (MEAS)	-249.00	-249.00
STRAIN A. (MECH)	290.54	272.54

STRAIN B. (MECH)	651.08
STRAIN C. (MECH)	-410.91
STRAIN X. (MECH)	-392.91
STRAIN Y. (MECH)	651.08
GAMMA XY. (MECH)	1080.00
PRIN.STR.1. (M)	880.14
PRIN.STR.2. (M)	-621.97
PHI X (DEGREES)	67.01
SIGMA XX (KSI)	2.86
SIGMA YY (KSI)	10.66
TAU XY (KSI)	4.33
YIELD STRESS (KSI)	39.82
I (KSI)	0.1017E 02
I/YIELD STRESS	0.2555E 00

27.50	
TEMPERATURE(DEG.FAHR)	125.00
STRAIN A. (MEAS)	570.00
STRAIN B. (MEAS)	494.00
STRAIN C. (MEAS)	-402.00
STRAIN A. (MECH)	809.49
STRAIN B. (MECH)	519.49
STRAIN C. (MECH)	-416.51
STRAIN X. (MECH)	-326.51
STRAIN Y. (MECH)	519.49
GAMMA XY. (MECH)	1026.00
PRIN.STR.1. (M)	761.39
PRIN.STR.2. (M)	-568.41
PHI X (DEGREES)	64.75
SIGMA XX (KSI)	7.38
SIGMA YY (KSI)	13.66
TAU XY (KSI)	3.81
YIELD STRESS (KSI)	39.64
I (KSI)	0.1232E 02
I/YIELD STRESS	0.3107E 00

29.00	
TEMPERATURE(DEG.FAHR)	154.00
STRAIN A. (MEAS)	194.00
STRAIN B. (MEAS)	350.00
STRAIN C. (MEAS)	-284.00
STRAIN A. (MECH)	245.50
STRAIN B. (MECH)	395.50
STRAIN C. (MECH)	-258.50
STRAIN X. (MECH)	-408.53
STRAIN Y. (MECH)	395.50
GAMMA XY. (MECH)	504.00
PRIN.STR.1. (M)	467.45
PRIN.STR.2. (M)	-480.98
PHI X (DEGREES)	73.98
SIGMA XX (KSI)	11.62
SIGMA YY (KSI)	17.53

STRAIN B. (MECH)	323.54	326.54
STRAIN C. (MECH)	-339.46	-255.46
STRAIN X. (MECH)	-339.46	-339.46
STRAIN Y. (MECH)	320.54	326.54
GAMMA XY. (MECH)	600.00	528.00
PRIN.STR.1. (M)	436.52	421.54
PRIN.STR.2. (M)	-455.45	-404.77
PHI X (DEGREES)	88.86	77.15
SIGMA XX (KSI)	-1.65	-1.29
SIGMA YY (KSI)	3.30	3.48
TAU XY (KSI)	2.29	1.98
YIELD STRESS (KSI)	39.96	39.96
I (KSI)	0.5388E 01	0.4427E 01
I/YIELD STRESS	0.1273E 00	0.1233E 00

25.50		
TEMPERATURE(DEG.FAHR)	84.00	84.00
STRAIN A. (MEAS)	438.00	503.00
STRAIN B. (MEAS)	522.00	535.00
STRAIN C. (MEAS)	-243.00	-279.00
STRAIN A. (MECH)	441.88	447.88
STRAIN B. (MECH)	525.88	567.88
STRAIN C. (MECH)	-302.12	-234.12
STRAIN X. (MECH)	-388.12	-434.12
STRAIN Y. (MECH)	525.88	567.88
GAMMA XY. (MECH)	744.00	732.00
PRIN.STR.1. (M)	655.37	693.28
PRIN.STR.2. (M)	-516.61	-560.52
PHI X (DEGREES)	70.90	71.51
SIGMA XX (KSI)	-0.24	-0.29
SIGMA YY (KSI)	0.60	2.00
TAU XY (KSI)	2.79	2.75
YIELD STRESS (KSI)	39.92	39.92
I (KSI)	0.7316E 01	0.7705E 01
I/YIELD STRESS	0.1833E 00	0.1930E 00

26.00		
TEMPERATURE(DEG.FAHR)	103.00	104.00
STRAIN A. (MEAS)	630.00	707.00
STRAIN B. (MEAS)	606.00	649.00
STRAIN C. (MEAS)	-351.00	-417.00
STRAIN A. (MECH)	645.08	657.55
STRAIN B. (MECH)	619.08	634.55
STRAIN C. (MECH)	-404.91	-416.45
STRAIN X. (MECH)	-377.91	-396.45
STRAIN Y. (MECH)	619.08	634.55
GAMMA XY. (MECH)	1050.00	1074.00
PRIN.STR.1. (M)	841.65	867.16
PRIN.STR.2. (M)	-601.48	-626.26
PHI X (DEGREES)	66.66	67.01
SIGMA XX (KSI)	2.93	2.95
SIGMA YY (KSI)	10.53	10.71

TAU XY (KSI)	1.85	
YIELD STRESS (KSI)	39.34	
I (KSI)	0.1563E 02	
I/YIELD STRESS	0.3973E 00	

29.00

TEMPERATURE(DEG.FAHR)	215.00	
STRAIN A. (MEAS)	-526.00	
STRAIN B. (MEAS)	470.00	
STRAIN C. (MEAS)	-66.00	
STRAIN A. (MECH)	-641.64	
STRAIN B. (MECH)	548.36	
STRAIN C. (MECH)	-27.64	
STRAIN X. (MECH)	-1017.64	
STRAIN Y. (MECH)	548.36	
GAMMA XY. (MECH)	-414.00	
PRIN.STR.1. (")	575.26	
PRIN.STR.2. (")	-1044.54	
PHI X (DEGREES)	82.60	
SIGMA XX (KSI)	17.24	
SIGMA YY (KSI)	28.48	
TAU XY (KSI)	-1.49	
YIELD STRESS (KSI)	38.40	
I (KSI)	0.2476E 02	
I/YIELD STRESS	0.6447E 00	

30.00

TEMPERATURE(DEG.FAHR)	260.00	75.00
STRAIN A. (MEAS)	-868.00	240.00
STRAIN B. (MEAS)	674.00	237.00
STRAIN C. (MEAS)	48.00	-61.00
STRAIN A. (MECH)	-785.64	313.89
STRAIN B. (MECH)	750.36	349.89
STRAIN C. (MECH)	84.36	-70.11
STRAIN X. (MECH)	-1451.64	-106.11
STRAIN Y. (MECH)	750.36	349.89
GAMMA XY. (MECH)	-870.00	384.00
PRIN.STR.1. (")	833.18	419.96
PRIN.STR.2. (")	-1534.46	-176.18
PHI X (DEGREES)	79.22	69.95
SIGMA XX (KSI)	21.81	0.12
SIGMA YY (KSI)	37.28	3.55
TAU XY (KSI)	-3.06	1.44
YIELD STRESS (KSI)	37.32	39.99
I (KSI)	0.3230E 02	0.4064E 01
I/YIELD STRESS	0.8655E 00	0.1016E 00

31.00

TEMPERATURE(DEG.FAHR)	286.00
STRAIN A. (MEAS)	-1018.00

TAU XY (KSI)	3.92	4.01
YIELD STRESS (KSI)	39.82	39.81
I (KSI)	0.9837E 01	0.1019E 02
I/YIELD STRESS	0.2470E 00	0.2559E 00

26.50

TEMPERATURE(DEG.FAHR)	129.00	129.00
STRAIN A. (MEAS)	654.00	713.00
STRAIN B. (MEAS)	456.00	487.00
STRAIN C. (MEAS)	-441.00	-483.00
STRAIN A. (MECH)	678.11	678.11
STRAIN B. (MECH)	483.11	492.11
STRAIN C. (MECH)	-479.89	-467.89
STRAIN X. (MECH)	-281.89	-281.89
STRAIN Y. (MECH)	483.11	492.11
GAMMA XY. (MECH)	1158.00	1146.00
PRIN.STR.1. (")	792.22	776.56
PRIN.STR.2. (")	-594.00	-586.33
PHI X (DEGREES)	61.67	62.02
SIGMA XX (KSI)	8.51	8.55
SIGMA YY (KSI)	14.16	14.29
TAU XY (KSI)	4.29	4.25
YIELD STRESS (KSI)	39.00	39.00
I (KSI)	0.1265E 02	0.1298E 02
I/YIELD STRESS	0.3246E 00	0.3278E 00

27.00

TEMPERATURE(DEG.FAHR)	165.00	163.00
STRAIN A. (MEAS)	542.00	541.00
STRAIN B. (MEAS)	234.00	307.00
STRAIN C. (MEAS)	-339.00	-363.00
STRAIN A. (MECH)	391.09	329.73
STRAIN B. (MECH)	203.09	335.73
STRAIN C. (MECH)	-352.91	-324.27
STRAIN X. (MECH)	-246.91	-330.27
STRAIN Y. (MECH)	203.09	335.73
GAMMA XY. (MECH)	744.00	654.00
PRIN.STR.1. (")	475.25	469.44
PRIN.STR.2. (")	-437.37	-463.98
PHI X (DEGREES)	62.08	67.76
SIGMA XX (KSI)	15.13	14.00
SIGMA YY (KSI)	18.99	18.68
TAU XY (KSI)	2.72	2.40
YIELD STRESS (KSI)	39.21	39.23
I (KSI)	0.1762E 02	0.1718E 02
I/YIELD STRESS	0.4494E 00	0.4380E 00

27.50

TEMPERATURE(DEG.FAHR)	201.00	198.00
STRAIN A. (MEAS)	-96.00	-91.00

STRAIN B. (MEAS)	778.00
STRAIN C. (MEAS)	-24.00
STRAIN A. (MECH)	-951.66
STRAIN B. (MECH)	838.34
STRAIN C. (MECH)	-3.66
STRAIN X. (MECH)	-1793.66
STRAIN Y. (MECH)	838.34
GAMMA XY. (MECH)	-948.00
PRIN.STR.1. (")	921.10
PRIN.STR.2. (")	-1876.42
PHI X (DEGREES)	80.13
SIGMA XX (KSI)	23.35
SIGMA YY (KSI)	41.59
TAU XY (KSI)	-3.28
YIELD STRESS (KSI)	36.50
I (KSI)	0.3597E 02
I/YIELD STRESS	0.9854E 00

33.00

TEMPERATURE(DEG.FAHR)	305.00
STRAIN A. (MEAS)	-1042.00
STRAIN B. (MEAS)	848.00
STRAIN C. (MEAS)	-144.00
STRAIN A. (MECH)	-995.09
STRAIN B. (MECH)	888.91
STRAIN C. (MECH)	-143.09
STRAIN X. (MECH)	-2027.09
STRAIN Y. (MECH)	888.91
GAMMA XY. (MECH)	-852.00
PRIN.STR.1. (")	949.87
PRIN.STR.2. (")	-2088.05
PHI X (DEGREES)	81.86
SIGMA XX (KSI)	24.58
SIGMA YY (KSI)	44.57
TAU XY (KSI)	-2.92
YIELD STRESS (KSI)	35.81
I (KSI)	0.3855E 02
I/YIELD STRESS	0.1077E 01

35.00

TEMPERATURE(DEG.FAHR)	309.00
STRAIN A. (MEAS)	-976.00
STRAIN B. (MEAS)	818.00
STRAIN C. (MEAS)	-284.00
STRAIN A. (MECH)	-934.06
STRAIN B. (MECH)	853.96
STRAIN C. (MECH)	-288.14
STRAIN X. (MECH)	-2076.04
STRAIN Y. (MECH)	853.96
GAMMA XY. (MECH)	-646.00
PRIN.STR.1. (")	869.15
PRIN.STR.2. (")	-2111.22

STRAIN B. (MEAS)	1[illegible]	329.00
STRAIN C. (MEAS)	-147.00	-201.00
STRAIN A. (MECH)	-[illegible]	-81.80
STRAIN B. (MECH)	261.51	374.20
STRAIN C. (MECH)	-140.49	-141.80
STRAIN X. (MECH)	-428.49	-597.80
STRAIN Y. (MECH)	261.51	374.20
GAMMA XY. (MECH)	114.00	60.00
PRIN.STR.1. (")	266.18	375.12
PRIN.STR.2. (")	-433.17	-598.73
PHI X (DEGREES)	85.31	88.23
SIGMA XX (KSI)	14.91	17.91
SIGMA YY (KSI)	24.89	26.94
TAU XY (KSI)	0.41	0.22
YIELD STRESS (KSI)	38.66	38.72
I (KSI)	0.2284E 02	0.2249E 02
I/YIELD STRESS	0.5907E 00	0.5751E 00

28.00

TEMPERATURE(DEG.FAHR)	295.00	295.00
STRAIN A. (MEAS)	-920.00	-373.00
STRAIN B. (MEAS)	288.00	491.00
STRAIN C. (MEAS)	-33.00	-99.00
STRAIN A. (MECH)	-348.38	-355.59
STRAIN B. (MECH)	369.62	506.41
STRAIN C. (MECH)	-16.38	-31.59
STRAIN X. (MECH)	-736.38	-655.59
STRAIN Y. (MECH)	369.62	506.41
GAMMA XY. (MECH)	-330.00	-324.00
PRIN.STR.1. (")	389.38	526.80
PRIN.STR.2. (")	-757.14	-914.04
PHI X (DEGREES)	81.04	83.53
SIGMA XX (KSI)	23.41	23.50
SIGMA YY (KSI)	31.22	30.33
TAU XY (KSI)	-1.17	-1.16
YIELD STRESS (KSI)	37.47	38.14
I (KSI)	0.2[illegible] 02	0.2[illegible] 02
I/YIELD STRESS	0.7394E 00	0.6[illegible] 00

28.50

TEMPERATURE(DEG.FAHR)	295.00	294.00
STRAIN A. (MEAS)	-[illegible]	-571.00
STRAIN B. (MEAS)	[illegible]	564.00
STRAIN C. (MEAS)	[illegible]	-63.00
STRAIN A. (MECH)	-564.69	-553.47
STRAIN B. (MECH)	579.11	616.53
STRAIN C. (MECH)	11.11	4.53
STRAIN X. (MECH)	-1362.89	-1165.47
STRAIN Y. (MECH)	579.11	616.53
GAMMA XY. (MECH)	-576.00	-558.00
PRIN.STR.1. (")	591.21	659.19
PRIN.STR.2. (")	-1113.99	-1208.13

PHI X (DEGREES)	83.78	
SIGMA XX (KSI)	24.68	
SIGMA YY (KSI)	44.72	
TAU XY (KSI)	-2.21	
YIELD STRESS (KSI)	35.65	
I (KSI)	0.3871E 02	
I/YIELD STRESS	0.1086E 01	

43.00		
TEMPERATURE(DEG.FAHR)	295.00	78.00
STRAIN A. (MEAS)	-838.00	306.00
STRAIN B. (MEAS)	614.00	357.00
STRAIN C. (MEAS)	-384.00	-91.00
STRAIN A. (MECH)	-780.33	379.89
STRAIN B. (MECH)	665.97	469.89
STRAIN C. (MECH)	-372.03	-100.11
STRAIN X. (MECH)	-1818.33	-190.11
STRAIN Y. (MECH)	665.97	469.89
GAMMA XY. (MECH)	-408.00	480.00
PRIN.STR.1. (")	682.61	547.93
PRIN.STR.2. (")	-1834.67	-268.15
PHI X (DEGREES)	85.36	71.99
SIGMA XX (KSI)	24.15	-0.38
SIGMA YY (KSI)	41.28	4.59
TAU XY (KSI)	-1.48	1.81
YIELD STRESS (KSI)	36.19	39.99
I (KSI)	0.3586E 02	0.9322E 01
I/YIELD STRESS	0.9910E 00	0.1331E 00

50.00		
TEMPERATURE(DEG.FAHR)	267.00	77.00
STRAIN A. (MEAS)	-778.00	648.00
STRAIN B. (MEAS)	410.00	261.00
STRAIN C. (MEAS)	-396.00	-493.00
STRAIN A. (MECH)	-698.79	721.82
STRAIN B. (MECH)	483.21	373.82
STRAIN C. (MECH)	-362.79	-502.18
STRAIN X. (MECH)	-1544.79	-154.18
STRAIN Y. (MECH)	483.21	373.82
GAMMA XY. (MECH)	-336.00	1224.00
PRIN.STR.1. (")	497.03	776.33
PRIN.STR.2. (")	-1558.61	-556.70
PHI X (DEGREES)	85.30	56.67
SIGMA XX (KSI)	21.20	-0.53
SIGMA YY (KSI)	35.40	3.44
TAU XY (KSI)	-1.16	4.61
YIELD STRESS (KSI)	37.12	40.01
I (KSI)	0.3080E 02	0.9271E 01
I/YIELD STRESS	0.8298E 00	0.1318E 00

PHI X (DEGREES)	79.99	81.91
SIGMA XX (KSI)	25.61	21.38
SIGMA YY (KSI)	36.04	34.33
TAU XY (KSI)	-2.02	-1.98
YIELD STRESS (KSI)	37.23	37.75
I (KSI)	0.3249E 02	0.2968E 02
I/YIELD STRESS	0.8726E 00	0.7859E 00

29.00		
TEMPERATURE(DEG.FAHR)	288.00	202.00
STRAIN A. (MEAS)	-774.00	-703.00
STRAIN B. (MEAS)	556.00	679.00
STRAIN C. (MEAS)	9.00	-63.00
STRAIN A. (MECH)	-717.00	-693.95
STRAIN B. (MECH)	514.59	731.59
STRAIN C. (MECH)	2.34	-68.95
STRAIN X. (MECH)	-1329.66	-1422.49
STRAIN Y. (MECH)	514.34	731.65
GAMMA XY. (MECH)	-723.00	-69[illegible]
PRIN.STR.1. (")	516.66	7[illegible]
PRIN.STR.2. (")	-1334.16	-1476.36
PHI X (DEGREES)	79.34	81.12
SIGMA XX (KSI)	27.39	22.42
SIGMA YY (KSI)	40.87	37.34
TAU XY (KSI)	-2.49	-2.42
YIELD STRESS (KSI)	36.36	37.26
I (KSI)	0.3597E 02	0.3261E 02
I/YIELD STRESS	0.9852E 00	0.8751E 00

30.00		
TEMPERATURE(DEG.FAHR)	312.00	248.00
STRAIN A. (MEAS)	-870.00	-92[illegible]
STRAIN B. (MEAS)	726.00	817.00
STRAIN C. (MEAS)	-63.00	-117.00
STRAIN A. (MECH)	-847.95	-825.06
STRAIN B. (MECH)	794.05	854.34
STRAIN C. (MECH)	-97.95	-[illegible]
STRAIN X. (MECH)	-1679.95	-1749.06
STRAIN Y. (MECH)	794.05	854.34
GAMMA XY. (MECH)	-750.00	-756.00
PRIN.STR.1. (")	810.00	90[illegible]
PRIN.STR.2. (")	-1795.97	-1[illegible]
PHI X (DEGREES)	81.53	81.[illegible]
SIGMA XX (KSI)	26.73	23.[illegible]
SIGMA YY (KSI)	45.49	41.[illegible]
TAU XY (KSI)	-2.56	-2.62
YIELD STRESS (KSI)	35.53	36.50
I (KSI)	0.3975E 02	0.3630E 02
I/YIELD STRESS	0.1119E 01	0.9944E 00

51.00

TEMPERATURE(DEG.FAHR)	77.00
STRAIN A. (MEAS)	750.00
STRAIN B. (MEAS)	255.00
STRAIN C. (MEAS)	-529.00
STRAIN A. (MECH)	823.82
STRAIN B. (MECH)	367.82
STRAIN C. (MECH)	-538.18
STRAIN X. (MECH)	-82.18
STRAIN Y. (MECH)	367.82
GAMMA XY. (MECH)	1362.00
PRIN.STR.1. (")	860.02
PRIN.STR.2. (")	-574.39
PHI X (DEGREES)	54.14
SIGMA XX (KSI)	0.26
SIGMA YY (KSI)	3.65
TAU XY (KSI)	5.12
YIELD STRESS (KSI)	40.00
I (KSI)	0.5272E 01
I/YIELD STRESS	0.1318E 00

52.00

TEMPERATURE(DEG.FAHR)	78.00
STRAIN A. (MEAS)	882.00
STRAIN B. (MEAS)	417.00
STRAIN C. (MEAS)	-433.00
STRAIN A. (MECH)	955.89
STRAIN B. (MECH)	529.89
STRAIN C. (MECH)	-442.11
STRAIN X. (MECH)	-16.11
STRAIN Y. (MECH)	529.89
GAMMA XY. (MECH)	1398.00
PRIN.STR.1. (")	1007.31
PRIN.STR.2. (")	-493.53
PHI X (DEGREES)	55.67
SIGMA XX (KSI)	1.81
SIGMA YY (KSI)	5.92
TAU XY (KSI)	5.26
YIELD STRESS (KSI)	39.99
I (KSI)	0.6584E 01
I/YIELD STRESS	0.1646E 00

52.50

TEMPERATURE(DEG.FAHR)	80.00
STRAIN A. (MEAS)	1038.00
STRAIN B. (MEAS)	615.00
STRAIN C. (MEAS)	-385.00
STRAIN A. (MECH)	1112.09
STRAIN B. (MECH)	728.09
STRAIN C. (MECH)	-393.91
STRAIN X. (MECH)	-9.91
STRAIN Y. (MECH)	728.09

32.00

TEMPERATURE(DEG.FAHR)	328.00	310.00
STRAIN A. (MEAS)	-840.00	0.00
STRAIN B. (MEAS)	828.00	0.00
STRAIN C. (MEAS)	-225.00	-237.00
STRAIN A. (MECH)	-841.64	-28.32
STRAIN B. (MECH)	832.36	11.68
STRAIN C. (MECH)	-283.64	-215.32
STRAIN X. (MECH)	-1957.64	-255.32
STRAIN Y. (MECH)	832.36	11.68
GAMMA XY. (MECH)	-556.00	187.00
PRIN.STR.1. (")	859.99	41.16
PRIN.STR.2. (")	-1985.27	-284.81
PHI X (DEGREES)	84.34	72.50
SIGMA XX (KSI)	29.21	40.65
SIGMA YY (KSI)	48.07	42.47
TAU XY (KSI)	-1.89	0.64
YIELD STRESS (KSI)	34.84	35.91
I (KSI)	0.4184E 02	0.4161E 02
I/YIELD STRESS	0.1202E 01	0.1169E 01

35.00

TEMPERATURE(DEG.FAHR)	321.00	311.00
STRAIN A. (MEAS)	-720.00	0.00
STRAIN B. (MEAS)	774.00	0.00
STRAIN C. (MEAS)	-375.00	369.00
STRAIN A. (MECH)	-734.66	-29.62
STRAIN B. (MECH)	789.32	10.38
STRAIN C. (MECH)	-622.66	-348.62
STRAIN X. (MECH)	-1910.68	-388.62
STRAIN Y. (MECH)	789.32	10.38
GAMMA XY. (MECH)	-282.00	319.00
PRIN.STR.1. (")	796.04	66.00
PRIN.STR.2. (")	-1924.01	-444.55
PHI X (DEGREES)	87.03	70.68
SIGMA XX (KSI)	28.24	39.45
SIGMA YY (KSI)	46.62	42.17
TAU XY (KSI)	-0.96	1.09
YIELD STRESS (KSI)	33.15	35.57
I (KSI)	0.4304E 02	0.4092E 02
I/YIELD STRESS	0.1296E 01	0.1150E 01

40.00

TEMPERATURE(DEG.FAHR)	296.00	294.00
STRAIN A. (MEAS)	-982.00	0.00
STRAIN B. (MEAS)	964.00	0.00
STRAIN C. (MEAS)	-429.00	-411.00
STRAIN A. (MECH)	-537.15	-13.03
STRAIN B. (MECH)	608.85	29.97
STRAIN C. (MECH)	-447.15	-371.03
STRAIN X. (MECH)	-1593.15	-411.03
STRAIN Y. (MECH)	608.85	29.97

GAMMA XY. (MECH)	1506.00
PRIN.STR.1. (#)	1197.65
PRIN.STR.2. (#)	-479.46
PHI X (DEGREES)	58.05
SIGMA XX (KSI)	3.01
SIGMA YY (KSI)	8.56
TAU XY (KSI)	5.66
YIELD STRESS (KSI)	39.98
I (KSI)	0.8574E 01
I/YIELD STRESS	0.2145E 00

53.00

TEMPERATURE(DEG.FAHR)	84.00
STRAIN A. (MEAS)	1254.00
STRAIN B. (MEAS)	753.00
STRAIN C. (MEAS)	-409.00
STRAIN A. (MECH)	1328.72
STRAIN B. (MECH)	866.72
STRAIN C. (MECH)	-417.28
STRAIN X. (MECH)	44.72
STRAIN Y. (MECH)	866.72
GAMMA XY. (MECH)	1746.00
PRIN.STR.1. (#)	1420.63
PRIN.STR.2. (#)	-509.19
PHI X (DEGREES)	57.61
SIGMA XX (KSI)	4.91
SIGMA YY (KSI)	11.09
TAU XY (KSI)	6.56
YIELD STRESS (KSI)	39.95
I (KSI)	0.1060E 02
I/YIELD STRESS	0.2652E 00

53.50

TEMPERATURE(DEG.FAHR)	93.00
STRAIN A. (MEAS)	1350.00
STRAIN B. (MEAS)	705.00
STRAIN C. (MEAS)	-397.00
STRAIN A. (MECH)	1427.09
STRAIN B. (MECH)	821.09
STRAIN C. (MECH)	-402.91
STRAIN X. (MECH)	203.09
STRAIN Y. (MECH)	821.09
GAMMA XY. (MECH)	1830.00
PRIN.STR.1. (#)	1477.86
PRIN.STR.2. (#)	-453.67
PHI X (DEGREES)	54.33
SIGMA XX (KSI)	8.25
SIGMA YY (KSI)	12.89
TAU XY (KSI)	6.86
YIELD STRESS (KSI)	39.89
I (KSI)	0.1218E 02
I/YIELD STRESS	0.3054E 00

GAMMA XY. (MECH)	-90.00	361.00
PRIN.STR.1. (#)	609.76	94.43
PRIN.STR.2. (#)	-1594.37	-475.48
PHI X (DEGREES)	88.83	70.35
SIGMA XX (KSI)	26.82	36.33
SIGMA YY (KSI)	41.98	39.37
TAU XY (KSI)	-0.31	1.25
YIELD STRESS (KSI)	36.38	36.22
I (KSI)	0.3681E 02	0.3799E 02
I/YIELD STRESS	0.1020E 01	0.1049E 01

54.00

TEMPERATURE(DEG.FAHR)	109.00
STRAIN A, (MEAS)	1170.00
STRAIN B, (MEAS)	483.00
STRAIN C, (MEAS)	-265.00
STRAIN A, (MECH)	1252.03
STRAIN B, (MECH)	604.03
STRAIN C, (MECH)	-265.97
STRAIN X, (MECH)	382.03
STRAIN Y, (MECH)	604.03
GAMMA XY, (MECH)	1518.00
PRIN.STR.1, (M)	1260.10
PRIN.STR.2, (M)	-274.04
PHI X (DEGREES)	49.16
SIGMA XX (PSI)	11.75
SIGMA YY (KSI)	13.41
TAU XY (KSI)	5.67
YIELD STRESS (KSI)	39.80
I (KSI)	0.1332E 02
I/YIELD STRESS	3.3346E 00

55.55

TEMPERATURE(DEG.FAHR)	123.00
STRAIN A, (MEAS)	780.00
STRAIN B, (MEAS)	345.00
STRAIN C, (MEAS)	-145.00
STRAIN A, (MECH)	872.21
STRAIN B, (MECH)	476.21
STRAIN C, (MECH)	-135.79
STRAIN X, (MECH)	260.21
STRAIN Y, (MECH)	476.21
GAMMA XY, (MECH)	1308.00
PRIN.STR.1, (M)	883.65
PRIN.STR.2, (M)	-147.23
PHI X (DEGREES)	51.05
SIGMA XX (KSI)	13.37
SIGMA YY (KSI)	14.97
TAU XY (KSI)	3.74
YIELD STRESS (KSI)	39.66
I (KSI)	0.1463E 02
I/YIELD STRESS	0.3688E 00

55.00

TEMPERATURE(DEG.FAHR)	144.00
STRAIN A, (MEAS)	474.00
STRAIN B, (MEAS)	363.00
STRAIN C, (MEAS)	-115.00
STRAIN A, (MECH)	580.45
STRAIN B, (MECH)	508.45

STRAIN C. (MECH)	-91.99
STRAIN X. (MECH)	-19.55
STRAIN Y. (MECH)	505.45
GAMMA XY. (MECH)	677.00
PRIN.STR.1. (")	671.76
PRIN.STR.2. (")	-187.86
PHI X (DEGREES)	64.28
SIGMA XX (KSI)	14.41
SIGMA YY (KSI)	19.30
TAU XY (KSI)	2.48
YIELD STRESS (KSI)	39.45
I (KSI)	3.1692E 02
I/YIELD STRESS	8.4285E 00

50.00

TEMPERATURE(DEG.FAHR)	184.00
STRAIN A. (MEAS)	276.00
STRAIN B. (MEAS)	495.00
STRAIN C. (MEAS)	5.00
STRAIN A. (MECH)	409.01
STRAIN B. (MECH)	667.01
STRAIN C. (MECH)	55.01
STRAIN X. (MECH)	-202.99
STRAIN Y. (MECH)	667.01
GAMMA XY. (MECH)	354.00
PRIN.STR.1. (")	701.04
PRIN.STR.2. (")	-237.67
PHI X (DEGREES)	78.93
SIGMA XX (KSI)	25.61
SIGMA YY (KSI)	26.93
TAU XY (KSI)	1.29
YIELD STRESS (KSI)	38.94
I (KSI)	0.2447E 02
I/YIELD STRESS	0.6284E 00

TEMPERATURE(DEG.FAHR)	213.00
STRAIN A. (MEAS)	114.00
STRAIN B. (MEAS)	543.00
STRAIN C. (MEAS)	-7.00
STRAIN A. (MECH)	259.83
STRAIN B. (MECH)	727.83
STRAIN C. (MECH)	55.80
STRAIN X. (MECH)	-412.23
STRAIN Y. (MECH)	727.80
GAMMA XY. (MECH)	204.00
PRIN.STR.1. (")	736.86
PRIN.STR.2. (")	-421.25
PHI X (DEGREES)	84.93
SIGMA XX (KSI)	24.07
SIGMA YY (KSI)	32.71
TAU XY (KSI)	0.71

YIELD STRESS (KSI)		38.44
1 (KSI)		0.2904E 02
I/YIELD STRESS		0.7554E 00
50.00		
TEMPERATURE(DEG.FAHR)		232.00
STRAIN A, (MEAS)		42.00
STRAIN B, (MEAS)		595.00
STRAIN C, (MEAS)		-7.00
STRAIN A, (MECH)		191.05
STRAIN B, (MECH)		743.05
STRAIN C, (MECH)		59.05
STRAIN X, (MECH)		-492.94
STRAIN Y, (MECH)		743.05
GAMMA XY, (MECH)		132.00
PRIN.STR.1, (M)		746.57
PRIN.STR.2, (M)		-496.46
PHI X (DEGREES)		86.95
SIGMA XX (KSI)		28.75
SIGMA YY (KSI)		35.56
TAU XY (KSI)		0.47
YIELD STRESS (KSI)		38.04
1 (KSI)		0.3210E 02
I/YIELD STRESS		0.8438E 00
60.00		
TEMPERATURE(DEG.FAHR)	244.00	261.07
STRAIN A, (MEAS)	-526.00	-42.00
STRAIN B, (MEAS)	290.00	579.00
STRAIN C, (MEAS)	-336.00	35.00
STRAIN A, (MECH)	-439.47	101.96
STRAIN B, (MECH)	370.53	761.96
STRAIN C, (MECH)	-295.47	95.96
STRAIN X, (MECH)	-1105.47	-564.04
STRAIN Y, (MECH)	370.53	761.96
GAMMA XY, (MECH)	-664.00	0.00
PRIN.STR.1, (M)	374.03	761.97
PRIN.STR.2, (M)	-1160.97	-564.04
PHI X (DEGREES)	87.21	89.87
SIGMA XX (KSI)	21.15	31.38
SIGMA YY (KSI)	31.60	40.70
TAU XY (KSI)	-0.51	0.02
YIELD STRESS (KSI)	37.75	37.29
1 (KSI)	0.2786E 02	0.3693E 02
I/YIELD STRESS	0.7390E 00	0.9903E 00
65.00		
TEMPERATURE(DEG.FAHR)		271.00
STRAIN A, (MEAS)		-300.00
STRAIN B, (MEAS)		369.00

STRAIN C. (MEAS)	227.33
STRAIN A. (MECH)	-160.97
STRAIN B. (MECH)	547.03
STRAIN C. (MECH)	283.33
STRAIN X. (MECH)	-424.97
STRAIN Y. (MECH)	547.03
GAMMA XY. (MECH)	-444.00
PRIN.STR.1. (")	595.33
PRIN.STR.2. (")	-473.27
PHI X (DEGREES)	77.72
SIGMA XX (KSI)	33.89
SIGMA YY (KSI)	40.68
TAU XY (KSI)	-1.55
YIELD STRESS (KSI)	36.99
I (KSI)	0.3769E 02
I/YIELD STRESS	0.1019E 01

70.00		
TEMPERATURE(DEG.FAHR)	226.00	264.00
STRAIN A. (MEAS)	-624.00	-650.00
STRAIN B. (MEAS)	210.33	255.00
STRAIN C. (MEAS)	-264.00	311.00
STRAIN A. (MECH)	-337.46	-308.29
STRAIN B. (MECH)	298.54	435.71
STRAIN C. (MECH)	-223.46	360.71
STRAIN X. (MECH)	-899.46	-374.29
STRAIN Y. (MECH)	298.54	435.71
GAMMA XY. (MECH)	-114.00	-478.00
PRIN.STR.1. (")	301.34	550.86
PRIN.STR.2. (")	-862.26	-497.44
PHI X (DEGREES)	87.19	78.03
SIGMA XX (KSI)	28.13	33.14
SIGMA YY (KSI)	28.48	36.81
TAU XY (KSI)	-0.41	-2.37
YIELD STRESS (KSI)	30.17	37.15
I (KSI)	0.2528E 02	0.3621E 02
I/YIELD STRESS	0.6422E 00	0.9749E 00

90.00	
TEMPERATURE(DEG.FAHR)	245.00
STRAIN A. (MEAS)	-624.00
STRAIN B. (MEAS)	105.00
STRAIN C. (MEAS)	383.07
STRAIN A. (MECH)	-671.61
STRAIN B. (MECH)	292.39
STRAIN C. (MECH)	448.39
STRAIN X. (MECH)	-919.61
STRAIN Y. (MECH)	292.39
GAMMA X . (MECH)	-924.00
PRIN.STR.1. (")	340.54
PRIN.STR.2. (")	-567.76
PHI X (DEGREES)	41.76

SIGMA XX (KSI)	29.47
SIGMA YY (KSI)	33.73
TAU XY (KSI)	-3.27
YIELD STRESS (KSI)	37.72
E (KSI)	0.3163E 02
E/YIELD STRESS	0.8385E 00

93.33

TEMPERATURE(DEG.FAH)	220.00
STRAIN A. (MEAS)	-696.00
STRAIN B. (MEAS)	-9.00
STRAIN C. (MEAS)	401.00
STRAIN A. (MECH)	-567.23
STRAIN B. (MECH)	178.77
STRAIN C. (MECH)	466.77
STRAIN X. (MECH)	-256.23
STRAIN Y. (MECH)	178.77
GAMMA XY. (MECH)	-1314.00
PRIN.STR.1. (M)	512.06
PRIN.STR.2. (M)	-592.51
PHI C (DEGREES)	56.65
SIGMA XX (KSI)	26.50
SIGMA YY (KSI)	29.63
TAU XY (KSI)	-3.62
YIELD STRESS (KSI)	38.13
E (KSI)	0.2833E 02
E/YIELD STRESS	0.7344E 00

100.00

TEMPERATURE(DEG.FAH)	196.33	213.33
STRAIN A. (MEAS)	-202.00	-754.00
STRAIN B. (MEAS)	122.00	-99.00
STRAIN C. (MEAS)	-132.00	401.00
STRAIN A. (MECH)	-184.73	-610.20
STRAIN B. (MECH)	193.27	85.80
STRAIN C. (MECH)	-100.73	489.80
STRAIN X. (MECH)	-478.73	-232.20
STRAIN Y. (MECH)	193.27	85.80
GAMMA XY. (MECH)	-84.00	-1074.00
PRIN.STR.1. (M)	195.89	496.85
PRIN.STR.2. (M)	-481.34	-633.24
PHI C (DEGREES)	86.44	53.25
SIGMA XX (KSI)	19.17	23.66
SIGMA YY (KSI)	23.83	25.94
TAU XY (KSI)	-0.30	-3.86
YIELD STRESS (KSI)	38.75	38.44
E (KSI)	0.2180E 02	0.2965E 02
E/YIELD STRESS	0.5625E 00	0.7712E 00

TEMPERATURE(DEG.FAHR)		169.03
STRAIN A. (MEAS)		-858.00
STRAIN B. (MEAS)		-405.00
STRAIN C. (MEAS)		305.33
STRAIN A. (MECH)		-734.25
STRAIN B. (MECH)		+242.25
STRAIN C. (MECH)		343.75
STRAIN X. (MECH)		-144.25
STRAIN Y. (MECH)		-242.25
GAMMA XY. (MECH)		-1080.00
PRIN.STR.1. (")		347.88
PRIN.STR.2. (")		-736.38
PHI X (DEGREES)		42.46
SIGMA XX (KSI)		19.06
SIGMA YY (KSI)		14.35
TAU XY (KSI)		-3.95
YIELD STRESS (KSI)		39.14
1 (KSI)		0.1431E 02
1/YIELD STRESS		0.3655E 00

200.00

TEMPERATURE(DEG.FAHR)	150.00	145.00
STRAIN A. (MEAS)	-70.00	-876.00
STRAIN B. (MEAS)	53.30	-549.00
STRAIN C. (MEAS)	40.00	274.00
STRAIN A. (MECH)	-21.32	-768.45
STRAIN B. (MECH)	92.68	-402.85
STRAIN C. (MECH)	50.68	299.15
STRAIN X. (MECH)	-63.32	-66.85
STRAIN Y. (MECH)	92.68	-402.85
GAMMA XY. (MECH)	-72.00	-1069.00
PRIN.STR.1. (")	100.54	324.96
PRIN.STR.2. (")	-71.22	-794.65
PHI X (DEGREES)	77.61	36.27
SIGMA XX (KSI)	13.55	18.72
SIGMA YY (KSI)	14.70	8.25
TAU XY (KSI)	-0.26	-3.94
YIELD STRESS (KSI)	39.39	39.44
1 (KSI)	0.1413E 02	0.9096E 01
1/YIELD STRESS	0.3587E 00	0.2306E 00

300.00

TEMPERATURE(DEG.FAHR)	129.00	125.01
STRAIN A. (MEAS)	-5.00	-876.00
STRAIN B. (MEAS)	37.00	-651.00
STRAIN C. (MEAS)	78.00	221.00
STRAIN A. (MECH)	28.11	-782.51
STRAIN B. (MECH)	60.11	-518.51
STRAIN C. (MECH)	96.11	231.49
STRAIN X. (MECH)	94.11	-32.51
STRAIN Y. (MECH)	60.11	-518.51
GAMMA XY. (MECH)	-19.00	-1014.00

PRIN.STR.1. (M)	77.13	286.72
PRIN.STR.2. (M)	24.09	-837.74
PHI X (DEGREES)	62.13	32.20
SIGMA XX (KSI)	17.46	8.91
SIGMA YY (KSI)	29.65	3.20
TAU XY (KSI)	-7.14	-3.74
YIELD STRESS (KSI)	36.67	39.69
I (KSI)	C.12948E 02	0.4849E 01
I/YIELD STRESS	C.2462E 00	0.1221E 00

600.00

TEMPERATURE(DEG.FAHR)	185.00	185.00
STRAIN A. (MEAS)	2.00	-856.00
STRAIN B. (MEAS)	8.00	-717.00
STRAIN C. (MEAS)	146.00	185.00
STRAIN A. (MECH)	22.03	-775.97
STRAIN B. (MECH)	22.03	-905.97
STRAIN C. (MECH)	119.03	184.03
STRAIN X. (MECH)	119.03	4.03
STRAIN Y. (MECH)	22.03	-905.97
GAMMA XY. (MECH)	-98.00	-960.00
PRIN.STR.1. (M)	137.91	270.07
PRIN.STR.2. (M)	2.15	-862.01
PHI X (DEGREES)	77.50	29.00
SIGMA XX (KSI)	4.63	3.85
SIGMA YY (KSI)	5.91	-1.43
TAU XY (KSI)	-5.14	-3.58
YIELD STRESS (KSI)	37.80	39.83
I (KSI)	C.6214E 01	0.2224E 01
I/YIELD STRESS	C.1641E 00	0.5582E-01

900.00

TEMPERATURE(DEG.FAHR)	95.00	95.00
STRAIN A. (MEAS)	-4.00	-858.00
STRAIN B. (MEAS)	-4.00	-717.00
STRAIN C. (MEAS)	128.00	173.00
STRAIN A. (MECH)	11.79	-780.21
STRAIN B. (MECH)	5.79	-600.21
STRAIN C. (MECH)	89.79	167.79
STRAIN X. (MECH)	95.79	-12.21
STRAIN Y. (MECH)	5.79	-600.21
GAMMA XY. (MECH)	-78.00	-948.00
PRIN.STR.1. (M)	110.34	251.94
PRIN.STR.2. (M)	-8.76	-863.94
PHI X (DEGREES)	28.46	29.10
SIGMA XX (KSI)	4.39	8.91
SIGMA YY (KSI)	3.71	-3.98
TAU XY (KSI)	-2.29	-3.15
YIELD STRESS (KSI)	39.88	39.89
I (KSI)	0.1982E 01	0.2339E 01
I/YIELD STRESS	0.4987E-01	0.5916E-01

1100.00		
TEMPERATURE(DEG.FAHR)	89.00	88.00
STRAIN A, (MEAS)	-4.00	-858.00
STRAIN B, (MEAS)	-4.00	-717.00
STRAIN C, (MEAS)	126.00	167.00
STRAIN A, (MECH)	9.88	-782.38
STRAIN B, (MECH)	3.88	-602.38
STRAIN C, (MECH)	93.88	159.62
STRAIN X, (MECH)	99.88	-20.38
STRAIN Y, (MECH)	3.88	-602.38
GAMMA XY, (MECH)	-84.00	-942.00
PRIN.STR.1, (")	119.66	242.24
PRIN.STR.2, (")	-11.90	-865.02
PHI X (DEGREES)	20.59	29.15
SIGMA XX (KSI)	3.27	-0.55
SIGMA YY (KSI)	2.99	-4.92
TAU XY (KSI)	-0.32	-3.53
YIELD STRESS (KSI)	39.92	39.93
I (KSI)	0.7888E 01	0.3343E 01
I/YIELD STRESS	0.[illegible]E-11	0.[illegible]E-31

1600.00		
TEMPERATURE(DEG.FAHR)	84.00	83.00
STRAIN A, (MEAS)	-16.00	-952.00
STRAIN B, (MEAS)	2.00	-725.00
STRAIN C, (MEAS)	138.00	161.00
STRAIN A, (MECH)	-7.96	-777.48
STRAIN B, (MECH)	9.14	-615.46
STRAIN C, (MECH)	139.14	192.54
STRAIN X, (MECH)	93.14	-5.46
STRAIN Y, (MECH)	9.14	-615.46
GAMMA XY, (MECH)	-100.37	-930.03
PRIN.STR.1, (")	119.55	242.54
PRIN.STR.2, (")	-17.27	-867.47
PHI X (DEGREES)	28.06	28.46
SIGMA XX (KSI)	2.63	-1.45
SIGMA YY (KSI)	2.33	-4.33
TAU XY (KSI)	-0.41	-3.49
YIELD STRESS (KSI)	39.94	39.96
I (KSI)	0.2107E 01	0.4352E 01
I/YIELD STRESS	0.527[illegible]E-01	0.1089E 00

CORE USAGE OBJECT CODE= 9600 BYTES,ARRAY AREA= 6468 BYTES,TOTAL AREA AVAILABLE= 26722 BYTES

COMPILE TIME= 0.37 SEC,EXECUTION TIME= 0.86 SEC, ATFIV - VERSION 1 LEVEL 2 AUGUST 1970 DATE= 73/121

TEST NO. 5 (CONTINUED): 3.00 INCH TRANSVERSE DISTANCE FROM THE CENTERLINE AT CENTER OF PLATE:

Time (Seconds)	Temperature (°F)	ϵ_x (Measured) (Microstrain)	ϵ_y (Measured) (Microstrain)	ϵ_x (Mechanical) (Microstrain)	ϵ_y (Mechanical) (Microstrain)
0.00	78.00	-39.00	21.00	-32.83	27.17
10.00	78.00	-80.00	6.00	-34.83	- 8.83
15.00	78.00	-85.00	-24.00	-39.83	-38.83
20.00	78.00	-25.00	-89.00	20.17	-103.83
25.00	78.00	125.00	-39.00	170.17	-53.83
26.00	78.00	155.00	76.00	200.17	61.17
27.00	78.00	155.00	116.00	200.17	101.17
28.00	80.00	190.00	116.00	235.00	101.00
30.00	80.00	270.00	51.00	315.00	36.00
32.00	87.00	395.00	-34.00	439.94	-49.06
35.00	101.00	410.00	-89.00	456.94	-102.06
40.00	127.00	155.00	-84.00	211.20	-87.00
45.00	144.00	-90.00	-34.00	-25.48	-29.48
50.00	152.00	-260.00	16.00	-191.31	24.69
60.00	166.00	-425.00	61.00	-349.06	76.94

Time (Seconds)	Temperature (^{o}F)	ε_x(Measured) (Microstrain)	ε_y(Measured) (Microstrain)	ε_x(Mechanical) (Microstrain)	ε_y(Mechanical) (Microstrain)
75.00	169.00	-475.00	91.00	-397.55	108.45
100.00	167.00	-430.00	96.00	-353.55	112.45
200.00	143.00	-220.00	96.00	-155.99	100.01
300.00	127.00	-150.00	96.00	-93.80	92.20
600.00	104.00	-100.00	91.00	-52.31	78.69
900.00	94.00	-85.00	81.00	-39.39	66.61
1200.00	89.00	-70.00	81.00	-24.94	66.06
1800.00	85.00	-70.00	76.00	-25.12	60.88

References:

1. Hill, H. N., "Residual Welding Stresses in Aluminum Alloys," Metal Progress, 80 (2), 92-96 (1961).

2. Masubuchi, K., "Residual Stresses and Distortion in Welded Aluminum Structures and Their Effects on Service Performance," Welding Research Council Bulletin No. 174, July, 1972.

3. Masubuchi, K., "Residual Stress Analysis Techniques for Weldment Studies - A summary of M.I.T. Studies," May, 1972, International Institute of Welding, Commission X Document X-675-72. Also presented before the 1972 Spring Meeting of SESA, Cleveland, Ohio, May 23-26, 1972.

4. Masubuchi, K., "Integration of NASA Sponsored Studies on Aluminum Welding Second Edition," Under Contract No. NAS 8-24364 to George C. Marshall Space Flight Center, NASA, June, 1971.

5. Masubuchi, K., "Third Draft-Interpretive Report on Residual Stresses and Distortion in Welded Aluminum Structures and Their Effects on Service Performance," April, 1972.

6. Klein, K. and Masubuchi, K., "Investigation of Welding Thermal Stresses in High Strength Steels for Marine Applications," Paper presented before the Second International Ocean Development Conference held October 5-7, 1972, Tokyo, Japan.

7. Klein, K., "Investigation of Welding Thermal Strains in Marine Steels," M.S. Thesis, M.I.T., May 1971.

8. Masubuchi, K., "Control of Distortion and Shrinkage in Welding," Welding Research Council Bulletin No. 149, April, 1970.

9. Tall, L., "Residual Stresses in Welded Plates--A Theoretical Study," The Welding Journal, 43 (1), Research Supplement, 10-s to 23-s.(1964).

10. Masubuchi, K., Simmons, F. B., and Monroe, R. E., "Analysis of Thermal Stresses and Metal Movement During Welding," RSIC-820, Redstone Scientific Information Center, Redstone Arsenal, Alabama, July, 1969.

11. Andrews, J. B., et. al., "Analysis of Thermal Stress and Metal Movement During Welding," NTIS Document No. N71-26143, 15 December 1970.

12. Hirsch, K. A., "Investigation of Thermal Stress and Buckling During Welding of Tantalum and Columbium Sheet," M.S. Thesis, MIT, January, 1972.

13. Masubuchi, K. and Iwaki, T., "Welding Stress Analysis by Numerical Experiments by Finite Element Method," Additional paper to the report "Residual Stress-Analysis Techniques for Weldment Study" by K. Masubuchi presented at 1972 SESA Spring Meeting, Cleveland, Ohio, May 23-26.

14. Andrews, J. B., and Masubuchi, K., "Analysis of Thermal Stresses and Metal Movement During Welding," Phase Report under Contract No. NAS8-24365, to George C. Marshall Space Flight Center, MIT Department of Ocean Engineering, Sept., 1971.

15. Wang, B., "Elasto-plastic Analysis of Orthotropic Plates and Shells," MIT Department of Civil Engineering, Report No. R68-83, October, 1968.

16. Marcal, P. V., and King, I. P., "Elastic-plastic Analysis of Two Dimensional Stress Systems by the Finite Element Method," Int. J. Mech. Sci., Pergamon Press, 1969, Vol. 9, 153-155.

17. Yamada, Y., "Recent Developments in Matrix Displacement Method for Elastic-plastic Problems in Japan," Recent Advances in Matrix Methods of Structural Analysis and Design, ed. R. H. Gallagher, Y. Yamada, J. T. Oden, University of Alabama Press, University of Alabama, pp. 283-316.

18. Hibbit, H. D., and Marcal, P. V., "A Numerical Thermo-Mechanical Model for the Welding and Subsequent Loading of a Fabricated Structure," Dept. of Navy, NSRDC Contract No. N00014-67-A-0191-0006, Technical Report No. 2, March, 1972.

19. Shin, D. B., "Finite Element Analysis of Out-of-plane Distortion of Panel Structures," MIT M.S. Thesis, May, 1972.

20. Muraki, T., and Masubuchi, K., First Interim Report on Phase B of Thermal Analysis of M551 Experiment for Materials Processing in Space, under Contract NAS8-28732, to G. C. Marshall Space Flight Center, January, 1973.

21. Richard, R. M., "Elastoplastic Analysis," Lecture Notes, Finite Element Short Course, Dept. of Civil Engineering and Mechanical Engineering, University of Arizona, April, 1971.

22. Tong, P., Lecture Notes for Course 16.28, "Variational and Matrix Methods," MIT, Spring, 1972.

23. Arpaci, V. S., Conduction Heat Transfer, Addison-Wesley, Reading, Massachusetts, 1966.

24. Zienkiewicz, O. C., The Finite Element Method in Engineering Science, McGraw-Hill, London, 1971.

25. Visser, W., "A Finite Element Method for the Determination of Non-stationary Temperature Distribution and Thermal Deformations," Proceedings of the First Conference on Matrix Methods in Structural Mechanics, Wright Patterson Air Force Base, Ohio, 1965.

26. Gallagher, R. H., and Mallett, R., "Efficient Solution Processes for Finite Element Analysis of Transient Heat Conduction," ASME Publication 69WA/HT-32, New York, 1969.

27. Wilson, E. L., and Michell, R. E., "Application of the Finite Element Method to Heat Conduction Analysis," Nuclear Engineering and Design (4), pp. 276-286, Amsterdam, 1966.

28. Thompson, J. J., and Chen, P. Y. P., "Discontinuous Finite Elements in Thermal Analysis," Nuclear Engineering and Design (14), pp. 211-222, Amsterdam, 1970.

29. Richardson, P. D., and Shum, Y. M., "Use of Finite Element Methods in Solutions of Transient Heat Conduction Problems," ASME Publication 69-WA/HT-36, New York, 1969.

30. Velikoivanenko, E. A. and Makhenko, V. I., "Numerical Solution of the Plane Problem in the Theory of Non-isothermal Plastic Flow as Applied to Welding Heating," University of California Radiation Laboratories Translation No. 10577, December, 1971.

31. ----------, Aerospace Structural Metals Handbook, AFML-TR-68-115, Air Force Materials Laboratory, Air Force Systems Command, Wright-Patterson Air Force Base, Ohio, 1970.

32. Alcoa Research Laboratories, "Typical Tensile Stress-Strain Curves for 6061 and 6062-T6 at Room Temperature, 212, 300, 400, 500, 600, and 700°F," Physical Test No. 010758-G Data Sheets, (March 6 and 31, 1958).

33. Mantell, C. L., Ed., Engineering Materials Handbook, McGraw-Hill, New York, 1958.

34. Brungraber, R. J., and Nelson, F. G., "Effect of Welding Variables on Aluminum Alloy Weldments," Welding Journal, 52, (3), 1973, pp. 97-s to 103-s.

35. --------, Alcoa Aluminum Handbook, Aluminum Company of America, pp. 43-45.

36. --------, Material Properties Handbook, Volume I, Aluminum Alloys, The Royal Aeronautical Society, London, 1966.

37. Touloukian, Y. S., Ed., Thermophysical Properties of High Temperature Solid Materials, Thermophysical Properties Research Center, Purdue University, the Macmillan Company, New York, 1967.

38. --------, Aluminum Standards and Data, The Aluminum Association, New York, 1969.

39. Van Horn, K. R., Ed., Aluminum, Volume I, Properties, Physical Metallurgy and Phase Diagrams, American Society for Metals, Metals Park, Ohio, 1967.

40. Murray, W. M., "Fundamental Concepts for Strain Gages," Lecture Series, MIT, (1970).

41. Murray, W. M., "Basic Electric Circuits for Strain Gages," Lecture Series, MIT, (1969).

42. Murray, W. M., "Rosette Analysis," Lecture Series, MIT, (1970).

43. Masubuchi, K., "Analytical Investigation of Residual Stresses and Distortions Due to Welding," the Welding Journal, 39, (12), Research Supplement, 525-s to 537-s, (1960).

44. Mendelson, A., Plasticity: Theory and Application, Macmillan Company, New York, 1968.